COMPLEMENTING SUBARACHNOID HEMORRHAGE

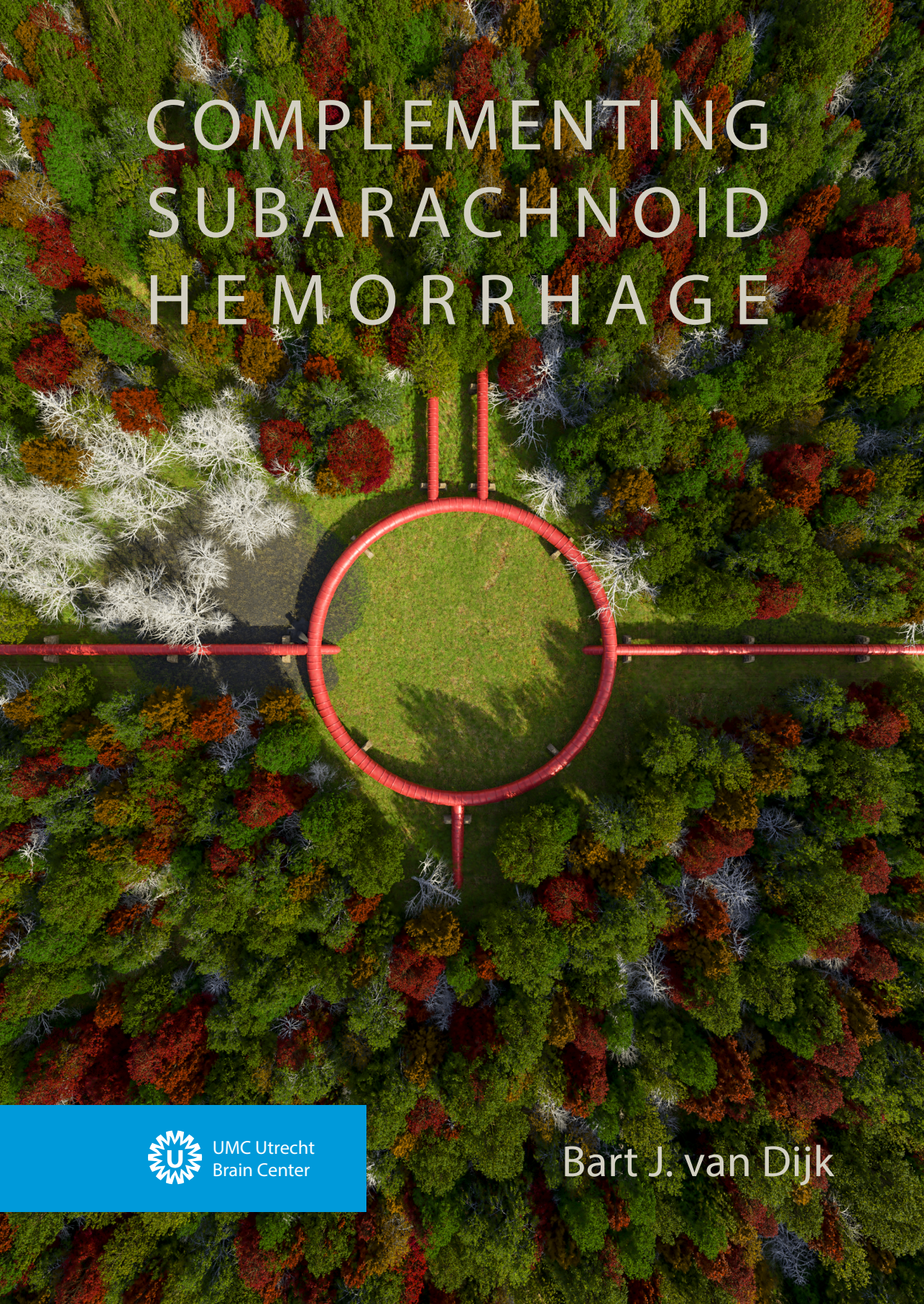

UMC Utrecht
Brain Center

Bart J. van Dijk

Complementing Subarachnoid Hemorrhage

Bart Jan van Dijk

About the cover

This thesis cover represents a metaphore between Subarachnoid Hemorrhage and an oil leak in a forest. Both cause damage to the surrounding environment. In this metaphore, the pipelines are in the shape of the Circle of Willis, with incoming pipes from the ground up, and distributing pipes to either side, representing the Middle Cerebral Arteries, and upwards, representing the anterior cerebral arteries. The trees represent the brain cells, closely resembling the astrocytes, with their countless processes as leaves. There is an oil leakage at the bifurcation of the left pipeline, resulting in dead trees.

Colofon

Copyright © 2020 Bart J. van Dijk
ISBN: 978-94-93184-69-5
DOI: 10.33540/210
Author: Bart J. van Dijk
Cover design: Bart J. van Dijk
Layout: Bart J. van Dijk
Print: Proefschrift All In One | www.proefschrift-AIO.nl

Complementing Subarachnoid Hemorrhage

Het complementeren van een subarachnoïdale bloeding
(met een samenvatting in het Nederlands)

Proefschrift

ter verkrijging van de graad van doctor aan de
Universiteit Utrecht
op gezag van de rector magnificus, prof. dr. H.R.B.M. Kummeling,
ingevolge het besluit van het college voor promoties
in het openbaar te verdedigen op
dinsdag 17 november 2020 des middags te 12.45 uur.

door

Bart Jan van Dijk
geboren op 23 augustus 1985 te Utrecht

Promotoren:
Prof. dr. E.M. Hol
Prof. dr. G.J.E Rinkel

Copromotor:
Dr. M.D.I. Vergouwen

TABLE OF CONTENTS

Prefix

Complementing Subarachnoid Hemorrhage

B.J. van Dijk

Complementing Subarachnoid Hemorrhage.

Aneurysmal subarachnoid hemorrhage (SAH) is a severe type of stroke with a high case fatality rate. The hemorrhage is caused by the rupture of an aneurysm; an outpouching of an artery. The median age on which an aneurysmal SAH occurs is around 55 years. Because of the young age it occurs, and the poor outcome, the loss of productive life years is high.[1] One-third of the patients dies within 3 months after ictus, and surviving patients often have long-lasting functional and cognitive impairments.
In this thesis, we will focus on the brain injury from aneurysmal SAH. Upon rupture of the aneurysm, blood spurs into the subarachnoid space, a cavity between the membranes around the brain. Subsequently, several factors lead to brain injury. The subarachnoid space is constrained by the skull, and therefore the intracranial pressure rises and may become as high as blood pressure. As a result, the blood supply to the brain is compromised, which leads to ischemic brain injury. Furthermore, there is a rapid degradation of erythrocytes within the cerebrospinal fluid. Many of these breakdown products of blood are toxic to the brain, which may cause further brain injury.[2]
The rupture of an aneurysm, ischemic brain injury and the breakdown products in the subarachnoid space all trigger molecular and cellular pathways, such as the complement system and glia activation.[3]

The complement system is an immune pathway which consists of over 30 components.[4] The pathways can get activated *via* three different routes, all leading to the production of a key component: C3 (Figure 1). From there, cleavage products of C3 activate immune cells. Furthermore, C5 and its cleavage components enhance the immune response. Moreover, it can generate the membrane attack complex, that can damage cells by making pores into cell membrane. This can be beneficial in case of a bacterial infection, but it causes additional damage to brain cells.

> **Figure 1**. **Scheme of the complement system.** The complement system consists of over 30 components that activate after damage or infections. Three initiating pathways, the classical, lectin, and alternative pathway lead to the convertase of C3, the main component of the complement system. From there, a cascade of responses triggers the production of anaphylatoxins C3a and C5a, leading to chemotaxis (recruitment of immune cells) and inflammation. Furthermore, the Membrane Attack Complex is formed, that makes pores into the membrane of cells, inducing cell death.

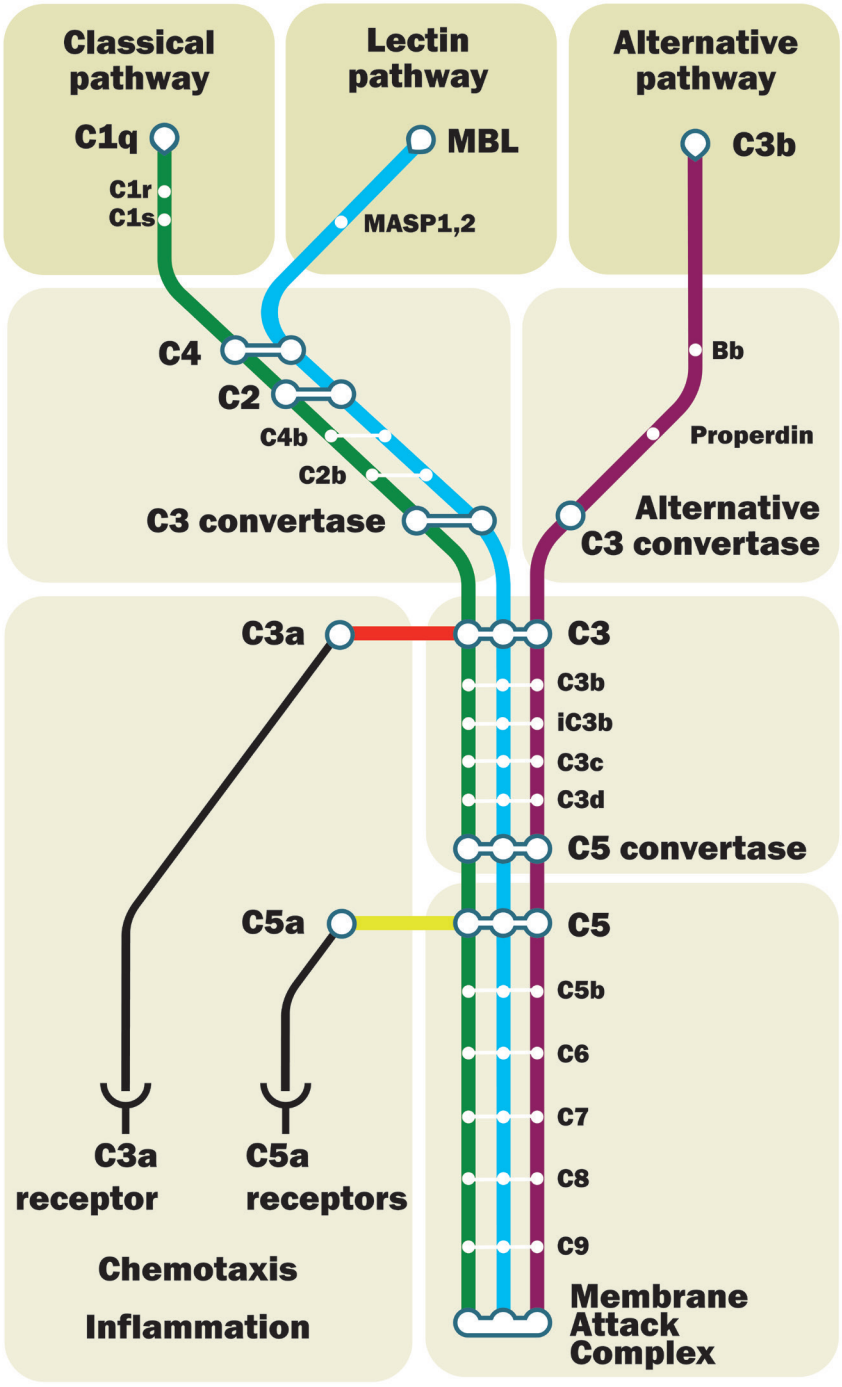
Classical pathway
Lectin pathway
Alternative pathway
C1q
C1r
C1s
MBL
MASP1,2
C3b
C4
C2
C4b
C2b
C3 convertase
Bb
Properdin
Alternative C3 convertase
C3a
C3
C3b
iC3b
C3c
C3d
C5 convertase
C5a
C5
C5b
C6
C7
C8
C9
Membrane Attack Complex
C3a receptor
C5a receptors
Chemotaxis
Inflammation

The activation of immune cells after SAH, in part by the complement system, happens both in the peripheral circulation, and in the brain.[5] In the brain, the immune response is mainly orchestrated by glia. The definition of glia, classically described in the Oxford dictionary as "The connective tissue of the nervous system, consisting of several different types of cell associated with neurons," is much more than that. Whereas neurons simply are conveying electro-chemical signals, glia cells have a long list of functions that support brain functioning. Amongst other functions, they maintain and support the synapse,[6] regulate the number of synapses,[7,8] regulate the blood flow and control energy consumption,[9] and facilitate action potentials through the axon.[10] Therefore, glia are crucial for the functioning of the brain. The main glia cell types in the mammalian brain are astrocytes, microglia, and oligodendrocytes (Figure 2).

> Figure 2. Illustrations of three main glial cells in the mammalian brain, and their main functions. Astrocytes have countless fine processes that make contact with synapses, axonal nodes of Ranvier, glia limitans and blood vessels. By doing so, they keep homeostasis of ions and water, recycle neurotransmitters from synaptic clefts, but also release gliotransmitters themselves. Furthermore, they take up nutrition from blood vessels, while regulating the vessel constriction/dilation. Moreover, they respond to damage to the brain or during a disease process, and becoming immune activated. Microglia, while not immune activated, have long thin motile protrusions that scan the area for damage. Furthermore, these protrusions sense weak synapses, and can eliminate these synapses by pruning. Upon brain damage, their processes become smaller and thicker, ultimately forming an amoeboid cell. They produce cytokines, enhancing the immune response, and phagocytose cell debris. Oligodendrocytes reside in the white matter of the brain where axons of neurons cross the brain. The oligodendrocytes have short processes that enwrap the axons with myelin sheets. They thereby isolate the axons, making action potentials go faster through the axon. Oligodendrocytes also produce trophic factors that support axons.

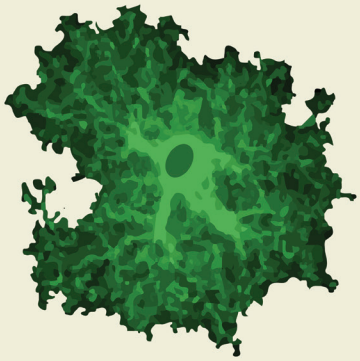

Astrocyte

- Keep ion and water homeostasis
- Regulate synaptic transmission
- Synapse formation, elimination
- Regulate bloodflow
- Gliosis

Microglia

- Developmental cues for axon guidance, myelination
- Synapse formation, elimination
- Immune response, gliosis
- Phagocytosis

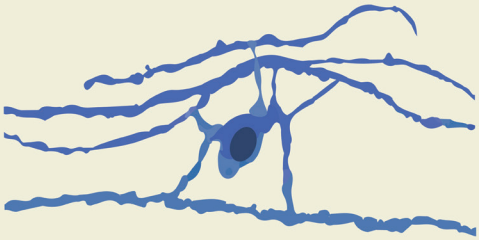

Oligodendrocyte

- Myelination
- Axon support
- Action potential facilitation

In response to damage, glial cells respond by a process called gliosis.[12] Mainly the astrocytes and microglia change their functions upon damage and become immune activated. Gliosis is a spectrum, from mild cytokine production, to a severe form of a glial scar around damaged tissue.[13] The response can be neuroprotective, but, can also further damage the brain.[14] This is partly because the glia do not execute their homeostatic functions anymore, which will lead to brain dysfunction. Furthermore, the production of too many cytokines can be toxic to the environment.[15]
Upon SAH, both complement and the glial response is supposed to reduce the damage inflicted to brain. However, a sustained glia response can enhance the damage of the SAH, thus complement the subarachnoid hemorrhage.

In **chapter 1,** we systematically reviewed the literature on the glial response after SAH until July 2015.[15] In chapter 1, we also give insights into the functional consequences and clinical implications of the glia response. An update is given in the other chapters and in the discussion.

In **chapter 2**, we studied the role of the complement system in the development of brain injury after SAH. We investigated the presence of complement components C1q and C3 in the brain of SAH patients. Furthermore, we studied whether single nucleotide polymorphisms in complement genes are associated with poor functional outcome in patients. Moreover, we measured complement components levels in plasma and cerebrospinal fluid of over time for up to 17 days. In a mouse model for SAH, we studied whether mice lacking C5a receptors have reduced microglia response and reduced neural cell death. Moreover, wildtype mice were treated with an antibody that prevents the cleavage of C5 into C5a and C5b, to investigate the possibilities for therapeutic interventions.

In **chapter 3,** we investigated long-term cognitive outcome of SAH. Many patients who survive SAH have long-term cognitive impairments. Many domains are affected, such as memory and attention. We subjected mice with and without SAH to behavioral tests. We investigated whether the complement/glial response is associated with cognitive impairments.

Is the glial response then only detrimental? In **chapter 4,** we investigated whether the glial response can be beneficial, by having regenerative proper-

ties. The adult brain has neurogenic astrocytes capable to produce newborn neurons.[16] Furthermore, upon damage, glia can start to proliferate, and migrate to the lesion site.[17] We investigated the amount of proliferative neurogenic astrocytes in the neurogenic niches of the mouse brain after SAH.

In the **General Discussion**, we discuss our findings on the complement and glia response after SAH, and their clinical implications. We also give an overview of the SAH and glia articles that were published after our search in July 2015.[15] We also discuss future possibilities for clinical practice to reduce the detrimental properties of gliosis, while stimulating the neuroprotective capabilities.

References

1. van Gijn J, Kerr RS, Rinkel GJ. Subarachnoid haemorrhage. *The Lancet*. 2007;369(9558):306-318. doi:10.1016/S0140-6736(07)60153-6

2. Robinson SR, Dang TN, Dringen R, Bishop GM. Hemin toxicity: a preventable source of brain damage following hemorrhagic stroke. *Redox Rep*. 2009;14(6):228-235. doi:10.1179/135100009X12525712409931

3. Merle NS, Grunenwald A, Rajaratnam H, et al. Intravascular hemolysis activates complement via cell-free heme and heme-loaded microvesicles. *JCI Insight*. 2018;3(12). doi:10.1172/jci.insight.96910

4. Merle NS, Church SE, Fremeaux-Bacchi V, Roumenina LT. Complement System Part I â€“ Molecular Mechanisms of Activation and Regulation. *Front Immunol*. 2015;6. doi:10.3389/fimmu.2015.00262

5. Merle NS, Noe R, Halbwachs-Mecarelli L, Fremeaux-Bacchi V, Roumenina LT. Complement System Part II: Role in Immunity. *Front Immunol*. 2015;6. doi:10.3389/fimmu.2015.00257

6. Allen NJ, Eroglu C. Cell Biology of Astrocyte-Synapse Interactions. *Neuron*. 2017;96(3):697-708. doi:10.1016/j.neuron.2017.09.056

7. Stogsdill JA, Ramirez J, Liu D, et al. Astrocytic neuroligins control astrocyte morphogenesis and synaptogenesis. *Nature*. 2017;551:192.

8. Stephan AH, Barres BA, Stevens B. The Complement System: An Unexpected Role in Synaptic Pruning During Development and Disease. *Annu Rev Neurosci*. 2012;35(1):369-389. doi:10.1146/annurev-neuro-061010-113810

9. Bélanger M, Allaman I, Magistretti PJ. Brain Energy Metabolism: Focus on Astrocyte-Neuron Metabolic Cooperation. *Cell Metab*. 2011;14(6):724-738. doi:10.1016/j.cmet.2011.08.016

10. Michalski J-P, Kothary R. Oligodendrocytes in a Nutshell. *Front Cell Neurosci*. 2015;9. doi:10.3389/fncel.2015.00340

11. Farmer WT, Murai K. Resolving Astrocyte Heterogeneity in the CNS. *Front Cell Neurosci*. 2017;11. doi:10.3389/fncel.2017.00300

12. Burda JE, Sofroniew MV. Reactive Gliosis and the Multicellular Response to CNS Damage and Disease. *Neuron*. 2014;81(2):229-248. doi:10.1016/j.neuron.2013.12.034

13. Pekny M, Pekna M, Messing A, et al. Astrocytes: a central element in neurological diseases. *Acta Neuropathol (Berl)*. 2016;131(3):323-345. doi:10.1007/s00401-015-1513-1

14. Liddelow SA, Barres BA. Reactive Astrocytes: Production, Function, and Therapeutic Potential. *Immunity*. 2017;46(6):957-967. doi:10.1016/j.immuni.2017.06.006

15. van Dijk BJ, Vergouwen MD, Kelfkens MM, Rinkel GJ, Hol EM. Glial cell response after aneurysmal subarachnoid hemorrhage - Functional consequences and clinical implications. *BiochimBiophysActa*. 2016;1862(0006-3002 (Print)):492-505. doi:10.1016/j.bbadis.2015.10.013

16. Magnusson JP, Frisén J. Stars from the darkest night: unlocking the neurogenic potential of astrocytes in different brain regions. *Development*. 2016;143(7):1075-1086. doi:10.1242/dev.133975

17. Saha B, Peron S, Murray K, Jaber M, Gaillard A. Cortical lesion stimulates adult subventricular zone neural progenitor cell proliferation and migration to the site of injury. *Stem Cell Res*. 2013;11(3):965-977. doi:10.1016/j.scr.2013.06.006

CHAPTER 1

Glial cell response after aneurysmal subarachnoid hemorrhage – functional consequences and clinical implications

Bart J. van Dijk[1,2], Mervyn D.I. Vergouwen[2], Myrna M. Kelfkens[1], Gabriel J.E. Rinkel[2] and Elly M. Hol[1,3,4]

1. Department of Translational Neuroscience, Brain Center Rudolf Magnus, University Medical Center Utrecht, 3584 CG Utrecht, The Netherlands;
2. Department of Neurology and Neurosurgery, Brain Center Rudolf Magnus, University Medical Center Utrecht, 3584 CG Utrecht, The Netherlands,
3. Netherlands Institute for Neuroscience, An Institute of the Royal Netherlands Academy of Arts and Sciences, 1105 BA Amsterdam, The Netherlands;
4. Swammerdam Institute for Life Sciences, Center for Neuroscience, University of Amsterdam, 1098 XH Amsterdam, The Netherlands.

Published in Biochim Biophys Acta. 2016 March;1862(3):492-505.

Abstract

Glial cells, both astrocytes and microglia, respond to neurodegenerative processes and to brain damage by a process called reactive gliosis. This response is highly context dependent, varies from mild to severe, and can be protective or detrimental for neural functioning. In patients with a subarachnoid hemorrhage from a ruptured aneurysm, the acute glial response is important to restrict the initial damage. Patients who survive the hemorrhage and early brain injury, often suffer from delayed cerebral ischemia or persisting cognitive impairment. Glia emerge as versatile cells that can modulate synapses and can control the microcirculatory blood flow in the brain. Therefore, a sustained activation of glial cells can affect normal brain functioning. Here we review the current literature on the glial response induced by aneurysmal subarachnoid hemorrhage in humans and in animal models. We discuss how reactive gliosis can affect brain functioning and how it may contribute to early brain injury, delayed cerebral ischemia and cognitive impairment after aneurysmal subarachnoid hemorrhage.

Keywords
Stroke, reactive gliosis, astrocytes, microglia, cognitive impairment, subarachnoid hemorrhage

Abbreviations
ADAMTS-13, a disintegrin and metalloproteinase with a thrombospondin type 1 motif, member 13; AQP1/4, Aquaporin 1/4; BBB, Blood Brain Barrier; BK, Big Potassium; CSD, Cortical Spreading Depression; CSF, cerebrospinal fluid; DCI, delayed cerebral ischemia; EBI, Early Brain Injury; ERK1/2, Extracellular signal-regulated protein kinases 1 and 2; ET-1, Endothelin-1; GABA, γ-aminobutyric acid; GFAP, Glial fibrillary acidic protein; Gln, Glutamine; GLT-1, Glutamate Transporter-1; GSN, Gelsolin; HMGB1, High Mobility Group Box-1; HO-1, Heme-Oxygenase-1; HSP47/70, Heat Shock Protein 47/70; IBA-1, ionized calcium-binding adapter molecule 1; IL-1α/1β/6/8/33, interleukin-1α/1β/6/8/33; iNOS, inducible Nitric Oxide Synthase; KIR4.1, inwardly rectifying potassium channel; LCA, Leukocyte Common Antigen; MAPk, Mitogen activated protein kinase; mGluR5, metabotropic Glutamate Receptor 5; MyD88, myeloid differentiation 88; NFκB, Nuclear Factor κB; Ngb, neuroglobin; OPN, Osteopontin; p-p38MAPK, phosphorylated p38 Mitogen-activated protein kinase; Pk-Cα, Protein Kinase Cα; RAGE, Receptor for Advanced

Glycation End products; SAH, subarachnoid hemorrhage; SENP3, SUMO1/Sentrin/SMT3 Specific Peptidase 3; TGF-β, Transforming Growth Factor β; TLR4, Toll-Like Receptor 4.

1. Introduction

Subarachnoid hemorrhage (SAH) from a ruptured aneurysm is a subtype of stroke that occurs in relatively young patients (median age around 55 years of age) and has high rates of case fatality and morbidity [138]. The most important determinants of poor functional outcome after aneurysmal SAH are Early Brain Injury (EBI) in the first 72 hours after the SAH, rebleeding of the aneurysm, and Delayed Cerebral Ischemia (DCI) 4 to 14 days after ictus. Many survivors, even those with good functional outcome, have cognitive impairment in the long-term. Since the pathogenesis of EBI, DCI and cognitive impairment remains unclear, no effective treatments are available to improve outcome. These data also stress the need to focus on other pathogenic processes that might be involved, such as reactive gliosis.

Reactive gliosis is a broad term, used for the acute response of astrocytes and microglia to a central nervous system injury, but also for the chronic reactivity state of these cells in neurodegenerative diseases. Classically reactive gliosis is seen as a scarring response, but this needs readjustment. Currently, reactive gliosis is recognized as a context dependent spectrum of heterogeneous multi-cellular responses [125]. Recent developments in glia biology have revealed that glial cells are versatile, they control the microcirculatory blood flow in the brain, contribute to synaptic plasticity by pruning and modifying synapses, and are actively involved in neuronal communication. The sustained activation state of astrocytes and microglia, which is a form of mild reactive gliosis after brain damage or during a degenerative disease, emerges as a contributing factor to cognitive decline [11,28,37,42]. Activation of astrocytes and microglia has also been implicated to be involved in vasospasm, microcirculatory vasoconstriction, edema, cortical spreading depression, and neuronal damage after SAH [40,53,120,149]. Therefore, reactive gliosis might be an important cellular process in the development of complications and long-term sequelae after SAH. In recent years, both preclinical and clinical studies have described the activation of glia induced by SAH. Here we review the literature on the glial response after SAH and its potential role in EBI, DCI and cognitive impairment after SAH. We performed a PubMed search on 13-07-2015 with the following search term: ((‘microg-

lia[MeSH Terms]' OR 'microgli*[Title/Abstract]' OR 'astrocytes[MeSH Terms]' OR 'astrogli*[Title/Abstract]' OR 'astrocyt*[Title/Abstract]') AND ('subarachnoid hemorrhage[MeSH Terms]' OR 'subarachnoid haemorrhage[Title/Abstract]' OR 'subarachnoid bleeding[Title/Abstract]')). We included all research articles written in English that investigated an interaction between aneurysmal SAH and glial cells on a cellular and a molecular level *in-vivo* and *ex-vivo*.

2. Subarachnoid hemorrhage

2.1 Subarachnoid hemorrhage: pathophysiology

World-wide the incidence of SAH is 6-7 per 100.000 people per year and the median age it occurs is 55 years [138]. The incidence increases with age and women have a 1.6 times higher risk than men. The case fatality rate is high: about 35% of SAH patients die, including the 10-15% of patients who die before reaching the hospital [84]. Of those who survive, one-third needs lifelong care [130]. SAH is a type of stroke characterized by the extravasation of blood into the subarachnoid space of the brain. SAH can be caused by trauma or occur spontaneously, by the rupture of an aneurysm. In this review we will focus on spontaneous aneurysmal SAH that account for 85% of SAH cases. The prevalence of intracranial aneurysms in the general adult population is approximately 3% [102]. Intracranial aneurysms are usually located at arterial branch points at the base of the brain, mostly at bifurcations at the circle of Willis (figure 1). The most characteristic symptom of aneurysmal SAH is an acute and severe headache or neck pain, which mostly peaks within a few seconds after bleeding. SAH causes an abrupt increase in intracranial pressure, which causes a decrease in blood perfusion pressure. Blood pressure increases to balance the perfusion pressure, however, this is often not sufficient. Accordingly, the brain receives insufficient blood supply to function. Therefore, patients often have a decreased level of consciousness or focal neurological signs. These acute cerebral insults cause the onset of EBI [116].

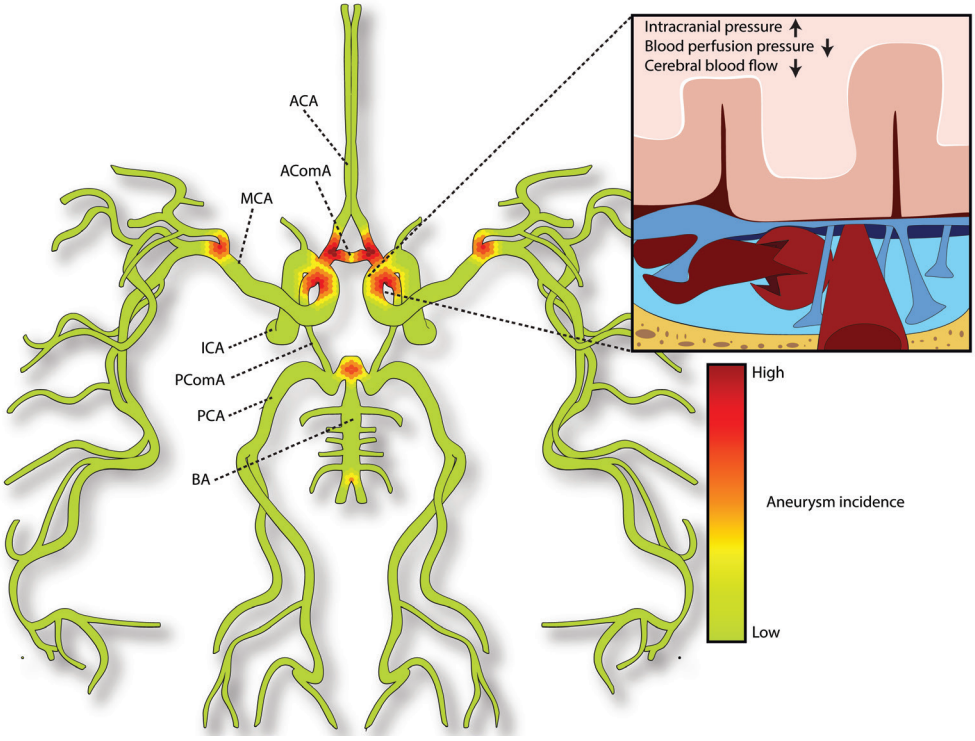

Figure 1. Cerebral arterial vasculature and predilection sites of intracranial aneurysms. Basal view of the brains arteries. Aneurysms arise most frequently at the bifurcation of the anterior communicating artery (AComA), the middle cerebral artery (MCA), the posterior communicating artery (PComA), the basilar artery (BA), and the posterior inferior cerebellar artery (PICA). Insert: In case of a ruptured aneurysm, blood flows into the subarachnoid space, causing increased intracranial pressure, reduced blood perfusion pressure, and reduced cerebral blood flow. Red color in the arteries indicates common locations of aneurysms, green color in the arteries indicates rare locations of aneurysms. ACA, anterior cerebral artery; ICA, Internal carotid artery; PCA, posterior cerebral artery.

2.3 Early brain injury

EBI is supposed to result from increased intracranial pressure, acute hydrocephalus, microvascular alterations, platelet aggregation, acute vasospasm, and reperfusion injury [8,117-119]. SAH also induces an increase in pro-inflammatory cytokines and reactive oxygen species and contributes to cell death of neurons, astrocytes, oligodendrocytes and endothelial cells [116]. Global cerebral edema occurs during the first 24 hours after ictus [20]. Endothelin-1 and nitric oxide can induce microcirculatory vasoconstriction [116],

which occurs in 70% of the arterioles within the first three days after SAH [30]. Moreover, microthrombi occlude arterioles, and are also evident within the first three days [30]. Reactive gliosis is involved in several of the mechanisms contributing to EBI. Their potential role in these mechanisms will be discussed in sections 3 and 4.

2.4 Delayed cerebral ischemia

DCI occurs in about 30% of surviving SAH patients [13,142]. These patients develop uni- or multifocal areas of ischemia, which are not limited to the arterial supply or border zone territories. Clinical symptoms include focal neurological deficits and reduced level of consciousness with a gradual onset. The pathogenesis of DCI is not completely understood. Traditionally, arterial narrowing ('vasospasm') in the circle of Willis was considered to be the cause of DCI, even to such an extent that the term vasospasm was used as a synonym for DCI. Recent studies suggest that this is a too simplistic view [69]. Several factors have now been implicated in DCI pathogenesis, including blood brain barrier (BBB) damage, impaired cerebral autoregulation, neuroinflammation, microvascular spasms, microthrombosis, and cortical spreading depressions [13]. However, none of these processes can induce DCI by itself. The current view is that the pathogenesis of DCI is multifactorial [24,93,141,154]. Since reactive gliosis is involved in several of the described mechanisms, it may be an interesting target for intervention. In this review, we will discuss the role of glia activation in the factors associated with the onset of DCI (see section 3 and 4).

2.5 Cognitive impairment

Cognitive impairment is present in about a third of the surviving SAH patients [1,22,104]. Cognitive domains that are most often affected include visual memory, verbal memory, reaction time, executive function, visuospatial function, and language function [77]. Cognitive impairment can remain for many years after the hemorrhage and reduce quality of life. These cognitive impairments also occur in patients who have made a good physical recovery and have regained independence in daily life. Cognitive impairment after SAH is associated with the severity of the hemorrhage indicated by the state of the patient at hospitalization, older age, fewer years of education, and aneurysms in the anterior circulation [41,60]. We propose that sustained reactive gliosis can contribute to the cognitive impairment after SAH (see paragraphs 5.1 and 5.2).

3. Microglia and their response in SAH

Microglia, the immune cells in the CNS, reside in the parenchyma of the brain where they scan their environment for unwanted infiltrating cells, the presence of aggregated proteins, or injury. Upon activation, they rapidly change to phagocytose any unwanted particles and release pro-inflammation cytokines to facilitate an immune response [50]. In recent years, microglia have been implicated to be more than the immune cells of the brain. Besides the pro-inflammatory response, microglia also possess neuroprotective properties, helping to restore the brain after injury [83]. Furthermore, in the healthy brain, microglia are never resting [85]. They have a ramified morphology with long processes that interact with both neurons and astrocytes. In the quadripartite synapse (consisting of the neuronal presynaptic terminal, the postsynaptic dendritic spine, the perisynaptic astrocyte processes, and microglial processes), microglia are actively involved in modulating neuronal circuitry [112]. They eliminate synapses by phagocytosis of complement component C1q and C3 positive synapses [129]. Moreover, microglia respond to neurotransmitters, which changes their activity [29]. Contrary to the elimination of synapses, microglia are also regulating the maturation of synapses [92,103]. Finally, microglia are involved in neurogenesis in the hippocampus [31].

3.1 Inflammatory response

Microglia respond to SAH in several ways. The cellular and molecular changes in microglia after SAH are summarized in table 1 and figure 2. They turn into activated microglia having a morphology with shorter processes [96], suggesting a phenotype that is associated with macrophage-like cells [124,148]. Microglial response described in human SAH studies is very limited. The phagocytic marker CD68 expression has been investigated in human post mortem tissue samples [115]. CD68 positive microglia are increased between 5 to 15 days after ictus in patients with SAH [115]. Furthermore, several neuroprotective (Interleukin (IL)-10) and pro-inflammatory cytokines (IL-1β, IL-6, IL-8, TNFα) are all increased after 7 days in the cerebrospinal fluid (CSF) of patients [114]. However, the majority of studies investigating the microglial response is performed in animal models (for references see table 1 and box 1). Microglia start a sustained expression of pro-inflammatory cytokines [115,121]. The pro-inflammatory cytokine and transcription factor high-mobility group box 1 protein (HMGB1) is upregulated in microglia, in the parenchyma of the brainstem, the hippocampus and the cortex [82,132].

This suggests that the activation of microglia is diffuse, causing a systemic response in the brain. HMGB1 expression contributes to brain injury as it further activates other microglia to express IL-1β and Toll-like receptor 4 (TLR4). Indeed, TLR4 is abundantly expressed by microglia after SAH [63,157], but this could also be triggered by the blood metabolite methemoglobin [63]. Since in TLR4 knock out mice the occurrence of vasospasm and neuronal death is reduced, it is conceivable that microglial activation contributes to these SAH induced processes [40]. The expression of receptor for advanced glycation (RAGE) and myeloid differentiation 88 (MyD88) is upregulated in microglia after SAH. Both proteins are associated with the pro-inflammation response [65,131]. Major cytokines in this response are microglia-derived Tumor Necrosis Factor alpha (TNF-α), IL-1β, IL-6, and IL-8 [115]. These cytokines contribute to apoptosis in neurons [43]. The upregulation of IL-33 after SAH in neurons and astrocytes is positively associated with secretion of IL-1 by microglia [33,47]. This suggests that microglia activate astrocytes in SAH. Ablation of microglia, by ganciclovir activation of a suicide gene (HSVTK) driven by the CD11b promotor, results in a significant reduction of apoptotic neurons after SAH [115]. Activated microglia contribute to neuronal damage after SAH, but it requires further investigation whether this is an acute or a sustained response.

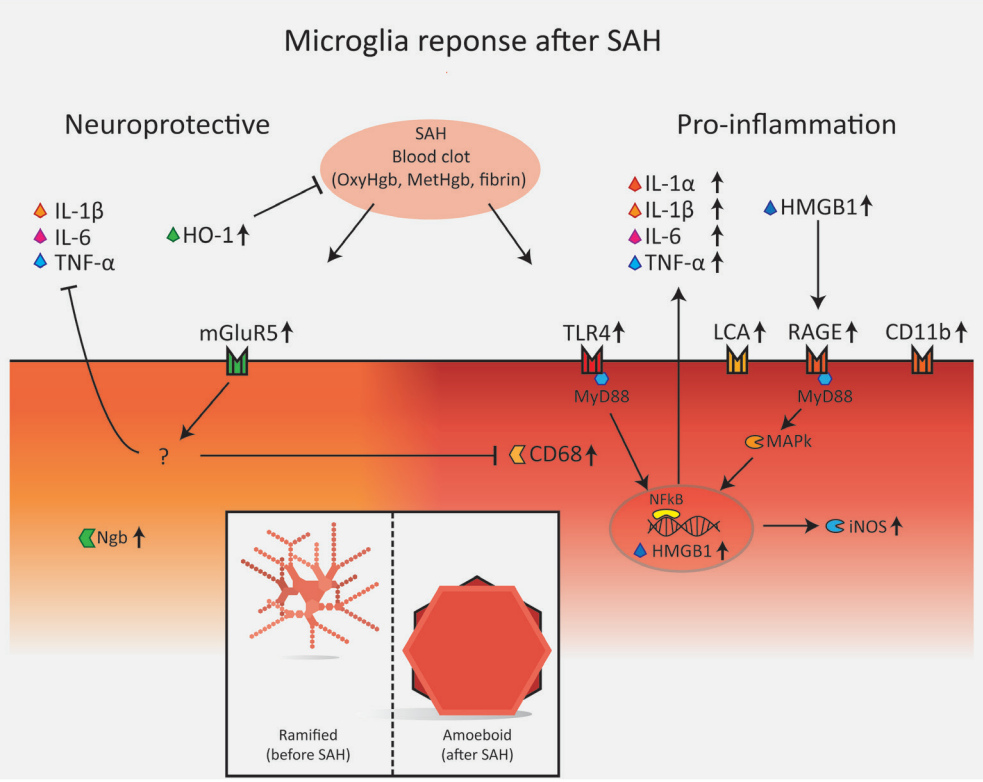

Figure 2. Current knowledge of the changes in microglia after SAH. In the non-injured brain quiescent microglia have a ramified morphology. The motile microglia processes are in close contact with synapses and astrocyte processes and scan the brain parenchyma for injured cells, possible intruders, and danger signals. SAH leads to a response in microglia to the brain injury and to the blood clot. In brain areas where these cells are triggered to phagocytose injured cells, they adapt an amoeboid morphology, and the microglia will highly express the phagocytic marker CD68. The microglia start expressing neuroprotective cytokines or can engage in a pro-inflammatory response. These are two extremes of a spectrum, and it is likely that several microglia with in-between phenotypes can be found in brain tissue after SAH. HO-1 helps with clearance of the blood clot. HMGB1, High Mobility Group Box-1; HO-1, Heme-Oxygenase-1; HSP47/70, Heat Shock Protein 47/70; IL-1α/1β/6/8, interleukin-1α/1β/6/8; iNOS, inducible Nitric Oxide Synthase; LCA, Leukocyte Common Antigen; MAPk, Mitogen activated protein kinase; MetHb, Methemoglobin; mGluR5, metabotropic Glutamate Receptor 5; myD88, myeloid differentiation 88; Ngb, neuroglobin; NFkB, Nuclear Factor κB; OxyHb, Oxyhemoglobin; RAGE, Receptor for Advanced Glycation End products; SAH, subarachnoid hemorrhage; TLR4, Toll-Like Receptor 4; TNF-α, Tumor Necrosis Factor-α.

3.2 Neuroprotective properties

The activation of microglia also leads to the expression of several neuroprotective proteins (figure 2). Microglia upregulate the metabotropic Glutamate Receptor 5 (mGluR5) after SAH in rats. Treatment with mGluR5 agonists limits brain injury by reducing the production of pro-inflammatory cytokines, subsequently reducing neuronal apoptosis and reduced edema [158]. The mechanism by which mGluR5 activation reduces the inflammatory response is still unknown. SAH activated microglia also express neuroglobin (Ngb), which protects neurons by reducing oxidative stress [66]. Another neuroprotective factor that is upregulated in microglia is heme-oxygenase (HO), which is induced by the presence of heme in the subarachnoid space. HO-1 is a stress response protein that metabolizes heme into biliverdin, Fe^{2+}, and carbon monoxide (CO). Microglial HO production is not only elevated in the vicinity of the hemorrhage, but also throughout the brain [75]. That HO-expression is neuroprotective was clearly shown in a study in which HO-1 expression in microglia was knocked out. SAH in these mice led to impaired phagocytosis, increased blood clot volume, increased neuronal injury, and cognitive impairment, as observed by a decrease in spatial memory [114].

3.3 Complement components

The complement system is involved in the initial inflammation reaction after SAH [70]. Complement components, such as C3a and C5a are upregulated after SAH and CSF levels of these complement components have been correlated to functional outcome [49,71,89]. In addition, the microglial C3 receptor CD11b/CD18 is activated by fibrin, a coagulation factor involved in the formation of (micro)thrombi [21,105]. Fibrin is found diffusely in the brain of SAH patients [141]. The expression of the C1q and C3 receptors is involved in pruning of synapses during development [128]. This complement activated pruning can also occur after brain injury and can be induced by activation of microglia by LPS in adult mouse brains [57]. SAH causes loss of synapses in rats and complement factors are increased, thus suggesting a potential involvement of microglial pruning [39]. As microglia remain activated for several weeks after SAH, excessive pruning by activated microglia may therefore cause disruption in neuronal circuitry and may be detrimental for cognitive functions. In the complement cascade, C5 is cleaved into C5a and C5b. C5a causes smooth muscle contraction, suggesting a role in vasospasm. C5b forms, together with C6 to C9, the complement membrane attack complex (MAC), which causes cell death by dysregulation of the membrane of

the cell. In SAH, MAC is upregulated 3 days after ictus, causing brain edema [156]. Taken together, activation of the complement cascade after SAH potentially has a detrimental effect on the brain and might be involved in the pathogenesis of both DCI and cognitive impairment.

3.4 The origin of the activated microglia cells

The initial immune response of infiltrating leukocytes is an important aspect of the pathogenic response after and SAH. Upon rupture of an aneurysm, blood flows into the subarachnoid space, which is normally filled with cerebrospinal fluid. Hemoglobin from erythrolysis initiates an inflammatory response that activates endothelial cells of cerebral arteries to produce cell adhesion molecules, in particular endothelial (E)-selectin. Interaction of E-selectins and monocytes allows for the infiltration of these cells to blood in the subarachnoid space. Macrophages then remove the debris from the CSF and are actively involved in the initial inflammation response [18,81]. Iba-1 expression is increased in the brain, suggesting an increase of Iba-1 positive cells, either by proliferation or migration in the brain [82]. Thus, the increase in Iba-1, CD68 and CD11b positive cells after SAH might both reflect the proliferation of microglia in situ, but also the recruitment of peripheral macrophages, as these markers express in both cell types. In a recent study, it was shown that the majority of the Iba-1/CD68/CD11b positive cells in the parenchymal brain tissue are microglia and not infiltrated peripheral monocytes [115]. The increase in Iba-1 positive cells is therefore likely a result of microglial proliferation. Although monocytes play a role in the initial inflammation after SAH, microglia remain activated for a prolonged period, potentially causing long-term sequelae.

4. Astrocytes and their response in SAH

Astrocytes are present in all regions of the CNS [126]. Astrocytes make numerous contacts with blood vessels through their perivascular endfeet. In addition, astrocytes contact neurons on either their cell bodies, synapses or the axons [3]. With their thin processes, they closely enwrap synapses, forming the tripartite synapse [4]. A single astrocyte in rodents can contact about 100,000 synapses, and human astrocytes even up to 2 million [86]. Astrocytes are connected to each other with gap junctions, through which cell signaling molecules can be propagated, causing Ca^{2+} waves and enabling astrocytes to communicate with each other [37].

Astrocytes perform several functions in healthy CNS. First, they influence the microvasculature by regulating vessel contraction with their endfeet that are close to the pericytes in the neurovascular unit [5]. The endfeet take up glucose, and release vasodilating and vasoconstricting factors. They do so in combination with keeping a balanced K^+ concentration and by the production of arachidonic acid metabolites EET, lactate, PGE_2, or 20HETE [72]. As a result, astrocytes contribute to the regulation of microvascular blood flow. As astrocytes are also in contact with neurons, they are perfectly positioned to regulate blood flow according to local neuronal activity and metabolic demands. Astrocytic endfeet are close to the BBB, which is formed by endothelial cells and pericytes. The endothelial cells form tight junctions and are surrounded by a basal lamina. The BBB restricts the diffusion of molecules from the systemic circulation into the brain tissue. The astrocytes are important in the induction of barrier properties in cerebral endothelium [126]. Finally, astrocytes have multiple homeostatic functions in the brain [143], they express the water channel aquaporin 4 (AQP4) and transporters for K^+ and H^+, in order to regulate the ion, pH, and fluid balance. Astrocytes also control the level of neurotransmitters, as they clear the neurotransmitters glutamate, gamma-aminobutyric acid (GABA), and glycine from the synaptic cleft via transporters. The astrocyte specific enzyme glutamine synthetase converts the glutamate taken up from the synaptic cleft into glutamine, which is then transported back to neurons where it is used to form *de novo* glutamate and GABA [143]. In addition to maintaining homeostasis in the synapse, astrocytes have also been shown to actively modulate synaptic transmission by releasing gliotransmitters, such as glutamate, adenosine triphosphate (ATP), adenosine, GABA, and D-serine. This release occurs in response to synaptic activity and can lead to either an increase or decrease in neuronal activity. In this way, astrocytes contribute directly to neurotransmission [4]. However, there is still some controversy surrounding the involvement of astrocytes in synaptic transmission [123].

4.1 Astrocytes – reactive gliosis

Astrocytes respond to a chronic degenerative disease or to acute brain injury by becoming reactive. The reactive astrocytes are part of a multicellular response, which is collectively called reactive gliosis. It is important to describe the exact nature of this response in the disease context, as it has many faces [16]. After acute brain injury, astrocytes form a scar around the damaged area, which provides a barrier between the injured and healthy

brain tissue [125]. On the other end of the spectrum, a chronic response of astrocytes will affect neuronal functioning, as they upregulate immune genes and downregulate neuron support genes [88]. Clearly, the function of astrocytes changes when they become reactive, although the exact nature of this change is not fully known yet and is most likely disease dependent [88]. For example, astrocytes respond differently to inflammation and to stroke [155]. A major problem in any type of brain injury is neuronal cell death. The astrocytic response to brain injury can have both positive and negative consequences on neuron survival [17,26]. It is likely that activation of distinct pathways lead to beneficial or detrimental consequences [12,45,87]. After SAH, the astrocytic pathways leading to either neural protection or to the death of neurons have not yet been elucidated. However, in SAH, the robustness of initial response of the astrocytes seems to correlate with the severity of the hemorrhage [59]. Several SAH induced changes in the expression of astrocyte genes have been reported and are summarized in table 2. Most of these changes can lead to functional consequences in the astrocytic perivascular endfeet and the perisynaptic processes, as summarized in figure 3.

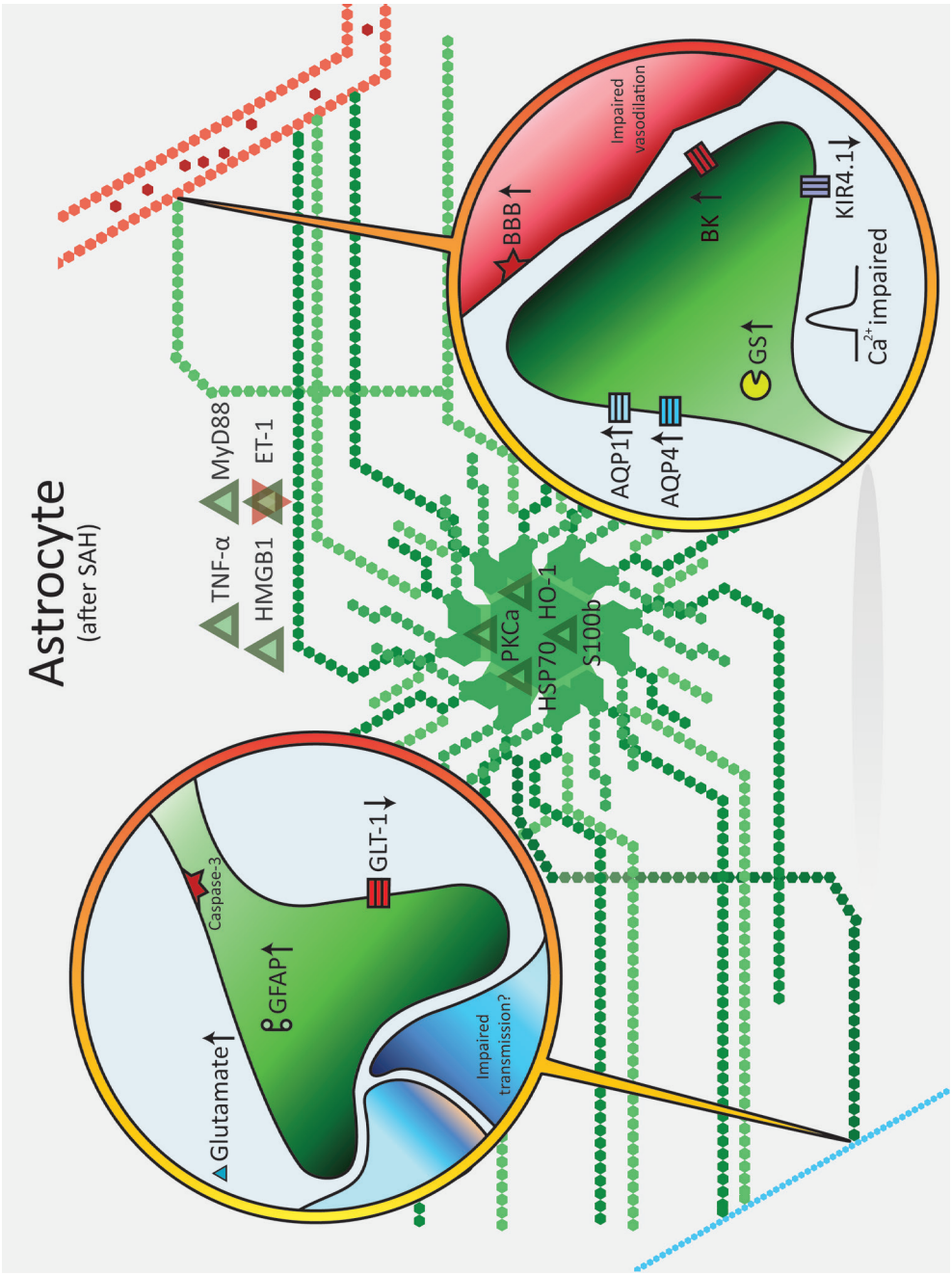
Astrocyte
(after SAH)
TNF-α
MyD88
HMGB1
ET-1
PKCa
HO-1
HSP70
S100b
Glutamate
GFAP
Caspase-3
GLT-1
Impaired transmission?
BBB
Impaired vasodilation
AQP1
AQP4
GS
BK
KIR4.1
Ca2+ impaired

< Figure 3. Current knowledge of the molecular and cellular changes in astrocytes after SAH. At the perivascular end feet, SAH causes inversed neurovascular coupling and edema. At the perisynaptic processes, glutamate clearance is decreased, possibly causing impaired synaptic transmission. Triangles up at the soma represent increased levels, triangle down represents reduced levels of the indicated mRNAs or proteins. AQP1/4, Aquaporin 1/4; BBB, Blood Brain Barrier; BK, Large conductance potassium channels; Caspase-3, cleaved Caspase 3, apoptosis marker; ET-1, Endothelin-1; GFAP, Glial fibrillary acidic protein; GS, Glutamine Synthetase; GLT-1, Glutamate Transporter-1; HMGB1, High Mobility Group Box-1; HO-1, Heme-Oxygenase-1; HSP70, Heat Shock Protein 70; KIR4.1, inwardly rectifying potassium channel; MyD88, myeloid differentiation 88; NFκB, Nuclear Factor κB; Pk-Cα, Protein Kinase Cα; TNF-α, Tumor Necrosis Factor-α.

Glial fibrillary acidic protein (GFAP) is an astrocyte specific intermediate filament protein that is highly upregulated in reactive astrocytes after SAH [67,82,99,133,152,153]. Increased GFAP expression is more evident at the site of the hemorrhage, but an increase is also observed in scattered astrocytes further away from the insult area. This is likely to occur through release of platelet-derived growth factor (PDGF) by platelets present in the blood clot, which diffuses into the brain parenchyma [153]. Astrocytes start to express HO-1 and Heat Shock Protein 70 (HSP70) after SAH [136]. The upregulation of HO-1 is spread over the brain, further indicating that the astrocyte response is not only close to the bleeding but is diffuse throughout the grey matter. Furthermore, reactive oxygen species (ROS) can be formed from oxyhemoglobin in the extravasated blood, and this can also lead to a response in astrocytes [73]. Reactive astrocytes, based on an increased GFAP expression, are also found in areas more distally from the bleeding, suggesting that the blood clot is not the only factor that activates astrocytes. Another trigger can be the acute reduction in cerebral blood flow that follows SAH. This leads to ischemia, which in turn can lead to a response in astrocytes to compensate for the lack of energy resulting in gliosis [100]. Furthermore, SAH leads to an increase in fibrin in the brain's capillaries where it is involved in microthrombosis. Fibrin binds to astrocytes and can induce glial scar formation through the Transforming Growth Factor β (TGF-β)/Smad signaling pathway [111]. This response is also likely to occur at the microscale around capillaries with thrombi.

4.2 Inflammatory response

Astrocytes contribute to the inflammatory response, as they, just as microglia do, start to produce the pro-inflammatory cytokine TNF-α after SAH [73].

Moreover, in an *in-vitro* model it has been shown that exposing cultured astrocytes to oxyhemoglobin induces the expression of pro-inflammatory cytokines TNF-α, IL-1β, IL-6 and matrix metallopeptidase 9 (MMP9) [91]. Furthermore, MyD88, which is expressed in astrocytes after SAH, can regulate the inflammatory response [6,131]. In addition, IL-33 is upregulated in astrocytes, which is associated with an increase in the secretion of IL-1 by microglia [33,47]. Taken together, there are indications that astrocytes are involved in the inflammatory response after SAH.

4.3 Neurotoxicity

Glutamate toxicity is a common phenomenon after SAH [67,158]. In physiological conditions, astrocytes clear intracellular glutamate through glutamate transporters and metabolize extensive glutamate into glutamine with the use of glutamine synthetase. One of the causes of glutamate toxicity is that in reactive astrocytes, the glutamate transporter 1 (GLT-1; EAAT2) is downregulated and thus is less able to clear glutamate from the synaptic cleft [27,61,67]. Indeed, GLT-1 is also downregulated after SAH and this can contribute to the neuronal damage [9,158]. In astrocytes, glutamine synthetase metabolizes glutamate into glutamine, a substrate that is used in neurons to produce glutamate and GABA. In humans, microdialysis after SAH revealed failing glutamine synthesis during energy crisis, presumably caused by ischemic events. Failing glutamine synthesis results in high interstitial glutamate concentration [108-110]. Another possibility of increased glutamate levels is the release of glutamate by blood platelets, as seen after SAH [9]. Platelets are activated in the process of microthrombi formation and are a source of glutamate that can exceed a local extracellular concentration of 300 μM that can be toxic to neurons [9]. When astrocytes are unable to clear the increased levels of glutamate because of the downregulation of glutamate transporters, it may lead to glutamate toxicity after SAH.

4.4 Edema, vasospasm and BBB breakdown

Edema is a severe complication after SAH [20]. Astrocytes regulate the water homeostasis of the brain by aquaporin-1 (AQP1) and aquaporin-4 (AQP4) [90,122]. In SAH patients, both AQP1 and AQP4 are upregulated [7]. Following SAH in a rat, the gene expression of AQP4 is increased and of the inwardly rectifying potassium channels KIR 4.1 is decreased at the astrocytic perivascular endfeet [149]. Astrocytes swell due to the impaired AQP4 and KIR4.1 channel expression by the increasing uptake of water, which can lead

to cytotoxic edema [149].
Vasospasm of the major intracranial arteries may occur within 3 days after SAH but peaks at day 6 to 8 [69]. Endothelin-1 (ET-1) is a protein that is associated with vasospasm [147]. It enables the endothelial cells to upregulate adhesion molecules on their membrane by which they interact with leukocytes. After SAH, ET-1 is also expressed in astrocytes and its expression is associated with worse outcome in mice [152]. Targeted overexpression of ET-1 in astrocytes leads to more vasospasm and mortality in experimental SAH. The astrocytic ET-1 can bind to two receptors, ET-R-a and ET-R-b1. After SAH, ET-R-a expression is increased, leading to an increase in PKC-α levels, causing disruption of K^+ channels [152,153]. This leads to vasoconstriction and may contribute to DCI. However, DCI can also develop without vasospasm and vasospasm not always leads to DCI [101]. Moreover, the use of ET-1 receptor antagonists in clinical trials reduced the risk of vasospasm but did not affect DCI and functional outcome [139], which implies that the pathogenesis of DCI is multifactorial.
Astrocytes cover the microvasculature with the endfeet. Reactive astrocytes start to express osteopontin three days after SAH, which is known to reduce BBB breakdown. Therefore, reactive astrocytes seem to protect the BBB after SAH [133], although more evidence is needed to be able to draw this conclusion.

4.5 Microcirculatory vasoconstriction
Together with the astrocytic ET-1 expression after SAH and its associated vasospasm in basal arteries, astrogliosis after SAH can also have a persistent effect on the regulation of microcirculatory blood flow. SAH leads to a dysregulation of several ion channels on astrocytic endfeet, which results in vasoconstriction [53]. The change in the astrocytic K^+ channel (KIR4.1) not only has an effect on the water balance, but also leads to reversed neurovascular coupling due to the impaired K^+ balance at the perivascular space [53]. Astrocytes react to neuronal activity by adjusting the K^+ concentrations in the perivascular space. There, K^+ affects smooth muscle cells constriction because of a depolarizing shift in the K^+ equilibrium potential and activation of voltage-dependent Ca^{2+} channels on the smooth muscle cells. This leads to dilation or constriction of arterioles, dependent on the perivascular K^+ concentrations. In SAH, K^+ homeostasis is impaired, likely caused by impaired astrocytic intracellular Ca^{2+} signaling and their associated response on Ca^{2+} activated Big Potassium (BK) channels [53]. During physiological conditions,

neuronal activity leads to dilation of the arterioles, providing more nutrition. After SAH, it leads to vasoconstriction. Whereas active neurons need more nutrition, vasoconstriction after neuronal activity leads to ischemia. Although the exact mechanism leading to reverse neurovascular coupling is not clear, it has been shown that Ca^{2+}-permeable Transient Receptor Potential Vanilloid 4 (TRPV4) channels at the astrocytic endfeet are not responsible for the impaired Ca^{2+} oscillations and inversion of neurovascular coupling after SAH [56]. In conclusion, through the mechanism of inversed neurovascular coupling, activated astrocytes can cause reduced blood flow, resulting in impaired nutrition delivery and ischemia after SAH.

4.6 Cortical Spreading Depression

Cortical Spreading depression (CSD) starts when a minimum critical volume of brain tissue is simultaneously depolarized. This leads to prolonged suppression of neuronal activity. CSD is well described after SAH in both animal models as well as in humans [23,24,94,146]. Astrocytes are key players in the onset of CSD and therefore reactive astrocytes could potentially be involved in CSD after SAH [55,95]. Impaired K^+ and glutamate clearance by astrocytes cause propagation of the spreading depolarization. Extracellular K^+ and glutamate depolarize neurons, causing more K^+ and glutamate excretion in neighboring neurons and SD slowly propagates in grey matter. As discussed above, both glutamate and K^+ concentrations are increased in SAH, due to changes in ion channels at the perivascular endfeet of astrocytes and therefore this may contribute to the onset of CSD [53,55]. Moreover, AQP4 regulates the frequency and velocity of CSD [151] and AQP4 expression is also increased after SAH. ET-1 is also implicated to induce CSD [48]. As described above, astrocytic production of ET-1 is upregulated after SAH. In addition, ET-1 induces Ca^{2+} responses in the processes of astrocytes by activation of Gq protein–coupled endothelin receptors [127]. These Ca^{2+} responses may result in many processes, including propagation through gap junctions, leading to Ca^{2+} oscillations, impaired K^+ balance and the release gliotransmitters [51]. In conclusion, these changes in expression in astrocytes may lead to more CSD events after SAH.

5. Contribution of the glial response to cognitive impairment after SAH

Evidence is emerging that both microglia activation and reactive astrocytes can affect neuronal communication, and therefore can contribute to cognitive impairment.

5.1 Microglia

Microglia are actively involved in the maintenance of the neuronal circuitry, both in the healthy and diseased brain [113]. Activated microglia release many pro-inflammatory cytokines, which can induce apoptosis in neurons. This leads to an impairment of the neuronal circuitry and can contribute to a decline in cognitive functions. With their processes, the microglia monitor their environment and interact with synapses and other cellular compartments. The pruning of neuronal dendritic spines by microglia is induced by astrocytic release of TGF-β, which results in an increase of the complement component C1q on the plasma membrane of synapses [10,129]. The surveilling microglia interact with these C1q positive synapses with the complement receptors present on their processes. Microglial contact modulates the size of the synapses, thus altering the neuronal circuitry [135]. By doing so, the microglia participate in the quadripartite synapse [112]. The microglia-related pruning of synapses is an active process during development in the healthy brain, however, it is also implicated to occur in neurodegenerative diseases, such as Multiple Sclerosis [79]. Excessive pruning of synapses can be a pathological process and may impair neuronal circuitry, thereby affecting memory and other cognitive functions. Whether excessive pruning by microglia occurs in SAH brains is unknown. However, SAH can cause a loss of synapses, without detectable neuronal loss [39]. This suggests that synapses are actively eliminated. Furthermore, SAH causes complement cascade activation [49,71,89]. Taken together, these data suggest a possible role for microglia in the elimination of synapses after SAH. This process could contribute to cognitive impairment after SAH.

5.2 Astrocytes

Astrocytes have been implicated to modulate the synapse in several ways. Astrocytes are involved in the elimination of synapses with the use of MEGF10 and MERTK phagocytic pathways [19]. Moreover, astrocytes are part of the tripartite synapse and as such can modulate synaptic transmission [4]. Astrocytes can respond to synaptic released neurotransmitters such as cannabinoids, which are involved in long-term depression in synapses, and alter working memory in mice [38]. Astrocytes can also regulate synaptic plasticity by the release of the gliotransmitters D-serine, glutamate, ATP/adenosine, and γ-amino-butyric acid (GABA) [38,44,64]. It remains to be investigated whether SAH alters these modulatory capacities of astrocytes. However, SAH causes a decrease in GLT-1 and KIR4.1, leading to excitotoxicity and changes

in neurovascular coupling (see also section 4). Moreover, astrocytes respond differently to electrical field stimulation after SAH [53,109,152]. Disruption of Ca^{2+} balance causes impaired synaptic transmission [52]. Endothelin-1, abundantly expressed after SAH, causes Ca^{2+} waves in astrocytic microdomains [127,152]. Ca^{2+} is an important second messenger for many astrocytic processes, including the release of gliotransmitters. In Huntington disease, decreased KIR4.1 expression in astrocytes contributes to neuronal dysfunctions [134], and it is conceivable that the decreased KIR4.1 expression after SAH can also contribute to cognitive impairment. Finally, glutamine synthetase is downregulated during energy crisis after SAH. Failing glutamine synthesis results in high interstitial glutamate concentration [108-110]. Furthermore, it results in reduced glutamine in neurons, leading to reduced glutamate and GABA production and affects neuronal signaling [2]. These changes in astrocyte response may thus have an impact on the synaptic transmission.
Taken together, the response of astrocytes induced by SAH can have a detrimental effect on normal brain functioning, and may contribute to cognitive impairment after SAH. Therapeutic intervention targeting reactive astrocytes may help to prevent cognitive impairment after SAH. Several of these therapeutics have been proposed in preclinical studies and are discussed below.

5.3 Therapeutic intervention

Recovery after aneurysmal SAH is a long and highly variable process. Patients often continue to recover over months to years after SAH, but some patients fail to improve [32,145]. Presently, rehabilitation is the only treatment to stimulate recovery after SAH. Despite rehabilitation, many survivors are left cognitively impaired. Rehabilitation focuses on adaptation to cognitive impairment, but does not reduce the underlying brain injury. There is a high need for new therapies that improve cognitive recovery in the long-term. As described above, glia response may affect neuronal circuitry and may contribute to cognitive impairment after SAH. Therapeutic intervention or suppression of the glial response may therefore help to prevent cognitive impairment. Several therapeutics have been implicated to prevent or suppress glial response. The adenosine A3R agonist, 2-chloro-N^6-(3-iodobenzyl)-adenosine-5'-N-methyluronamide (CL-IB-MECA) reduces microglia activation and its production of pro-inflammation cytokines TNF-α and IL-1β [68]. The statin rosuvastatin reduces superoxide production, nuclear factor-kappa B (NF-κB) activation, and the increase in activated microglial cells after SAH. This leads to reduced neuronal death and reduced BBB breakdown [137]. Similar effects

have been found for Heparin and Apigenin [121,157]. In a preclinical study, recombinant ADAMTS-13 decreases microthrombosis and an attenuated microglia response in knock out mice of the same protein [140]. Opposed to the reduction of the inflammatory response, stimulating the neuroprotective properties of microglia might also be beneficial for the outcome of SAH. For example, mGluR5 agonists (RS)-2-chloro-5-hydroxyphenylglycine (CHPG) and the mGluR5 positive allosteric modulator N-Cyclobutyl-6-[2-(3-fluorophenyl)ethynyl]-3-pyridinecarboxamide hydrochloride (VU0360172) reduce microglial production of pro-inflammatory cytokines IL-1β, IL-6 and TNF-α after SAH, resulting in reduced neuronal damage [158]. Preventing detrimental effects of reactive astrocytes is also possible. Baicalein attenuates glutamate toxicity by preserving GLT-1 expression in astrocytes [61]. Ceftriaxone and Rosiglitazone cause a similar effect [27,67]. Furthermore, pifithrin-α inhibits the transcription factor P53, which is associated with astrocyte reactivity [107]. Treatment with pifithrin-α after SAH results in recovered KIR4.1 and AQP4 expression in astrocytes and reduces edema [149]. The attenuation of brain damage after preventing or suppressing the response of microglia and astrocytes suggests a potential therapeutic window for treatment, to prevent the devastating complications after SAH.

6. Discussion and future directions

SAH is a severe medical emergency that often causes profound brain injury, both shortly after the hemorrhage (EBI), or at a later stage (DCI). Both microglia and astrocytes respond to the acute cerebral injury induced by SAH. Microglia start to produces inflammatory factors and can change into phagocytic-like cells [40,96]. Astrocytes become reactive [82], as shown by an increase in the expression of the cytoskeletal intermediate filament proteins [46,80]. The SAH induced glia response, together with the initial infiltration of peripheral immune cells and the release of blood coagulation factors, might be an important modulator in the pathogenesis of EBI, DCI, and cognitive impairment. As glia are intrinsically associated with neuroprotective capabilities, they are also potential targets for therapeutic interventions [15,52]. The number of studies describing the glial response in SAH patients is very limited. Microglial CD68 expression is increased in human post mortem brain samples [115], suggesting that these microglia are phagocytosing cell debris. However, this can also imply that these active microglia are pathologically pruning synapses, leading to a decline in neuronal functioning. Astrocytes respond to SAH by a change in glutamate metabolism, and an increase in AQP1

and AQP4. Furthermore, spreading depolarization has been associated with reactive astrocytes after SAH [7,24,109]. This suggests a role for astrocytes in the development of edema and glutamate toxicity after SAH in humans. In SAH animal models, sustained glia reactivity is observed, and this chronic response is likely to occur in SAH patients as well. Thus, both activated microglia and reactive astrocytes can potentially contribute to EBI, DCI and cognitive impairment after SAH.

Although most factors that contribute to the development of both early and delayed injury after SAH overlap, there is a clear distinction in the timing of EBI and DCI. In the first three days after SAH, EBI causes damage to the brain. Thereafter, even in patients without apparent neurological deficits during the first few days, DCI can occur. As described above, glia activation might contribute to most factors associated with EBI and DCI (section 3 and 4). Glia cells are activated from hours to up to at least 28 days after SAH (see table 1 and 2). However, studies investigating reactive gliosis and microglia activation longitudinally are very limited, and studies including time points after 28 days have not been reported. Recently, CD68 positive microglia were found to be increased, peaking at 5 to 15 days after SAH in humans [115]. This indicates that in humans, microglia are predominantly activated during the period in which DCI occurs. However, more research is needed to link glial contribution to either EBI or DCI.
To determine whether the glia response is causally related to cognitive impairment, it is required to perform long-term follow-up studies in animal models. Presently, most studies investigating molecular, cellular, and behavioral changes after SAH only consider a relatively short period after the induction of the hemorrhage. The activation of microglia is present up to 28 days and reactive astrocytes are observed to be present up to 21 days after SAH, as summarized in tables 1 and 2 [59,115]. However, it is unknown whether this activation sustains for a longer time. Glia activation starts within hours after the hemorrhage, causing both neuroprotective and detrimental effects. The neuroprotective effects of activated glia seem to only occur in the first few days after the hemorrhage, while the detrimental effect continues to be present for a longer period [115,158]. This chronic and detrimental glia activation is likely to be involved in the cognitive impairment. However, it remains to be elucidated whether the neuroprotective effects are lost after the first few days after the hemorrhage.

Conclusion

We gave an overview of the response of microglia and astrocytes induced by SAH. The initial glia activation is triggered by blood metabolites, such as oxyhemoglobin and methemoglobin, and coagulation factors, such as fibrin. This leads to a cascade of events including the production of pro-inflammatory cytokines by infiltrating monocytes and activated microglia, impaired blood flow regulation, edema, BBB breakdown, neuro-axonal damage and apoptosis, vasospasm, spreading depolarization, and increased glutamate levels. The glia response is not only detrimental, as the production of HO-1 and neuroglobin by microglia are neuroprotective, reducing brain damage and preventing cognitive impairment. Astrocytic osteopontin helps reducing BBB breakdown. There appears to be a temporal therapeutic window during which adequate treatment that enhances the protective effects and reduces the detrimental effect of activated glia could help to reduce the damage following SAH. Indeed, preclinical studies show that therapeutics targeting the glia response have great potential in reducing neuronal damage and cognitive impairment. Targeting the glia response may therefore be a promising novel therapeutic target to help to improve functional and cognitive outcome of SAH patients.

Acknowledgements

The work of the authors is supported by the Netherlands Organization for Scientific Research (EMH 865.09.003) and the Dutch Heart Foundation (MDIV 2011T18).

References

[1] T. Al-Khindi, R.L. Macdonald, T.A. Schweizer, Cognitive and functional outcome after aneurysmal subarachnoid hemorrhage, Stroke 41 (2010) p.e519-e536.

[2] J. Albrecht, M. Sidoryk-Wegrzynowicz, M. Zielinska, M. Aschner, Roles of glutamine in neurotransmission, Neuron Glia Biol. 6 (2010) pp. 263-276.

[3] N.J. Allen and B.A. Barres, Neuroscience: Glia - more than just brain glue, Nature 457 (2009) pp. 675-677.

[4] A. Araque, G. Carmignoto, P.G. Haydon, S.H. Oliet, R. Robitaille, A. Volterra, Gliotransmitters travel in time and space, Neuron 81 (2014) pp. 728-739.

[5] D. Attwell, A.M. Buchan, S. Charpak, M. Lauritzen, B.A. Macvicar, E.A. Newman, Glial and neuronal control of brain blood flow, Nature 468 (2010) pp. 232-243.

[6] A.A. Babcock, H. Toft-Hansen, T. Owens, Signaling through MyD88 regulates leukocyte recruitment after brain injury, J. Immunol. 181 (2008) pp. 6481-6490.

[7] J. Badaut, J.F. Brunet, L. Grollimund, M.F. Hamou, P.J. Magistretti, J.G. Villemure, L. Regli, Aquaporin 1 and aquaporin 4 expression in human brain after subarachnoid hemorrhage and in peritumoral tissue, Acta Neurochir. Suppl 86 (2003) pp. 495-498.

[8] J.B. Bederson, A.L. Levy, W.H. Ding, R. Kahn, C.A. DiPerna, A.L. Jenkins, III, P. Vallabhajosyula, Acute vasoconstriction after subarachnoid hemorrhage, Neurosurgery 42 (1998) pp. 352-360.

[9] J.D. Bell, T.C. Thomas, E. Lass, J. Ai, H. Wan, J. Lifshitz, A.J. Baker, R.L. Macdonald, Platelet-mediated changes to neuronal glutamate receptor expression at sites of microthrombosis following experimental subarachnoid hemorrhage, J. Neurosurg. 121 (2014) pp. 1424-1431.

[10] A.R. Bialas and B. Stevens, TGF-beta signaling regulates neuronal C1q expression and developmental synaptic refinement, Nat. Neurosci. 16 (2013) pp. 1773-1782.

[11] T. Blank and M. Prinz, Microglia as modulators of cognition and neuropsychiatric disorders, Glia 61 (2013) pp. 62-70.

[12] R. Brambilla, V. Bracchi-Ricard, W.H. Hu, B. Frydel, A. Bramwell, S. Karmally, E.J. Green, J.R. Bethea, Inhibition of astroglial nuclear factor kappaB reduces inflammation and improves functional recovery after spinal cord injury, J. Exp. Med. 202 (2005) pp. 145-156.

[13] K.P. Budohoski, M. Guilfoyle, A. Helmy, T. Huuskonen, M. Czosnyka, R. Kirollos, D.K. Menon, J.D. Pickard, P.J. Kirkpatrick, The pathophysiology and treatment of delayed cerebral ischaemia following subarachnoid haemorrhage, J. Neurol. Neurosurg. Psychiatry 85 (2014) pp. 1343-1353.

[14] D. Buhler, K. Schuller, N. Plesnila, Protocol for the induction of subarachnoid hemorrhage in mice by perforation of the Circle of Willis with an endovascular filament, Transl. Stroke Res. 5 (2014) pp. 653-659.

[15] J.E. Burda, A.M. Bernstein, M.V. Sofroniew, Astrocyte roles in traumatic brain injury, Exp. Neurol. (2015).

[16] J.E. Burda and M.V. Sofroniew, Reactive gliosis and the multicellular response to

CNS damage and disease, Neuron 81 (2014) pp. 229-248.

[17] T.G. Bush, N. Puvanachandra, C.H. Horner, A. Polito, T. Ostenfeld, C.N. Svendsen, L. Mucke, M.H. Johnson, M.V. Sofroniew, Leukocyte infiltration, neuronal degeneration, and neurite outgrowth after ablation of scar-forming, reactive astrocytes in adult transgenic mice, Neuron 23 (1999) pp. 297-308.

[18] C.Z. Chang, S.C. Wu, A.L. Kwan, C.L. Lin, S.L. Hwang, 6-Mercaptopurine reverses experimental vasospasm and alleviates the production of endothelins in NO-independent mechanism-a laboratory study, Acta Neurochir. (Wien.) 153 (2011) pp. 939-949.

[19] W.S. Chung, L.E. Clarke, G.X. Wang, B.K. Stafford, A. Sher, C. Chakraborty, J. Joung, L.C. Foo, A. Thompson, C. Chen, S.J. Smith, B.A. Barres, Astrocytes mediate synapse elimination through MEGF10 and MERTK pathways, Nature 504 (2013) pp. 394-400.

[20] J. Claassen, J.R. Carhuapoma, K.T. Kreiter, E.Y. Du, E.S. Connolly, S.A. Mayer, Global cerebral edema after subarachnoid hemorrhage: frequency, predictors, and impact on outcome, Stroke 33 (2002) pp. 1225-1232.

[21] D. Davalos, J.K. Ryu, M. Merlini, K.M. Baeten, M.N. Le, M.A. Petersen, T.J. Deerinck, D.S. Smirnoff, C. Bedard, H. Hakozaki, M.S. Gonias, J.B. Ling, H. Lassmann, J.L. Degen, M.H. Ellisman, K. Akassoglou, Fibrinogen-induced perivascular microglial clustering is required for the development of axonal damage in neuroinflammation, Nat. Commun. 3 (2012) p.1227.

[22] N.W. Dorsch and M.T. King, A review of cerebral vasospasm in aneurysmal subarachnoid haemorrhage Part I: Incidence and effects, J. Clin. Neurosci. 1 (1994) pp. 19-26.

[23] J.P. Dreier, O. Windmuller, G. Petzold, U. Lindauer, K.M. Einhaupl, U. Dirnagl, Ischemia triggered by red blood cell products in the subarachnoid space is inhibited by nimodipine administration or moderate volume expansion/hemodilution in rats, Neurosurgery 51 (2002) pp. 1457-1465.

[24] J.P. Dreier, J. Woitzik, M. Fabricius, R. Bhatia, S. Major, C. Drenckhahn, T.N. Lehmann, A. Sarrafzadeh, L. Willumsen, J.A. Hartings, O.W. Sakowitz, J.H. Seemann, A. Thieme, M. Lauritzen, A.J. Strong, Delayed ischaemic neurological deficits after subarachnoid haemorrhage are associated with clusters of spreading depolarizations, Brain 129 (2006) pp. 3224-3237.

[25] F. Espinosa, B. Weir, T. Overton, W. Castor, M. Grace, D. Boisvert, A randomized placebo-controlled double-blind trial of nimodipine after SAH in monkeys. Part 1: Clinical and radiological findings, J. Neurosurg. 60 (1984) pp. 1167-1175.

[26] J.R. Faulkner, J.E. Herrmann, M.J. Woo, K.E. Tansey, N.B. Doan, M.V. Sofroniew, Reactive astrocytes protect tissue and preserve function after spinal cord injury, J. Neurosci. 24 (2004) pp. 2143-2155.

[27] D. Feng, W. Wang, Y. Dong, L. Wu, J. Huang, Y. Ma, Z. Zhang, S. Wu, G. Gao, H. Qin, Ceftriaxone alleviates early brain injury after subarachnoid hemorrhage by increasing excitatory amino acid transporter 2 expression via the PI3K/Akt/NF-kappaB signaling pathway, Neuroscience 268 (2014) pp. 21-32.

[28] R.D. Fields, A. Araque, H. Johansen-Berg, S.S. Lim, G. Lynch, K.A. Nave,

M. Nedergaard, R. Perez, T. Sejnowski, H. Wake, Glial biology in learning and cognition, Neuroscientist. 20 (2014) pp. 426-431.

[29] A.M. Fontainhas, M. Wang, K.J. Liang, S. Chen, P. Mettu, M. Damani, R.N. Fariss, W. Li, W.T. Wong, Microglial morphology and dynamic behavior is regulated by ionotropic glutamatergic and GABAergic neurotransmission, PLoS. One. 6 (2011) p.e15973.

[30] B. Friedrich, F. Muller, S. Feiler, K. Scholler, N. Plesnila, Experimental subarachnoid hemorrhage causes early and long-lasting microarterial constriction and microthrombosis: an in-vivo microscopy study, J. Cereb. Blood Flow Metab 32 (2012) pp. 447-455.

[31] C. Gemma and A.D. Bachstetter, The role of microglia in adult hippocampal neurogenesis, Front Cell Neurosci. 7 (2013) p.229.

[32] P. Greebe, G.J. Rinkel, J.W. Hop, J.M. Visser-Meily, A. Algra, Functional outcome and quality of life 5 and 12.5 years after aneurysmal subarachnoid haemorrhage, J. Neurol. 257 (2010) pp. 2059-2064.

[33] A.D. Greenhalgh, D. Brough, E.M. Robinson, S. Girard, N.J. Rothwell, S.M. Allan, Interleukin-1 receptor antagonist is beneficial after subarachnoid haemorrhage in rat by blocking haem-driven inflammatory pathology, Dis. Model. Mech. 5 (2012) pp. 823-833.

[34] A.D. Greenhalgh, N.J. Rothwell, S.M. Allan, An Endovascular Perforation Model of Subarachnoid Haemorrhage in Rat Produces Heterogeneous Infarcts that Increase with Blood Load, Transl. Stroke Res. 3 (2012) pp. 164-172.

[35] I. Gules, M. Satoh, B.R. Clower, A. Nanda, J.H. Zhang, Comparison of three rat models of cerebral vasospasm, Am. J. Physiol Heart Circ. Physiol 283 (2002) p.H2551-H2559.

[36] E. Guresir, P. Schuss, V. Borger, H. Vatter, Experimental subarachnoid hemorrhage: double cisterna magna injection rat model--assessment of delayed pathological effects of cerebral vasospasm, Transl. Stroke Res. 6 (2015) pp. 242-251.

[37] M.M. Halassa and P.G. Haydon, Integrated brain circuits: astrocytic networks modulate neuronal activity and behavior, Annu. Rev. Physiol 72 (2010) pp. 335-355.

[38] J. Han, P. Kesner, M. Metna-Laurent, T. Duan, L. Xu, F. Georges, M. Koehl, D.N. Abrous, J. Mendizabal-Zubiaga, P. Grandes, Q. Liu, G. Bai, W. Wang, L. Xiong, W. Ren, G. Marsicano, X. Zhang, Acute cannabinoids impair working memory through astroglial CB1 receptor modulation of hippocampal LTD, Cell 148 (2012) pp. 1039-1050.

[39] S.M. Han, H. Wan, G. Kudo, W.D. Foltz, D.C. Vines, D.E. Green, T. Zoerle, A. Tariq, S. Brathwaite, J. D'Abbondanza, J. Ai, R.L. Macdonald, Molecular alterations in the hippocampus after experimental subarachnoid hemorrhage, J. Cereb. Blood Flow Metab 34 (2014) pp. 108-117.

[40] K.A. Hanafy, The role of microglia and the TLR4 pathway in neuronal apoptosis and vasospasm after subarachnoid hemorrhage, J. Neuroinflammation. 10 (2013) p.83.

[41] T. Haug, A. Sorteberg, W. Sorteberg, K.F. Lindegaard, T. Lundar, A. Finset, Cognitive outcome after aneurysmal subarachnoid hemorrhage: time course of recovery

and relationship to clinical, radiological, and management parameters, Neurosurgery 60 (2007) pp. 649-656.

[42] M.T. Heneka, M.J. Carson, K.J. El, G.E. Landreth, F. Brosseron, D.L. Feinstein, A.H. Jacobs, T. Wyss-Coray, J. Vitorica, R.M. Ransohoff, K. Herrup, S.A. Frautschy, B. Finsen, G.C. Brown, A. Verkhratsky, K. Yamanaka, J. Koistinaho, E. Latz, A. Halle, G.C. Petzold, T. Town, D. Morgan, M.L. Shinohara, V.H. Perry, C. Holmes, N.G. Bazan, D.J. Brooks, S. Hunot, B. Joseph, N. Deigendesch, O. Garaschuk, E. Boddeke, C.A. Dinarello, J.C. Breitner, G.M. Cole, D.T. Golenbock, M.P. Kummer, Neuroinflammation in Alzheimer's disease, Lancet Neurol. 14 (2015) pp. 388-405.

[43] M.T. Heneka, M.P. Kummer, E. Latz, Innate immune activation in neurodegenerative disease, Nat. Rev. Immunol. 14 (2014) pp. 463-477.

[44] C. Henneberger, T. Papouin, S.H. Oliet, D.A. Rusakov, Long-term potentiation depends on release of D-serine from astrocytes, Nature 463 (2010) pp. 232-236.

[45] J.E. Herrmann, T. Imura, B. Song, J. Qi, Y. Ao, T.K. Nguyen, R.A. Korsak, K. Takeda, S. Akira, M.V. Sofroniew, STAT3 is a critical regulator of astrogliosis and scar formation after spinal cord injury, J. Neurosci. 28 (2008) pp. 7231-7243.

[46] E.M. Hol and M. Pekny, Glial fibrillary acidic protein (GFAP) and the astrocyte intermediate filament system in diseases of the central nervous system, Curr. Opin. Cell Biol. 32 (2015) pp. 121-130.

[47] L.T. Huang, H. Li, Q. Sun, M. Liu, W.D. Li, S. Li, Z. Yu, W.T. Wei, C.H. Hang, IL-33 expression in the cerebral cortex following experimental subarachnoid hemorrhage in rats, Cell Mol. Neurobiol. 35 (2015) pp. 493-501.

[48] D. Jorks, S. Major, A.I. Oliveira-Ferreira, J. Kleeberg, J.P. Dreier, Endothelin-1(1-31) induces spreading depolarization in rats, Acta Neurochir. Suppl 110 (2011) pp. 111-117.

[49] H. Kasuya and T. Shimizu, Activated complement components C3a and C4a in cerebrospinal fluid and plasma following subarachnoid hemorrhage, J. Neurosurg. 71 (1989) pp. 741-746.

[50] H. Kettenmann, U.K. Hanisch, M. Noda, A. Verkhratsky, Physiology of microglia, Physiol Rev. 91 (2011) pp. 461-553.

[51] B.S. Khakh and K.D. McCarthy, Astrocyte calcium signaling: from observations to functions and the challenges therein, Cold Spring Harb. Perspect. Biol. 7 (2015) p.a020404.

[52] B.S. Khakh and M.V. Sofroniew, Diversity of astrocyte functions and phenotypes in neural circuits, Nat. Neurosci. 18 (2015) pp. 942-952.

[53] M. Koide, A.D. Bonev, M.T. Nelson, G.C. Wellman, Inversion of neurovascular coupling by subarachnoid blood depends on large-conductance Ca2+-activated K+ (BK) channels, Proc. Natl. Acad. Sci. U. S. A 109 (2012) p.E1387-E1395.

[54] M. Koide, A.D. Bonev, M.T. Nelson, G.C. Wellman, Subarachnoid blood converts neurally evoked vasodilation to vasoconstriction in rat brain cortex, Acta Neurochir. Suppl 115 (2013) pp. 167-171.

[55] M. Koide, I. Sukhotinsky, C. Ayata,

G.C. Wellman, Subarachnoid hemorrhage, spreading depolarizations and impaired neurovascular coupling, Stroke Res. Treat. 2013 (2013) p.819340.

[56] M. Koide and G.C. Wellman, Activation of TRPV4 channels does not mediate inversion of neurovascular coupling after SAH, Acta Neurochir. Suppl 120 (2015) pp. 111-116.

[57] S. Kondo, S. Kohsaka, S. Okabe, Long-term changes of spine dynamics and microglia after transient peripheral immune response triggered by LPS in vivo, Mol. Brain 4 (2011) p.27.

[58] E. Kooijman, C.H. Nijboer, C.T. van Velthoven, A. Kavelaars, J. Kesecioglu, C.J. Heijnen, The rodent endovascular puncture model of subarachnoid hemorrhage: mechanisms of brain damage and therapeutic strategies, J. Neuroinflammation. 11 (2014) p.2.

[59] E. Kooijman, C.H. Nijboer, C.T. van Velthoven, W. Mol, R.M. Dijkhuizen, J. Kesecioglu, C.J. Heijnen, Long-term functional consequences and ongoing cerebral inflammation after subarachnoid hemorrhage in the rat, PLoS. One. 9 (2014) p.e90584.

[60] K.T. Kreiter, D. Copeland, G.L. Bernardini, J.E. Bates, S. Peery, J. Claassen, Y.E. Du, Y. Stern, E.S. Connolly, S.A. Mayer, Predictors of cognitive dysfunction after subarachnoid hemorrhage, Stroke 33 (2002) pp. 200-208.

[61] C.P. Kuo, L.L. Wen, C.M. Chen, B. Huh, C.H. Cherng, C.S. Wong, W.J. Liaw, C.C. Yeh, B.F. Lin, C.T. Wu, Attenuation of neurological injury with early baicalein treatment following subarachnoid hemorrhage in rats, J. Neurosurg. 119 (2013) pp. 1028-1037.

[62] M. Kuroki, K. Kanamaru, H. Suzuki, S. Waga, R. Semba, Effect of vasospasm on heme oxygenases in a rat model of subarachnoid hemorrhage, Stroke 29 (1998) pp. 683-688.

[63] M.S. Kwon, S.K. Woo, D.B. Kurland, S.H. Yoon, A.F. Palmer, U. Banerjee, S. Iqbal, S. Ivanova, V. Gerzanich, J.M. Simard, Methemoglobin is an endogenous toll-like receptor 4 ligand-relevance to subarachnoid hemorrhage, Int. J. Mol. Sci. 16 (2015) pp. 5028-5046.

[64] S. Lee, B.E. Yoon, K. Berglund, S.J. Oh, H. Park, H.S. Shin, G.J. Augustine, C.J. Lee, Channel-mediated tonic GABA release from glia, Science 330 (2010) pp. 790-796.

[65] H. Li, W. Wu, Q. Sun, M. Liu, W. Li, X.S. Zhang, M.L. Zhou, C.H. Hang, Expression and cell distribution of receptor for advanced glycation end-products in the rat cortex following experimental subarachnoid hemorrhage, Brain Res. 1543 (2014) pp. 315-323.

[66] W.D. Li, Q. Sun, X.S. Zhang, C.X. Wang, S. Li, W. Li, C.H. Hang, Expression and cell distribution of neuroglobin in the brain tissue after experimental subarachnoid hemorrhage in rats: a pilot study, Cell Mol. Neurobiol. 34 (2014) pp. 247-255.

[67] B.F. Lin, C.Y. Kuo, L.L. Wen, C.M. Chen, Y.F. Chang, C.S. Wong, C.H. Cherng, M.Y. Chuang, Z.F. Wu, Rosiglitazone attenuates cerebral vasospasm and provides neuroprotection in an experimental rat model of subarachnoid hemorrhage, Neurocrit. Care 21 (2014) pp. 316-331.

[68] C. Luo, B. Yi, G. Tao, M. Li, Z. Chen, W. Tang, J.H. Zhang, H. Feng, Adenosine A3 receptor agonist reduces early brain injury

in subarachnoid haemorrhage, Neuroreport 21 (2010) pp. 892-896.

[69] R.L. Macdonald, Delayed neurological deterioration after subarachnoid haemorrhage, Nat. Rev. Neurol. 10 (2014) pp. 44-58.

[70] W.J. Mack, A.F. Ducruet, Z.L. Hickman, M.C. Garrett, E.J. Albert, C.P. Kellner, J. Mocco, E.S. Connolly, Jr., Early plasma complement C3a levels correlate with functional outcome after aneurysmal subarachnoid hemorrhage, Neurosurgery 61 (2007) pp. 255-260.

[71] W.J. Mack, A.F. Ducruet, Z.L. Hickman, M.C. Garrett, E.J. Albert, C.P. Kellner, J. Mocco, E.S. Connolly, Jr., Early plasma complement C3a levels correlate with functional outcome after aneurysmal subarachnoid hemorrhage, Neurosurgery 61 (2007) pp. 255-260.

[72] B.A. MacVicar and E.A. Newman, Astrocyte regulation of blood flow in the brain, Cold Spring Harb. Perspect. Biol. 7 (2015).

[73] A. Maddahi, G.K. Povlsen, L. Edvinsson, Regulation of enhanced cerebrovascular expression of proinflammatory mediators in experimental subarachnoid hemorrhage via the mitogen-activated protein kinase kinase/extracellular signal-regulated kinase pathway, J. Neuroinflammation. 9 (2012) p.274.

[74] S. Marbacher, J. Fandino, N.D. Kitchen, Standard intracranial in vivo animal models of delayed cerebral vasospasm, Br. J. Neurosurg. 24 (2010) pp. 415-434.

[75] P. Matz, C. Turner, P.R. Weinstein, S.M. Massa, S.S. Panter, F.R. Sharp, Heme-oxygenase-1 induction in glia throughout rat brain following experimental subarachnoid hemorrhage, Brain Res. 713 (1996) pp. 211-222.

[76] P.G. Matz, S.M. Massa, P.R. Weinstein, C. Turner, S.S. Panter, F.R. Sharp, Focal hyperexpression of hemeoxygenase-1 protein and messenger RNA in rat brain caused by cellular stress following subarachnoid injections of lysed blood, J. Neurosurg. 85 (1996) pp. 892-900.

[77] S.A. Mayer, K.T. Kreiter, D. Copeland, G.L. Bernardini, J.E. Bates, S. Peery, J. Claassen, Y.E. Du, E.S. Connolly, Jr., Global and domain-specific cognitive impairment and outcome after subarachnoid hemorrhage, Neurology 59 (2002) pp. 1750-1758.

[78] J.F. Megyesi, B. Vollrath, D.A. Cook, J.M. Findlay, In vivo animal models of cerebral vasospasm: a review, Neurosurgery 46 (2000) pp. 448-460.

[79] I. Michailidou, J.G. Willems, E.J. Kooi, E.C. van, S.M. Gold, J.J. Geurts, F. Baas, I. Huitinga, V. Ramaglia, Complement C1q-C3-associated synaptic changes in multiple sclerosis hippocampus, Ann. Neurol. 77 (2015) pp. 1007-1026.

[80] J. Middeldorp and E.M. Hol, GFAP in health and disease, Prog. Neurobiol. 93 (2011) pp. 421-443.

[81] B.A. Miller, N. Turan, M. Chau, G. Pradilla, Inflammation, vasospasm, and brain injury after subarachnoid hemorrhage, Biomed. Res. Int. 2014 (2014) p.384342.

[82] K. Murakami, M. Koide, T.M. Dumont, S.R. Russell, B.I. Tranmer, G.C. Wellman, Subarachnoid Hemorrhage Induces Gliosis and Increased Expression of the Pro-inflam-

matory Cytokine High Mobility Group Box 1 Protein, Transl. Stroke Res. 2 (2011) pp. 72-79.

[83] J. Neumann, M. Gunzer, H.O. Gutzeit, O. Ullrich, K.G. Reymann, K. Dinkel, Microglia provide neuroprotection after ischemia, FASEB J. 20 (2006) pp. 714-716.

[84] D.J. Nieuwkamp, L.E. Setz, A. Algra, F.H. Linn, N.K. de Rooij, G.J. Rinkel, Changes in case fatality of aneurysmal subarachnoid haemorrhage over time, according to age, sex, and region: a meta-analysis, Lancet Neurol. 8 (2009) pp. 635-642.

[85] A. Nimmerjahn, F. Kirchhoff, F. Helmchen, Resting microglial cells are highly dynamic surveillants of brain parenchyma in vivo, Science 308 (2005) pp. 1314-1318.

[86] N.A. Oberheim, T. Takano, X. Han, W. He, J.H. Lin, F. Wang, Q. Xu, J.D. Wyatt, W. Pilcher, J.G. Ojemann, B.R. Ransom, S.A. Goldman, M. Nedergaard, Uniquely hominid features of adult human astrocytes, J. Neurosci. 29 (2009) pp. 3276-3287.

[87] S. Okada, M. Nakamura, H. Katoh, T. Miyao, T. Shimazaki, K. Ishii, J. Yamane, A. Yoshimura, Y. Iwamoto, Y. Toyama, H. Okano, Conditional ablation of Stat3 or Socs3 discloses a dual role for reactive astrocytes after spinal cord injury, Nat. Med. 12 (2006) pp. 829-834.

[88] M. Orre, W. Kamphuis, L.M. Osborn, J. Melief, L. Kooijman, I. Huitinga, J. Klooster, K. Bossers, E.M. Hol, Acute isolation and transcriptome characterization of cortical astrocytes and microglia from young and aged mice, Neurobiol. Aging 35 (2014) pp. 1-14.

[89] J.R. Ostergaard, B.O. Kristensen, S.E. Svehag, B. Teisner, T. Miletic, Immune complexes and complement activation following rupture of intracranial saccular aneurysms, J. Neurosurg. 66 (1987) pp. 891-897.

[90] Y. Otsu, K. Couchman, D.G. Lyons, M. Collot, A. Agarwal, J.M. Mallet, F.W. Pfrieger, D.E. Bergles, S. Charpak, Calcium dynamics in astrocyte processes during neurovascular coupling, Nat. Neurosci. 18 (2015) pp. 210-218.

[91] H. Pan, H. Wang, L. Zhu, L. Mao, L. Qiao, X. Su, Depletion of Nrf2 enhances inflammation induced by oxyhemoglobin in cultured mice astrocytes, Neurochem. Res. 36 (2011) pp. 2434-2441.

[92] R.C. Paolicelli, K. Bisht, M.E. Tremblay, Fractalkine regulation of microglial physiology and consequences on the brain and behavior, Front Cell Neurosci. 8 (2014) p.129.

[93] F.A. Pennings, G.J. Bouma, C. Ince, Direct observation of the human cerebral microcirculation during aneurysm surgery reveals increased arteriolar contractility, Stroke 35 (2004) pp. 1284-1288.

[94] G.C. Petzold, K.M. Einhaupl, U. Dirnagl, J.P. Dreier, Ischemia triggered by spreading neuronal activation is induced by endothelin-1 and hemoglobin in the subarachnoid space, Ann. Neurol. 54 (2003) pp. 591-598.

[95] D. Pietrobon and M.A. Moskowitz, Chaos and commotion in the wake of cortical spreading depression and spreading depolarizations, Nat. Rev. Neurosci. 15 (2014) pp. 379-393.

[96] B.A. Plog, K.M. Moll, H. Kang, J.J. Iliff, M.L. Dashnaw, M. Nedergaard, G.E. Vates, A novel technique for morphometric quan-

tification of subarachnoid hemorrhage-induced microglia activation, J. Neurosci. Methods 229 (2014) pp. 44-52.

[97] R.M. Pluta, J. Bacher, B. Skopets, V. Hoffmann, A non-human primate model of aneurismal subarachnoid hemorrhage (SAH), Transl. Stroke Res. 5 (2014) pp. 681-691.

[98] R.M. Pluta, R.J. Boock, J.K. Afshar, K. Clouse, M. Bacic, H. Ehrenreich, E.H. Oldfield, Source and cause of endothelin-1 release into cerebrospinal fluid after subarachnoid hemorrhage, J. Neurosurg. 87 (1997) pp. 287-293.

[99] G.F. Prunell, N.A. Svendgaard, K. Alkass, T. Mathiesen, Delayed cell death related to acute cerebral blood flow changes following subarachnoid hemorrhage in the rat brain, J. Neurosurg. 102 (2005) pp. 1046-1054.

[100] G.F. Prunell, N.A. Svendgaard, K. Alkass, T. Mathiesen, Inflammation in the brain after experimental subarachnoid hemorrhage, Neurosurgery 56 (2005) pp. 1082-1092.

[101] A.A. Rabinstein, J.A. Friedman, S.D. Weigand, R.L. McClelland, J.R. Fulgham, E.M. Manno, J.L. Atkinson, E.F. Wijdicks, Predictors of cerebral infarction in aneurysmal subarachnoid hemorrhage, Stroke 35 (2004) pp. 1862-1866.

[102] G.J. Rinkel, M. Djibuti, A. Algra, G.J. van, Prevalence and risk of rupture of intracranial aneurysms: a systematic review, Stroke 29 (1998) pp. 251-256.

[103] J.T. Rogers, J.M. Morganti, A.D. Bachstetter, C.E. Hudson, M.M. Peters, B.A. Grimmig, E.J. Weeber, P.C. Bickford, C. Gemma, CX3CR1 deficiency leads to impairment of hippocampal cognitive function and synaptic plasticity, J. Neurosci. 31 (2011) pp. 16241-16250.

[104] Y.B. Roos, R.J. de Haan, L.F. Beenen, R.J. Groen, K.W. Albrecht, M. Vermeulen, Complications and outcome in patients with aneurysmal subarachnoid haemorrhage: a prospective hospital based cohort study in the Netherlands, J. Neurol. Neurosurg. Psychiatry 68 (2000) pp. 337-341.

[105] J.K. Ryu, D. Davalos, K. Akassoglou, Fibrinogen signal transduction in the nervous system, J. Thromb. Haemost. 7 Suppl 1 (2009) pp. 151-154.

[106] M. Sabri, A. Kawashima, J. Ai, R.L. Macdonald, Neuronal and astrocytic apoptosis after subarachnoid hemorrhage: a possible cause for poor prognosis, Brain Res. 1238 (2008) pp. 163-171.

[107] J.J. Salazar, R. Gallego-Pinazo, H.R. de, M.D. Pinazo-Duran, B. Rojas, A.I. Ramirez, M. Serrano, J.M. Ramirez, "Super p53" mice display retinal astroglial changes, PLoS. One. 8 (2013) p.e65446.

[108] C. Samuelsson, L. Hillered, P. Enblad, E. Ronne-Engstrom, Microdialysis patterns in subarachnoid hemorrhage patients with focus on ischemic events and brain interstitial glutamine levels, Acta Neurochir. (Wien.) 151 (2009) pp. 437-446.

[109] C. Samuelsson, L. Hillered, M. Zetterling, P. Enblad, G. Hesselager, M. Ryttlefors, E. Kumlien, A. Lewen, N. Marklund, P. Nilsson, K. Salci, E. Ronne-Engstrom, Cerebral glutamine and glutamate levels in relation to compromised energy metabolism: a microdialysis study in subarachnoid hemorrhage patients, J. Cereb. Blood Flow Metab 27 (2007) pp. 1309-1317.

[110] C. Samuelsson, T. Howells, E. Kumlien, P. Enblad, L. Hillered, E. Ronne-Engstrom, Relationship between intracranial hemodynamics and microdialysis markers of energy metabolism and glutamate-glutamine turnover in patients with subarachnoid hemorrhage. Clinical article, J. Neurosurg. 111 (2009) pp. 910-915.

[111] C. Schachtrup, J.K. Ryu, M.J. Helmrick, E. Vagena, D.K. Galanakis, J.L. Degen, R.U. Margolis, K. Akassoglou, Fibrinogen triggers astrocyte scar formation by promoting the availability of active TGF-beta after vascular damage, J. Neurosci. 30 (2010) pp. 5843-5854.

[112] D.P. Schafer, E.K. Lehrman, B. Stevens, The "quad-partite" synapse: microglia-synapse interactions in the developing and mature CNS, Glia 61 (2013) pp. 24-36.

[113] D.P. Schafer and B. Stevens, Microglia Function in Central Nervous System Development and Plasticity, Cold Spring Harb. Perspect. Biol. (2015).

[114] N. Schallner, R. Pandit, R. LeBlanc, III, A.J. Thomas, C.S. Ogilvy, B.S. Zuckerbraun, D. Gallo, L.E. Otterbein, K.A. Hanafy, Microglia regulate blood clearance in subarachnoid hemorrhage by heme oxygenase-1, J. Clin. Invest 125 (2015) pp. 2609-2625.

[115] U.C. Schneider, A.M. Davids, S. Brandenburg, A. Muller, A. Elke, S. Magrini, E. Atangana, K. Turkowski, T. Finger, A. Gutenberg, C. Gehlhaar, W. Bruck, F.L. Heppner, P. Vajkoczy, Microglia inflict delayed brain injury after subarachnoid hemorrhage, Acta Neuropathol. (2015).

[116] F.A. Sehba and V. Friedrich, Early events after aneurysmal subarachnoid hemorrhage, Acta Neurochir. Suppl 120 (2015) pp. 23-28.

[117] F.A. Sehba, J. Hou, R.M. Pluta, J.H. Zhang, The importance of early brain injury after subarachnoid hemorrhage, Prog. Neurobiol. 97 (2012) pp. 14-37.

[118] F.A. Sehba, G. Mostafa, V. Friedrich, Jr., J.B. Bederson, Acute microvascular platelet aggregation after subarachnoid hemorrhage, J. Neurosurg. 102 (2005) pp. 1094-1100.

[119] F.A. Sehba, G. Mostafa, J. Knopman, V. Friedrich, Jr., J.B. Bederson, Acute alterations in microvascular basal lamina after subarachnoid hemorrhage, J. Neurosurg. 101 (2004) pp. 633-640.

[120] J.L. Seidel, C. Escartin, C. Ayata, G. Bonvento, C.W. Shuttleworth, Multifaceted roles for astrocytes in spreading depolarization: A target for limiting spreading depolarization in acute brain injury?, Glia (2015).

[121] J.M. Simard, C. Tosun, S. Ivanova, D.B. Kurland, C. Hong, L. Radecki, C. Gisriel, R. Mehta, D. Schreibman, V. Gerzanich, Heparin reduces neuroinflammation and transsynaptic neuronal apoptosis in a model of subarachnoid hemorrhage, Transl. Stroke Res. 3 (2012) pp. 155-165.

[122] M. Simard and M. Nedergaard, The neurobiology of glia in the context of water and ion homeostasis, Neuroscience 129 (2004) pp. 877-896.

[123] S.A. Sloan and B.A. Barres, Looks can be deceiving: reconsidering the evidence for gliotransmission, Neuron 84 (2014) pp. 1112-1115.

[124] S. Smithason, S.K. Moore, J.J. Proven-

cio, Systemic administration of LPS worsens delayed deterioration associated with vasospasm after subarachnoid hemorrhage through a myeloid cell-dependent mechanism, Neurocrit. Care 16 (2012) pp. 327-334.

[125] M.V. Sofroniew, Astrocyte barriers to neurotoxic inflammation, Nat. Rev. Neurosci. 16 (2015) pp. 249-263.

[126] M.V. Sofroniew and H.V. Vinters, Astrocytes: biology and pathology, Acta Neuropathol. 119 (2010) pp. 7-35.

[127] R. Srinivasan, B.S. Huang, S. Venugopal, A.D. Johnston, H. Chai, H. Zeng, P. Golshani, B.S. Khakh, Ca(2+) signaling in astrocytes from Ip3r2(-/-) mice in brain slices and during startle responses in vivo, Nat. Neurosci. 18 (2015) pp. 708-717.

[128] A.H. Stephan, B.A. Barres, B. Stevens, The complement system: an unexpected role in synaptic pruning during development and disease, Annu. Rev. Neurosci. 35 (2012) pp. 369-389.

[129] B. Stevens, N.J. Allen, L.E. Vazquez, G.R. Howell, K.S. Christopherson, N. Nouri, K.D. Micheva, A.K. Mehalow, A.D. Huberman, B. Stafford, A. Sher, A.M. Litke, J.D. Lambris, S.J. Smith, S.W. John, B.A. Barres, The classical complement cascade mediates CNS synapse elimination, Cell 131 (2007) pp. 1164-1178.

[130] J.I. Suarez, R.W. Tarr, W.R. Selman, Aneurysmal subarachnoid hemorrhage, N. Engl. J. Med. 354 (2006) pp. 387-396.

[131] Q. Sun, Y. Dai, X. Zhang, Y.C. Hu, D. Zhang, W. Li, X.S. Zhang, J.H. Zhu, M.L. Zhou, C.H. Hang, Expression and cell distribution of myeloid differentiation primary response protein 88 in the cerebral cortex following experimental subarachnoid hemorrhage in rats: a pilot study, Brain Res. 1520 (2013) pp. 134-144.

[132] Q. Sun, W. Wu, Y.C. Hu, H. Li, D. Zhang, S. Li, W. Li, W.D. Li, B. Ma, J.H. Zhu, M.L. Zhou, C.H. Hang, Early release of high-mobility group box 1 (HMGB1) from neurons in experimental subarachnoid hemorrhage in vivo and in vitro, J. Neuroinflammation. 11 (2014) p.106.

[133] H. Suzuki, Y. Hasegawa, K. Kanamaru, J.H. Zhang, Mechanisms of osteopontin-induced stabilization of blood-brain barrier disruption after subarachnoid hemorrhage in rats, Stroke 41 (2010) pp. 1783-1790.

[134] X. Tong, Y. Ao, G.C. Faas, S.E. Nwaobi, J. Xu, M.D. Haustein, M.A. Anderson, I. Mody, M.L. Olsen, M.V. Sofroniew, B.S. Khakh, Astrocyte Kir4.1 ion channel deficits contribute to neuronal dysfunction in Huntington's disease model mice, Nat. Neurosci. 17 (2014) pp. 694-703.

[135] M.E. Tremblay, R.L. Lowery, A.K. Majewska, Microglial interactions with synapses are modulated by visual experience, PLoS. Biol. 8 (2010) p.e1000527.

[136] C.P. Turner, S.S. Panter, F.R. Sharp, Anti-oxidants prevent focal rat brain injury as assessed by induction of heat shock proteins (HSP70, HO-1/HSP32, HSP47) following subarachnoid injections of lysed blood, Brain Res. Mol. Brain Res. 65 (1999) pp. 87-102.

[137] K. Uekawa, Y. Hasegawa, M. Ma, T. Nakagawa, T. Katayama, D. Sueta, K. Toyama, K. Kataoka, N. Koibuchi, T. Kawano, J. Kuratsu, S. Kim-Mitsuyama, Rosuvastatin ameliorates early brain injury after

subarachnoid hemorrhage via suppression of superoxide formation and nuclear factor-kappa B activation in rats, J. Stroke Cerebrovasc. Dis. 23 (2014) pp. 1429-1439.

[138] J. van Gijn, R.S. Kerr, G.J. Rinkel, Subarachnoid haemorrhage, Lancet 369 (2007) pp. 306-318.

[139] M.D. Vergouwen, A. Algra, G.J. Rinkel, Endothelin receptor antagonists for aneurysmal subarachnoid hemorrhage: a systematic review and meta-analysis update, Stroke 43 (2012) pp. 2671-2676.

[140] M.D. Vergouwen, V.L. Knaup, J.J. Roelofs, O.J. de Boer, J.C. Meijers, Effect of recombinant ADAMTS-13 on microthrombosis and brain injury after experimental subarachnoid hemorrhage, J. Thromb. Haemost. 12 (2014) pp. 943-947.

[141] M.D. Vergouwen, M. Vermeulen, B.A. Coert, E.S. Stroes, Y.B. Roos, Microthrombosis after aneurysmal subarachnoid hemorrhage: an additional explanation for delayed cerebral ischemia, J. Cereb. Blood Flow Metab 28 (2008) pp. 1761-1770.

[142] M.D. Vergouwen, M. Vermeulen, G.J. van, G.J. Rinkel, E.F. Wijdicks, J.P. Muizelaar, A.D. Mendelow, S. Juvela, H. Yonas, K.G. Terbrugge, R.L. Macdonald, M.N. Diringer, J.P. Broderick, J.P. Dreier, Y.B. Roos, Definition of delayed cerebral ischemia after aneurysmal subarachnoid hemorrhage as an outcome event in clinical trials and observational studies: proposal of a multidisciplinary research group, Stroke 41 (2010) pp. 2391-2395.

[143] A. Verkhratsky, M. Nedergaard, L. Hertz, Why are astrocytes important?, Neurochem. Res. 40 (2015) pp. 389-401.

[144] D.C. Widenka, R.J. Medele, W. Stummer, K. Bise, H.J. Steiger, Inducible nitric oxide synthase: a possible key factor in the pathogenesis of chronic vasospasm after experimental subarachnoid hemorrhage, J. Neurosurg. 90 (1999) pp. 1098-1104.

[145] D.A. Wilson, P. Nakaji, F.C. Albuquerque, C.G. McDougall, J.M. Zabramski, R.F. Spetzler, Time course of recovery following poor-grade SAH: the incidence of delayed improvement and implications for SAH outcome study design, J. Neurosurg. 119 (2013) pp. 606-612.

[146] M.K. Winkler, Y. Chassidim, S. Lublinsky, G.S. Revankar, S. Major, E.J. Kang, A.I. Oliveira-Ferreira, J. Woitzik, N. Sandow, M. Scheel, A. Friedman, J.P. Dreier, Impaired neurovascular coupling to ictal epileptic activity and spreading depolarization in a patient with subarachnoid hemorrhage: possible link to blood-brain barrier dysfunction, Epilepsia 53 Suppl 6 (2012) pp. 22-30.

[147] A. Xie, Y. Aihara, V.A. Bouryi, E. Nikitina, B.S. Jahromi, Z.D. Zhang, M. Takahashi, R.L. Macdonald, Novel mechanism of endothelin-1-induced vasospasm after subarachnoid hemorrhage, J. Cereb. Blood Flow Metab 27 (2007) pp. 1692-1701.

[148] G.B. Xie, C.X. Wang, C.H. Zhou, H. Li, X.S. Zhang, X.M. Zhou, L. Zhang, C.H. Hang, M.L. Zhou, J.X. Shi, Expression of Cytoplasmic Gelsolin in Rat Brain After Experimental Subarachnoid Hemorrhage, Cell Mol. Neurobiol. 35 (2015) pp. 723-731.

[149] J.H. Yan, N.H. Khatibi, H.B. Han, Q. Hu, C.H. Chen, L. Li, X.M. Yang, C.M. Zhou, p53-induced uncoupling expression of aquaporin-4 and inwardly rectifying K+ 4.1 channels in cytotoxic edema after subarachnoid hemorrhage, CNS. Neurosci. Ther. 18

(2012) pp. 334-342.

[150] Y.Q. Yang, H. Li, X. Zhang, C.X. Wang, Q. Sun, S. Li, W. Li, W. Li, K. Ding, M. Liu, Z. Yu, C.H. Hang, Expression and cell distribution of SENP3 in the cerebral cortex after experimental subarachnoid hemorrhage in rats: a pilot study, Cell Mol. Neurobiol. 35 (2015) pp. 407-416.

[151] X. Yao, A.J. Smith, B.J. Jin, Z. Zador, G.T. Manley, A.S. Verkman, Aquaporin-4 regulates the velocity and frequency of cortical spreading depression in mice, Glia 63 (2015) pp. 1860-1869.

[152] P.K. Yeung, J. Shen, S.S. Chung, S.K. Chung, Targeted over-expression of endothelin-1 in astrocytes leads to more severe brain damage and vasospasm after subarachnoid hemorrhage, BMC. Neurosci. 14 (2013) p.131.

[153] M. Yokota, J.W. Peterson, E. Tani, I. Yamaura, The immunohistochemical distribution of protein kinase C isozymes is altered in the canine brain and basilar artery after subarachnoid hemorrhage, Neurosci. Lett. 180 (1994) pp. 171-174.

[154] K.D. Yundt, R.L. Grubb, Jr., M.N. Diringer, W.J. Powers, Autoregulatory vasodilation of parenchymal vessels is impaired during cerebral vasospasm, J. Cereb. Blood Flow Metab 18 (1998) pp. 419-424.

[155] J.L. Zamanian, L. Xu, L.C. Foo, N. Nouri, L. Zhou, R.G. Giffard, B.A. Barres, Genomic analysis of reactive astrogliosis, J. Neurosci. 32 (2012) pp. 6391-6410.

[156] C. Zhang, J.Y. Lee, R.F. Keep, A. Pandey, N. Chaudhary, Y. Hua, G. Xi, Brain edema formation and complement activation in a rat model of subarachnoid hemorrhage, Acta Neurochir. Suppl 118 (2013) pp. 157-161.

[157] T. Zhang, J. Su,B. Guo, K. Wang, X. Li, G. Liang, Apigenin protects blood-brain barrier and ameliorates early brain injury by inhibiting TLR4-mediated inflammatory pathway in subarachnoid hemorrhage rats, Int. Immunopharmacol. 28 (2015) pp. 79-87.

[158] Z.Y. Zhang, B.L. Sun, J.K. Liu, M.F. Yang, D.W. Li, J. Fang, S. Zhang, Q.L. Yuan, S.L. Huang, Activation of mGluR5 Attenuates Microglial Activation and Neuronal Apoptosis in Early Brain Injury After Experimental Subarachnoid Hemorrhage in Rats, Neurochem. Res. 40 (2015) pp. 1121-1132.

[159] Z.Y. Zhang, B.L. Sun, M.F. Yang, D.W. Li, J. Fang, S. Zhang, Carnosine attenuates early brain injury through its antioxidative and anti-apoptotic effects in a rat experimental subarachnoid hemorrhage model, Cell Mol. Neurobiol. 35 (2015) pp. 147-157.

Table 1. Changes in microglia after SAH. The changes in microglia after SAH including the species and what kind of SAH model is used, measure time after the ictus and important findings from the studies are summarized.

Changes in microglia	Species / strain	Model	Time after SAH	Remarks	Other outcome	References
HO-1	Sprague-Dawley Rats	Cisterna magna injection	1,2,3 and 4 days	Lysed blood injection	In both microglia and astrocytes	[75]
HO-1, *HO-1*	Sprague-Dawley Rats	Cisterna magna injection	1,2,3 and 4 days	Lysed blood injection	In both microglia and astrocytes	[76]
HO-1, **HSP70**, **HPS47**	Sprague-Dawley Rats	Cisterna magna injection	1 day	Lysed blood, oxyhemoglobin A_0 injection	Antioxidants may prevent HO-1 expression	[136]
iNOS	Wistar Rats	2x Cisterna magna blood injection, 24h apart	7 days	No clear data shown regarding the microglial expression	Mainly found in endothelial cells, smooth muscle cells adventitial cells	[144]
CD11b, TNF-α, IL-1β	Sprague-Dawley Rats	Endovascular perforation model	6, 12 and 24 hours	-	adenosine A3 receptor agonist reduces neuroinflammation	[68]
LCA (CD45), ***TNF-α***, ***IL-1***, ***IL-6***, **ET-1**	Sprague-Dawley Rats	Cisterna magna blood injection	5 days	Marker not specific; LCA is used as microglia and astrocyte marker	6-mp reduces *IL-1, IL-6, TNF-α* and ET-1 expression	[18]
HMGB1	New Zealand White Rabbits	1 or 2x Cisterna magna blood injection	2 and 5 days	-	GFAP and S100b increased, number of Iba-1 positive cells not increased	[82]
Amoeboid morphology	C57Bl/6 Mice	Subarachnoid vein transection	24 hours	SAH in combination with LPS injection, but one group SAH alone	CD11b antibody blocks vasospasms	[124]

Table 1 continued.

Amoeboid morphology	Wistar Rats	Endovascular perforation model	72 hours	-	BBB disruption and neuronal death	[34]
Il-1α	Wistar Rats	Endovascular perforation model	24, 48 hours	-	IL-1 receptor antagonist reduces BBB breakdown	[33]
CD68, **Iba-1**, **amoeboid morphology**	Wistar Rats	Unilateral blood injection	48 hours	-	Heparin reduces neuroinflammation and neuronal apoptosis	[121]
MyD88, ***MyD88***	Sprague-Dawley Rats	Prechiasmatic cistern blood injection	1 and 5 days	-	MyD88 expression also in neurons and astrocytes	[131]
TLR4	C57Bl/6 Mice	Cisterna magna blood injection	7 and 15 days	-	Ablation of microglia reduces vasospasms, apoptosis	[40]
Ngb, ***Ngb***	Sprague-Dawley Rats	Prechiasmatic cistern blood injection	24 hours	-	Ngb expression in neurons	[66]
RAGE, ***RAGE***	Sprague-Dawley Rats	Prechiasmatic cistern blood injection	1 day	-	RAGE expression in neurons	[65]
NFκB subunit p65, **Iba-1**	Sprague-Dawley Rats	Endovascular perforation model	24 hours	-	Rosuvastatin attenuates neuroinflammation and ROS expression	[137]
Iba-1, ***TNF-α***	Wistar rats	Endovascular perforation model	21 days	-	GFAP/astrocytes also upregulated after 21 days,	[59]
amoeboid morphology	Cx3cr1-eGFP/ C57BL/6N Mice	Cisterna magna blood injection	1, 2 and 7 days	-	Cell count and CD68 does not change	[96]
HMGB1 translocation	Sprague-Dawley Rats	Cisterna magna blood injection	2 hours, 1 day	-	HMGB1 mainly found in neurons	[132]

Table 1 continued.

CD68, **TNF-α**, **IL-1β**, **IL-6**, **amoeboid morphology**	Sprague-Dawley Rats	Cisterna magna blood injection	48 hours	-	Carnosine attenuates neuroinflammation and ROS expression	[159]
-	Sprague-Dawley Rats	Prechiasmatic cistern blood injection	24 hours	SENP3 not increased in microglia after SAH	SENP3 increased in neurons, not in astrocytes	[150]
amoeboid morphology, GSN, *GSN*	Sprague-Dawley Rats	Prechiasmatic cistern blood injection	1 day	-	GSN downregulated in astrocytes and neurons	[148]
NFκB subunit p65, **TLR4**, ***TLR4***, **TNF-α**	Wistar Rats, N9 microglia	Unilateral MetHgb injection	24 hours	MetHgb injections, partly *in-vitro*	-	[63]
CD68, **mGluR5**, **amoeboid morphology**, **TNF-α**, **IL-1β**, **IL-6**, ***TNF-α***	Sprague-Dawley Rats	Endovascular perforation model	24 hours	-	CHPG and VU0360172 reduces neuroinflammation and neuronal apoptosis	[158]
CD68 cells, **Iba1 cells,** ***TNF-α***, ***IL-1β***, ***IL-6***, ***IL2r***, ***Il6r***, ***Tnfr***	Human, C57BL/6 Mice	Endovascular perforation mouse model	4, 14 and 28 days	-	Neuro-axonal injury	[115]
HO-1, ***HO-1, IL-1β, IL-6, IL-8, TNF-α, IL-10***	Human, C57BL/6 Microglia HO-1 KO And other genetic mouse models	Prechiasmatic cistern blood injection	7 days	-	HO-1 and CO attenuates cognitive impairment, blood volume and vasospasm	[114]
TLR4	Sprague-Dawley Rats	Endovascular perforation mouse model	24 hours	-	Apigenin attenuates neuroinflammation, brain edema, BBB disruption, cell apoptosis	[157]

Typeface in first column: **Bold** represents upregulated genes/proteins, underlined represents downregulated genes/proteins, *italics* represents mRNAs and normal typeface represents proteins. 6-mp, 6-mercaptopurine; BBB, Blood Brain Barrier; CHPG; *RS*)-2-chloro-5-hydroxyphenylgly-

cine; CO, carbon monoxide; Cx3cr1-eGFP mice, CX3C chemokine receptor 1 - enhanced Green Fluorescence Protein mice; EBI, Early Brain Injury; GFAP, Glial fibrillary acidic protein; GSN, Gelsolin; HMGB1, High Mobility Group Box-1; HO-1, Heme-Oxygenase-1; HSP47/70, Heat Shock Protein 47/ 70; IBA-1, ionized calcium-binding adapter molecule 1; IL-1α/1β/6/8, interleukin-1α/1β/6/8; IL2r, Interleukin 2 receptor; IL6r, Interleukin 6 receptor; iNOS, inducible Nitric Oxide Synthase; LCA, Leukocyte common antigen; MetHgb, Methemoglobin; mGluR5, metabotropic Glutamate Receptor 5; MyD88, myeloid differentiation 88; NFκB, Nuclear Factor κB; Ngb, neuroglobin; RAGE, Receptor for Advanced Glycation End products; ROS, Reactive Oxygen Species; SENP3, SUMO1/Sentrin/SMT3 Specific Peptidase 3; TLR4, Toll-Like Receptor 4; TNF-α, Tumor Necrosis Factor-α; TNFr, Tumor Necrosis Factor receptor; VU0360172, Metabotropic Glutamate Receptor 5 Positive Allosteric Modulator.

Table 2. Changes in astrocytes after SAH. The changes in astrocytes after SAH including the species and what kind of SAH model is used, measure time after the ictus and important findings from the studies are summarized.

Changes in astrocyte	Species/strain	Model	Time after ictus	Remarks	Other outcome	References
Pk-Cα, **GFAP**	Mongrel Dogs	1 or 2x Cisterna magna blood injection, 48h apart	2 and 7 days	No clear data shown	-	[153]
HO-1	Sprague-Dawley Rats	Cisterna magna injection	1,2,3 and 4 days	Lysed blood injection	In both microglia and astrocytes	[75]
ET-1, **ET-1** increase after hypoxia	Cynomolgus monkeys, primary rat astrocyte culture	Subarachnoid preclotted blood injection	6, 24 and 48 hours	No *in-vivo* control	-	[98]
HO-1	Sprague-Dawley Rats	Cisterna magna injection	24 hours	Lysed blood injection	-	[62]
HO-1, **HSP70,**	Sprague-Dawley Rats	Cisterna magna injection	1 day	Lysed blood, oxyhemoglobin A_0 injection	Antioxidants may prevent HO-1 expression	[136]

Table 2 continued.

AQP1, **AQP4**	Human	Neo-cortex biopsy during surgery	Not determined	Controls from epileptic surgery	AQP1, AQP4 also up regulated after gliomas	[7]
GFAP	Sprague-Dawley Rats	Endovascular perforation mouse model and Prechiasmatic cistern blood injection	2 and 7 days	-	DNA damage in neurons, astrocytes, oligodendroglia	[99]
Gln synthesis during energy crisis	Human	Microdialysis	Hourly	No control patients		[109]
Apoptosis by **cleaved caspase-3**	Mongrel Dogs	Cisterna magna blood injection	7 days	-	In both neurons and astrocytes	[106]
Initial interstitial Gln levels lower in patients with poor clinical admittance status, Gln lower during ischemia	Human	Microdialysis	Hourly	-	-	[108]
Interstitial Glt during high ICP and low CPP	Human	Microdialysis	Hourly	-	-	[110]
OPN, **GFAP**	Sprague-Dawley Rats	Endovascular perforation model	72 hours	Weak contrast in stainings	OPN exacerbated neurologic impairment and BBB breakdown	[133]
S100b, **GFAP**	New Zealand White Rabbits	1 or 2x Cisterna magna blood injection	2 and 5 days	-	HMGB1 expressed in microglia	[82]
volume astrocyte endfeet/ mitochondria, P53, **GFAP**, **p-p38MAPK**, KIR4.1, **AQP4**	Sprague-Dawley Rats	Endovascular perforation model	24 hours	Inconsistent double immunofluorescence stainings shown	p53 inhibitor pifithrin-*α* reduces edema, recovers KIR4.1 and AQP4 expression	[149]

Table 2 continued.

Inversed neuro-vascular coupling, **increased Ca^{2+} oscillations**, enhanced **BK** channel activity	Sprague-Dawley Rats	2x Cisterna magna blood injection, 24 hours apart	4 days	-	-	[53,54]
TNF-α	Sprague-Dawley Rats	Prechiasmatic cistern blood injection	24 hours		Activation of the MAPK-ERK1/2 pathway	[73]
MyD88, ***MyD88***	Sprague-Dawley Rats	Prechiasmatic cistern blood injection	1 and 5 days	-	MyD88 expression in neurons, microglia	[131]
GFAP, GLT-1	Wistar rats	2x Prechiasmatic cistern blood injection, 48 hours apart	1 and 7 days	-	Baicalein reduces brain damage, edema, recovers GLT-1 expression	[61]
GFAP, **ET-1**	Non-transgenic and GET-1(GFAP-ET-1) Mice	Endovascular perforation model	3 days	-	Astrocytic **ET-1** overexpression causes more brain injury	[152]
-	Sprague-Dawley Rats	Prechiasmatic cistern blood injection	1 day	-	RAGE expression in neurons and microglia, not in astrocytes	[65]
GFAP, ***TNF-α***	Wistar rats	Endovascular perforation model	21 days	-	Iba-1/microglia also upregulated after 21 days	[59]
GLT-1, **Glt**, *GLT-1*	Sprague-Dawley Rats	Cisterna magna blood injection	6 hours to 5 days	-	Ceftriaxone reduces brain damage, recovers *GLT-1*	[27]
GFAP, GLT-1	Wistar rats	2x Prechiasmatic cistern blood injection, 48 hours apart	7 days	-	Rosiglitazone attenuates vasospasm, recovers GLT-1	[67]
IL-33	Sprague-Dawley Rats	Prechiasmatic cistern blood injection	1 day	Immunofluorescence not convincing	-	[47]

Table 2 continued.

-	Sprague-Dawley Rats	Prechiasmatic cistern blood injection	24 hours	SENP3 not increased in astrocytes after SAH	SENP3 increased in neurons, not in microglia	[150]
GSN, *GSN*	Sprague-Dawley Rats	Prechiasmatic cistern blood injection	12 hours	-	amoeboid morphology in microglia	[148]
-	Sprague-Dawley Rats	Endovascular perforation mouse model	24 hours	TLR4 is not elevated in astrocytes	Apigenin attenuates neuroinflammation, brain edema, BBB disruption, cell apoptosis	[157]

Typeface in first column: **Bold** represents upregulated genes/proteins, underlined represents downregulated genes/proteins, *italics* represents mRNAs and normal typeface represents proteins. AQP1/4, Aquaporin 1/4; BBB, Blood Brain Barrier; CPP, Cerebral Perfusion Pressure; EAAT2, Excitatory amino-acid transporter 2; ERK1/2, Extracellular signal-regulated protein kinases 1 and 2; ET-1, Endothelin-1; GFAP, Glial fibrillary acidic protein; Gln, Glutamine; GLT-1, Glutamate Transporter-1; GSN, Gelsolin; HMGB1, High Mobility Group Box-1; HO-1, Heme-Oxygenase-1; HSP70, Heat Shock Protein 70; IBA-1, ionized calcium-binding adapter molecule 1; ICP, Intracranial Pressure; IL-33, interleukin-33; KIR4.1, inwardly rectifying potassium channel; MyD88, myeloid differentiation 88; NFκB, Nuclear Factor κB; Ngb, neuroglobin; OPN, Osteopontin; p-p38MAPK, phosphorylated p38 Mitogen-activated protein kinase; Pk-Cα, Protein Kinase Cα; SENP3, SUMO1/Sentrin/SMT3 Specific Peptidase 3; TLR4, Toll-Like Receptor 4; TNF-α, Tumor Necrosis Factor-α; RAGE, Receptor for Advanced Glycation End products.

Box 1. Animal models for SAH

The case fatality rate in patients with SAH is high and limited treatment options are available to reduce brain damage after the hemorrhage. In order to investigate SAH pathophysiology and discover new therapeutic targets, suitable animal models are needed [58]. These models should mimic the human situation as closely as possible. Several species have been used in the past to mimic human SAH, including mice, rats, rabbits, dogs, and nonhuman primates [74]. Several techniques for the induction of experimental SAH exist, of which only three are frequently applied: endovascular vessel puncture, intracisternal blood injection, and blood clot placement. The choice of an animal model for SAH depends on the aim of the research and practical considerations. Furthermore, no animal model can mimic the complete pathophysiology of SAH [74].

Endovascular puncture

The endovascular puncture model is applied in mice and rats [74]. In this model, SAH is induced by insertion of a nylon filament into the external carotid artery, which is moved through the internal carotid artery until the circle of Willis is reached. The filament is then pushed through the vessel wall in order to puncture it [14]. The filament is removed as soon as possible, in order to limit the ischemic period, which serves to mimic the clinical situation as closely as possible.

The advantage of the endovascular puncture model is the resemblance of the induction method to the natural pathophysiology of SAH, since an artery at the circle of Willis is ruptured in the process and pressurized arterial blood flows into the subarachnoid space [35]. This is important for the development of EBI and DCI. Furthermore, the histological changes observed in cerebral arteries in the endovascular puncture model resemble the changes found in humans. An increase in the mean arterial blood pressure and intracranial pressure is observed in both humans and animals. The mortality rate in this model is high: up to 50% in the first 24 hours and the extent of the hemorrhage in this model shows a large variation, both aspects mimic the clinical situation [35,36].

Intracisternal blood injection

Intracisternal blood injection is used to simulate SAH in mice, rats, rabbits, dogs, and nonhuman primates [74]. In this model, blood is injected into a subarachnoid cistern, usually the cisterna magna. Blood injection can be achieved by means of a surgical approach, involving insertion of a tube into the cistern, or by puncturing the cistern transcutaneously with a needle. The injected blood is usually autologous arterial blood, but autologous venous blood, allogenous arterial blood, and CSF and blood mixtures are also used. The method described above is the single- hemorrhage model. In the double-hemorrhage model, a second blood injection is given after either 24h or 48h. In the double-hemorrhage model, the time course of vasospasm is similar to that in humans, with maximum vasospasm present on day 7 after SAH induction [35,36]. Furthermore, vasospasm in the double-hemorrhage model is more severe compared to other models. The histological changes found in the double-hemorrhage model are the same as in humans, although this also applies to the endovascular and single-hemorrhage model. However, the changes are more consistent and severe in the double-hemorrhage model.

Blood clot model

A third approach to study SAH in animals is the blood clot model [97]. This model is used in Cynomolgus monkeys. The arachnoid over the proximal portion of the middle cerebral artery (MCA) and the bifurcation of the internal carotid artery (ICA) is opened. There, the arteries are covered with 5 ml of preclotted arterial blood after removal of 3 to 4 ml of cerebrospinal fluid. Thereafter, the dura is closed [25]. It is the most consistent model in mimicking development of vasospasm after SAH [78].

CHAPTER 2

Complement C5 contributes to brain injury after subarachnoid hemorrhage

Bart J. van Dijk, MSc;[1,2] Joost C.M. Meijers, PhD;[3,4] Anne T. Kloek, MD;[5] Veronique L. Knaup, MSc;[3] Gabriel J.E. Rinkel, MD FRCP(E);[2] B. Paul Morgan, MD PhD;[6] Marije J. van der Kamp, BSc;[1] Koji Osuka, MD PhD;[7] Eleonora Aronica, MD PhD;[8] Ynte M. Ruigrok, MD 1. PhD;[2] Diederik van de Beek, MD PhD;[5] Matthijs Brouwer, MD PhD;[5] Marcela Pekna, MD PhD;[9] Elly M. Hol, PhD;[1,10] Mervyn D.I. Vergouwen, MD PhD[2]

1. UMC Utrecht Brain Center, Department of Translational Neurosciences, University Medical Center Utrecht, Utrecht University, Heidelberglaan 100, Utrecht, The Netherlands
2. UMC Utrecht Brain Center, Department of Neurology and Neurosurgery, University Medical Center Utrecht, Utrecht University, Heidelberglaan 100, Utrecht, The Netherlands
3. Department of Experimental Vascular Medicine, Academic Medical Center, Meibergdreef 9, Amsterdam, The Netherlands
4. Department of Plasma Proteins, Sanquin Research, Plesmanlaan 125, Amsterdam, The Netherlands
5. Department of Neurology, Amsterdam Neuroscience, Academic Medical Center, Meibergdreef 9, Amsterdam, The Netherlands
6. Systems Immunity Research Institute, Cardiff University, Heath Park, Cardiff, United Kingdom
7. Department of Neurological Surgery, Aichi Medical University, 1-1 Karimatayazako, Aichi, Japan
8. Department of Neuropathology, Academic Medical Center, Meibergdreef 9, Amsterdam, The Netherlands
9. Department of Clinical Neuroscience, Institute of Neuroscience and Physiology, Sahlgrenska Academy at University of Gothenburg, Medicinaregatan 9A, Gothenburg, Sweden
10. Netherlands Institute for Neuroscience, an institute of the Royal Netherlands Academy of Arts and Sciences, Meibergdreef 47, Amsterdam, The Netherlands

Published in Translational Stroke Research. 2020 Aug;11(4):678-688.

Abstract
Previous studies showed that complement activation is associated with poor functional outcome after aneurysmal subarachnoid hemorrhage (SAH). We investigated whether complement activation is underlying brain injury after aneurysmal SAH (n=7) and if it is an appropriate treatment target. We investigated complement expression in brain tissue of aneurysmal SAH patients (n=930), and studied the role of common genetic variants in C3 and C5 genes in outcome. We analyzed plasma levels (n=229) to identify the functionality of a Single Nucleotide Polymorphism (SNP) associated with outcome. The time course of C5a levels was measured in plasma (n=31) and CSF (n=10). In an SAH mouse model, we studied the extent of microglia activation and cell death in wildtype mice, mice lacking the C5a receptor, and in mice treated with C5-specific antibodies (n=15 per group). Brain sections from aneurysmal SAH patients showed increased presence of complement components C1q and C3/C3b/iC3B compared to controls. The complement component 5 (*C5*) SNP correlated with C5a plasma levels and poor disease outcome. Serial measurements in CSF revealed that C5a was >1400-fold increased 1 day after aneurysmal SAH and then gradually decreased. C5a in plasma was two-fold increased at days 3-10 after aneurysmal SAH. In the SAH mouse model, we observed a ≈40% reduction in both microglia activation and cell death in mice lacking the C5a receptor, and in mice treated with C5-specific antibodies. These data show that C5 contributes to brain injury after experimental SAH, and support further study of C5-specific antibodies as novel treatment option to reduce brain injury and improve prognosis after aneurysmal SAH.

Key Words
Aneurysmal subarachnoid hemorrhage; complement system; brain injury.

Introduction

Aneurysmal SAH is a devastating subtype of stroke, caused by rupture of an aneurysm of an intracranial artery in the subarachnoid space. Although the prognosis after aneurysmal SAH has improved over the last decades, 90-day case-fatality is still around 30% in hospital-based studies [1]. The most important determinant of poor functional outcome after aneurysmal SAH is early brain injury directly related to the initial bleeding [1,2]. Other major determinants of poor functional outcome are rebleeding of the aneurysm and delayed cerebral ischemia, which may occur 4-14 days after the initial haemorrhage [1,3]. No treatment exists for early brain injury, while the effect of calcium antagonist nimodipine in preventing delayed cerebral ischemia is only modest [4]. Therefore, new treatment options are needed to reduce brain injury after SAH.

Poor functional outcome after SAH can partially be predicted using models that include factors such as age, World Federation of Neurological Surgeons (WFNS) scale at admission, and premorbid history of hypertension [5]. However, these models do not take into account the inflammatory response after SAH, which is considered to play a key role in the pathogenesis of early brain injury and delayed cerebral ischemia after aneurysmal SAH [6,7]. The inflammatory response after SAH is independently associated with poor clinical condition on admission, delayed cerebral ischemia, disability, and death [6,8,9]. The inflammatory response in the brain is reflected by the activation of microglia and astrocytes [10]. The complement system may be a major component of this acute injury induced neuroinflammation after aneurysmal SAH. The classical pathway of the complement system is initiated by C1q, which then activates a cascade of other soluble or membrane bound proteins. Activation of the complement system leads to the cleavage of C5, resulting in C5a and the lytic C5b-9 membrane attack complex. Anaphylatoxins C3a and C5a are important proinflammatory mediators and have the potential to produce vasoconstriction and activate coagulation by aggregation of platelets and regulation of tissue factor activity [11–15]. All these processes occur after aneurysmal SAH and are associated with early brain injury and delayed cerebral ischemia [16–21]. Plasma levels of mannose-binding lectin, C3a and C5a early after SAH correlate with outcome at discharge [22,23]. Despite the observed associations between complement activation and measures of brain injury after SAH, it remains unclear if these are causal relationships. If so, this would represent an appealing target to decrease

brain injury and improve prognosis after SAH.

We investigated the role of complement activation after SAH. In an autopsy study, we examined local complement expression in brains of patients who died from aneurysmal SAH. We evaluated the association between common complement component polymorphisms and functional outcome and delayed cerebral ischemia, and elucidated the time-course of complement activation in CSF and plasma after SAH using serial measurements. We then confirmed our results in a SAH mouse model and studied whether treatment with a C5-specific monoclonal antibody affects brain injury after SAH.

Methods

Autopsy study
We used autopsy material from seven SAH patients (two males, five females, median age 56 years (range 34-77 years)) who died within 11 days after aneurysmal SAH. All patients had delayed cerebral ischemia [3]. We isolated cortical areas with both white and grey matter. From autopsy material from five control patients (three males, two females, median age 72 years (range 52-75 years)) who died from non-neurological causes (myocardial infarction: n=3; heart failure: n=1; pulmonary embolism: n=1) we isolated corresponding areas. Sections were stained with hematoxylin and eosin to distinguish infarcted from non-infarcted areas. For analysis, only non-infarcted areas were used. Complement component C1q acts as the initiating molecule in the classical pathway of the complement cascade, whereas C3b and iC3b are biologically active fragments of C3, a central molecule in the complement system. Deposition of C3/C3b/iC3b in the tissue indicates that the complement pathway reached a proinflammatory state [24]. We performed immunohistochemistry to investigate the presence of C1q (Polyclonal Rabbit, anti-human C1q complement, #F0254, DAKO, 1:200) and C3/C3b/iC3b (Polyclonal Rabbit, Anti-human C3c complement, #F0201, DAKO, 1:100). We were unable to evaluate the presence of C5a or C5b-9 (Membrane Attack Complex), as these antibodies do not work on the paraffin embedded post-mortem material. The immunohistochemistry of C1q and C3/C3b/iC3b on human brain sections resulted in heterogenous staining patterns, as shown in high magnification (100x) images in Supplementary Figure 1. Optical density measurements were used for quantitative assessments. Images were analyzed with FIJI software (ImageJ 2.0.0). After manually selecting the entire

non-infarcted area per brain slide, selections were automatically quantified, expressed as a mean total of -log transformed grey scales, to calculate a mean per patient. The investigators who analysed the immunohistochemistry images were blinded to the experimental group.

Genotyping study

The cohort of the genetic study consisted of 930 patients who were admitted between 1983 and 2011 to the University Medical Center Utrecht, the Netherlands, which is a tertiary referral center for patients with SAH (Table 1). We used the University Medical Center Utrecht Subarachnoid Hemorrhage database, which is a prospectively collected database of consecutive patients with confirmed SAH, to collect the following variables: age, sex, clinical condition on admission according to the WFNS grading scale [25], aneurysm location, the occurrence of rebleeding and delayed cerebral ischemia, and functional outcome. After centrifugation of blood samples, the cell pellets were used to extract DNA for genotyping. The primary outcome was poor functional outcome, which was defined as a Glasgow Outcome Scale score of 1-3, three months after ictus [26]. Secondary outcome was clinical deterioration due to delayed cerebral ischemia, for which we used the definition that was proposed by an international multidisciplinary research group [3]. The occurrence of rebleeding was recorded between admission and aneurysm treatment, and defined as a sudden clinical deterioration with signs of increased hemorrhage on CT scan compared with previous CT imaging or found at autopsy, or a sudden clinical deterioration suspect for rebleeding with fresh blood in the ventricular drain in which no CT scan or autopsy was obtained. During collection of clinical data, the investigators were blinded for the results of genotyping.

Genotyping

The following common allele variants with a frequency of >5% were investigated: C3 rs1047286, C3 rs2230199 and C5 rs17611. Genotyping was done using TaqMan SNP Genotyping Assays with the Lightcycler® 480. In case of unsuccessful genotyping of C5 rs17611, we used data from a previous Genome Wide Association Study, which partly included the same patients as in the present study [27]. Due to the supplementary Genome Wide Association Study data, genotype success rate for the C5 rs17611 SNP increased from 94.1% to 98.0%. Genotyping was performed on coded DNA samples, so clinical information remained unknown to the laboratory personnel.

Table 1. Patient characteristics.

	Cohort (N=930)
Median age (year, Interquartile range)	50 (43-59)
Female sex (number, %)	653 (70)
WFNS grading scale on admission (number/total, %) **1** **2** **3** **4** **5**	 481/905 (53) 188/905 (21) 60/905 (7) 115/905 (13) 61/905 (7)
Location of aneurysm in anterior circulation (number/total, %)	802/911 (88)
In-hospital complications (number/total, %) **Rebleeding** **Clinical deterioration due to Delayed cerebral ischemia**	 125/914 (14) 174/913 (19)
Glasgow Outcome Scale Score at 3 months (%) **1. Death** **2. Vegetative state** **3. Severe disability** **4. Moderate disability** **5. Good recovery**	 73 (8) 4 (0) 112 (12) 224 (24) 517 (56)

C5a levels in plasma of genotyped patients

To determine the relationship between the C5 rs17611 SNP and C5a levels in plasma, we used plasma samples in a subset of 229 patients who presented with aneurysmal SAH between 2007 and 2011 (63 males, 176 females, median age 57 years (range 19-88 years)). Blood samples were obtained in EDTA tubes between days 1 to 14 after ictus. The samples were centrifuged and C5a levels in plasma were measured with the use of Human Complement C5a ELISA Kit (LifeSpan Biosciences) according to the manufacturers' instructions.

Serial measurement of C5a in CSF and plasma

We performed serial blood withdrawals in 31 patients with aneurysmal SAH (13 males, 18 females, median age 53 years (range 32-74 years)) and single measurements in 17 healthy control patients (6 males, 11 females, median age 53 years (range 30-63 years)). Blood samples in SAH patients were ob-

tained in citrate tubes on days 1, 3, 5, 7, 10, 14 and 17 (+/- 1 day), with day of ictus defined as day 0. The samples were centrifuged and plasma C5a levels were measured with the use of a C5a EIA kit (Quidel) according to the manufacturers' guidelines (standard curves R^2 ranging from 0.9998 to 1, lower limit of detection: 0.05 ng/ml).

CSF samples were collected from 10 patients with aneurysmal SAH (three males, seven females, median age 57 years (range 41-75 years)) and three controls in whom CSF was collected during surgery for an unruptured aneurysm (one male, two females, ages: 49, 60 and 60 years). In 6 patients, CSF samples were collected from external ventricular drains and in 4 patients from lumbar drains. CSF was sampled on days 1, 3, 5, 7, 10, 12 and 14 after SAH with day of ictus defined as day 0. All CSF samples were immediately centrifuged upon collection, and the supernatants were stored at −80 °C until analysis. C5a levels were measured with the use of a C5a EIA kit (Quidel) according to the manufacturers' guidelines.

SAH animal model

To model SAH in mice, we applied the prechiasmatic blood injection model as described previously, with injection of 60 µL of blood in the prechiasmatic cistern [28,29]. Body temperature was maintained at 37 °C. Cerebral blood flow was measured between 7.5 min prior to and up to 15 min after blood injection, with a laser Doppler flow meter (BLF22; Transonics Systems, New York, NY, USA). The success of SAH creation was confirmed by a sharp reduction in cerebral blood flow during blood injection. Mean cerebral blood flow during blood injection dropped to ≤25% of baseline in all groups, which is a reflection of an acute increase in intracranial pressure that is also seen in patients with aneurysmal SAH. Mice were killed 48 hours after blood injection. After intracardiac perfusion-fixation with 4% paraformaldehyde in PBS, brains were removed and post-fixed for 48 hours in 4% paraformaldehyde in PBS, pH7.4. Coronal cuts were made with a mouse brain matrix (Zivic Instruments, Pittsburgh, PA, USA). Slices were dehydrated and embedded in paraffin, and cut into 7-µm sections with a microtome.

The following experimental groups were investigated: (a) wildtype (WT) mice (BALB/c, male, n=15) with prechiasmatic injection of 60 µL of blood from a donor WT mouse (BALB/c, male, n=15); (b) WT mice (BALB/c, male, n=15) with prechiasmatic injection of 60 µL of blood from a donor WT mouse

(BALB/c, male, n=15) and with a subsequent intraperitoneal injection of a neutralizing monoclonal antibody directed against murine C5 (20 min after creation of SAH, 1 mg per mouse; clone BB5.1; [30]; and (c) *C5aR*$^{-/-}$ mice (C.129S4(B6)-*C5ar1*^{tm1Cge}/J, 15 times back crossed to BALB/c, obtained from the Jackson Laboratory, male, n = 15) with prechiasmatic injection of 60 µL of blood from a donor *C5aR*$^{-/-}$ mouse, male, n=15). All mice were 2 months of age. The experiments were performed in random order.

Immunocytochemistry
Iba1 and cleaved caspase-3 immunofluorescence imaging was performed on coronal 7-µm sections that were taken 3 mm anterior to the cerebellum of the mice. Iba1 (polyclonal rabbit, 1:4000, #019-19741, Wako), cleaved caspase 3 (polyclonal rabbit, Antibody #9661, 1:100, Cell Signalling) and NeuN (monoclonal, 1:500, Mab377, Chemicon) were used as primary antibodies. Hoechst 33258 (1:1000, Sigma-Aldrich) was used to visualize cell nuclei. We selected four predefined areas of cerebral cortex to quantify protein expression. Images were taken with the use of an epifluorescence microscope (20x objective, Axio Scope A1, Zeiss) and processed with the use of Axiovision (Zeiss). We calculated the threshold area percentage of Iba1 positive cells with the use of FIJI software (ImageJ, NIH). The investigators who analysed Iba1 and cleaved caspase 3 positive cells were blinded to the experimental group.

Statistical analysis – autopsy study
Optical density values were presented as mean with SEM, compared between areas of SAH patients and controls, and analysed with a Student's t-test for the C1q analysis, and a Mann Whitney test for the C3/C3b/iC3b analysis.

Statistical analysis – genetic analysis
The number of patients in our cohort (n=930) was based on a variant with a minor allele frequency of 0.36 and a study power of >80%, to detect an association of the variant with poor functional outcome with an odds ratio of ≥1.8 (http://pngu.mgh.harvard.edu/~purcell/gpc/). We calculated whether the genotype frequencies concurred with the Hardy-Weinberg equilibrium by use of an X^2 test with one degree of freedom with a p-value of less than 0.05 to indicate significance. Differences in genotype frequencies were analysed with a two-tailed X^2 test. Statistical analyses were performed with SPSS

version 20.0 for Windows (IBM, Armonk, New York, USA). We calculated odds ratios with 95% confidence intervals, and performed logistic regression analyses with adjustments for age, sex and WFNS grading scale on admission to calculate adjusted odds ratio. C5a levels per genotype of the C5 SNP rs17611 were analysed by the Kruskal-Wallis test followed by Dunn's multiple comparison test. Correlation between plasma C5a levels and functional outcome 3 months after ictus, measured with the Glasgow Outcome Scale, was analysed by Partial Spearman's Rho correlation test, and controlled for WFNS grading scale score on admission.

Statistical analysis – serial C5a measurements in CSF and plasma
Concentrations were presented as mean with SEM. Means of each serial C5a measurement in plasma were compared with the mean of the controls, calculated with ANOVA followed by the Dunnett's multiple comparisons test. Each serial C5a measurement in CSF was compared with the controls, calculated with Kruskal-Wallis test, followed by the Dunn's multiple comparisons test.

Statistical analysis – animal experiments
The number of mice (n=15) was based on an assumed mortality rate of 6% (leaving 14 mice available for analysis), a minimum difference in extent of microglia/macrophage activation or cells undergoing apoptosis of 25% between groups with and without C5a ablation, a standard deviation of 20% in both groups, 5% error, and 80% power.

The results of Iba1 and cleaved caspase-3 immunofluorescence stainings were presented as means with SD. Differences between groups were calculated with Kruskal-Wallis test, followed by the Dunn's multiple comparisons test. Probability values of <0.05 were considered to be of statistical significance.

Results

Complement expression in brains of SAH patients
In autopsy brain tissue from SAH patients and controls, we found a higher expression in SAH patients compared to controls of complement component C1q (control mean±SEM: 0.129± 0.007, n=5; versus SAH mean±SEM: 0.155 ± 0.007, n=7; t=2,66 df=10; $p<0.05$, Fig. 1A and 1B) and complement compo-

nent C3/C3b/iC3b (control mean±SEM: 0.114±0.001 versus SAH mean±SEM: 0.148±0.005; U=0, p<0.01, Fig. 1C and 1D). These results show that C1q and C3/C3b/iC3b immunoreactivity is increased in the brain after SAH.

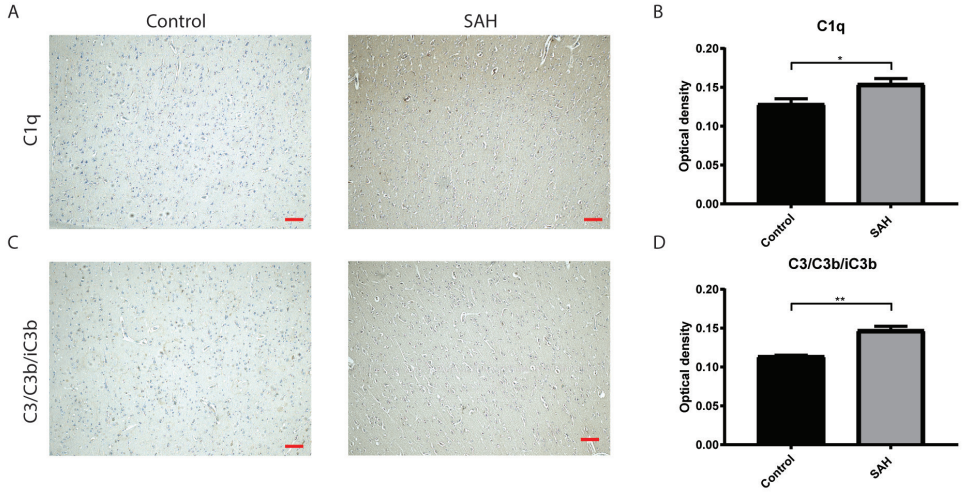

Figure 1. Complement expression in human autopsy brain sections. A) Representative images of immunohistochemical staining of C1q on autopsy brain sections of a control patient, and a subarachnoid hemorrhage patient; B) Average optical density measurements of C1q; C) Representative images of immunohistochemical staining of C3/C3b/iC3b on autopsy brain sections of a control patient, and a subarachnoid hemorrhage patient; D) Average optical density measurements of C3/C3b/iC3b. Scale bar: 100µm, Student's t-test; * p=<0.05; ** p=<0.01; mean±SEM.

Genetic association study of common allele variants of the complement C3 and C5 genes

Inter-individual differences in the inflammatory response resulting from common polymorphisms in the complement system may explain part of the heterogeneity in disease severity and outcome following aneurysmal SAH. Previously, it was shown that these polymorphisms are involved in central nervous system inflammation [31]. We performed a genetic association study to investigate if common allele variants in C3 and C5 genes are associated with functional outcome and delayed cerebral ischemia. Characteristics of the 930 patients included in the genetic study are shown in Table 1. Poor functional outcome, measured by the Glasgow Outcome Score 1-3 at three months, occurred in 189 of the 930 patients (20%). Data on genotyping success rate are shown in Table 2. All genotype frequencies were in concurrence with the Hardy-Weinberg equilibrium.

Table 2. Allele frequency, Hardy-Weinberg equilibrium and genotyping success rate of common complement component polymorphisms in 930 patients with aneurysmal subarachnoid hemorrhage

Gene	SNP ID	A %	B %	AA	AB	BB	HWE p-value	Success rate
C3	rs1047286	80.1%	19.9%	545	267	35	p=0.750	91 %
C3	rs2230199	77.6%	22.4%	590	277	37	p=0.534	97 %
C5	rs17611	43.7%	56.3%	182	432	297	p=0.274	98 %

HWE= Hardy-Weinberg equilibrium; SNP= Single Nucleotide Polymorphism.

The relationship between genotyping and outcome is shown in Table 3. The C3 SNP frequencies were similar in patients with poor and good functional outcome, and in patients with and without delayed cerebral ischemia. The C5 rs17611 allele A was associated with poor functional outcome (Odds Ratio 1.49; 95% Confidence Interval: 1.04-2.14; adjusted Odds Ratio 1.53; 95% CI: 1.02-2.28; Table 3), but not with delayed cerebral ischemia (Odds Ratio 1.09; 95% CI 0.78-1.52; adjusted Odds Ratio 1.10; 95% Confidence Interval 0.79-1.55; Table 4).

Since the C5 rs17611 allele A was associated with poor functional outcome, we subsequently measured plasma C5a levels in 229 genotyped patients with SAH in blood samples drawn between days 1 and 14 after the hemorrhage. Patients carrying allele A of the C5 rs17611 SNP had lower plasma C5a levels (Genotype AA median: 5.3 ng/ml [95% Confidence Interval: 5.3-7.1 ng/ml]; AG median: 13.0 ng/ml [95% Confidence Interval: 13.1-16.0 ng/ml]; GG median: 19.3 ng/ml [95% Confidence Interval: 18.2-25.9 ng/ml; H= 117.9, $p<0.0001$, Fig. 2A). No correlation was found between plasma C5a levels and poor functional outcome, measured by the Glasgow Outcome Scale, 3 months after subarachnoid hemorrhage (Partial Spearman's Rho correlation: -0.09, p=0.16, controlled for WFNS grading scale on admission).

Table 3. Genotyping analysis of common complement component polymorphisms in 741 patients with favourable outcome and 189 patients with unfavourable outcome.

Gene	Allele	SNP ID	Favourable outcome			Unfavourable outcome			OR (95%CI)	aOR (95%CI)
			AA	AB	BB	AA	AB	BB		
C3	**C**/T	rs1047286	422	220	27	123	47	8	1.31 (0.92-1.87)	1.46 (0.98-2.17)
C3	**C**/G	rs2230199	462	227	28	128	50	9	0.84 (0.59-1.18)	0.75 (0.51-1.11)
C5	**A**/G	rs17611	144	333	249	38	99	48	1.49 (1.04-2.14)	1.53 (1.02-2.28)

aOR= adjusted odds ratio (adjusted for gender, age at time of ictus, and WFNS grading scale on admission); CI= confidence interval; OR= odds ratio; SNP= Single Nucleotide Polymorphism. Allele in bold is used for analysis

Table 4. Genotyping analysis of common complement component polymorphisms in 725 patients without DCI and 169 patients with DCI.

Gene	Allele	SNP ID	No DCI			DCI			OR (95%CI)	aOR (95%CI)
			AA	AB	BB	AA	AB	BB		
C3	**C**/T	rs1047286	432	214	28	103	47	7	0.93 (0.67-1.30)	0.95 (0.67-1.33)
C3	**C**/G	rs2230199	467	222	29	113	49	7	1.11 (0.80-1.53)	1.10 (0.79-1.53)
C5	**A**/G	rs17611	152	334	239	27	91	51	1.09 (0.78-1.52)	1.10 (0.79-1.55)

aOR= adjusted odds ratio (adjusted for gender, age at time of ictus and WFNS grading scale on admission); CI= confidence interval; DCI= delayed cerebral ischemia; OR= odds ratio; SNP= Single Nucleotide Polymorphism. Allele in bold is used for analysis

Serial C5a measurements in CSF and plasma of subarachnoid hemorrhage patients

We investigated the time-course of plasma C5a levels in 31 patients with aneurysmal SAH. Blood samples were taken at days 1, 3, 5, 7, 10, 14, and 17 (+/- 1 day) after aneurysmal SAH. Plasma C5a levels steadily increased with a peak on day 5 after SAH (control mean±SEM: 7.8±0.9 ng/ml; SAH day 5 mean±SEM: 17.9±2.0 ng/ml, F= 3.305, $p<0.01$) and dropped thereafter (Fig. 2B). Furthermore, we used serial CSF samples from 10 patients with aneurysmal SAH up to day 14 after ictus and single CSF samples from 3 controls with unruptured aneurysms. The CSF levels of C5a were >1400 times increased 1 day after aneurysmal SAH (control mean±SEM: 0.05±0.03 ng/ml; SAH day 1 mean±SEM: 71.9±26.4 ng/ml, H=23.21, $p<0.001$) and slowly decreased over time (Fig. 2C). These data show that complement activation is strongly increased in the acute phase of SAH, in particular in the central nervous system.

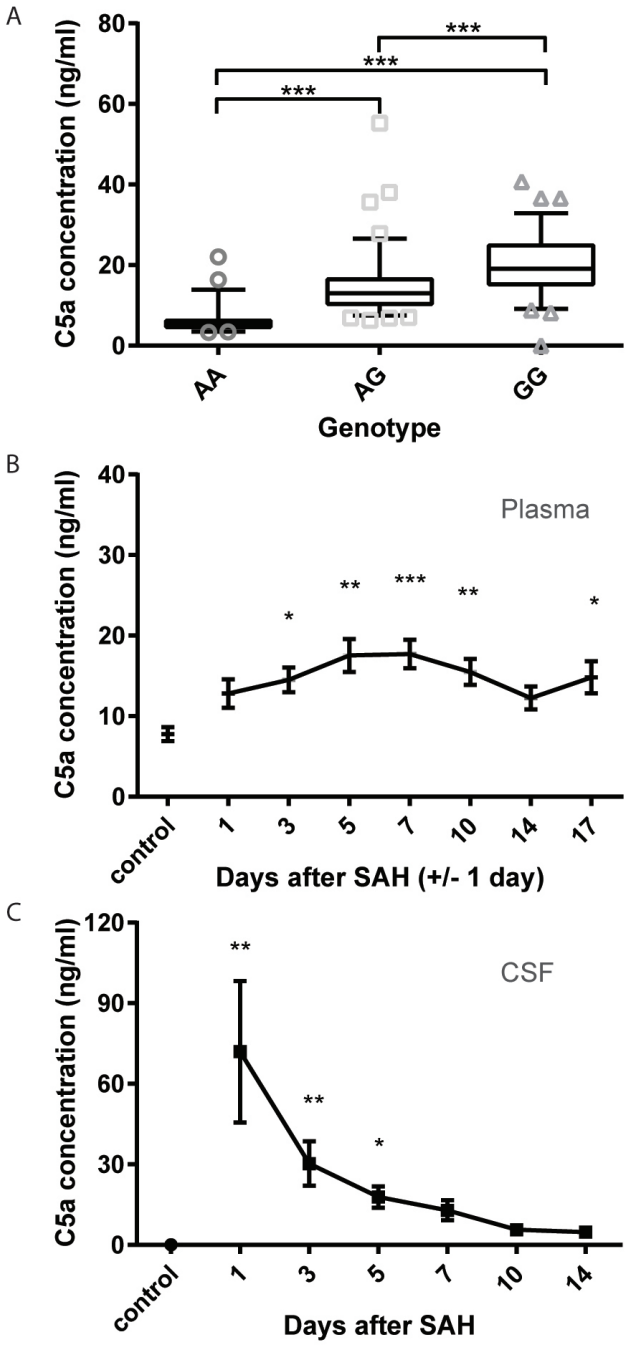
A
C5a concentration (ng/ml)
80
60
40
20
0
***
***
***
AA
AG
GG
Genotype
B
C5a concentration (ng/ml)
40
30
20
10
0
Plasma
*
**
***
**
*
control
1
3
5
7
10
14
17
Days after SAH (+/- 1 day)
C
C5a concentration (ng/ml)
120
90
60
30
0
CSF
**
**
*
control
1
3
5
7
10
14
Days after SAH

< Figure 2. C5a levels measured in plasma and CSF of aneurysmal subarachnoid hemorrhage patients. A) Plasma C5a levels (ng/ml) of genotyped patients, grouped per genotype of the C5 Single Nucleotide Polymorphism rs17611; blood samples were obtained between day 1 and day 14 post-subarachnoid hemorrhage; AA; n=53, AG; n=98, GG; n=78; Kruskal-Wallis, Dunn's multiple comparison, ***p=<0.001, median±5-95 percentile. B) Sequentially measured C5a levels in plasma of aneurysmal subarachnoid hemorrhage patients (n=31), versus plasma C5a levels of healthy controls (n=17). Blood samples were taken on days 1, 3, 5, 7, 10, 14, and 17 (+/- 1 day) after subarachnoid hemorrhage. * p=<0.05, ** p=<0.01, *** p=<0.001, ANOVA, Dunnett's post-hoc; mean±SEM. C) Sequentially measured C5a levels in CSF of aneurysmal subarachnoid hemorrhage patients (n=10) versus CSF C5a levels of patients with an unruptured aneurysm (n=3). CSF obtained on days 1, 3, 5, 7, 10, 12 and 14 after subarachnoid hemorrhage. * p=<0.05, ** p=<0.01, Kruskal-Wallis test, Dunn's post-hoc; mean±SEM.

Functional analysis of the role of C5 and C5a in an SAH mouse model

To investigate if C5 contributes to brain injury after SAH and to study the effect of C5-specific antibodies on the extent of brain injury, we used 3 groups of mice in which SAH was created with the prechiasmatic blood injection model [29]. We assessed microglia/macrophage activation and cell death 48 hours after SAH induction. We found that Iba1 expression, a microglia/macrophage marker, was reduced in the $C5aR^{-/-}$ mice compared to wildtype controls. Moreover, the mice treated with C5 specific antibody showed similar reduction in Iba1 expression ($C5aR^{-/-}$ mean±SD: 6.3±0.9%; control BALB/c mean±SD: 10.8±2.1%; C5 antibody treated mice mean±SD: 6.7±1.0%; Kruskal-Wallis, Dunn's post-hoc, H=22.9, p=<0.001; Fig. 3A; quantified in Fig. 3C), indicating a reduced activation of microglia/macrophages, the innate immune cells of the brain. No difference in Iba1 expression between the $C5aR^{-/-}$ and C5 antibody treated wildtype mice was found, showing the potency of this treatment. Furthermore, the density of cells positive for cleaved caspase 3, marker for cells undergoing apoptosis, was reduced to a similar degree in the $C5aR^{-/-}$ mice and mice treated with C5 antibody compared to wild type controls ($C5aR^{-/-}$ mean±SD: 28±24; C5 antibody treated BALB/c mean±SD: 26±16; control BALB/c mean±SD: 47±22; Kruskal-Wallis, Dunn's post-hoc, H=8.6, p=<0.05; Fig. 3B; quantified in Fig. 3D), indicating a reduction in the number of cells undergoing apoptosis. The majority of cleaved caspase 3 positive cells were also positive for NeuN, a neuronal marker (Fig. 3B).

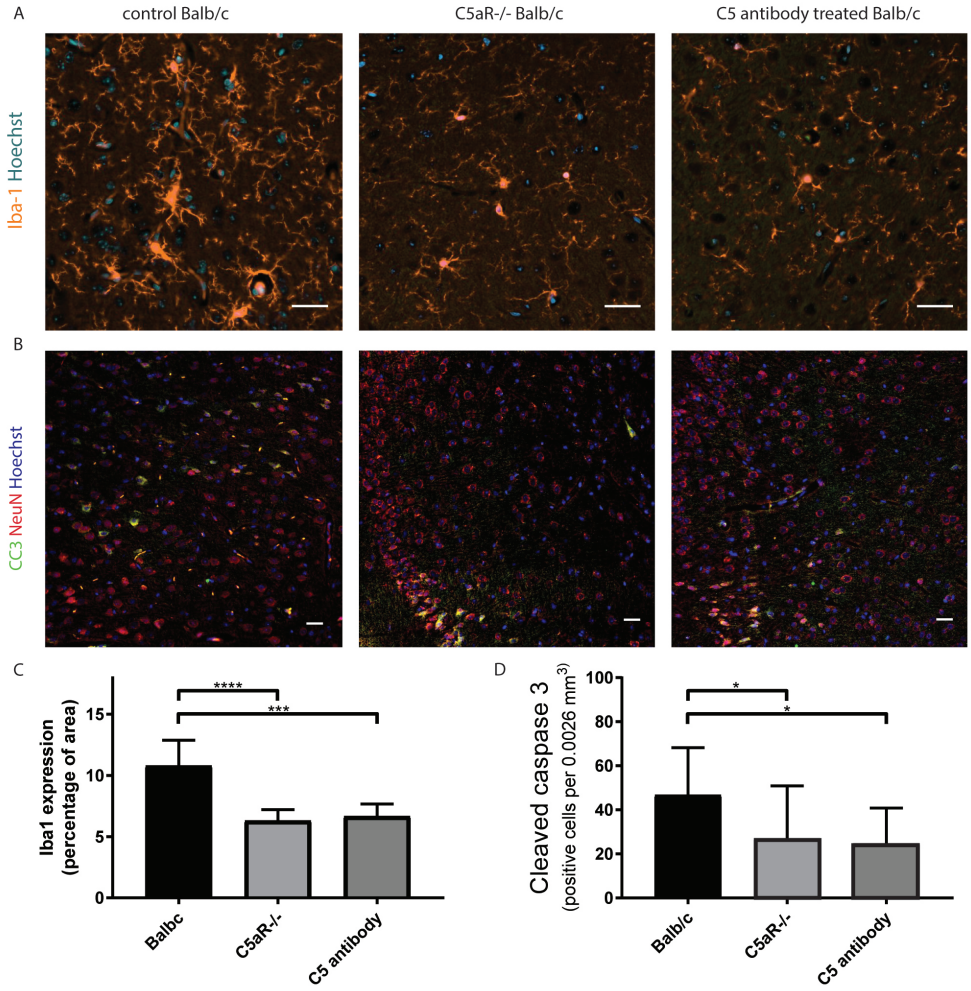

Figure 3. C5 antibody treatment reduces brain injury in experimental subarachnoid hemorrhage. A) Representative images of mouse cortex stained with antibody against Iba-1 (orange); cell nuclei in blue (Hoechst). B) Representative images of mouse cortex stained with antibody against Cleaved caspase 3 (CC3; green); NeuN (red) and cell nuclei in blue (Hoechst). C) C5a receptor deficient ($C5aR^{-/-}$) and wildtype mice treated with C5-specific antibodies had a >38% reduction in microglia/macrophage activation compared to untreated wildtype mice. Kruskal-Wallis, Dunn's post hoc; D) $C5aR^{-/-}$ mice and control BALB/c mice treated with C5-specific monoclonal antibodies had >39% reduction in cells undergoing apoptosis, compared to untreated wildtype mice 48 hours after subarachnoid hemorrhage. Kruskal-Wallis, Dunn's post hoc; n=15 mice per group; ****p=<0.0001, ***p=<0.001, *p=<0.05; mean±SD; scale bars: 30 µm.

Discussion

We are the first to show in a multilevel approach that complement factor C5 contributes to brain injury after SAH. We showed that the complement system is activated in the brain following SAH, as reflected by the increased immunoreactivity for C1q and C3/C3b/iC3b in brain tissue of patients who died after SAH compared with brain tissue of patients who died from non-neurological causes. C5 rs17611 SNP correlated with functional outcome after SAH and with plasma C5a levels, and that C5a levels in CSF were markedly increased on day 1 after ictus and gradually decreased within the next two weeks. Plasma C5a levels were increased at a later stage, with a peak concentration around days 3-10 after ictus. In a mouse model of SAH, mice lacking C5a receptor had a ≈40% reduction of brain injury as reflected by reduced microglia/macrophage activation and cell apoptosis. This indicates that C5a is involved in the pathogenesis of brain injury after experimental SAH. Similarly, mice treated with C5 neutralizing antibodies directly after the hemorrhage had reduced brain injury. As the mice were treated short after the induction of SAH and sacrificed two days after SAH, this suggests that the inhibition of C5 has a long-lasting effect. These data indicate that C5 antibodies may be a promising new treatment option to decrease brain injury. Importantly, C5 antibodies are already used for other clinical indications [32–34]. Furthermore, studies showed that C5 antibodies are a promising new treatment option for patients with other neurological diseases, such as pneumococcal meningitis, neuromyelitis optica, and myasthenia gravis [31,35,36].

The C5 rs17611 SNP correlated with poor functional outcome. This SNP has also been linked to poor outcome after pneumococcal meningitis [31], adverse cardiovascular outcomes [37] and periodontitis [38]. Recently, the functional basis for these disease associations was clarified [39]. Allele G of the C5 rs17611 SNP causes a missense mutation in the C5 gene, increases the rate of proteolytic activation of C5 and C5a generation. As a result, patients carrying allele G have increased C5a plasma levels [39]. This is in accordance with the results from our study, in which we found that patients carrying allele G of the C5 rs17611 SNP had higher plasma C5a levels than patients with allele A. Although patients with allele A had lower plasma C5a levels and were at increased risk of poor functional outcome, the plasma levels were not correlated with poor functional outcome. Since complement

activation was much stronger upregulated in the CSF than in plasma, it remains to be investigated if C5a levels in CSF correlate better with functional outcome than C5a levels in plasma.

There are a number of mechanisms by which complement activation can contribute to brain injury. The complement system has been linked to the regulation of synapse numbers [40]. In particular, complement components C1q and C3 have been implicated to facilitate the removal of synapses [41]. Unwanted synapses are tagged with C1q and C3, thereby becoming eligible for elimination. Microglia recognize these components and start to remove the synapse [42]. Synaptic pruning by microglia occurs during development, but also in diseases such as glaucoma and Alzheimer's disease and after viral infection[41,43,44]. Therefore, complement activation in response to SAH may also induce excessive synapse pruning. However, while early complement components are involved in synapse elimination, the involvement of downstream components, such as C5 and C5a, remain to be investigated. Another mechanism by which complement activation may contribute to brain injury is by the membrane attack complex, formed by C5b-C9 complexes. Hemolysis of blood in the CSF is thought to be complement system mediated by activation of the membrane attack complex [45,46]. The membrane attack complex may also bind bystander cells, such as endothelial cells, ependymal cells and other brain cells, and thereby induce brain injury.

To address the specific involvement of C5 and C5a in brain injury after SAH, we used *C5aR*$^{-/-}$ and wildtype mice treated with neutralizing antibody against C5. While the antibody treatment inhibits the generation of both activation products of C5, namely C5a and C5b, only the C5aR-mediated functions of C5a are absent in the *C5aR*$^{-/-}$ mice. Our experimental data show that apoptosis and microglia activation are reduced in mice lacking C5aR as well as mice treated with a single dose of neutralizing antibody against C5. These findings provide evidence for the detrimental role of C5a in brain injury after SAH and are in line with previous studies in which C5aR deficiency as well as treatment with a C5aR antagonist resulted in reduced apoptosis, increased cell viability and reduced infarct volume after ischemic stroke [47,48]. As C5a promotes neuronal apoptosis by acting directly through neuronal C5aR *in-vitro* [48], it is conceivable that the same neuronal mechanism is involved in brain injury after SAH.

C5aR is also expressed by microglia which upregulate C5aR in response to injury [49–51]. Thus, the reduced activation of microglia in the *C5aR*$^{-/-}$ and anti-C5 antibody treated mice may not only be an indirect effect of reduced cell death but may also be explained by direct effects of the intervention on these cells. In experimental spinal cord injury, C5aR signaling in the acute phase has been shown to contribute to tissue damage through local proinflammatory cytokine production and the recruitment of inflammatory monocytes/macrophages [52]. As Iba1 is expressed in microglia as well as in blood born monocytes/macrophages, it is possible that recruited inflammatory cells together with activated microglia play a role in SAH-induced brain injury.

The effects of C5a in the context of brain tissue injury may not be solely detrimental. C5a has been shown to be neuroprotective during neuronal maturation [53] and to protect neurons against glutamate-mediated toxicity [54]. Through the upregulation of microglial glutamate receptor GLT-1, C5a can also increase the capacity of microglia to clear excessive glutamate [55]. In addition, in the post-acute stage after spinal cord injury, signaling through the C5a-C5aR axis appears to serve a protective and/or reparative role [52]. Thus, in light of the potential beneficial effects of C5a, the timing of the therapeutic intervention targeting C5aR after SAH may need to be carefully determined.

Interestingly, C5a can bind to Gpr77, also termed C5a-like receptor 2 (C5L2; [56]). The function of C5L2 is controversial, as both pro- and anti-inflammatory properties of this receptor have been described [56]. Our results that C5aR deficiency and inhibition of C5 activation reduced brain injury to the same extent support the contention that the deleterious effects of C5a in the acute phase after SAH are mediated mainly by its canonical receptor C5aR. In addition to the release of C5a, the proteolytic activation of C5 triggers the formation of the membrane attack complex, C5b-9, leading to neuronal death through apoptosis [57] or cell lysis [55]. However, in light of our findings of the comparable effect of C5aR deficiency and anti-C5 antibody treatment, a substantial contribution of C5b-9 to brain injury after SAH appears unlikely.

There are potential limitations to our study. The human brain tissue used in the autopsy study was from deceased patients. The increased expres-

sion of complement C1q and C3/C3b/iC3b may not reflect the situation of patients with a more favorable outcome. However, the CSF used to measure C5 levels was of patients of both favorable and unfavorable outcomes, and showed a sharp increase in complement C5 levels after SAH. This suggests activation of the complement cascade both in good and poor grade SAH.

In conclusion, the present study highlights the role of C5a in the development of brain injury after SAH and identifies C5 antibodies as a potential novel treatment strategy to reduce brain injury after SAH.

Funding

This study was financially supported by a personal grant from the Dutch Heart Foundation to MDIV (2011T18).

Compliance with Ethical Standards

Written informed consent was obtained from all participating patients or their legally authorized representatives, and controls. Approval for the genetic study was obtained from the Institutional Research Ethics Board, University Medical Center Utrecht, Utrecht, the Netherlands. All procedures performed in studies involving human participants were in accordance with the ethical standards of the Institutional Research Ethics Board and with the 1964 Helsinki declaration and its later amendments or comparable ethical standards. All animal experiments were approved by the Institutional Animal Care and Use Committee of the Academic Medical Center, Amsterdam, the Netherlands.

Potential Competing Interests

A patent was filed by the University Medical Center Utrecht, based on the data described in this manuscript (Methods of reducing brain injury after aneurysmal subarachnoid hemorrhage using anti-C5 or anti C5a antibodies [application number 62820860]).

References

1. Vergouwen MD, Jong-Tjien-Fa AV, Algra A, Rinkel GJ. Time trends in causes of death after aneurysmal subarachnoid hemorrhage: A hospital-based study. Neurology. 2016;86:59–63.

2. Roos YB, de Haan RJ, Beenen LF, Groen RJ, Albrecht KW, Vermeulen M. Complications and outcome in patients with aneurysmal subarachnoid haemorrhage: a prospective hospital based cohort study in the Netherlands. J Neurol Neurosurg Psychiatry. 2000;68:337–41.

3. Vergouwen MD, Vermeulen M, van Gijn J, Rinkel GJ, Wijdicks EF, Muizelaar JP, et al. Definition of delayed cerebral ischemia after aneurysmal subarachnoid hemorrhage as an outcome event in clinical trials and observational studies: proposal of a multidisciplinary research group. Stroke. 2010;41:2391–5.

4. Dorhout Mees S, Rinkel GJ, Feigin VL, Algra A, van den Bergh WM, Vermeulen M, et al. Calcium antagonists for aneurysmal subarachnoid haemorrhage. Cochrane Database Syst Rev [Internet]. John Wiley & Sons, Ltd; 2007. Available from: http://onlinelibrary.wiley.com/doi/10.1002/14651858.CD000277.pub3/abstract

5. Jaja BNR, Saposnik G, Lingsma HF, Macdonald E, Thorpe KE, Mamdani M, et al. Development and validation of outcome prediction models for aneurysmal subarachnoid haemorrhage: the SAHIT multinational cohort study. BMJ. 2018;j5745.

6. Yoshimoto Y, Tanaka Y, Hoya K. Acute systemic inflammatory response syndrome in subarachnoid hemorrhage. Stroke. 2001;32:1989–93.

7. Ibrahim GM, Morgan BR, Macdonald RL. Patient phenotypes associated with outcomes after aneurysmal subarachnoid hemorrhage: a principal component analysis. Stroke. 2014;45:670–6.

8. Dumont AS, Dumont RJ, Chow MM, Lin CL, Calisaneller T, Ley KF, et al. Cerebral vasospasm after subarachnoid hemorrhage: putative role of inflammation. Neurosurgery. 2003;53:123–33.

9. Dhar R, Diringer MN. The burden of the systemic inflammatory response predicts vasospasm and outcome after subarachnoid hemorrhage. NeurocritCare. 2008;8:404–12.

10. van Dijk BJ, Vergouwen MD, Kelfkens MM, Rinkel GJ, Hol EM. Glial cell response after aneurysmal subarachnoid hemorrhage - Functional consequences and clinical implications. BiochimBiophysActa. 2016;1862:492–505.

11. Bjork J, Hugli TE, Smedegard G. Microvascular effects of anaphylatoxins C3a and C5a. JImmunol. 1985;134:1115–9.

12. Saadi S, Holzknecht RA, Patte CP, Stern DM, Platt JL. Complement-mediated regulation of tissue factor activity in endothelium. JExpMed. 1995;182:1807–14.

13. Ikeda K, Nagasawa K, Horiuchi T, Tsuru T, Nishizaka H, Niho Y. C5a induces tissue factor activity on endothelial cells. ThrombHaemost. 1997;77:394–8.

14. Fortin JP, Bouthillier J, St-Pierre SA, Marceau F. Contractile effect of anaphylatoxin C5a and of a mimetic peptide on the human umbilical artery: further evidence for leukocyte-dependent vasomotion. JCardiovascPharmacol. 2002;40:815–21.

15. Guo RF, Ward PA. Role of C5a in inflammatory responses. AnnuRevImmunol. 2005;23:821–52.

16. Ohkuma H, Suzuki S, Kimura M, Sobata E. Role of platelet function in symptomatic cerebral vasospasm following aneurysmal subarachnoid hemorrhage. Stroke. 1991;22:854–9.

17. Hirashima Y, Nakamura S, Suzuki M, Kurimoto M, Endo S, Ogawa A, et al. Cerebrospinal fluid tissue factor and thrombin-antithrombin III complex as indicators of tissue injury after subarachnoid hemorrhage. Stroke. 1997;28:1666–70.

18. Hirashima Y, Nakamura S, Endo S, Kuwayama N, Naruse Y, Takaku A. Elevation of platelet activating factor, inflammatory cytokines, and coagulation factors in the internal jugular vein of patients with subarachnoid hemorrhage. NeurochemRes. 1997;22:1249–55.

19. Nissen JJ, Mantle D, Gregson B, Mendelow AD. Serum concentration of adhesion molecules in patients with delayed ischaemic neurological deficit after aneurysmal subarachnoid haemorrhage: the immunoglobulin and selectin superfamilies. JNeurolNeurosurgPsychiatry. 2001;71:329–33.

20. Frijns CJ, Kasius KM, Algra A, Fijnheer R, Rinkel GJ. Endothelial cell activation markers and delayed cerebral ischaemia in patients with subarachnoid haemorrhage. JNeurolNeurosurgPsychiatry. 2006;77:863–7.

21. Vergouwen MD, Bakhtiari K, van GN, Vermeulen M, Roos YB, Meijers JC. Reduced ADAMTS13 activity in delayed cerebral ischemia after aneurysmal subarachnoid hemorrhage. JCerebBlood Flow Metab. 2009;29:1734–41.

22. Mack WJ, Ducruet AF, Hickman ZL, Garrett MC, Albert EJ, Kellner CP, et al. Early plasma complement C3a levels correlate with functional outcome after aneurysmal subarachnoid hemorrhage. Neurosurgery. 2007;61:255–60.

23. Cai JY, Sun J, Yu ZQ. Serum mannose-binding lectin levels after aneurysmal subarachnoid hemorrhage. Acta NeurolScand. 2016;134:360–7.

24. Ricklin D, Lambris JD. Complement in immune and inflammatory disorders: therapeutic interventions. JImmunol. 2013;190:3839–47.

25. Teasdale GM, Drake CG, Hunt W, Kassell N, Sano K, Pertuiset B, et al. A universal subarachnoid hemorrhage scale: report of a committee of the World Federation of Neurosurgical Societies. JNeurolNeurosurgPsychiatry. 1988;51:1457.

26. Jennett B, Teasdale G, Braakman R, Minderhoud J, Knill-Jones R. Predicting outcome in individual patients after severe head injury. Lancet. 1976;1:1031–4.

27. Yasuno K, Bilguvar K, Bijlenga P, Low SK, Krischek B, Auburger G, et al. Genome-wide association study of intracranial aneurysm identifies three new risk loci. NatGenet. 2010;42:420–5.

28. Sabri M, Ai J, Lakovic K, Macdonald RL. Mechanisms of microthrombosis and microcirculatory constriction after experimental subarachnoid hemorrhage. Acta NeurochirSuppl. 2013;115:185–92.

29. Sabri M, Ai J, Lass E, D'Abbondanza J, Macdonald RL. Genetic elimination of eNOS

reduces secondary complications of experimental subarachnoid hemorrhage. JCerebBlood Flow Metab. 2013;33:1008–14.

30. Frei Y, Lambris JD, Stockinger B. Generation of a monoclonal antibody to mouse C5 application in an ELISA assay for detection of anti-CS antibodies. Mol Cell Probes. 1987;1:141–9.

31. Woehrl B, Brouwer MC, Murr C, Heckenberg SG, Baas F, Pfister HW, et al. Complement component 5 contributes to poor disease outcome in humans and mice with pneumococcal meningitis. JClinInvest. 2011;121:3943–53.

32. Hillmen P, Hall C, Marsh JC, Elebute M, Bombara MP, Petro BE, et al. Effect of eculizumab on hemolysis and transfusion requirements in patients with paroxysmal nocturnal hemoglobinuria. NEnglJMed. 2004;350:552–9.

33. Rother RP, Rollins SA, Mojcik CF, Brodsky RA, Bell L. Discovery and development of the complement inhibitor eculizumab for the treatment of paroxysmal nocturnal hemoglobinuria. NatBiotechnol. 2007;25:1256–64.

34. Legendre CM, Licht C, Muus P, Greenbaum LA, Babu S, Bedrosian C, et al. Terminal complement inhibitor eculizumab in atypical hemolytic-uremic syndrome. NEnglJMed. 2013;368:2169–81.

35. Howard JF Jr, Barohn RJ, Cutter GR, Freimer M, Juel VC, Mozaffar T, et al. A randomized, double-blind, placebo-controlled phase II study of eculizumab in patients with refractory generalized myasthenia gravis. Muscle Nerve. 2013;48:76–84.

36. Pittock SJ, Lennon VA, McKeon A, Mandrekar J, Weinshenker BG, Lucchinetti CF, et al. Eculizumab in AQP4-IgG-positive relapsing neuromyelitis optica spectrum disorders: an open-label pilot study. Lancet Neurol. 2013;12:554–62.

37. Hoke M, Speidl W, Schillinger M, Minar E, Zehetmayer S, Schonherr M, et al. Polymorphism of the complement 5 gene and cardiovascular outcome in patients with atherosclerosis. EurJClinInvest. 2012;42:921–6.

38. Chai L, Song YQ, Zee KY, Leung WK. Single nucleotide polymorphisms of complement component 5 and periodontitis. JPeriodontal Res. 2010;45:301–8.

39. Giles JL, Choy E, van den Berg C, Morgan BP, Harris CL. Functional analysis of a complement polymorphism (rs17611) associated with rheumatoid arthritis. JImmunol. 2015;194:3029–34.

40. Stephan AH, Barres BA, Stevens B. The Complement System: An Unexpected Role in Synaptic Pruning During Development and Disease. Annu Rev Neurosci. 2012;35:369–89.

41. Stevens B, Allen NJ, Vazquez LE, Howell GR, Christopherson KS, Nouri N, et al. The Classical Complement Cascade Mediates CNS Synapse Elimination. Cell. 2007;131:1164–78.

42. Weinhard L, di Bartolomei G, Bolasco G, Machado P, Schieber NL, Neniskyte U, et al. Microglia remodel synapses by presynaptic trogocytosis and spine head filopodia induction. Nat Commun [Internet]. 2018 [cited 2019 Jan 7];9. Available from: http://www.nature.com/articles/s41467-018-03566-5

43. Hong S, Beja-Glasser VF, Nfonoyim BM, Frouin A, Li S, Ramakrishnan S, et al. Complement and microglia mediate early synapse loss in Alzheimer mouse models. Science. 2016;352:712–6.

44. Vasek MJ, Garber C, Dorsey D, Durrant DM, Bollman B, Soung A, et al. A complement–microglial axis drives synapse loss during virus-induced memory impairment. Nature. 2016;534:538–43.

45. Park CC, Shin ML, Simard JM. The complement membrane attack complex and the bystander effect in cerebral vasospasm. J Neurosurg. 1997;87:294–300.

46. Peterson JW, Kwun B-D, Teramura A, Hackett JD, Morgan JA, Nishizawa S, et al. Immunological reaction against the aging human subarachnoid erythrocyte. J Neurosurg. 1989;718–26.

47. Kim GH, Mocco J, Hahn DK, Kellner CP, Komotar RJ, Ducruet AF, et al. Protective effect of C5a receptor inhibition after murine reperfused stroke. Neurosurgery. 2008;63:122–5.

48. Pavlovski D, Thundyil J, Monk PN, Wetsel RA, Taylor SM, Woodruff TM. Generation of complement component C5a by ischemic neurons promotes neuronal apoptosis. FASEB J. 2012;26:3680–90.

49. Gasque P, Singhrao SK, Neal JW, Gotze O, Morgan BP. Expression of the receptor for complement C5a (CD88) is up-regulated on reactive astrocytes, microglia, and endothelial cells in the inflamed human central nervous system. AmJPathol. 1997;150:31–41.

50. van Beek J, Bernaudin M, Petit E, Gasque P, Nouvelot A, MacKenzie ET, et al. Expression of receptors for complement anaphylatoxins C3a and C5a following permanent focal cerebral ischemia in the mouse. ExpNeurol. 2000;161:373–82.

51. Orre M, Kamphuis W, Osborn LM, Jansen AH, Kooijman L, Bossers K, et al. Isolation of glia from Alzheimer's mice reveals inflammation and dysfunction. NeurobiolAging. 2014;35:2746–60.

52. Brennan FH, Gordon R, Lao HW, Biggins PJ, Taylor SM, Franklin RJ, et al. The Complement Receptor C5aR Controls Acute Inflammation and Astrogliosis following Spinal Cord Injury. JNeurosci. 2015;35:6517–31.

53. Benard M, Gonzalez BJ, Schouft MT, Falluel-Morel A, Vaudry D, Chan P, et al. Characterization of C3a and C5a receptors in rat cerebellar granule neurons during maturation. Neuroprotective effect of C5a against apoptotic cell death. JBiolChem. 2004;279:43487–96.

54. Osaka H, Mukherjee P, Aisen PS, Pasinetti GM. Complement-derived anaphylatoxin C5a protects against glutamate-mediated neurotoxicity. JCell Biochem. 1999;73:303–11.

55. Persson M, Pekna M, Hansson E, Ronnback L. The complement-derived anaphylatoxin C5a increases microglial GLT-1 expression and glutamate uptake in a TNF-alpha-independent manner. EurJNeurosci. 2009;29:267–74.

56. Li R, Coulthard LG, Wu MC, Taylor SM, Woodruff TM. C5L2: a controversial receptor of complement anaphylatoxin, C5a. FASEB J. 2013;27:855–64.

57. Nauta AJ, Daha MR, Tijsma O, van de

Water B, Tedesco F, Roos A. The membrane attack complex of complement induces caspase activation and apoptosis. Eur J Immunol. 2002;32:783–92.

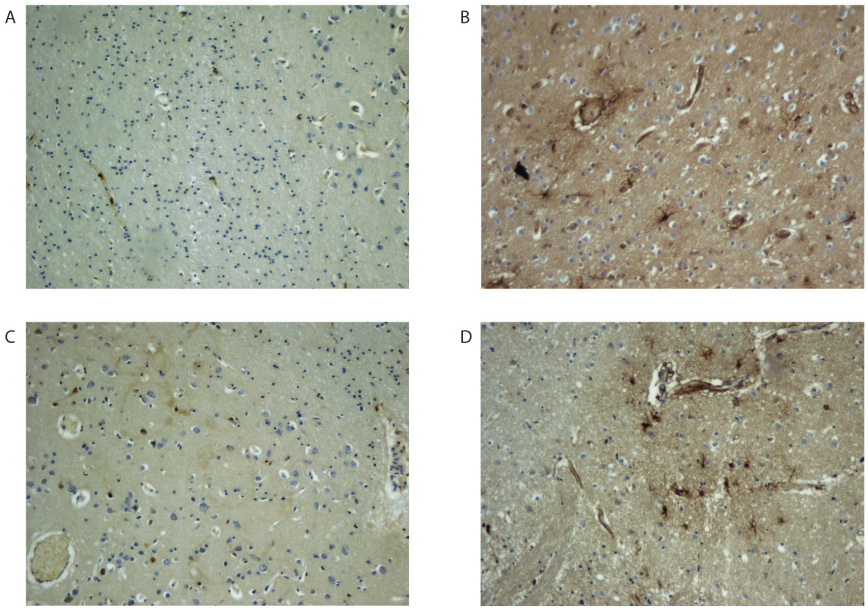

Supplementary Figure 1. Heterogenous complement expression in human autopsy brain sections. A) Image of immunohistochemical staining of C1q on autopsy brain sections of a control patient with only little immunoreactivity; B) Image of immunohistochemical staining of C1q on autopsy brain sections of a SAH patient with high immunoreactivity; C) Image of immunohistochemical staining of C3/C3b/iC3b on autopsy brain sections of a control patient with little immunoreactivity; D) Image of immunohistochemical staining of C3/C3b/iC3b on autopsy brain sections of a SAH patient with high immunoreactivity; 100x magnification

CHAPTER 3

Complement C3 is increased in astrocytes after subarachnoid hemorrhage with cognitive impairment.

B.J. van Dijk, MSc;[1,2] V. al-Naqib, MSc;[1] I. Koopman, MD;[2] I. Matias, PhD;[3] M.J. van der Kamp, MSc;[1] C.J. Frijns, PhD, MD;[2] J.A. Sluijs, BSc;[1] Z. Baldew, MSc;[1] D. Vonk, BSc;[1] G.J.E. Rinkel, PhD, FRCP(E);[2] M.D.I. Vergouwen, MD, PhD;*[2] E.M. Hol, PhD.*[1]

1. UMC Utrecht Brain Center, Department of Translational Neuroscience, University Medical Center Utrecht, Utrecht University, Utrecht, The Netherlands
2. UMC Utrecht Brain Center, Department of Neurology and Neurosurgery, University Medical Center Utrecht, Utrecht University, Utrecht, The Netherlands
3. Institute of Biomedical Sciences, Federal University of Rio de Janeiro, Rio de Janeiro, Brazil

* Shared last author.

Manuscript in preparation

Abstract
Aneurysmal subarachnoid hemorrhage (SAH) is a subtype of stroke that causes a high case fatality and morbidity. Patients who survive the initial weeks after the hemorrhage often have cognitive impairment, which reduces the quality of life substantially. The pathogenesis of the cognitive impairment in aneurysmal SAH survivors is poorly understood. Here, we studied the glial reaction in the post-mortem human frontal cortex of 11 aneurysmal SAH patients and 11 control patients, and found reactive astrocytes and active microglia after SAH. In the endovascular perforation SAH mouse model, which results in memory impairments after SAH, we studied the complement system-mediated activation of glia, which is associated with the detrimental effect of gliosis. In the hippocampal CA1 region of mice, the microglia were activated and the astrocytes expressed higher complement C3 after SAH than after sham operation, but these differences between SAH and control mice were not found in the prefrontal cortex. The expression levels of complement C3 within the hippocampal astrocytes correlated to memory impairments.

Introduction
Aneurysmal subarachnoid hemorrhage (SAH) is a severe subtype of stroke with a 90-day case-fatality rate of 30%. Patients who survive the initial weeks after the hemorrhage often have cognitive impairments, which can consist of reduced initiation of social interaction, impaired executive functions, anxiety, attention problems, and visual- and verbal memory loss *(1, 2)*. These impairments affect the daily practice of patients and reduce quality of life. The occurrence of these deficits are associated with the severity of the hemorrhage indicated by the clinical condition on admission, however, the deficits can also occur in patients that initially show a favorable prognoses *(1, 3)*. The pathogenesis of long-lasting cognitive impairment after SAH remains unclear. Reactive gliosis and complement activation may play a role in this *(4)*. Reactive gliosis is a response of microglia and astrocytes to central nervous system damage or disease *(5, 6)*. This immune response can be initially protective, but sustained activation of glial cells will affect normal brain functioning and becomes detrimental *(7)*. Moreover, astrocytes and microglia can become neurotoxic when the complement system, an immune initiating pathway, is also activated *(8)*. Microglia release a combination of cytokines, e.g. interleukin1-beta, tumor necrosis factor alpha, and comple-

ment component C1q, which induces a phenotypic switch in the astrocytes *(9)*. These astrocytes start producing more complement components and secrete neurotoxic agents. Another detrimental mechanism in which glia and early complement components are involved, is the pathological pruning of synapses *(10)*. Early complement components C1q, C3, and C4 can tag synapses. Microglia sense and remove these tagged synapses, a process called pruning. Therefore, prolonged reactive gliosis might be a maladaptive cellular response to SAH, as glia convert into a neurotoxic state contributing to excessive synapse pruning, and therefore reactive gliosis may induce cognitive deficits.

Upregulation of the complement cascade is associated with poor functional outcome after SAH. Levels of complement components C3a and C4 in plasma and cerebrospinal fluid of SAH patients correlates with poor functional outcome *(11)*. Furthermore, complement component C5 contributes to brain injury after aneurysmal subarachnoid hemorrhage *(12)*.

This study aims to determine reactive gliosis and the presence of complement components in glia after SAH in patient material. To provide mechanistic evidence on the interaction between gliosis and cognitive impairment after SAH, we used an SAH mouse model to investigate whether the glial response and complement activation is associated with cognitive impairment after SAH.

Materials and Methods

Human post mortem brain tissue

Post mortem brain tissue of 11 patients (2 males, 9 females, median age 71 years (range 45-85 years)), who died within 20 days after aneurysmal SAH was obtained from the pathology department of the University Medical Centre Utrecht. Detailed characteristics of SAH patients are shown in Table 1. The brain tissue originated from the medial frontal gyrus. Post mortem brain tissue from 11 non-demented neurological controls was provided by the Netherlands Brain Bank, and was obtained based on informed consent of the brain donor (3 males, 8 females, median age 72 years (range 47-84 years)). Detailed characteristics of control patients are shown in Table 2.

Table 1. Aneurysmal SAH patient characteristics.

Case	Sex	Age	WFNS score on admission	Number of rebleeds	Day of death after ictus	Aneurysm location
1	F	85	5	0	1	BA
2	M	70	5	3	20	Acom
3	F	54	2	1	1	Right pericallosal artery
4	F	74	1	2	17	Acom
5	F	79	4	0	1	Left MCA
6	F	71	4	0	8	Left ICA
7	F	74	2	2	18	Acom
8	F	74	4	0	1	Acom
9	F	67	5	0	6	Acom
10	F	61	2	1	9	Acom
11	M	45	1	4	9	Acom

WFNS: World Federation of Neurosurgical Surgeons; F: Female; M: Male; BA: Basilar artery; Acom: Anterior communicating artery; MCA: Middle cerebral artery; ICA: Internal carotid artery.

Table 2. Clinicopathological information of neurological control donors.

NBB number	Sex	Age (yrs)	Cause of death	Braak score	Amy-loid	PMD (h:min)	pH CSF
2001-077	f	47	Malignancy	1	0	04:00	6.9
2001-140	f	53	Respiratory failure	0	0	07:25	unknown
2014-043	f	60	Malignancy	0	0	08:10	6.6
2015-055	f	72	Malignancy	1	A	06:50	7.2
2000-127	f	76	Ischemic stroke	1	0	04:50	7.2
2011-072	f	76	Malignancy	2	0	07:15	6.9
2004-049	f	77	Renal failure	1	A	08:20	6.5
2009-042	f	84	Malignancy	1	0	06:55	unknown
2011-069	m	49	Malignancy	0	0	06:15	6.2
2005-034	m	56	Unknown	0	0	14:00	7.0
2005-044	m	80	Renal failure	0	0	07:15	5.8

PMD: post mortem delay of obduction, CSF: cerebrospinal fluid; Braak score: tau score for Alzheimer pathology, Amyloid: score for amyloid plaque pathology.

Endovascular perforation mouse model
All animal experiments were approved by the Institutional Animal Care and Use Committee of the University Medical Center Utrecht, the Netherlands. Mice were purchased from Jackson Laboratory, USA, and further bred at the University Medical Center Utrecht. Mice were weaned at 21 days, ear punched for identification purposes, and housed with littermates of the same sex in groups of 6-8 mice per cage. Adult male C57bl6/J mice of 2-3 months of age were randomly assigned to the sham control or SAH group. Before anesthesia, mice were injected intraperitoneally with an analgesic (Carprofen; 5 mg/kg, in a dose for 100 µl/10g). Anesthesia was induced by intraperitoneal injection of Ketamine; 75 mg/kg, and Medetomidine; 1 mg/kg. The surgery was performed according to a previously published method *(13)*. An incision was made on the right side of the neck of the mouse, and the external carotid artery was exposed. A black nylon filament with a blunt tip (size 5-0) was inserted into the external carotid artery and moved into the internal carotid artery. During filament insertion, a clip and sutures around the external carotid artery prevented the spilling of blood. In SAH mice, the nylon filament was advanced into the circle of Willis, and pushed further to perforate the vessel wall of the middle cerebral artery. Thereafter, the filament was retracted quickly to restore normal blood flow into the internal carotid artery and induce an SAH. In the sham control mice, the nylon filament was retracted before hitting the vessel wall. After removal of the nylon filament, the right external carotid artery of mice was ligated. Mice received one dose of analgesic 24h after the surgery.

Mice were housed in groups, with a normal day-night cycle (white lights on from 7:00-19:00 hr). Cages were enriched with sawdust and tissues. Regular chow and water were provided ad libitum. After surgery, the chow was provided in heated water to soften the chow. Cages were placed on top of a heater at 37°C after the surgery for 2h. The cages were placed half over the heating plate for up to 48h, for the mice to choose between heated or normal temperature. Mouse weight and neurological scores were measured daily for the first two weeks after surgery and 3 times a week thereafter. Neurological scoring was performed according to the method of Sugawara et al. *(14)*. Mice that lost >20% of their weight after the surgery, without showing signs of improved neurological scores were killed and were removed from the experiment. Mice were killed at 2 weeks (sham control n=16, SAH n=21), and at 1 month (sham control n=13, SAH n=15) after sham control/SAH sur-

gery for further morphological analyses (Figure 3A).

Fluorescence immunohistochemistry of the human paraffin-embedded brain tissue

Formalin-fixed paraffin-embedded human brain tissue was cut in 7 µm sections using a microtome. Sections were mounted on super frost plus slides (VWR) and stored at room temperature until further use. After deparaffination by dipping the sections in xylene (VWR International) for 2x 10 minutes, the sections were rehydrated in graded ethanol with a final 2x 5 minutes step in dH_20. Epitope retrieval was performed in 10 mM sodium citrate solution (Sigma), 0.05% Tween 20 (Millipore Corporation), pH 6.0, by heating the sections in a steamer at 96°C for 20 minutes. Sections were washed twice in phosphate buffer (PB: 0.05 mM $Na_2HPO_4 \cdot 2H_2O$, 0.05 mM $NaH_2PO_4 \cdot H_2O$, pH 7.4). PB with 10% normal donkey serum (Gene Tex) and 0.4% Triton-X 100 (Roche Diagnostics) applied at room temperature for 1 hour, to permeabilize the tissue and to block aspecific binding of the primary antibodies. Primary antibodies were diluted in PB with 0.4% Triton-X 100, 3% Normal Donkey Serum, and the incubation was performed in a humidified chamber at room temperature overnight, followed by washing in PB before secondary antibodies were applied. Secondary antibodies were incubated at 10 µg/ml in PB at room temperature for 1.5 hours. The antibodies used for this study are shown in Table 3. Nuclei were stained with Hoechst (1:1000; Invitrogen H3569, Life Technologies). Subsequently, the sections were washed in PB, and to reduce autofluorescence the sections were incubated in Sudan Black (0.3% Sudan Black dissolved in 70% EtOH (Sigma)) for 7 minutes, and then washed with 70% EtOH for 1 minute. Finally, the sections were washed in PB and embedded with Mowiol (0.1M Tris-HCl, pH 8.5, 25% Glycerol; Millipore Corporation), 10% w/v/ Mowiol 4-88 (EMD Chemicals).

Table 3. Primary antibody characteristics.

Antibody	Host	catalog number	Manufacturer	Dilution
Iba1	Rabbit polyclonal	019-19741	Wako	1:2000
GFAP-pan	Rabbit polyclonal	Z0334	Dako	1:4000 (mouse) 1:2000 (human)
C3	Rat monoclonal	ab11862	Abcam	1:50
PSD-95	Rabbit monoclonal	3450	Cell Signaling	1:500
Synaptophysin 1	Mouse monoclonal	101 011	Synaptic Systems	1:500

Fluorescence immunohistochemistry on mouse brain sections
At the end of the behavioral test battery, the mice were transcardially perfused with 4% paraformaldehyde in PBS, pH 7.4. After brain removal, brains were kept in 4% paraformaldehyde in PBS for 48h, and subsequently transferred into a 30% sucrose solution in PBS. After at least 48h in the sucrose solutions, the brains were snap-frozen in isopentane on dry ice and stored at -80°C. Brains were cut using a cryostat in 20 um thick sections that were thaw-mounted on Super Frost glass slides (VWR), and stored at -80°C until use. The slides were post-fixed by incubation in 4% paraformaldehyde in PBS for 10 minutes, then washed in PB. The protocols for epitope retrieval and immunofluorescence staining were the same as the protocols used for the human paraffin-embedded tissue, except that the mouse sections were not treated with Sudan Black.

Chromogenic Immunohistochemistry on mouse brain sections
Endogenous peroxidases were quenched by 2% hydrogen peroxide in water. After 10 minutes, the slides were washed in PBS with 0.5% Tween (PBST) and then treated for antigen retrieval. Epitope retrieval was performed the same way as for human paraffin-embedded tissue. Slides were washed in PBST two times for ten minutes. Blocking was done in 1% bovine serum albumin (BSA), followed by an incubation with primary antibodies and 1% BSA in PBS overnight. The slides were washed in PBST, then incubated with goat-derived biotinylated antibodies for 2 hours, and subsequently washed twice in PBST for 10 minutes. The sections were incubated with the avidin-biotin complex for 30 minutes and then washed in PBST. This was followed by an incuba-

tion in 3,3'-Diaminobenzidine (DAB; 20 µl/ml) in PBS for 11 minutes. Sections were quickly rinsed in water, dehydrated in graded ethanol and xylene. Finally, the sections were mounted in Entellan (EMD Millipore).

Image acquisition and analysis
Images of human brain sections were taken at three randomly selected locations within the grey matter of one brain section. At the time of imaging, the investigator was blinded for the experimental group (control or SAH). The sections were imaged with a 20x magnification on an epifluorescent microscope (Zeiss AxioImager M2 fluorescent microscope with N-Achroplan objectives, AxioCam MRm camera and Software Zen 2011). Images were evaluated and analyzed with the program ImageJ 2.0 (NIH). For the microglia analysis (Iba-1 staining), the images were binarized using the triangle auto threshold algorithm in ImageJ. The percentage of the total area covered by Iba-1 immunopositive staining was measured. Particles larger than 100 pixels were considered as single cells. The morphology of randomly chosen Iba-1 positive microglia (average of 4 cells per patient) was determined by making z-stack imaging on a confocal microscope (Zeiss LSM800, 63x magnification). The maximum intensity images were analyzed using ImageJ (NIH). The processes of the cells were tracked with the use of the Simple Neurotracer plugin. Microglia are highly ramified in a homeostatic state and, upon damage, the processes are retracted. The roundness of the cells is a sign of immune activation. Sholl analysis was performed using the Sholl analysis plugin to determine the complexity of the microglial processes. To analyze the activation of astrocytes, the intensity of the GFAP immunostaining was quantified by calculating the mean intensity per image. Furthermore, the percentage area of the GFAP immune-positive area was quantified. In the mouse brain tissue, the complement C3 and GFAP intensity was measured on the total area of each image. Particles larger than 100 pixels were considered as cells to determine cell count. Regions of interest (ROI) were created for each particle, and the intensity of C3 and GFAP immunostaining were measured within each ROI. The C3/GFAP ratio was calculated for each ROI. Ratios were then divided into bins per 0.05, and the percentage of ROIs per bin was determined. For correlations of C3/GFAP intensity with outcomes of the novel object discrimination task, the average C3/GFAP intensity of all ROIs was calculated per mouse. Immunostainings of presynaptic marker Synaptophysin and postsynaptic marker PSD-95 were used to investigate the number of synapses in the CA1 region of the hippocampus. ROIs were selected on areas with positive

staining, excluding negative stained tissue, likely caused by nuclei or other cells. Mean intensities were calculated per ROI.

Behavioral tests
Behavioral tests were performed at 1 week, 2 weeks, and 1 month after surgery. Mice were handled by one and the same investigator wearing gloves and a laboratory coat. All test chambers, cages, and objects were cleaned with non-fragranced disinfectant (1:200; Anistel) before each trial to avoid smells of prior mice.

Open field test
With the open field test, we measured whether the mice are more or less anxious to cross the arena and spend time in the center of an open field. Furthermore, we measured the velocity of the mice as well, which is an indication of the quality of their motor functions. Mice were placed in a large round cage (diameter 70 cm; height 40 cm) without markings on the floor or the walls. Mouse movement was observed with a ceiling camera and was traced using Ethovision version 11.5 (Noldus, the Netherlands) for 5 minutes. Parameters for analysis were body location and velocity (cm/s). A digital center circle of 25 cm was assigned and the total time of body location spent in the center versus the outer zones was calculated.
Novel object recognition test
To investigate non-social memory, the novel object recognition test was used. Both short and long-term memory were measured. During this task, the ability to discriminate between a novel and familiar object was measured, based on the innate preference of mice for novel over familiar stimuli. Mice were placed in a cage with two identical objects for 5 minutes (T0). To measure short-term memory, the mice were placed back into their home cage for an inter-trial interval (ITI) of 1h (T1), before returning to the test cage. Now, one of the objects was replaced for a novel object. The location of the novel object was assigned at random, to avoid the possibility that mice spend more time at a preferred location. The mice were allowed to freely explore the objects for 5 minutes. For long-term memory, this procedure was repeated after an ITI of 24h (T24) from T0, but with a different novel object. Objects used were transparent bottles for familiar objects, a round metal flask for T1 novel object, and a tall round glass without print for T24 novel object. Mice were unable to mount the objects. Mouse movements were recorded with a camera. The time spent at objects was measured manually with the

use of stopwatches. Video file names were blinded to the investigator. Discrimination capacity was calculated as the preference for the novel versus the familiar object following the formula: tN/(tN+tF), where tN is time spent exploring the novel object and tF is the time spent exploring the familiar object. A ratio above 0.5 indicates a preference for the novel object. Passive contact with objects and attempts to climb the objects were not scored as object exploration. Mice that explored none of the objects for ≥1 sec were excluded from analysis.

Three chamber social interaction test

To measure memory in a social context, as well as social initiating behavior, the three-chamber social interaction test was used. The test chamber consists of 3 separate compartments, separated with transparent walls with doors. Mice were habituated in the middle chamber for 5 minutes. Thereafter, the doors were opened. Both outer chambers have a small round open cage with iron bars, for the mice to be able to see and smell each other. At T0, one cage is empty, the other has an unfamiliar stimulus mouse inside. Stimulus mice were non-litter mates, and housed in separate rooms from the test mice. During T0, the test mouse could freely move between the three chambers for 10 minutes. Mouse movement was recorded with a camera. Time spent exploring both cages was measured. Discrimination capacity was calculated as the preference for the mouse versus the empty cage following the formula: tM/(tM+tE), where tM is time spent exploring the cage with the mouse and tE is the time spent exploring the empty cage. A ratio above 0.5 indicates a preference towards the mouse, indicating social initiation behavior. After T0, the test mouse is placed back into its home cage for 5 minutes. During this time, a novel stimulus mouse is placed into the empty round cage. During this task, the ability to discriminate between a novel and familiar mouse was measured, based on the innate preference of mice for novel over familiar stimuli. The test mouse was placed back and could freely move between the three chambers for 10 minutes (T1). Time spent exploring both smaller cages was measured manually. Discrimination capacity was calculated as the preference for the novel mouse versus the familiar mouse using the formula: tNm/(tNm+tFm), where tNm is time spent exploring the cage with the novel mouse and tFn is the time spent exploring the familiar mouse cage. A ratio above 0.5 indicates a discrimination towards the novel mouse, indicating normal social memory. The investigator doing the analyses was blinded for the experimental condition of the mouse (SAH vs. control).

Statistical analysis

A p-value of ≤0.05 was considered statistically significant. The Student's t-test was used to compare two groups with normal distribution, and a Mann-Whitney when the data were not normally distributed. Normal distribution was determined with a Shapiro-Wilk test. One sample t-test was performed to calculate whether groups of mice could distinguish between the novel versus the familiar object in the novel object recognition task and between the novel/familiar mouse in the three-chamber social interaction test, and were tested against a theoretical mean of 50%. Correlations between discrimination of Novel object and C3/GFAP ratios and the Synaptophysin/PSD-95 intensities were tested with the Pearson r-test.

Results

Glial reaction after aneurysmal SAH in human cortex

First, we aimed to determine whether astrocytes and microglia in the human brain respond to an aneurysmal SAH and show signs of reactive gliosis. We found a doubling of the microglia surface area in the grey matter in SAH patients compared to controls (representative images of controls and SAH patients in Figure 1A and 1B, respectively; Statistic characteristics in Supplementary Table 1; Figure 1C) and also a doubling in the number of Iba-1$^+$ microglia after SAH compared to controls (Statistic characteristics in Supplementary Table 1; Figure 1D). We did not find a difference in length of Iba-1$^+$ processes when comparing control to SAH (Supplementary Figure 1A). Our Sholl analysis of Iba-1$^+$ positive cells showed that the number of intersections was slightly reduced after SAH, however, presumably due to high variation between cells, this was not significantly different between the groups (Supplementary Figure 1B).

The immunopositive surface of the astrocytic intermediate filament protein GFAP was significantly increased in the grey matter of the frontal cortex in patients with an SAH (representative images for controls and SAH patients in Figure 2A and 2B, respectively; Statistic characteristics in Supplementary Table 1; Figure 2C). The intensity of the GFAP immunostaining was increased after SAH (Statistic characteristics in Supplementary Table 1; Figure 2D). Taken together, we show here that there is a clear indication that microglia and astrocytes are activated after SAH.

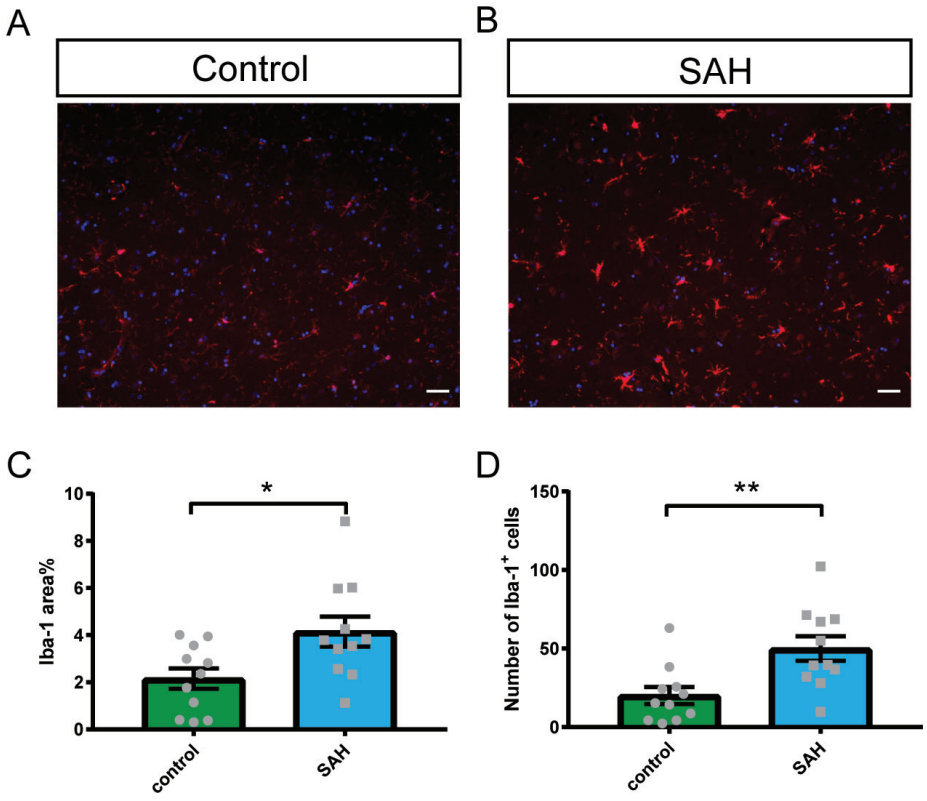

Figure 1. Microglia/macrophage activation in the grey matter of the frontal cortex after SAH in patients. A) Representative image of Iba-1^{+} cells in the human frontal cortex of a control donor, and B) a SAH patient. C) Iba-1 is increased after human SAH. D) The number of Iba1^{+} cells is increased after human SAH. Scale bars: 40µm, points in graphs represent individuals; Student's t-tests; * p=<0.05; ** p=<0.01; Bars and error bars in mean±SEM.

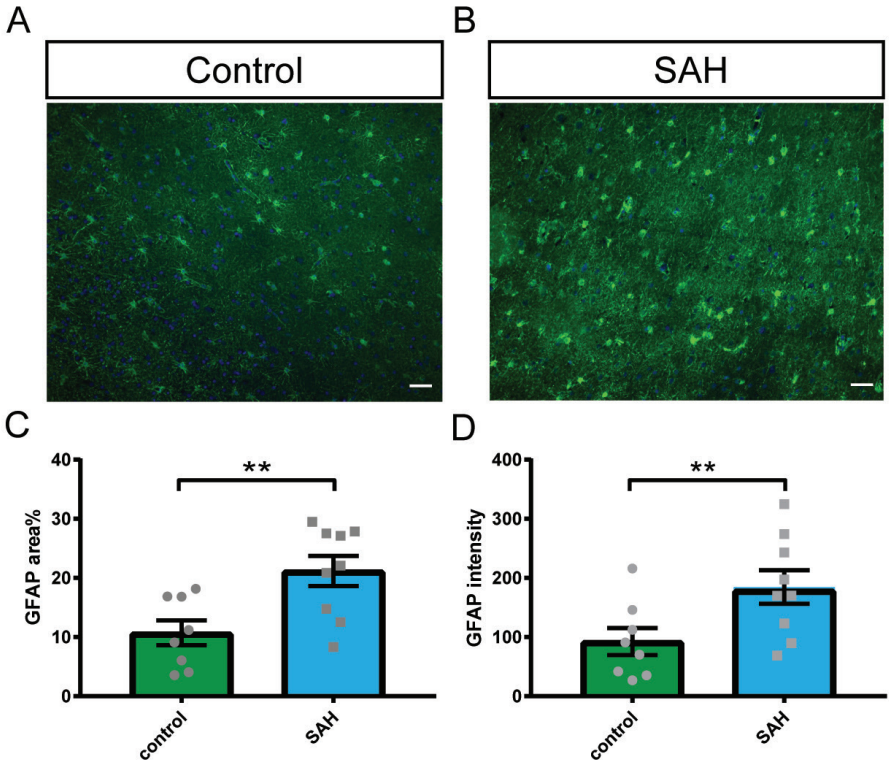

Figure 2. **Astrocyte activation in the frontal cortex after SAH in patients.** A) Representative image of GFAP positive cells in the human frontal cortex of a control donor, and B) SAH patient. C) GFAP area is increased after human SAH. D) The intensity of GFAP is also increased after human SAH. Scale bars: 40µm; points in graphs represent individuals; Student's t-tests; ** p=<0.01; Bars and error bars in mean±SEM.

The endovascular perforation SAH mouse model mimics SAH in patients based on the number of survivors and neurological condition.

An overview of the mouse experiments is shown in Figure 3A. All control mice survived the sham surgery, and in the SAH group, 68% survived the initial 14 days after the experimental SAH surgery. Both control and SAH mice lost weight after surgery, but the control mice quickly gained weight from day 2 after surgery. The SAH mice dropped in weight until day 4 and started to gain weight thereafter (Figure 3B). All mice were assessed for motor, balance, and sensory behavior problems, with a maximum score of 18 in unaffected mice. All control mice were neurologically unaffected, as these

mice had a maximum score of 18 on day 1 after surgery. The SAH mice clearly showed a drop in the neurological score on day 1 after surgery, but improved gradually in performance on each following day until reaching the maximum score of 18 on day 10 after surgery (Figure 3C).

SAH mice move with a higher velocity and spent more time in the center of an open field arena

To test whether SAH induced anxiety-related behavior, we performed the open field test. There was no difference between the control and SAH groups at 1 and 2 weeks after surgery (Statistic characteristics in Supplementary Table 2; Percentage in center at 1 week after surgery in Figure 3D; and at 2 weeks after surgery in Figure 3E). However, at 1 month after surgery, the SAH mice differed from the control group by spending more time in the center of the open field arena (Statistic characteristics in Supplementary Table 2; Figure 3F).
There was no difference in velocity between control and SAH mice at 1 and 2 weeks after surgery (Statistic characteristics in Supplementary Table 2; Velocity at 1 week in Figure 3G; and at 2 weeks in Figure 3H). SAH mice had a higher velocity than control mice at 1 month after surgery (Statistic characteristics in Supplementary Table 2; Figure 3I). Taken together, these results suggest that at 1 month after surgery the SAH mice are more active or less anxious than the control mice.

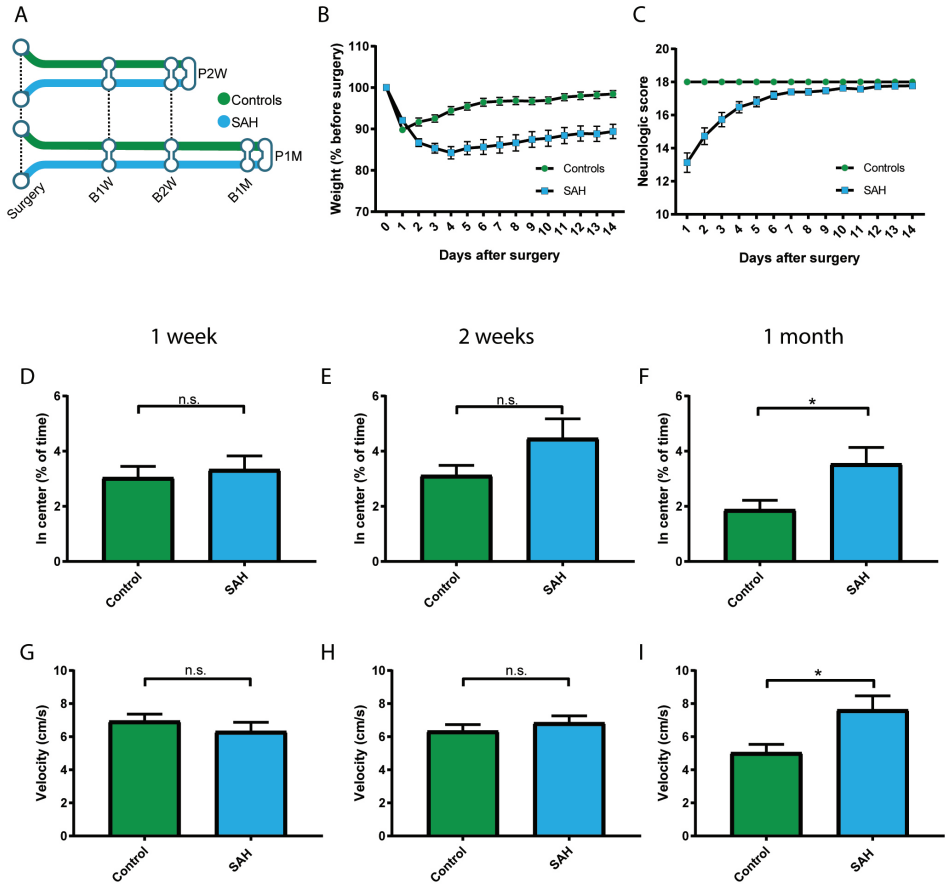

Figure 3. Study overview, mouse characteristics, and open field test. A) Mice were tested for behavioral impairments at 1 week (B1W), 2 weeks (B2W), and 1 month (B1M) after sham/SAH surgery. Mice were killed for morphological and immunocytochemical analysis at 2 weeks (P2W) or 1 month (P1M) after sham/SAH surgery. B) Repeated weight measurements, and C) Neurological scores in the first two weeks after surgery. D) Time spend in the center of the open field test between control and SAH mice at 1 week after surgery, E) at 2 weeks after surgery, and F) at 1 month after surgery. G) Velocity (cm/s) between control and SAH mice at 1 week after surgery, H) at 2 weeks surgery and I) at 1 month after surgery. Student's t-test for velocity at 1 week; Mann-Whitney test for velocity at 2 weeks and 1 month; Mann-Whitney test for % in center at 1 and 2 weeks after surgery, Student's t-test for % in center at 1 month after surgery; * p=<0.05; Bars and error bars in mean±SEM.

SAH mice display memory impairments

Next, we investigated whether the short- and long-term contextual memory was affected after an SAH by assessing the behavior of the mice in the novel object recognition test. With an ITI of 1 hour, testing the short term memory, control mice were able to distinguish the novel object from the familiar object, whereas the SAH mice were not, at 1 week after surgery (Statistic characteristics in Supplementary Table 3; Figure 4A). Both groups were able to distinguish the novel object from the familiar object at 2 weeks after surgery. However, when comparing the groups, the control mice were significantly better in recognizing the novel object than the SAH mice (Statistic characteristics in Supplementary Table 3; Figure 4B). At 1 month after surgery, both groups were also able to distinguish the novel object from the familiar object, without a significant difference between the groups (Statistic characteristics in Supplementary Table 3; Figure 4C).

We also tested long-term memory, with an ITI of 24 hours. Both groups were able to distinguish the novel object from the familiar object, at 1 week after surgery. However, there was no significant difference between the groups (Statistic characteristics in Supplementary Table 3; Figure 4D). Control mice were able to distinguish the novel object from the familiar object, whereas the SAH mice were not, at 2 weeks after surgery, and there was a significant difference between groups (Statistic characteristics in Supplementary Table 3; Figure 4E). Finally, control mice were able to distinguish the novel object from the familiar, whereas the SAH mice were not, at 1 month after surgery. (Statistic characteristics in Supplementary Table 3; Figure 4F). These data indicate that besides short term memory impairments, SAH mice also have long-lasting long-term memory impairments.

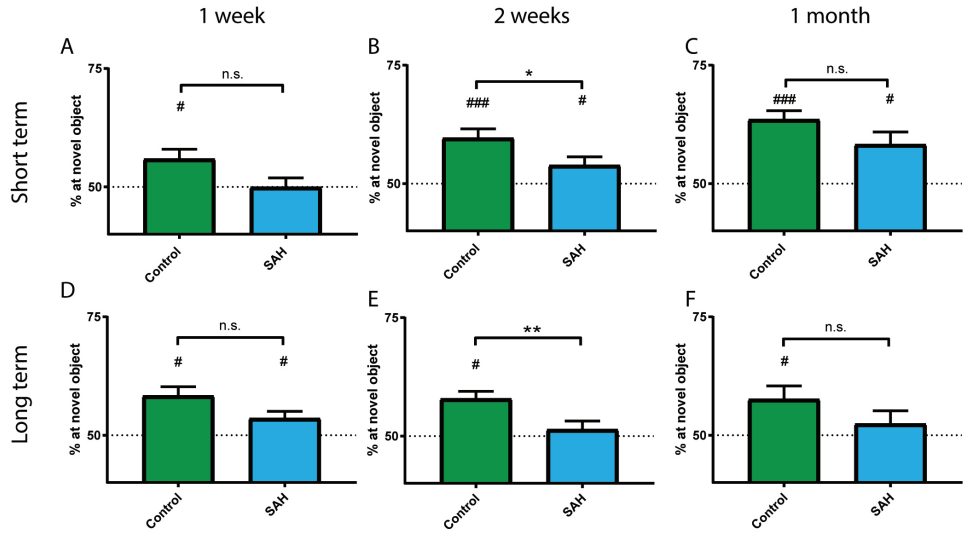

Figure 4. Short- and long-term memory impairments after SAH. A) Short-term novel object recognition at 1 week after surgery, B) at 2 weeks after surgery, and C) at 1 month after surgery. D) Long-term novel object recognition at 1 week after surgery, E) at 2 weeks after surgery, and F) at 1 month after surgery. Student's t-tests between groups, * p=<0.05, ** p=<0.01, one sample t-tests against a theoretical mean of 50%, # p=<0.05; ### p=<0.001; Bars and error bars in mean±SEM.

No social interaction deficits in mice with SAH

Next, we tested whether mice with SAH also had difficulties with social interactions towards unknown mice. We used the three-chamber social Interaction test for this. We did not find any significant differences between the control and SAH mice in interacting with the unknown mouse, at any time point (Statistic characteristics in Supplementary Table 4; 1 week in Supplementary Figure 2A, 2 weeks in Supplementary Figure 2B, and 1 month in Supplementary Figure 2C). Next, a novel mouse was put into the previously empty cage. Again, there is no preference toward the novel mouse over the familiar mouse, at any of the time points, by both control and SAH mice. Control and SAH mice are unable to distinguish the novel over the familiar mouse and there was no significant difference between the groups (Statistic characteristics in Supplementary Table 4; 1 week in Supplementary Figure 2D, 2 weeks in Supplementary Figure 2E, 1 month in Supplementary Figure 2F).

Glial activation after SAH in mice and Complement C3 in astrocytes is associated with long-term memory impairments.

The next step was to determine the cellular changes that could account for the behavioral changes. First, we assessed the extent of reactive gliosis in the hippocampus of the mice. We quantified the Iba-1 and GFAP immunofluorescence in the CA1 region of the hippocampus, as this area is implicated in contextual memory. We focused on brain tissue perfused at 2 weeks after surgery, as the memory impairments were most apparent at that time point. The Iba-1 area was larger in the hippocampus of SAH mice compared to controls (Representative images of control and SAH mice in Figure 5A and 5B, respectively; Statistic characteristics in Supplementary Table 1; Figure 5C). Moreover, the number of $Iba1^+$ cells was larger in the hippocampus of SAH mice compared to control mice (Statistic characteristics in Supplementary Table 1; Figure 5D).

To quantify the immune activation of astrocytes, we analyzed the GFAP and complement C3 protein expression by immunostaining (representative images of both control and SAH mice; Figure 6A). We assessed astrocyte activation in the medial prefrontal cortex (mPFC) and the hippocampus of mice. We included the mPFC as a control region. The number of $GFAP^+$ cells is higher in the medial prefrontal cortex of SAH mice than in control mice (Statistic characteristics in Supplementary Table 1; Figure 6B). GFAP intensity was similar between control mice and SAH mice, at 2 weeks after surgery (Statistic characteristics in Supplementary Table 1; Figure 6C). Furthermore, the amount of C3 in $GFAP^+$ cells in the medial prefrontal cortex did not differ between control and SAH mice (Figure 6D).

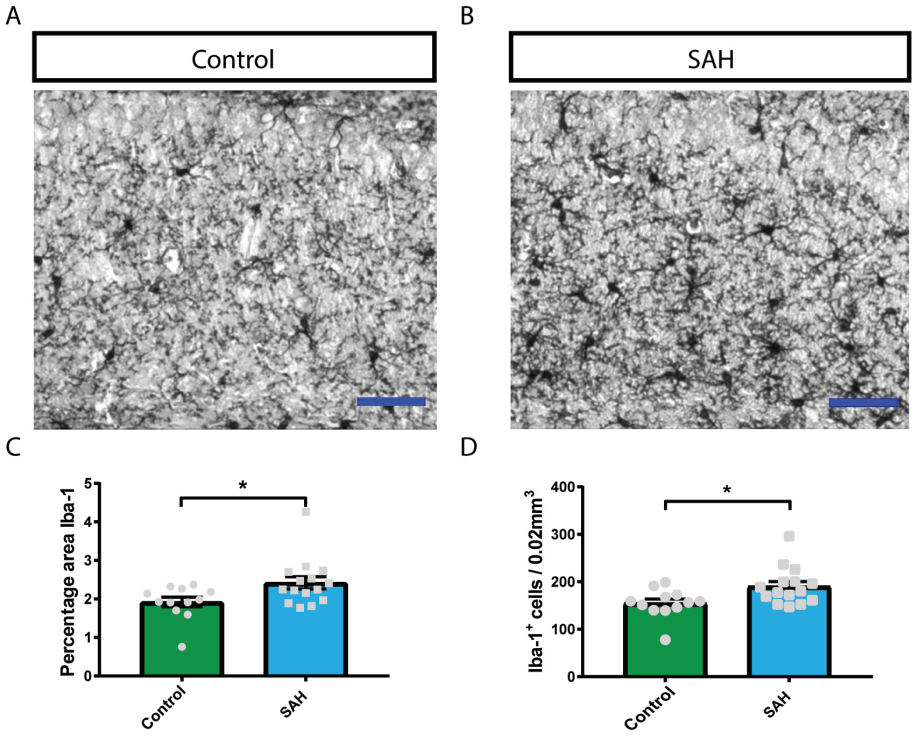

Figure 5. Iba-1 positive cells in the hippocampus of mice. Representative image of Iba-1 positive cells in the CA1 region of the hippocampus of A) control mice, and B) SAH mice. C) Iba-1 area and D) the number of Iba-1 cells in the CA1 region of the hippocampus were increased in SAH mice at 2 weeks after surgery. Scale bars: 40µm; points in graphs represent individual mice; Mann-Whitneys tests; * p=<0.05; Bars and error bars in mean±SEM.

> Figure 6. Complement C3 in astrocytes is associated with long-term memory impairments. A) representative images of complement C3 and GFAP immunostaining in the CA1 region of the hippocampus of a Sham control mouse and an SAH mouse. B) The number of $GFAP^+$ cells, C) GFAP intensity and D) the C3 abundance in $GFAP^+$ cells, in the medial prefrontal cortex at 2 weeks after surgery. E) the number of $GFAP^+$ cells, F) GFAP intensity, and G) the C3 abundance in $GFAP^+$ cells in the CA1 region of the hippocampus at 2 weeks after surgery. H) Correlation between C3 in $GFAP^+$ cells and short-term memory, indicated as the ability to recognize novel object over a familiar object at 1 hour after familiarization and I) Correlation between C3 in $GFAP^+$ cells and short-term memory, indicated as the ability to recognize novel object over a familiar object at 1 hour after familiarization. Students t-tests in C, D, E, F and in G; Mann-Whitney tests in B, Pearson's correlation in H and I, $*p<0.05$. Circles and squares in graphs are means of individual mice; Bars and error bars in mean±SEM.

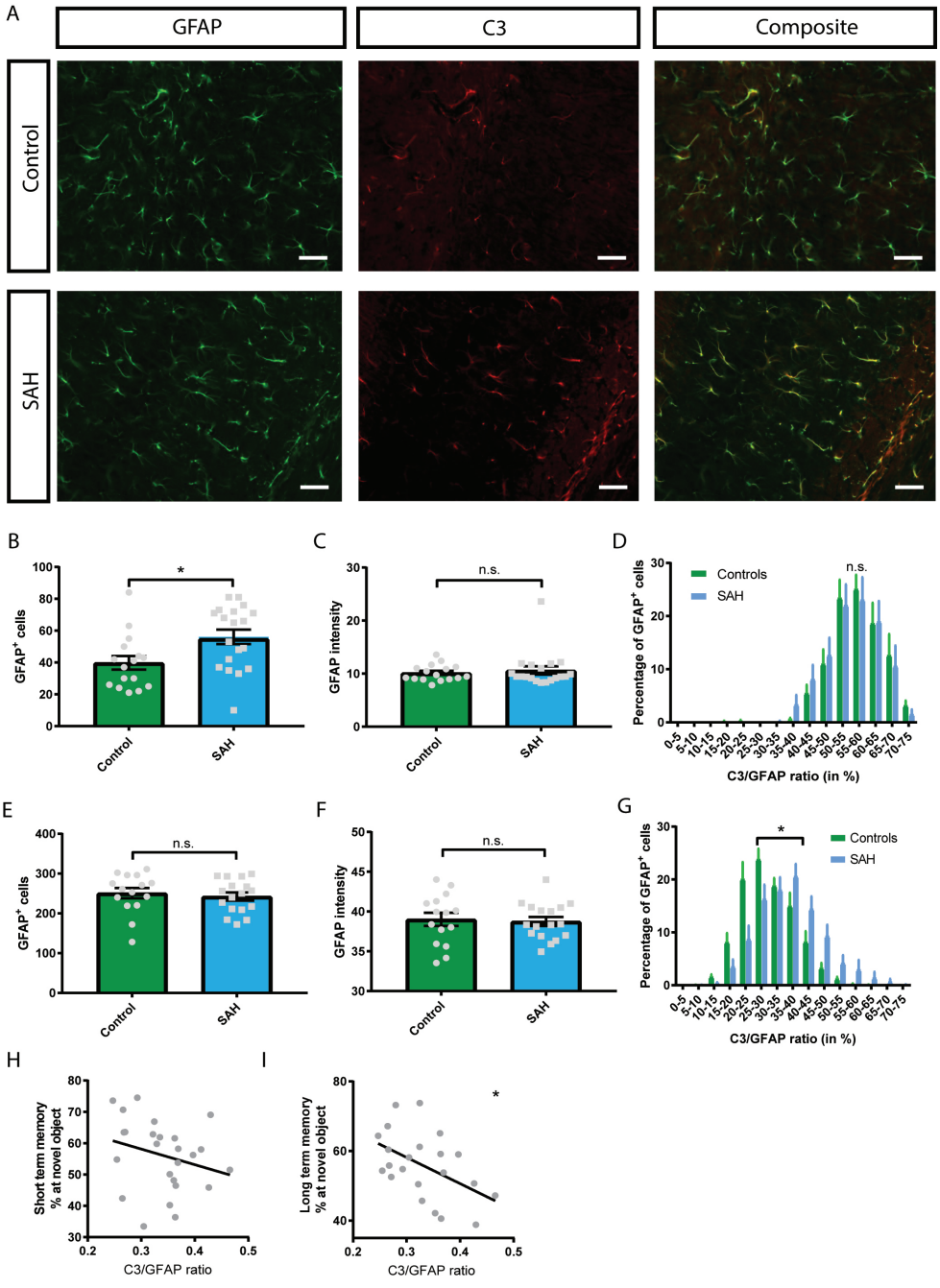
A
GFAP
C3
Composite
Control
SAH
B
GFAP+ cells
*
Control
SAH
C
GFAP intensity
n.s.
Control
SAH
D
Percentage of GFAP+ cells
Controls
SAH
n.s.
C3/GFAP ratio (in %)
E
GFAP+ cells
n.s.
Control
SAH
F
GFAP intensity
n.s.
Control
SAH
G
Percentage of GFAP+ cells
*
Controls
SAH
C3/GFAP ratio (in %)
H
Short term memory % at novel object
C3/GFAP ratio
I
Long term memory % at novel object
*
C3/GFAP ratio

Within the hippocampus, the number of GFAP$^+$ cells was similar between control and SAH mice at 2 weeks after surgery (Statistic characteristics in Supplementary Table 1; Figure 6E). Moreover, also the GFAP intensity was similar between control mice and SAH mice (Statistic characteristics in Supplementary Table 1; Figure 6F). Due to high variability in C3 positivity per cell within one image (Figure 6A), we assessed the C3 abundance per GFAP$^+$ cell, and calculated the C3/GFAP ratio within these cells. We found that GFAP$^+$ cells in SAH mice had higher C3 levels than in control mice, and that there were more cells with high C3/GFAP ratios in SAH than in control mice (Statistic characteristics in Supplementary Table 1; Figure 6G). Next, we calculated the average C3/GFAP ratio in GFAP$^+$ cells per mouse and tested whether there was a correlation with the memory impairments. The C3/GFAP ratio in GFAP$^+$ cells per mouse did not correlate to short-term memory performance (Pearson's r=-0.26, p=0.20; Figure 6H), but correlated negatively with long-term memory performance (Pearson's r=-0.48, p=0.02; Figure 6I).

Hippocampal synapse numbers are unaltered after SAH

Next, we investigated whether SAH could have impacted the communication between neurons. We hypothesized that the number of synapses in the hippocampus could be altered, in particular, due to excessive pruning by complement activated microglia. To test this, we performed immunostainings of the presynaptic marker Synaptophysin 1 and the postsynaptic marker PSD-95. We quantified the immunofluorescence of both markers in the CA1 region of the hippocampus (representative images of both control and SAH mice; respectively, Figures 7A and B). The intensities of both Synaptophysin and PSD-95 were similar between control mice and SAH mice, at 2 weeks after surgery (Synaptophysin: Statistic characteristics in Supplementary Table 1; Figure 7C and PSD-95: Statistic characteristics in Supplementary Table 1; Figure 7D). Furthermore, we investigated whether the ratio of pre- and postsynapses was changed. We tested this by correlating the intensities of both pre- and postsynaptic markers of all mice in each group. There were strong positive correlations between the pre- and postsynaptic markers, and these were comparable for both groups (control: Pearson's r=0.61; p=0.012 and SAH: Pearson's r=0.79; p=<0.0001; Figure 7E). These data indicate that the number is synapses in the hippocampus is unaltered after SAH.

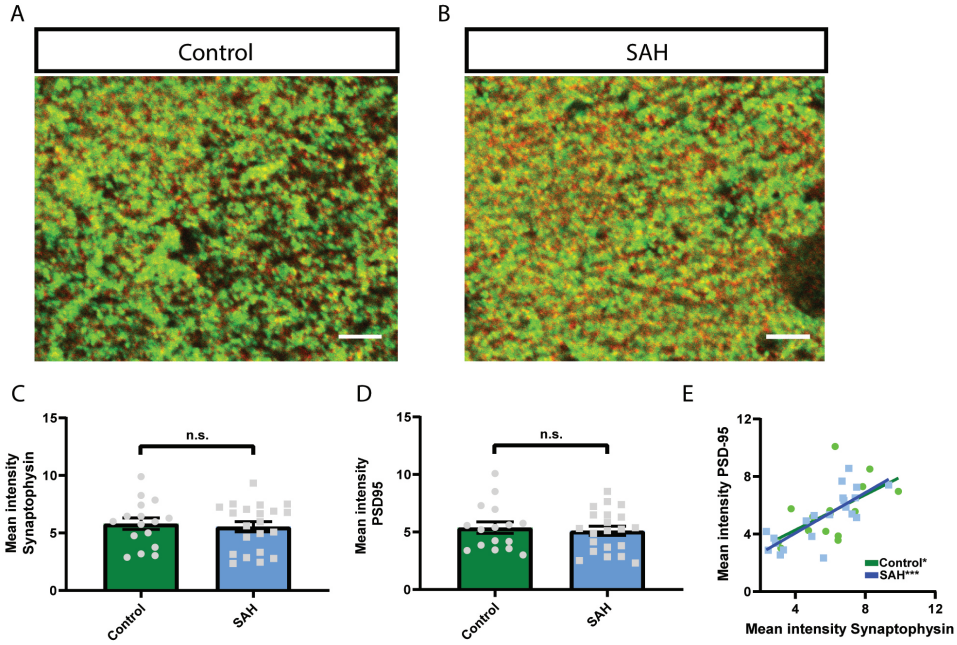

Figure 7. Pre- and postsynaptic markers are not altered after SAH, compared to controls. A) representative images of synaptophysin and PSD-95 immunostaining in the CA1 region of the hippocampus of a Sham control mouse and an SAH mouse. B) The mean intensity of Synaptophysin and C) PSD-95. D) Correlation between intensity of Synaptophysin PSD-95. Scale bars are 12µm; Circles and squares in graphs are means of individual mice; Student's t-tests in C and D, n.s.: not significant; Pearsons correlation in E, * p=<0,05; *** p=<0.0001. Bars and error bars in mean±SEM.

Discussion

We found that both microglia and astrocytes were activated in the brains of SAH patients and SAH mice. In our mouse model that showed highly similar characteristics to human pathology. We found differences in exploration between control and SAH mice, as well as memory impairments in SAH mice. These memory impairments correlated to the degree of C3 positive astrocytes in the hippocampus.

We investigated the glial response in the human frontal cortex. Our collection consists of a highly variable group of patients that died of aneurysmal SAH. Brain tissue of patients who died of an aneurysmal SAH is rare, however, we had access to tissue of 11 patients. Unfortunately, we neither had access to brain tissue of SAH patients who initially survived the insult, nor

of patients with known cognitive impairments. The aneurysm location was different in each case and patients died at different time points after the initial SAH, and at different ages. This resulted in a variability in glial activation. Yet, we found significant differences in the glial response between control patients and SAH patients. In human tissue of the frontal cortex, we found an immune activation of microglia or macrophages, as indicated by the increase in surface area stained for Iba-1, and the number of Iba-1$^+$ cells. We used Iba-1 immunostainings as a marker for microglia, the brain resident immune cells, however, Iba-1 is also a marker for macrophages *(15)*. Therefore, we could not make the distinction in microglia and macrophages. In rodent SAH studies, however, it has been shown that the glia response is primarily orchestrated by the microglia, and there is only little infiltration of macrophages *(16)*.

To investigate the glia response in humans, the focus has been primarily on the microglia response, and little is known about the astrocytic response in human SAH patients. Increased levels of GFAP and S100b were found in the serum of patients *(17)*. However, this might be due to increased cell death, rather than a cellular glial response. On a cellular level, a disruption in AQP4 was found in the hippocampus of human patients, suggesting that astrocytes do change in response to SAH *(18)*. Here, we have also shown an increase in the number of GFAP$^+$ astrocytes. GFAP positivity in cortical astrocytes is associated with their reactivity *(19)*, and this further suggests that there is indeed gliosis in the brains of SAH patients in which both microglia and astrocytes are involved.

To make the correlation with behavior, we have set up the endovascular perforation mouse model for SAH. We showed that in the mouse cortex the number of GFAP$^+$ cells was increased, but this was not obvious in the hippocampus. A possible explanation could be the heterogeneous response by different populations of astrocytes *(20)*. In the hippocampus, the astrocytic response may have been more subtle, and different markers for gliosis should be explored. However, we did find activated microglia in the hippocampus of these mice. This suggests that the microglia respond more fiercely to the insult than the astrocytes, at least at the two week time point. It would be interesting to investigate the glial response also at 1 month, as the SAH mice also show cognitive deficits at that timepoint.

We found several unexpected results in the behavioral tests. For the open field test, we did not expect that the SAH mice would have a higher velocity

at 1 month after surgery. We also did not expect that the SAH mice would be more prone to go into the center, indicating that SAH mice were less anxious. One explanation could be that these mice were less restrained. Although the behavioral traits affected after an SAH in patients is very heterogenous, impulsivity and disinhibited behavior are among these *(1, 21)*. However, it may also be that control mice become less explorative at their third time in the open field. We saw a trend of a decreased velocity between 2 weeks and 1 month. Moreover, control mice are significantly less in the center between 2 weeks and 1 month. This change in exploration between 2 weeks and 1 month was not observed in SAH mice. As we have found that memory is impaired in SAH, the SAH mice may not remember the Open Field test chamber as good as the control mice did, and thus explore it more each time they are in it.

The three-chamber social interaction test was performed to study how the mice interact with unknown mice as well as their interaction with a familiar mouse and a novel mouse. We were unable to find significant differences in performance between the control and SAH mice, at any time point. However, the absence of findings have been reported elsewhere, in which the three-chamber social interaction test gave unexpected results *(22)*. Unexpectedly, the control mice did not perform the task as it was reported before on normal C57bl/6J mice *(23)*. This may suggest that the control mice were also affected by their surgery (e.g. by the use of the anesthetics). We did not include an extra group of controls without any surgery, so it is not clear how well our sham-operated mice perform compared to non-operated mice. It would be interesting to examine the impact on behavior from the sham surgery alone.

Long-term memory impairments are common in SAH patients *(24)*. The SAH mice in this study also had memory impairments, as indicated by the disability to recognize the novel object over the familiar object after 1 hour and 24 hours, for short and long-term memory, respectively. The mice showed that SAH mice have difficulties with short-term memory, especially at 1 and 2 weeks after surgery, but seemed to improve after 1 month. This was surprising, as, in human patients, the memory impairments are long-lasting. However, at 1 month, SAH mice were unable to recognize the novel object during the long-term memory test, suggesting the long term memory impairments were long-lasting. To determine cellular changes, we focused on

the hippocampus, as this brain area is particularly involved in this type of memory *(25)*. We found an increase in microglia in the hippocampus but there was no increase in the classical astrocyte reactive gliosis marker GFAP. However, recent studies suggest that there are different ways to examine the reactivity of astrocytes; the neurotoxic "A1" type astrocytes could be detected with the complement C3 marker *(9)*. Indeed, we found that the $GFAP^+$ cells in the hippocampus of SAH mice have a higher C3/GFAP ratio. Interestingly, this ratio correlated negatively to the ability to recognize the novel object over the familiar object. This suggests an association between complement C3 in astrocytes and long-term memory impairments. Complement C3 has been linked with memory before, as C3 knockout mice have improved spatial memory compared to control mice *(26)*. Furthermore, the neurotoxic astrocytes may create a harmful environment that affect neuronal survival and changes their performance in maintaining memory *(27, 28)*. The mechanisms by which neurotoxic astrocytes become harmful is not yet fully understood, but fragmented mitochondria and other particles released from activated astrocytes are toxic to neurons *(7, 29)*. It would be interesting to investigate the toxicity of these astrocytes, e.g. by assessment of neuronal cell death. The other possibility for the memory impairments is that complement is involved in the maintenance of synapses. In association with microglia and astrocytes, complement-tagged synapses get pruned *(10)*. This happens both in normal development and healthy brains, but it is also associated with brain diseases, likely due to excessive pruning after uncontrolled complement activation *(30–32)*. However, our data does not indicate a change in the number of synapses after SAH. Recently, it was found that synapse function can be altered by microglia by remodeling the extracellular matrix *(33)*. It would be interesting to investigate whether the glial activation after SAH causes other types of altered neuronal communication.

In conclusion, we found both activated microglia and reactive astrocytes in the brain tissue of SAH patients. Using the endovascular perforation SAH mouse model, we also found activated microglia, reactive astrocytes in the PFC, and complement C3 activated astrocytes in the hippocampus of these mice. These mice also had memory impairments. Interestingly, there was a correlation between the C3 positive astrocytes and long-term memory. It would be interesting to investigate this further, to find out that this is not merely a correlation but also a cause of memory impairments after SAH.

References

1. T. Al-Khindi, R. L. Macdonald, T. A. Schweizer, Cognitive and Functional Outcome After Aneurysmal Subarachnoid Hemorrhage, *Stroke* **41** (2010), doi:10.1161/STROKEAHA.110.581975.

2. S. A. Mayer, K. T. Kreiter, D. Copeland, G. L. Bernardini, J. E. Bates, S. Peery, J. Claassen, Y. E. Du, E. S. Connolly, Global and domain-specific cognitive impairment and outcome after subarachnoid hemorrhage, *Neurology* **59**, 1750–1758 (2002).

3. P. Egeto, R. Loch Macdonald, T. J. Ornstein, T. A. Schweizer, Neuropsychological function after endovascular and neurosurgical treatment of subarachnoid hemorrhage: a systematic review and meta-analysis, *J. Neurosurg.* **128**, 768–776 (2018).

4. B. J. van Dijk, M. D. Vergouwen, M. M. Kelfkens, G. J. Rinkel, E. M. Hol, Glial cell response after aneurysmal subarachnoid hemorrhage - Functional consequences and clinical implications, *Biochim.Biophys.Acta* **1862**, 492–505 (2016).

5. M. Pekny, M. Pekna, A. Messing, C. Steinhäuser, J.-M. Lee, V. Parpura, E. M. Hol, M. V. Sofroniew, A. Verkhratsky, Astrocytes: a central element in neurological diseases, *Acta Neuropathol. (Berl.)* **131**, 323–345 (2016).

6. J. E. Burda, M. V. Sofroniew, Reactive Gliosis and the Multicellular Response to CNS Damage and Disease, *Neuron* **81**, 229–248 (2014).

7. R. M. Ransohoff, How neuroinflammation contributes to neurodegeneration, *Science* **353**, 777–783 (2016).

8. S. A. Liddelow, B. A. Barres, Reactive Astrocytes: Production, Function, and Therapeutic Potential, *Immunity* **46**, 957–967 (2017).

9. S. A. Liddelow, K. A. Guttenplan, L. E. Clarke, F. C. Bennett, C. J. Bohlen, L. Schirmer, M. L. Bennett, A. E. Münch, W.-S. Chung, T. C. Peterson, D. K. Wilton, A. Frouin, B. A. Napier, N. Panicker, M. Kumar, M. S. Buckwalter, D. H. Rowitch, V. L. Dawson, T. M. Dawson, B. Stevens, B. A. Barres, Neurotoxic reactive astrocytes are induced by activated microglia, *Nature* **541**, 481–487 (2017).

10. A. H. Stephan, B. A. Barres, B. Stevens, The Complement System: An Unexpected Role in Synaptic Pruning During Development and Disease, *Annu. Rev. Neurosci.* **35**, 369–389 (2012).

11. W. J. Mack, A. F. Ducruet, Z. L. Hickman, M. C. Garrett, E. J. Albert, C. P. Kellner, J. Mocco, E. S. Connolly Jr., Early plasma complement C3a levels correlate with functional outcome after aneurysmal subarachnoid hemorrhage, *Neurosurgery* **61**, 255–260 (2007).

12. B. J. van Dijk, J. C. M. Meijers, A. T. Kloek, V. L. Knaup, G. J. E. Rinkel, B. P. Morgan, M. J. van der Kamp, K. Osuka, E. Aronica, Y. M. Ruigrok, D. van de Beek, M. Brouwer, M. Pekna, E. M. Hol, M. D. I. Vergouwen, Complement C5 Contributes to Brain Injury After Subarachnoid Hemorrhage, *Transl. Stroke Res.* (2019), doi:10.1007/s12975-019-00757-0.

13. Z. V. Zheng, H. Lyu, S. Y. E. Lam, P. K. Lam, W. S. Poon, G. K. C. Wong, The Dynamics of Microglial Polarization Reveal the Resident Neuroinflammatory Responses After Subarachnoid Hemorrhage, *Transl.*

Stroke Res. **11**, 433–449 (2020).

14. T. Sugawara, R. Ayer, V. Jadhav, J. H. Zhang, A new grading system evaluating bleeding scale in filament perforation subarachnoid hemorrhage rat model, *J. Neurosci. Methods* **167**, 327–334 (2008).

15. Y. Imai, I. Ibata, D. Ito, K. Ohsawa, S. Kohsaka, A Novel Geneiba1in the Major Histocompatibility Complex Class III Region Encoding an EF Hand Protein Expressed in a Monocytic Lineage, *Biochem. Biophys. Res. Commun.* **224**, 855–862 (1996).

16. U. C. Schneider, A.-M. Davids, S. Brandenburg, A. Muller, A. Elke, S. Magrini, E. Atangana, K. Turkowski, T. Finger, A. Gutenberg, C. Gehlhaar, W. Bruck, F. L. Heppner, P. Vajkoczy, Microglia inflict delayed brain injury after subarachnoid hemorrhage., *Acta Neuropathol. (Berl.)* **130**, 215–231 (2015).

17. K. Nylén, L. Z. Csajbok, M. Öst, A. Rashid, K. Blennow, B. Nellgård, L. Rosengren, Serum Glial Fibrillary Acidic Protein Is Related to Focal Brain Injury and Outcome After Aneurysmal Subarachnoid Hemorrhage, *Stroke* **38**, 1489–1494 (2007).

18. J. Badaut, J. F. Brunet, L. Grollimund, M. F. Hamou, P. J. Magistretti, J. G. Villemure, L. Regli, in *Brain Edema XII*, T. Kuroiwa, A. Baethmann, Z. Czernicki, J. T. Hoff, U. Ito, Y. Katayama, A. Marmarou, B. A. D. Mendelow, H.-J. Reulen, Eds. (Springer Vienna, Vienna, 2003), pp. 495–498.

19. J. Middeldorp, E. M. Hol, GFAP in health and disease, *Prog. Neurobiol.* **93**, 421–443 (2011).

20. I. Matias, J. Morgado, F. C. A. Gomes, Astrocyte Heterogeneity: Impact to Brain Aging and Disease, *Front. Aging Neurosci.* **11**, 59 (2019).

21. T. F. Hasan, N. Haranhalli, N. Mbabuike, O. O. Akinduro, O. G. Garcia, B. K. Rush, O. Pedraza, R. G. Tawk, Aneurysmal subarachnoid hemorrhage: A pilot study for using longitudinal cognitive and neuropsychological testing for functional outcomes, *Clin. Neurol. Neurosurg.* **194**, 105941 (2020).

22. C. Fanizzi, A. D. Sauerbeck, M. Gangolli, G. J. Zipfel, D. L. Brody, T. T. Kummer, Minimal Long-Term Neurobehavioral Impairments after Endovascular Perforation Subarachnoid Hemorrhage in Mice, *Sci. Rep.* **7**, 7569 (2017).

23. S. Moy, J. Nadler, N. Young, A. Perez, L. Holloway, R. Barbaro, J. Barbaro, L. Wilson, D. Threadgill, J. Lauder, Mouse behavioral tasks relevant to autism: Phenotypes of 10 inbred strains, *Behav. Brain Res.* **176**, 4–20 (2007).

24. G. K. C. Wong, S. W. Lam, K. Ngai, A. Wong, D. Siu, W. S. Poon, V. Mok, Cognitive Dysfunction after Aneurysmal Subarachnoid Hemorrhage Investigators, J. Kwok, K. Y. Chan, P. Woo, C. Mak, P. Pang, Y. C. Po, T. Chan, W. K. Wong, S. Lee, C. K. Wong, M. Lee, R. Ng, A. Wong, V. Pang, Cognitive domain deficits in patients with aneurysmal subarachnoid haemorrhage at 1 year, *J. Neurol. Neurosurg. Psychiatry* **84**, 1054–1058 (2013).

25. N. J. Broadbent, S. Gaskin, L. R. Squire, R. E. Clark, Object recognition memory and the rodent hippocampus, *Learn. Mem.* **17**, 5–11 (2010).

26. M. Perez-Alcazar, J. Daborg, A. Stokowska, P. Wasling, A. Björefeldt, M. Kalm, H. Zetterberg, K. E. Carlström, K. Blomgren, C. T. Ekdahl, E. Hanse, M. Pekna, Altered cog-

nitive performance and synaptic function in the hippocampus of mice lacking C3, *Exp. Neurol.* **253**, 154–164 (2014).

27. A. Tariq, J. Ai, G. Chen, M. Sabri, H. Jeon, X. Shang, R. L. Macdonald, Loss of long-term potentiation in the hippocampus after experimental subarachnoid hemorrhage in rats, *Neuroscience* **165**, 418–426 (2010).

28. S. M. Han, H. Wan, G. Kudo, W. D. Foltz, D. C. Vines, D. E. Green, T. Zoerle, A. Tariq, S. Brathwaite, J. D'Abbondanza, J. Ai, R. L. Macdonald, Molecular Alterations in the Hippocampus after Experimental Subarachnoid Hemorrhage, *J. Cereb. Blood Flow Metab.* **34**, 108–117 (2014).

29. A. U. Joshi, P. S. Minhas, S. A. Liddelow, B. Haileselassie, K. I. Andreasson, G. W. Dorn, D. Mochly-Rosen, Fragmented mitochondria released from microglia trigger A1 astrocytic response and propagate inflammatory neurodegeneration, *Nat. Neurosci.* **22**, 1635–1648 (2019).

30. C. Wang, H. Yue, Z. Hu, Y. Shen, J. Ma, J. Li, X.-D. Wang, L. Wang, B. Sun, P. Shi, L. Wang, Y. Gu, Microglia mediate forgetting via complement-dependent synaptic elimination, *Science* **367**, 688–694 (2020).

31. S. Hong, V. F. Beja-Glasser, B. M. Nfonoyim, A. Frouin, S. Li, S. Ramakrishnan, K. M. Merry, Q. Shi, A. Rosenthal, B. A. Barres, C. A. Lemere, D. J. Selkoe, B. Stevens, Complement and microglia mediate early synapse loss in Alzheimer mouse models, *Science* **352**, 712–716 (2016).

32. D. P. Schafer, E. K. Lehrman, A. G. Kautzman, R. Koyama, A. R. Mardinly, R. Yamasaki, R. M. Ransohoff, M. E. Greenberg, B. A. Barres, B. Stevens, Microglia Sculpt Postnatal Neural Circuits in an Activity and Complement-Dependent Manner, *Neuron* **74**, 691–705 (2012).

33. P. T. Nguyen, L. C. Dorman, S. Pan, I. D. Vainchtein, R. T. Han, H. Nakao-Inoue, S. E. Taloma, J. J. Barron, A. B. Molofsky, M. A. Kheirbek, A. V. Molofsky, Microglial Remodeling of the Extracellular Matrix Promotes Synapse Plasticity, *Cell* **182**, 388-403.e15 (2020).

Supplementary Table 1. Results of immunohistochemistry in human and mouse brain tissue.

Measure	Group	Mean	SEM	Test statistic	Df	p-value
Human Iba-1 area (%)	Control	2.2	0.4			
	SAH	4.2	0.6	t= 2.6	20	**0.02**
Human Iba-1 cells	Control	20	5			
	SAH	50	8	t=3.1	20	**0.005**
Human Iba-1 process length (µm)	Control	129	18			
	SAH	119	16	t=0.7	20	0.68
Human GFAP area percentage (%)	Control	10.7	2.1			
	SAH	21.2	2.6	t=3.1	15	**0.007**
Human GFAP intensity (8bit)	Control	92	23			
	SAH	184	28	U: 39	15	**0.03**
Mouse Hipp Iba1 area (%)	Control	1.92	0.13			
	SAH	2.42	0.16	U: 46	25	**0.03**
Mouse Hipp iba1 cells	Control	155	9			
	SAH	190	10	U: 39	25	**0.01**
Mouse Hipp $GFAP^+$ cells	Control	251	13			
	SAH	242	10	t=0.51	30	0.61
Mouse Hipp GFAP intensity (8bit)	Control	39	1			
	SAH	39	1	t=0.3	30	0.79
Mouse prefrontal $GFAP^+$ cells	Control	40	17	U: 79	33	**0.02**
	SAH	56	20			
Mouse prefrontal GFAP intensity (8bit)	Control	10.1	0.4	t=0.52	33	0.61
	SAH	10.6	0.8			

Mouse Hipp Synaptophysin intensity (8bit)	Control	5.8	0.5	t=0.4	35	0.69
	SAH	5.5	0.4			
Mouse Hipp PSD-95 intensity (8bit)	Control	5.4	0.5	t=0.43	35	0.67
	SAH	5.1	0.4			

GFAP: Glial Fibrillary Acidic Protein (astrocyte marker); Iba-1: ionized calcium-binding adapter molecule 1 (microglia/macrophage marker); SAH: Subarachnoid Hemorrhage; 8bit: 2^8, or 256 greyscale values; Hipp: Hippocampus; PSD-95: Postsynaptic Density protein-95.

Supplementary Table 2. Results for the Open Field tests.

Measure	Group	Mean	SEM	Test statistic	Df	p-value
Mouse Velocity 1 week (cm/s)	Control	6.9	0.4			
	SAH	6.3	0.6	t=0.9	65	0.38
Mouse Velocity 2 weeks (cm/s)	Control	6.3	0.4			
	SAH	6.8	0.4	U=478	63	0.57
Mouse Velocity 1 month (cm/s)	Control	5.0	0.5			
	SAH	7.6	0.8	U=43	26	**0.01**
Mouse in center 1 week (%)	Control	3.0	0.4			
	SAH	3.3	0.5	U=547	65	0.89
Mouse in center 2 weeks (%)	Control	3.1	0.4			
	SAH	4.5	0.7	U=439	63	0.27
Mouse in center 1 month (%)	Control	1.9	0.3			
	SAH	3.5	2.3	t=2.4	26	**0.03**
SAH velocity (cm/s)	2 weeks	6.8	0.4			
	1 month	7.6	0.8	U=226	42	0.37
Control velocity (cm/s)	2 weeks	6.3	0.4			
	1 month	5.0	0.5	t=2.0	49	0.06
SAH in center (%)	2 weeks	4.5	0.7			
	1 month	3.5	2.3	U=259	42	0.81
Control in center (%)	2 weeks	3.1	0.4			
	1 month	1.9	0.3	t=2.1	49	**0.04**

Supplementary Table 3. Results for the Novel Object Recognition tests.

Measure	Group	Mean	SEM	Test statistic	Df	p-value
Short term memory; Mouse at novel object 1 week (%)	Control	55.9	2.0	t=2.0	44	0.05
	SAH	49.9	2.0			
	Control vs theoretical mean 50%			t=2.9	27	**0.008**
	SAH vs theoretical mean 50%			t=0.04	17	0.97
Short term memory; Mouse at novel object 2 weeks (%)	Control	59.6	1.9	t=2.2	46	**0.04**
	SAH	53.8	1.8			
	Control vs theoretical mean 50%			t=4.9	23	**0.0001**
	SAH vs theoretical mean 50%			t=2.1	23	**0.046**
Short term memory Mouse at novel object 1 month (%)	Control	63.5	1.9	t=1.7	13	0.12
	SAH	58.2	2.7			
	Control vs theoretical mean 50%			t=7.2	8	**0.0001**
	SAH vs theoretical mean 50%			t=3.1	5	**0.03**
Long term memory; Mouse at novel object 1 week (%)	Control	58.3	1.9	t=2.0	49	0.06
	SAH	53.5	1.9			
	Control vs theoretical mean 50%			t=4.3	18	**0.0004**
	SAH vs theoretical mean 50%			t=2.4	31	**0.02**
Long term memory; Mouse at novel object 2 weeks (%)	Control	57.9	1.6	t=2.6	53	**0.01**
	SAH	51.4	1.8			
	Control vs theoretical mean 50%			t=5.0	23	**0.0001**
	SAH vs theoretical mean 50%			t=0.7	30	0.46

Supplementary Table 3 continued.

Long term memory; Mouse at novel object 1 month (%)	Control	57.6	2.8	t=1.3	23	0.21
	SAH	52.4	2.8			
	Control vs theoretical mean 50%			t=2.7	10	**0.02**
	SAH vs theoretical mean 50%			t=0.9	13	0.41

Supplementary Table 4. Results for the Three Chamber Social Interaction tests.

Measure	**Group**	**Mean**	**SEM**	**Test statistic**	**Df**	**p-value**
Mouse vs empty cage; at mouse 1 week (%)	Control	48.5	2.7	t=1.9	57	0.068
	SAH	56.4	3.2			
	Control vs theoretical mean 50%			t=0.6	28	0.58
	SAH vs theoretical mean 50%			t=2.0	29	0.058
Mouse vs empty cage; at mouse 2 weeks (%)	Control	50.1	2.5	t=0.9	58	0.40
	SAH	53.4	2.7			
	Control vs theoretical mean 50%			t=0.1	28	0.95
	SAH vs theoretical mean 50%			t=1.2	30	0.23
Mouse vs empty cage; at mouse 1 month (%)	Control	52.5	3.4	t=1.0	26	0.31
	SAH	48.0	2.9			
	Control vs theoretical mean 50%			t=0.75	12	0.47
	SAH vs theoretical mean 50%			t=0.7	14	0.50
Novel vs familiar mouse; at novel mouse 1 week (%)	Control	52.7	3.9	t=0.001	48	0.99
	SAH	52.7	5.0			
	Control vs theoretical mean 50%			t=0.7	25	0.49
	SAH vs theoretical mean 50%			t=0.55	23	0.58

Novel vs familiar mouse; at novel mouse 2 weeks (%)	Control	49.9	3.6	t=0.4	51	0.71
	SAH	48.1	3.3			
	Control vs theoretical mean 50%			t=0.03	25	0.97
	SAH vs theoretical mean 50%			t=0.6	26	0.56
Novel vs familiar mouse; at novel mouse 1 month (%)	Control	50.7	10.0	t=0.5	22	0.61
	SAH	55.6	4.6			
	Control vs theoretical mean 50%			t=0.1	8	0.95
	SAH vs theoretical mean 50%			t=1.2	14	0.24

SAH: Subarachnoid Hemorrhage.

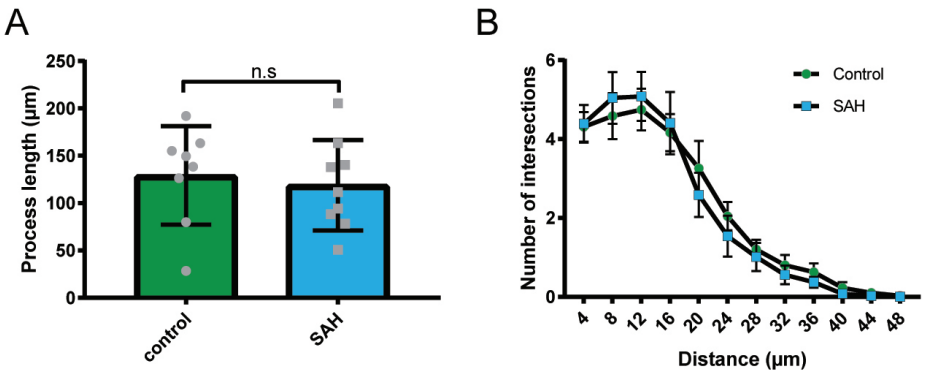

Supplementary Figure 1. Process length in microglia in the human cortex. A) The process length of Iba-1$^+$ cells was unchanged after SAH. B) Sholl analysis of Iba-1$^+$ positive cells showed a trend in higher short processes and fewer long processes after human SAH, as the number of intersections is up within 12µm of the soma and down from 20µm in the grey matter of the frontal cortex. Student's t-test in A; Bars and error bars in mean±SEM.

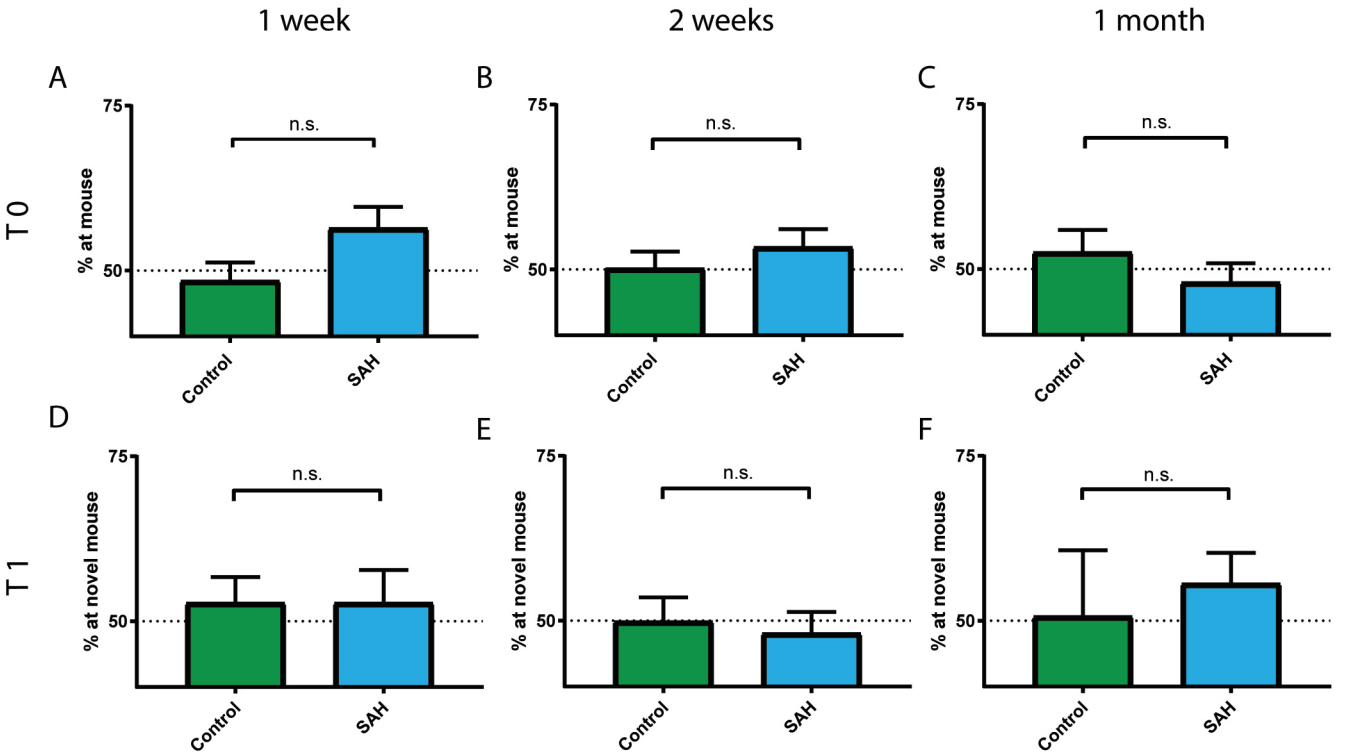

Supplementary Figure 2. Three chamber social interaction test. A) Mouse versus empty cage at 1 week after surgery, B) at 2 weeks after surgery, and C) at 1 month after surgery. D) novel mouse versus familiar mouse at 1 week after surgery, E) at 2 weeks after surgery, and F) at 1 month after surgery. Student's t-tests between groups, not significant, one-sample t-tests against a theoretical mean of 50%, not significant; Bars and error bars in mean±SEM.

CHAPTER 4

After experimental subarachnoid hemorrhage, the pool of quiescent neurogenic astrocytes in neurogenic niches is unaffected, showing potential to increase neuronal repair in the cortex.

B.J. van Dijk, MSc;[1]* C. Amboni, MSc;[1]* V. Donega, PhD;[1] J.A. Sluijs, BSc;[1] G.J.E. Rinkel, PhD, FRCP(E);[2] M.D.I. Vergouwen, MD, PhD;[2] E.M. Hol, PhD.[1]

1. Department of Translational Neurosciences, University Medical Center Utrecht Brain Center, University Utrecht, Utrecht, The Netherlands
2. Department of Neurology and Neurosurgery, University Medical Center Utrecht Brain Center, University Utrecht, Utrecht, The Netherlands

* Contributed equally

Manuscript in preparation

Abstract
Subarachnoid hemorrhage (SAH) from a ruptured intracranial aneurysm is a severe subtype of stroke leading to high case fatality and morbidity in patients. Subarachnoid hemorrhage causes profound brain damage due to an acute increase in intracranial pressure and ischemia due to cessation of the blood flow immediately after aneurysmal rupture. Secondary damage is likely caused by an immune response, orchestrated by the glial cells in the brain. Although the glial response to injury can be detrimental, it can also be neuroprotective and can facilitate repair. New-born cells derived from neurogenic astrocytes in the neurogenic niches of the adult brain can migrate towards the damaged area and differentiate into cells that contribute to the regenerative response. In the endovascular perforation SAH mouse model, we determined the number of quiescent neurogenic astrocytes and the fate of these cells near the damaged brain areas. Proliferating cells were labeled by 5-bromo-2-deoxyuridine (BrdU) and examined at 14 days after SAH. We found no differences in the number of $BrdU^+$ neurogenic astrocytes in the neurogenic niches between sham-operated (control; n=8) and SAH (n=14) mice, indicating that the pool of neurogenic astrocytes is not activated. However, by observing the brain sections of SAH mice, we found highly dense areas of $BrdU^+$ cells, of which some were also positive for the premature neuronal marker doublecortin, hinting towards intrinsic self-repair of damaged brain tissue.

Introduction

Subarachnoid hemorrhage from a ruptured intracranial aneurysm causes high case fatality and morbidity in patients *(1)*. The most important determinant of poor functional outcome after aneurysmal SAH is early brain injury directly related to the initial bleeding *(2, 3)*. Other major determinants of poor functional outcome are rebleeding of the aneurysm and delayed cerebral ischemia (DCI) *(4)*. Currently, there are no effective therapeutic interventions that prevent brain injury. Therapies that enhance repair mechanisms after injury may facilitate recovery after SAH.

One such repair mechanism is the brain's ability to generate new neurons *(5)* in two neurogenic niches, the subventricular zone (SVZ) in the lateral wall of the ventricles and the subgranular zone (SGZ) of the dentate gyrus in the hippocampus *(5, 6)*. During life, neurogenic astrocytes in these niches proliferate, migrate, and differentiate into new-born neurons. From the SVZ, a rostral migratory stream of neuroblasts migrate towards the olfactory bulb *(7)*, and the SGZ neurogenic astrocytes proliferate and migrate into the dentate gyrus *(6)*, in both cases these cells differentiate into glutamatergic and GABAergic neurons.

Upon injury, such as ischemic stroke and traumatic brain injury, neurogenesis is enhanced *(8, 9)*, as shown by an increase in the number of cycling cells. Furthermore, the migratory stream of new-born neurons diverts towards the injured brain areas, as a repair mechanism *(10)*. Although this mechanism has been investigated extensively in ischemic stroke, little is known about neurogenesis after SAH. One report shows a decrease in proliferation at the neurogenic niches in the first few days after SAH *(11)*. Two contradicting reports show both a stabilization and an increase *(11, 12)* in neurogenesis observed at 7 days after SAH. However, it is not known whether the change in cell proliferation sustains at later time points after SAH and what the fate is of the new-born cells. This information is required to determine whether the new-born cells facilitate brain repair in the damaged brain areas.

This study aimed to investigate whether there are long term changes in neurogenesis in the neurogenic niches after SAH, and whether there are indications of brain repair after SAH. We investigated this using the endovascular perforation mouse model and sham-operated control mice. Proliferating cells were labeled with BrdU before surgery and their number and fate were examined 14 days after SAH.

Materials and Methods

Endovascular perforation mouse model

All animal experiments were approved by the Institutional Animal Care and Use Committee of the University Medical Center Utrecht (UMCU), The Netherlands. Mice were originally purchased from Jackson Laboratory, USA, and further bred at the UMCU. Mice were weaned at 21 days, ear-punched for identification purposes, and housed with littermates in groups of 6-8 mice per cage. Adult male C57bl6/J mice of 2-3 months of age were randomly assigned to the sham (n=8) or SAH (n=14) group. Before anesthesia, mice were injected intraperitoneally with an analgesic (Carprofen; 5 mg/kg, in a volume of 100 µl/10g). Anesthesia was injected intraperitoneally in a volume of 100 µl/10g (Ketamine; 75 mg/kg, medetomidine; 1 mg/kg). The surgery was done according to a previously published method *(13)*. In short, an incision was made on the right side of the neck of the mouse, and the external carotid artery was exposed. A black nylon filament with a blunt tip (size 5-0, Ethicon) was inserted into the external carotid artery to the internal carotid artery. During filament insertion, a clip and sutures around the external carotid artery prevented the spilling of blood. In SAH mice, the nylon filament was advanced into the circle of Willis, and advanced further to perforate the vessel wall of the middle cerebral artery. Thereafter, the filament was retracted quickly to restore normal blood flow into the internal carotid artery and induce a SAH. In the sham control mice, the nylon filament was retracted before hitting the vessel wall. After removal of the nylon filament, the right external carotid artery of mice was ligated.

Post-surgery care

Mice were housed in groups, with a normal day-night cycle (white lights on from 7:00-19:00 hr). Cages were enriched with sawdust and tissues. Regular chow and water were provided ad libitum. After surgery, the chow was provided in heated water to soften it. Mice received one dose of analgesic 24h after the surgery. Cages were placed on top of a heating mat at 37°C after the surgery for 2h. The cages were placed half over the heating mat for up to 48h, for the mice to choose between heated or normal temperature. Mouse weight and neurologic scores were measured daily for the first two weeks after surgery and 3 times a week thereafter. Neurological scoring was performed according to the method of Sugawara et al. *(14)*. Mice that lost >20% of their weight after the surgery, without showing signs of improved neurological scores were killed and were removed from the experiment.

BrdU injections
Mice received 5-bromo-2-deoxyuridine (BrdU; 150 mg/kg/day in a dose for 100 µl/10g; Sigma) by intraperitoneal injection, on two consecutive days before the sham or SAH surgery and one injection during surgery *(15)*. Mice were killed 14 days after the surgery.

Immunofluorescent histochemistry
Brains were fixed by transcardial perfusion with 4% paraformaldehyde in phosphate-buffered saline (PBS: 0.137M NaCl; 0.0027M KCl; 0.01 M Na2HPO4; 0.0018M KH2PO4, pH= 7.4). Brains were kept in 4% paraformaldehyde in PBS for two days and then were transferred to 30% sucrose in PBS for two days. Brains were frozen in -55°C isopentane and stored at −80°C until slicing. Coronal cryosections of 20 µm were thaw-mounted on Superfrost Plus slides (VWR), dried at room temperature (RT) for 1 h, and stored at −80°C until use. The slides were post-fixed by incubation in 4% paraformaldehyde in PBS for 10 minutes and subsequently washed in PBS. Slides were either incubated in preheated HCl (2N) for 30 minutes in a 37°C incubator, followed by borate buffer (0.1M) at RT for 15 minutes to quench the acidity of HCl, or were incubated in 10 mM sodium citrate solution (Merck), 0.05% Tween 20 (Millipore Corporation), pH 6.0, by heating the sections in a steamer at 96°C for 20 minutes. Subsequently, slides were washed three times in PBS / 0.4% Triton-x100, and were incubated in the blocking buffer (0.25% BSA, 0.4% triton-X in PBS) at RT in a humidified chamber for 1 hour. Then, the slides were incubated with primary antibodies overnight (diluted in 0.25% BSA, 0.4% triton-X in PBS; overview of antibodies and dilutions in Table 1. The slides were washed for three times with PBS / 0.4% Triton-x100 for 10 minutes. Secondary antibodies were diluted in PBS / 0.25% Triton-x100 and incubated for at room temperature 1 hour. Donkey anti-rat 488 (1:1000; Dylight, Invitrogen) and Donkey anti-rabbit 594 (1:1000; Alexa Fluor, Thermo-Fisher) were used as secondary antibodies. Nuclei were stained with Hoechst (1:5000; Invitrogen H3569, Life Technologies). Finally, the sections were washed in PBS / 0.25% triton-X for three times 10 minutes and embedded with Fluorsave (Merck Millipore).

Table 1. Primary antibody characteristics of working antibodies.

Antibody	Host	Catalog number	Manufacturer	Dilution	Compatible with BrdU staining
BrdU	Rat monoclonal	Ab6326	Abcam	1:100	X
Iba1	Rabbit polyclonal	019-19741	Wako	1:2000	X
DCX	Goat polyclonal	SC8066	Santa Cruz	1:1000	X
Olig2	Rabbit polyclonal	18953	IBL	1:500	X
GFAP-pan	Rabbit polyclonal	Z0334	Dako	1:4000	X
NeuN	Mouse monoclonal	MAB377	Millipore	1:500	-
Sox9	Rabbit polyclonal	82630S	Cell signaling	1:1000	-
GFAPα	Goat polyclonal	SC-6170	Santa Cruz	1:400	-
GFAPδ mouse	Rabbit polyclonal	homemade	NIN	1:500	-

X: compatible with BrdU staining; -: not compatible with BrdU staining.

Image acquisition and analysis
The SVZ at the lateral ventricles and SGZ of the dentate gyrus were imaged. At the time of imaging, the investigator was blinded for the experimental group (SAH or sham). The sections were imaged with a 20x magnification on an epifluorescent microscope (Zeiss AxioImager M2 fluorescent microscope with N-Achroplan objectives, AxioCam MRm camera and Software Zen 2011) and with a 60x magnification on a confocal microscope (Olympus Fluoview FV1000 laser scanning microscope with a UPlan Apo N objective). $BrdU^+$ cells were counted manually. $BrdU^+/Iba1^+$ cells, that represented dividing microglia, were also counted manually. Cells up to 10µm from the lateral ventricles in the brain sections (left and right, anterior, and posterior) were counted. The mean number of cells for up to 4 lateral ventricles per mouse were calculated.

Statistical analysis
A p-value of <0.05 was considered statistically significant. Statistics were calculated using GraphPad Prism (GraphPad Software, Sandiego, USA). Student's t-tests were used for parametric testing and the Mann-Whitney test was used for non-parametric testing.

Results

Characteristics of the endovascular perforation SAH mouse model
An overview of the mouse experiments is shown in Figure 1A. Both control and SAH mice lost weight after surgery, but the control mice gradually gained weight from day 2 after surgery. The SAH mice dropped in weight until day 5 and started to gain weight thereafter (Figure 1B). All mice were assessed for balance, motor, and sensory behaviour problems, with a maximum score of 18 in unaffected mice. Most control mice were neurologically unaffected, with one control mouse that responded a bit slow to touch, resulting in a slightly lower mean neurological score during the first two days after the surgery (Figure 1C). The SAH mice clearly showed a drop in the neurological score on day 1 after surgery, but improved gradually in performance on each following day (Figure 1C). All control mice survived the sham surgery, and in the SAH group, 67% survived the initial 14 days after the experimental SAH surgery (Figure 1D).

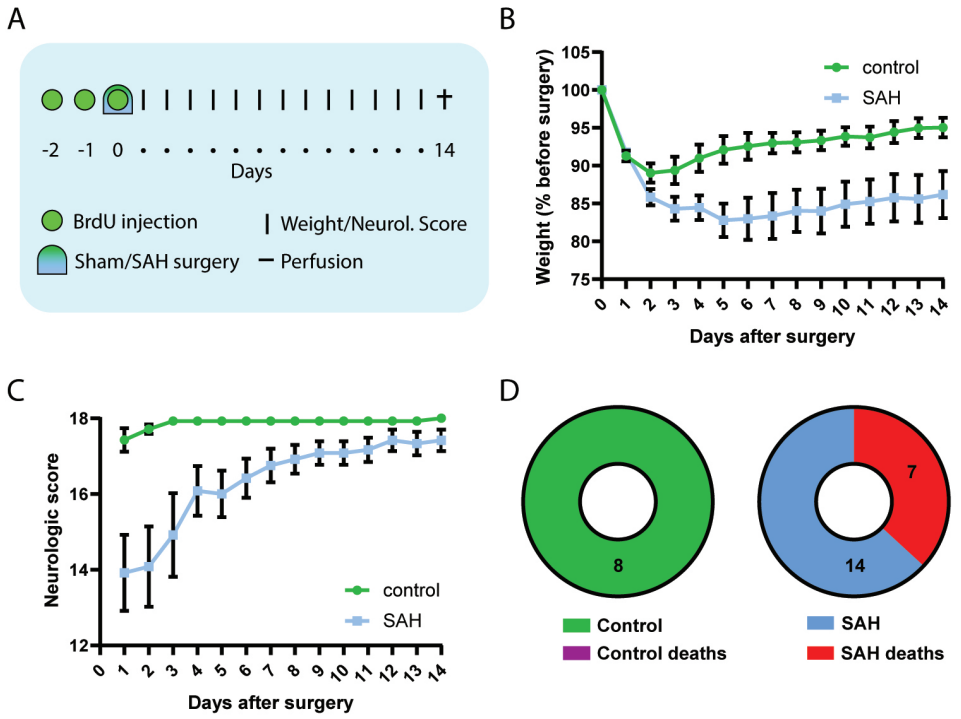

Figure 1. Study overview and mouse characteristics. A) Mice were injected with BrdU on days -2, -1, and the day of the Sham/SAH surgery (day 0). Mice were then weighted and tested for neurological scores daily for 14 days. Mice were killed and perfused for immunocytochemical analysis 14 days after sham/SAH surgery. B) Repeated weight measurements, and C) Neurological scores in the 14 days after surgery. D) Survival pie charts for sham-operated control mice and SAH mice. Mean ± SEM.

No difference in number of quiescent neurogenic astrocytes, but a decrease in the number of proliferating microglia in the SVZ after SAH.

To study whether the number of mitotic cells is changed after an SAH, we first counted the number of $BrdU^+$ neurogenic astrocytes in the SVZ, two weeks after surgery, as new-born neurons are the progeny of these cells. The neurogenic astrocytes are identified by immunostaining for both GFAP and BrdU. In both the control and SAH mice, most $BrdU^+$ cells in the SVZ co-localized with the GFAP-immunostaining, confirming that these cells were indeed neurogenic astrocytes (Figure 2A). We also observed $BrdU^+$ cells that did not co-localize with GFAP-immunostaining, close to the SVZ. These cells

were immunopositive for the microglia/macrophages marker Iba-1 (Figure 2B). With the combined BrdU and Iba-1 immunostaining, we could identify brain areas with increased microglia activity and make a distinction between the $BrdU^+$ neurogenic astrocytes and the mitotic microglia in the SVZ. Representative images are shown for both control (Figure 2C) and SAH mice (Figure 2D). Iba-1 positivity seemed to be increased after SAH, suggesting there were activated microglia after SAH (data not shown). We found no difference in the number of $BrdU^+$ cells that were negative for Iba-1 (hereafter referred to as $BrdU^+/Iba\text{-}1^-$ cells) in the SVZ between the SAH and control mice at 2 weeks after surgery and the last BrdU injection (control Mean ± SEM: 1.0 ± 0.2, n=8 mice; SAH: 1.3 ± 0.2, n=14 mice, Student's t-test t=0.8; p=0.41; Figure 2E). We found a reduction in the number of BrdU positive microglia/macrophages (hereafter referred to as $BrdU^+/Iba\text{-}1^+$ cells) in the SVZ of SAH compared to control mice 14 days after surgery and last BrdU injection (control: Mean ± SEM: 0.08 ± 0.03, n=8; SAH: 0.03 ± 0.01, n=13, Student's t-test t=2.2; p=0.04, Figure 2F).

No difference in the number of quiescent neurogenic astrocytes and the number of proliferating microglia in the SGZ after SAH.

Next, we quantified the number of $BrdU^+/Iba1^-$ and $BrdU^+/Iba1^+$ cells in the other neurogenic niche, the SGZ of the dentate gyrus. In both control mice and SAH mice, we found only a few $BrdU^+$ cells within the dentate gyrus (representative images are shown in Figures 2A and 2B). There was no difference in the number of $BrdU^+/Iba\text{-}1^-$ cells in the SGZ between the control and SAH mice at 2 weeks after surgery and the last BrdU injection (Control mean ± SEM: 5.5 ± 1.7, n=7; SAH: 5.1 ± 1.2,0 n=12; Student's t-test t=0.2; p=0.85; Figure 2C). Furthermore, there was also no difference in the number of $BrdU^+/Iba\text{-}1^+$ between the groups at the same time point (Control mean ± SEM: 1.6 ± 0.3, n=7; SAH: 1.3 ± 0.3, n=12; Mann-Whitney test U=27; p=0.22; Figure 2D).

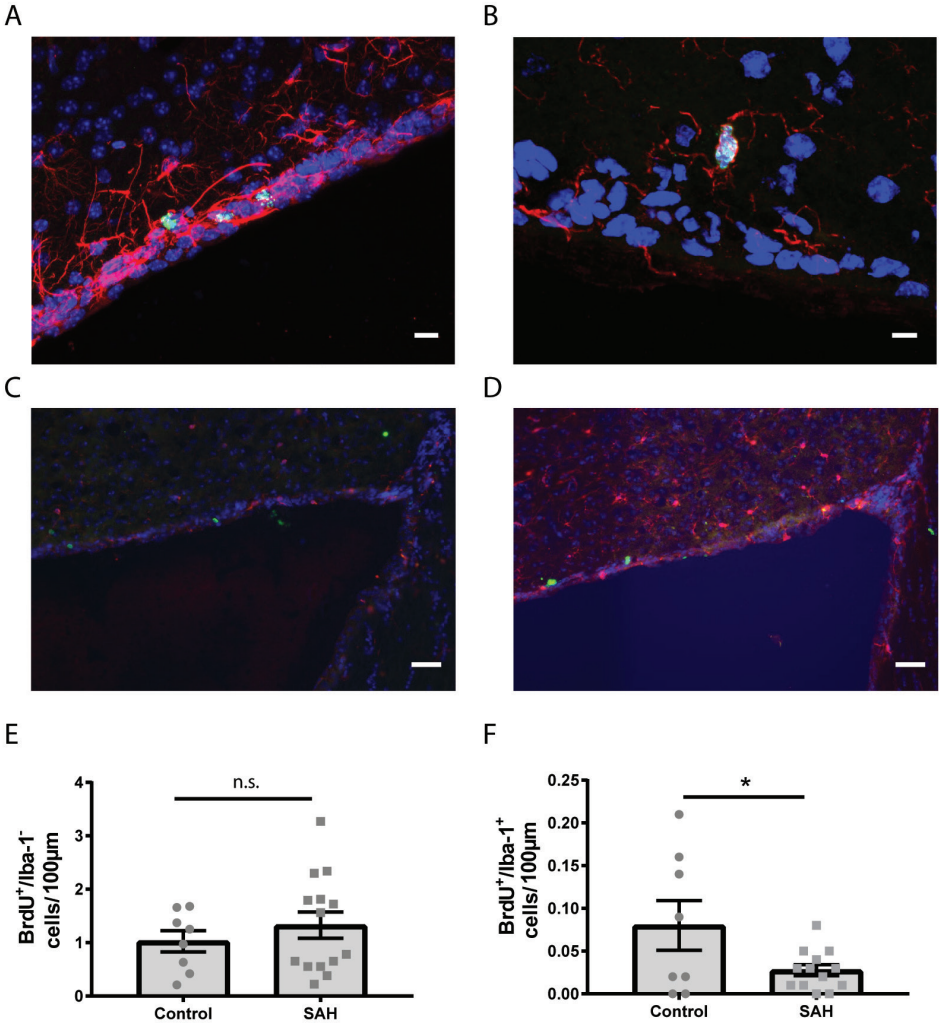

Figure 2. BrdU positive cells in the subventricular zone, two weeks after surgery, and the last BrdU injection. A) Close up of $BrdU^+/GFAP^+$ neurogenic astrocytes in the SVZ. B) Close up of a $BrdU^+/Iba\text{-}1^+$ cell near the SVZ. C) Representative image of $BrdU^+$ cells in the Sham SVZ and D) in the SAH SVZ. E) Quantification of the number of $BrdU^+/Iba\text{-}1^-$ cells per 100 µm SVZ, and F) $BrdU^+/Iba\text{-}1^+$ cells per 100 µm SVZ. For images: nucleic marker Hoechst in blue; BrdU staining in green; GFAP or Iba-1 in red; Scale bars for A = 10 µm, B = 5µm, C and D = 40 µm. Student's t-tests; n.s.: not significant, * $p<0.05$; Mean ± SEM; dots and squares represent mean per mouse.

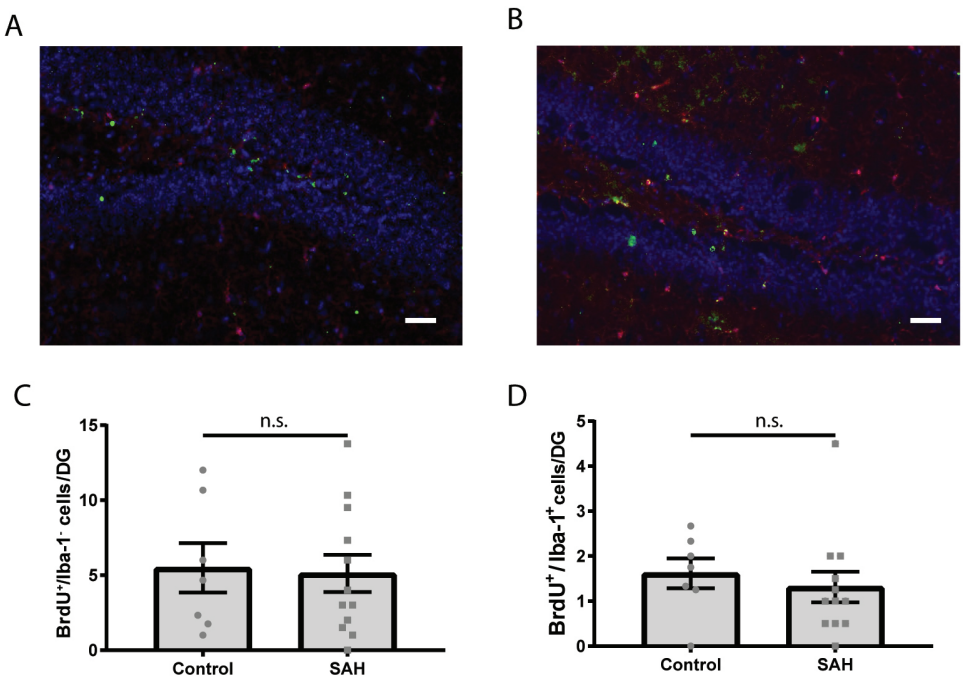

Figure 3. BrdU positive cells in the sub-granular zone of the dentate gyrus, two weeks after surgery and last the BrdU injection. A) Representative image of the dentate gyrus of a control and B) an SAH mouse. C) Quantification of the number of $BrdU^+/Iba\text{-}1^-$ cells and D) $BrdU^+/Iba\text{-}1^+$ cells in the dentate gyrus. For images: nucleic marker Hoechst in blue; BrdU staining in green and Iba-1 in red; Scale bar = 40µm; Student's t-tests; n.s.: not significant; Mean ± SEM; dots and squares represent mean per mouse.

$BrdU^+$ cells near cortical gliosis likely to play a role in neuronal repair.

Next, we investigated the location and the cell fate of $BrdU^+$ cells outside the neurogenic niches. We performed immunostainings for BrdU, in combination with several cell markers, i.e. Iba1 (microglia), DCX (new-born neurons), olig2 (oligodendrocytes), and pan-GFAP (astrocytes) (Table 1) to check $BrdU^+$ cell location and fate. We randomly selected sections of Sham control and SAH mice, for a qualitative analysis.

We observed many $BrdU^+$ cells along the RMS and within the olfactory bulb. Most $BrdU^+$ cells were DCX negative, suggesting these cells were neuronal precursors, mature neurons, or non-neuronal cells (Figure 3A). Next, we questioned whether there were also $BrdU^+$ cells outside the RMS and olfactory bulb. In control mice, we rarely observed $BrdU^+$ cells in the cortex, whereas these cells were more abundant after SAH (Figure 3B and 3C). We

found areas with high densities of $BrdU^+$ cells in SAH mice only. In these locations we also observed a higher number of Iba-1 + cells, suggesting that microglia in these areas were more activated in response to damage (Figure 3D). Most of these $BrdU^+$ cells were also Iba-1^+, showing an increase in dividing microglia in these areas. We also observed some cells that were both $BrdU^+/DCX^+$ (Figure $3E_1$ and E_2), indicating the presence of new-born neurons. The DCX^+ cells were observed in an area from the SVZ towards the damaged lateral cortex, suggesting a stream of new-born neurons diverting towards the damaged area. We performed several immunostainings for other cell markers at those damaged areas, and we showed that the $BrdU^+$ cells were negative to Olig2 and GFAP-pan, indicating that no new-born astrocytes and oligodendrocytes are present. For immunostaining for BrdU, sections had to be treated with either HCl or citrate buffer solution. The immunostaining for NeuN (mature neurons), Sox9 (oligodendrocyte precursor cells), and the GFAP isoforms GFAPα and GFAPδ to make a distinction between neurogenic astrocytes and other astrocytes *(16)*, were not compatible with the staining protocol for BrdU (Table 1).

> Figure 4. ***Cell fate of $BrdU^+$ cells outside the neurogenic niches.*** *A) Doublecortin (DCX^+) and $BrdU^+$ cells in the rostral migratory stream (dashed triangle) and olfactory bulb (neuroblasts migrate from the RMS into the olfactory bulb in the direction of the arrows). B) Sparse $BrdU^+$ cell in the cortex of a control mouse, the cell is DCX^-. C) Several $BrdU^+$cells in the cortex of an SAH mouse, with Iba-1^+ cells that are still ramified (insert depicts ramified microglia). D) Dense area of BrdU positive cells with highly active amoeboid Iba-1 positive cells (insert depicts amoeboid microglia). The left side of D is towards to cortex, the right side is towards the SVZ. E_1) DCX^+ positive cells, at the Iba1^+ dense damaged brain area as depicted in D. E_2) Same image as in E_1, but with BrdU positive cells in green to show some DCX^+/ $BrdU^+$ new-born neurons. Scale bars: A, B, C, D = 40µm, E = 5µm. Nucleic marker Hoechst in blue, BrdU in green, Doublecortin in red in A, B and $E_{1,2}$, Iba-1 in red in C and D.*

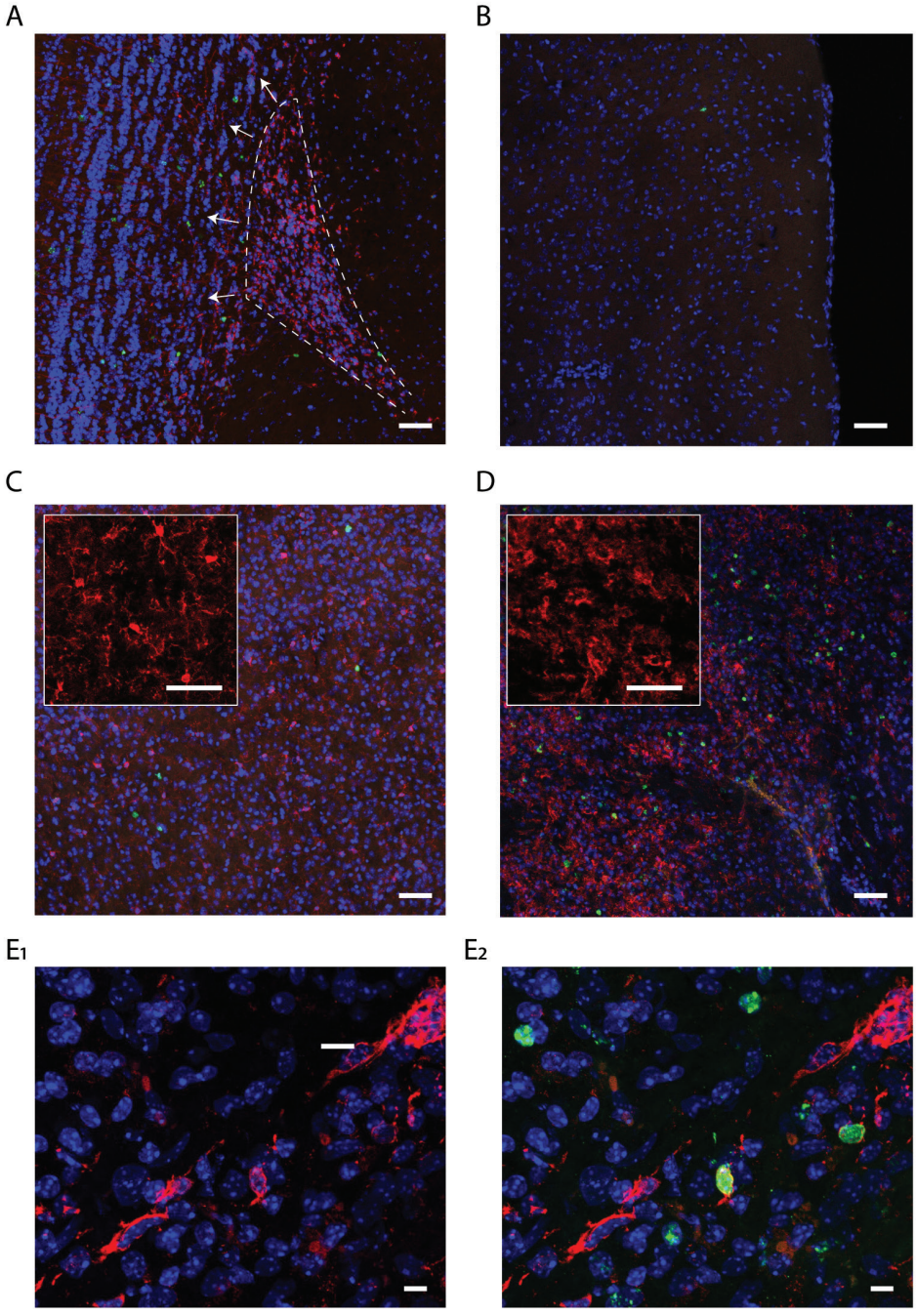
A
B
C
D
E1
E2

Discussion

Here we investigated whether there are signs of a beneficial glial response after SAH leading to increasing levels of self-repair. We investigated the neurogenic niches at two weeks after the induction of SAH. We did not find a difference in the number of $BrdU^+$ neurogenic astrocytes in either neurogenic niche between control and SAH mice. Interestingly, in SAH mice we found a reduction in the number of $BrdU^+$/Iba-1^+ microglia/macrophages in the SVZ and a trend in reduction in the SGZ, but an increase of these cells in other areas. Furthermore, we observed $BrdU^+$/DCX^+ cells close to the affected brain areas with highly activated microglia, suggesting there is intrinsic self-repair after SAH in mice.

Working with BrdU has practical limitations. BrdU only incorporates into dividing cells. The amount of incorporated BrdU is halved each time that a cell proliferates. After the proliferation of a neurogenic astrocyte, one daughter cell moves away, and the other stays to maintain a stable number of quiescent cells in the niche *(17)*. In our study, the cells that were counted as $BrdU^+$, two weeks after SAH, did not proliferate much, as otherwise the BrdU signal would have faded. These cells therefore remained mostly in a quiescent state. Active and highly proliferating neural stem cells will lose BrdU signal, and therefore, the counting at the neurogenic niches may be an underestimation of the neurogenic response.

It has been shown in several studies that ischemic stroke and traumatic brain injury leads to an increase in neurogenesis in the SVZ and SGZ, which is facilitated by an increase in proliferation of neurogenic astrocytes in the neurogenic niches*(8, 9)*. Neurogenesis in the first week after SAH has been described both to increase and decrease in the SVZ in rats *(12, 18)*. In mice, there was a decrease in neurogenesis in the first few days after SAH, thereafter the number of proliferating cells increased or stabilized *(11)*. The absence changes in quiescent neurogenic astrocytes in both neurogenic niches at two weeks after the SAH, suggests that in our model these cells were not activated to divide more rapidly.

We were also interested in the fate of the new-born cells originating from the neurogenic niches. In the healthy brain, migrating neuroblasts travel along the RMS towards the olfactory bulb *(19)*. After ischemic stroke, these cells have been shown to migrate towards ischemic areas in the striatum *(10)*. Others have found DCX^+ new-born neurons in the striatum at days 7 after SAH *(12)*. However, BrdU labeling was omitted in that study, so it is hard to

tell whether these cells are the progeny of SAH-induced dividing cells in the neurogenic niches. We observed more $BrdU^+$ cells in the cortex in SAH mice, suggesting an increase in new-born cells. These cells were also DCX^+, further suggesting a diversion of migrating new-born neurons from the SVZ/RMS to damaged brain areas after SAH. As we investigated the mice at two weeks after the SAH, some cells could have fully differentiated to mature neurons. Unfortunately, the marker to identify these cells, NeuN, did not work in combination with BrdU. It would be interesting to investigate this further, to test for other neuronal markers, and to add a full quantification of the number of $BrdU^+/DCX^+$ cells in all mice, to get a better understanding of the intrinsic self-repair mechanisms after SAH.

Besides the migration of neuroblasts from the SVZ towards the site of injury, there can be other sources of the new-born neurons in the damaged brain areas. In reaction to central nervous system injury, astrocytes outside the neurogenic niches also can proliferate *(20)*. This has been observed after a stab wound injury *(21)* and ischemic stroke *(22)*. These cells can then differentiate into neurons. Another source of new-born cells than the neurogenic niches are local proliferating oligodendrocyte precursor cells *(23)*. After traumatic brain injury, these cells start to proliferate faster *(24)*. Faster proliferation leads to doublets in the tissue sections, which we did not found, nor did we find $BrdU^+$ cells that were also positive for Olig2 or GFAP, suggesting oligodendrocytes and astrocytes were not among the $BrdU^+$ cells. There are also microglial stem cells that keep a homeostasis of the amount of microglia in a healthy brain *(25)*. In both our control and SAH mice, we found $BrdU^+/Iba\text{-}1^+$, which are likely the stem cell microglia. We found a reduction in $BrdU^+/Iba\text{-}1^+$ in the SVZ in the SAH group. This was unexpected, as after injury there usually are more microglia *(26)*, and we expected most of them would also be $BrdU^+$. There are two likely explanations for this result. Either the microglia moved out of the SVZ, or the microglia proliferated vigorously and therefore lost all BrdU signal. In the first scenario, there are more $BrdU^+$ cells elsewhere in the brain, likely near sites of injury as immune activated microglia are known to migrate towards the site of injury *(27)*. Although we did not quantify this, there was a clear increase in the number of $Iba1^+$ and $BrdU^+$ cells in cortical areas of SAH mice. In the second scenario there would also be more microglia in the damaged area, but these are not or lightly BrdU positive. Both could be true, and it would be interesting to study this further. We found indications of intrinsic self-repair after SAH, as we observed an increase in DCX^+ new-born neurons. Several studies on therapeutically stim-

ulating this response have found an increase in new-born cells, and outcome after SAH, at least in rodent models *(12, 28)*. However, having new-born neurons is not enough, they also need to integrate into the existing neuronal network, by axonal outgrowth and the formation of active synapses. Unfortunately, this often seems to fail *(29)*. These new-born neurons migrate into areas in which glial cells are highly immune activated. Although these activated glial cells produce neurotrophic factors, they also produce factors that adverse the outgrowth of axons *(30)*. Solely stimulating proliferation and migration of new-born neurons to the site of brain injury, therefore, is not enough, and should be combined with a blockade of the production of the adverse effects on axonal outgrowth by glial activation.

In conclusion, the number the quiescent neurogenic astrocytes in the SVZ and SGZ is not affected by SAH. There was a reduction in BrdU positive microglia in the SVZ, likely due to the increased migration of these cells towards damaged brain areas. We found signs of increased self-repair after SAH, as there were more DCX+ new-born neurons near the damaged brain area. Further investigation is needed to study this effect in detail, and should point out whether we can stimulate this beneficial glial response, as a treatment for SAH patients.

References

1. J. van Gijn, R. S. Kerr, G. J. Rinkel, Subarachnoid haemorrhage, The Lancet 369, 306–318 (2007).

2. Y. B. Roos, R. J. de Haan, L. F. Beenen, R. J. Groen, K. W. Albrecht, M. Vermeulen, Complications and outcome in patients with aneurysmal subarachnoid haemorrhage: a prospective hospital based cohort study in the Netherlands, J. Neurol. Neurosurg. Psychiatry 68, 337–341 (2000).

3. M. D. Vergouwen, A. V. Jong-Tjien-Fa, A. Algra, G. J. Rinkel, Time trends in causes of death after aneurysmal subarachnoid hemorrhage: A hospital-based study, Neurology 86, 59–63 (2016).

4. M. D. Vergouwen, M. Vermeulen, J. van Gijn, G. J. Rinkel, E. F. Wijdicks, J. P. Muizelaar, A. D. Mendelow, S. Juvela, H. Yonas, K. G. terBrugge, R. L. Macdonald, M. N. Diringer, J. P. Broderick, J. P. Dreier, Y. B. Roos, Definition of delayed cerebral ischemia after aneurysmal subarachnoid hemorrhage as an outcome event in clinical trials and observational studies: proposal of a multidisciplinary research group, Stroke 41, 2391–2395 (2010).

5. J. P. Magnusson, J. Frisén, Stars from the darkest night: unlocking the neurogenic potential of astrocytes in different brain regions, Development 143, 1075–1086 (2016).

6. J. T. Gonçalves, S. T. Schafer, F. H. Gage, Adult Neurogenesis in the Hippocampus: From Stem Cells to Behavior, Cell 167, 897–914 (2016).

7. M. S. Brill, J. Ninkovic, E. Winpenny, R. D. Hodge, I. Ozen, R. Yang, A. Lepier, S. Gascón, F. Erdelyi, G. Szabo, C. Parras, F. Guillemot, M. Frotscher, B. Berninger, R. F. Hevner, O. Raineteau, M. Götz, Adult generation of glutamatergic olfactory bulb interneurons, Nat. Neurosci. 12, 1524–1533 (2009).

8. A. Arvidsson, T. Collin, D. Kirik, Z. Kokaia, O. Lindvall, Neuronal replacement from endogenous precursors in the adult brain after stroke, Nat. Med. 8, 963 (2002).

9. B. Saha, S. Peron, K. Murray, M. Jaber, A. Gaillard, Cortical lesion stimulates adult subventricular zone neural progenitor cell proliferation and migration to the site of injury, Stem Cell Res. 11, 965–977 (2013).

10. T. Yamashita, M. Ninomiya, P. Hernandez Acosta, J. M. Garcia-Verdugo, T. Sunabori, M. Sakaguchi, K. Adachi, T. Kojima, Y. Hirota, T. Kawase, N. Araki, K. Abe, H. Okano, K. Sawamoto, Subventricular Zone-Derived Neuroblasts Migrate and Differentiate into Mature Neurons in the Post-Stroke Adult Striatum, J. Neurosci. 26, 6627–6636 (2006).

11. M. Mino, H. Kamii, M. Fujimura, T. Kondo, S. Takasawa, H. Okamoto, T. Yoshimoto, Temporal changes of neurogenesis in the mouse hippocampus after experimental subarachnoid hemorrhage, Neurol. Res. 25, 839–845 (2003).

12. W.-D. Lee, K.-C. Wang, Y.-F. Tsai, P.-C. Chou, L.-K. Tsai, C.-L. Chien, Subarachnoid Hemorrhage Promotes Proliferation, Differentiation, and Migration of Neural Stem Cells via BDNF Upregulation., PloS One 11, e0165460 (2016).

13. Z. V. Zheng, H. Lyu, S. Y. E. Lam, P. K. Lam, W. S. Poon, G. K. C. Wong, The Dynamics of Microglial Polarization Reveal the

Resident Neuroinflammatory Responses After Subarachnoid Hemorrhage, Transl. Stroke Res. 11, 433–449 (2020).

14. T. Sugawara, R. Ayer, V. Jadhav, J. H. Zhang, A new grading system evaluating bleeding scale in filament perforation subarachnoid hemorrhage rat model, J. Neurosci. Methods 167, 327–334 (2008).

15. W. Kamphuis, M. Orre, L. Kooijman, M. Dahmen, E. M. Hol, Differential cell proliferation in the cortex of the appsweps1de9 alzheimer's disease mouse model, Glia 60, 615–629 (2012).

16. S. A. Van Den Berge, J. Middeldorp, C. E. Zhang, M. A. Curtis, B. W. Leonard, D. Mastroeni, P. Voorn, W. D. J. Van De Berg, I. Huitinga, E. M. Hol, Longterm quiescent cells in the aged human subventricular neurogenic system specifically express GFAP-δ: GFAP-δ in aged human SVZ stem cells, Aging Cell 9, 313–326 (2010).

17. O. Basak, T. G. Krieger, M. J. Muraro, K. Wiebrands, D. E. Stange, J. Frias-Aldeguer, N. C. Rivron, M. van de Wetering, J. H. van Es, A. van Oudenaarden, B. D. Simons, H. Clevers, Troy+ brain stem cells cycle through quiescence and regulate their number by sensing niche occupancy, Proc. Natl. Acad. Sci. 115, E610–E619 (2018).

18. Y. Zuo, J. Wang, B. Enkhjargal, D. Doycheva, X. Yan, J. H. Zhang, F. Liu, Neurogenesis changes and the fate of progenitor cells after subarachnoid hemorrhage in rats, Exp. Neurol. 311, 274–284 (2019).

19. M. C. Whitman, C. A. Greer, Adult neurogenesis and the olfactory system, Prog. Neurobiol. 89, 162–175 (2009).

20. I. B. Wanner, M. A. Anderson, B. Song, J. Levine, A. Fernandez, Z. Gray-Thompson, Y. Ao, M. V. Sofroniew, Glial Scar Borders Are Formed by Newly Proliferated, Elongated Astrocytes That Interact to Corral Inflammatory and Fibrotic Cells via STAT3-Dependent Mechanisms after Spinal Cord Injury, J. Neurosci. 33, 12870–12886 (2013).

21. A. Buffo, I. Rite, P. Tripathi, A. Lepier, D. Colak, A.-P. Horn, T. Mori, M. Gotz, Origin and progeny of reactive gliosis: A source of multipotent cells in the injured brain, Proc. Natl. Acad. Sci. 105, 3581–3586 (2008).

22. J. P. Magnusson, C. Goritz, J. Tatarishvili, D. O. Dias, E. M. K. Smith, O. Lindvall, Z. Kokaia, J. Frisen, A latent neurogenic program in astrocytes regulated by Notch signaling in the mouse, Science 346, 237–241 (2014).

23. T. Maki, Novel roles of oligodendrocyte precursor cells in the developing and damaged brain, *Clin. Exp. Neuroimmunol.* **8**, 33–42 (2017).

24. C. Simon, M. Götz, L. Dimou, Progenitors in the adult cerebral cortex: Cell cycle properties and regulation by physiological stimuli and injury, *Glia* **59**, 869–881 (2011).

25. M. R. P. Elmore, A. R. Najafi, M. A. Koike, N. N. Dagher, E. E. Spangenberg, R. A. Rice, M. Kitazawa, B. Matusow, H. Nguyen, B. L. West, K. N. Green, Colony-Stimulating Factor 1 Receptor Signaling Is Necessary for Microglia Viability, Unmasking a Microglia Progenitor Cell in the Adult Brain, *Neuron* **82**, 380–397 (2014).

26. T. K. Ulland, Y. Wang, M. Colonna, Regulation of microglial survival and proliferation in health and diseases, *Semin. Immunol.* **27**, 410–415 (2015).

27. Y. Fan, L. Xie, C. Y. Chung, Signaling Pathways Controlling Microglia Chemotaxis, *Mol. Cells* **40**, 163–168 (2017).

28. C. H. Nijboer, E. Kooijman, C. T. van Velthoven, E. van Tilborg, I. A. Tiebosch, N. Eijkelkamp, R. M. Dijkhuizen, J. Kesecioglu, C. J. Heijnen, Intranasal Stem Cell Treatment as a Novel Therapy for Subarachnoid Hemorrhage., *Stem Cells Dev.* **27**, 313–325 (2018).

29. A. M. Turnley, H. S. Basrai, K. J. Christie, Is integration and survival of new-born neurons the bottleneck for effective neural repair by endogenous neural precursor cells?, *Front. Neurosci.* **8** (2014), doi:10.3389/fnins.2014.00029.

30. A. Sandvig, M. Berry, L. B. Barrett, A. Butt, A. Logan, Myelin-, reactive glia-, and scar-derived CNS axon growth inhibitors: Expression, receptor signaling, and correlation with axon regeneration, *Glia* **46**, 225–251 (2004).

Summary and General Discussion

B.J. van Dijk

Summary

Aneurysmal subarachnoid hemorrhage (SAH) can lead to poor functional outcome and cognitive impairment[1,2]. The most important determinant of poor functional outcome after aneurysmal SAH is early brain injury, which is directly related to the initial bleeding[3,4]. Other major determinants of poor functional outcome are rebleeding of the aneurysm, and delayed cerebral ischemia (DCI), which can occur 4-14 days after the initial bleeding[5]. In patients with cognitive impairment, many domains can be affected, such as memory, attention, executive function, and language. Upon SAH, there is an overwhelming immune response[6]. The immune response is supposed to limit the damage inflicted by the SAH. However, it probably also causes additional brain injury, which can contribute to functional outcome and cognitive impairment. We aimed to characterize the complement and glial responses after SAH, and identify their impact on the brain.
In **chapter 1,** we systematically reviewed the literature on the glial response after SAH until July 2015 (an update is presented in the text below). We also gave insights into the potential functional consequences and clinical implications of this glial response. We discussed how immune activated glial cells may affect brain functions after aneurysmal SAH. Furthermore, we focused on their contribution to early brain injury, DCI, and cognitive impairment.

In **chapter 2**, we studied the role of the complement system in the development of brain injury after SAH[7]. We found an increase in the presence of complement components C1q and C3 in the brain of SAH patients. Furthermore, we found an association between a single nucleotide polymorphisms in the complement gene C5 and poor functional outcome in patients. Patients with this risk allele had lower plasma C5a levels, although the plasma levels did not correlate with poor functional outcome. Moreover, we found that complement component C5a levels in cerebrospinal fluid were highly increased 1 day after SAH. In mice lacking the C5a receptor, we found a reduced microglia response and reduced neural cell death after experimentally induced SAH. Moreover, the microglia response and neural cell death were also reduced in wildtype mice which were given injections with an antibody that prevents the cleavage of C5 into C5a and C5b, after experimentally induced SAH.

In **chapter 3,** we investigated the glial response in the frontal cortex of SAH patients. The results suggested an activated state of both astrocytes and microglia in humans after SAH. Subsequently, we focused on the glial response and cognitive changes in an SAH mouse model and found that mice with SAH have memory impairment. Furthermore, there was an increased complement/glial response in the hippocampus of mice with SAH, which correlated with memory impairment. These results suggests that complement activation results in a glial response, which in turn contributes to cognitive impairment after SAH.

In **chapter 4,** we investigated whether the glial response can be beneficial, by having regenerative properties to repair brain tissue after SAH. We did not find a difference in the amount of proliferative neurogenic astrocytes within the neurogenic niches of the mouse brain two weeks after SAH. However, we observed a potential self-repair mechanism that led to induction of newborn neurons near highly damaged brain areas.

General discussion

In this part, we highlight and discuss the most important findings, methods, and their limitations. We propose an hypothesis on how the complement system and glial response are involved in both early and delayed injury after SAH. We will also discuss the methods used to study this. We will describe possible treatment options that can potentially reduce poor functional outcome and cognitive deficits after an SAH. And lastly, we will give an overview future directions for further studies, based on the results in this thesis.

To reduce the amount of patients inflicted with an SAH, prevention is key. Therefore, smoking should be avoided and hypertension needs to be treated, as these are the most common avoidable factors in aneurysm formation[8,9]. An estimated 3% of the adult population has an intracranial aneurysm[10,11], most of them unknowingly residing in the head. Population-wide screening for intracranial aneurysms is not cost-effective. Currently, most unruptured intracranial aneurysms remain untreated, since the risk of rupture needs to be weighed against the risk of complications from preventive endovascular or neurosurgical aneurysm treatment. As long as the formation and the bursting of aneurysms cannot be prevented, there will be patients with SAH. The incidence of aneurysmal SAH is 6.1 per 100.000 persons-years[1,12]. Prognosis has improved over the last 30 years, however, the case-fatality is still around 30% in hospital-based studies[3,13].

After an SAH, the initial hemorrhage is followed by physiological and cellular events that contribute to early brain damage, and is often followed by delayed cerebral ischemia and cognitive impairment[1]. Early brain injury is mostly caused by acute ischemia, resulting from the rise in intracranial pressure and a decline in cerebral perfusion pressure[14,15]. The acute ischemia in combination with blood in the subarachnoid space elicits several other processes such as a disturbed blood-brain barrier (BBB). Harmful compounds can pass the leaky BBB, damaging and dysregulating the brain parenchyma[16]. Subsequently, dysfunctional autoregulation and spreading depolarization may occur[16]. Moreover, the metabolites induced by hemostasis can also lead to microthrombi, reducing blood flow in the brain capillaries. All these early pathogenic responses probably also contribute to the later development of DCI[17]. In many of these responses, the complement system is involved[18–21]. The pathogenesis of cognitive impairment has not yet been clarified, however, the complement system is likely involved, as will be discussed in more detail below.

Immune activation

An SAH initiates an immune response in the subarachnoid space and brain parenchyma. The complement system is a major initiator and modulator of the innate immune response. Interestingly, the complement system has also been associated with aneurysm development and growth, however, in this discussion we will only focus on the complement response after aneurysm rupture[22]. Upon SAH, endogenous damage-associated molecular patterns (DAMPs) biomolecules are released by cells that are stressed or undergoing apoptosis[23]. DAMPs interact with the initiators of the complement pathway[24]. These initiators are C1q for the classical pathway, and Mannose-Binding Lectin (MBL)/Ficolins for the lectin pathway. In **Chapter 2**, we have shown that C1q is upregulated in brain tissue of SAH patients, suggesting the complement system gets activated via the classical pathway[7]. Besides this pathway, the lectin pathway also gets activated after SAH[25]. MBL, Ficolins, and several other factors of the lectin pathway are upregulated after SAH and have been associated with poor functional outcome[25–27]. In an ischemic stroke model, the lectin pathway is responsible for brain injury, and a treatment with C1 inhibitors targeted at the lectin pathway is beneficial[28].

All initiating complement pathways congregate into the conversion of C3, the main component of the complement system (Figure 1)[29]. C3 is then cleaved

into the active C3 peptide fragments: C3b, iC3b, and C3d. We have shown an increase of C3/C3b/iC3b in human brain tissue of SAH patients, showing that the complement system is activated through its main component. Conversion of C3 also produces the anaphylatoxin C3a, and C3b which converts C5 into the anaphylatoxin C5a. Together the anaphylatoxins C3a and C5a bind to receptors expressed on immune cells (e.g. B-, T-cells, macrophages, and microglia)[30]. Immune cells get attracted to the location of the hemorrhage to initiate an inflammatory response, and to phagocytose the blood cells and debris of dead cells[31]. Furthermore, peripheral immune cells produce coagulation and hemolysis factors[19]. Neutrophils, a type of white blood cells, interact with endothelial cells of blood vessels in the brain, which leads to the initiation of an immune response in the brain parenchyma[32]. Activated neutrophils also produce matrix metalloproteinase-9 (MMP-9), a proteinase that induces BBB damage[33,34]. Therefore, an immune response in the vasculature can be harmful by the substances they produce.

Microglia

Microglia are the first responders to initiate an immune response in the brain parenchyma. At a later stage, peripheral macrophages infiltrate the brain parenchyma, as shown after experimental SAH in mice[35]. Brain injury directly and indirectly activates microglia. Microglia directly respond to DAMPs released from stressed or dying cells and to blood breakdown products, reaching the brain parenchyma through leaky BBB. Microglia also react indirectly through the complement system receptors and the factors released by immune and endothelial cells[32,36]. In **chapter 1**, we gave an overview of these beneficial and detrimental consequences when microglia are immune activated after SAH[6]. Microglial response can be both beneficial, by removing cellular debris, and detrimental, by producing toxic levels of cytokines and reactive oxygen species[37]. Since the publication of our review paper[6], investigations into the glial response after SAH have ramped up considerably. An increasing number of studies have shown that microglia activation is detrimental to the brain after SAH [7,38–72]. A summary of these papers is shown in Supplementary Table 1. Especially, activation into a pro-inflammatory state seems to be detrimental, which in most of those papers is still classified as the so-called M1 microglia[38,39,59]. However, this classification is too blunt, as microglia can display a gradual spectrum of activation phenotypes between pro-inflammatory “M1” and neuroprotective “M2” microglia[73]. The pro-inflammatory microglia release cytokines in levels that are toxic to their environment,

mainly through the TLR4/NFkB pathways[37]. Many studies have tried to block or reduce microglia activation through these pathways after SAH[7,38–70]. This almost always led to reduced early brain injury in rodents. However, there may be a bias because of a lack of studies showing negative results. Nevertheless, all these studies corroborate the idea that the pro-inflammatory state of microglia is detrimental after SAH. In **Chapter 2,** we showed that we can reduce microglia activation in C5aR-/- mice. Furthermore, we observed a reduction in the number of apoptotic cells in C5aR-/- mice 2 days after SAH. Therefore, blockade of the interaction of the anaphylatoxin C5a and its receptor C5aR keeps microglia from being activated, and reduces brain injury. We also showed this by an alternative approach in which we treated mice with an antibody against C5, after experimentally induced SAH. This antibody prevents the cleavage of C5 into C5a and C5b. After treatment, we observed reduced microglia activation and reduced apoptosis. Several other studies, investigating traumatic brain injury and intracranial hemorrhage, have also shown that blockage of C5 cleavage and C5aR antagonists lead to reduced brain injury[74–76]. This further suggests that microglia activated by the complement system are in a pro-inflammatory state and are detrimental to the brain. Since microglia activation is both acute and long-lasting, treatment options against pro-inflammatory microglia activation may prevent acute as well as delayed brain injury.

As described in **Chapter 1**, the complement system and microglia are involved in maintaining synapses. The complement components C1q, C3, and C4 tag synapses, and these tagged synapses are subsequently recognized by microglia, and possibly astrocytes[77–79]. A study has shown that synapse numbers in the hippocampus are reduced in rats with SAH at 6 days[80], although we could not replicate this result in mice at 2 weeks after SAH. However, the same group found that neurons in the hippocampus have reduced long-term potentiation, in response to high-frequency stimulation[80]. It might be that weak synapses get eliminated or modulated after SAH, which is thought to happen in a complement-dependent manner[81–83]. The reduction in hippocampal potentiation may therefore induce the loss of synapses in a complement system orchestrated manner. A reduction in synapses may also underly the cognitive deficits after SAH. It would be interesting to investigate this further, to show a direct link between glial activation and memory impairment after SAH.

Astrocytes

The cognitive deficits could also be caused by astrocytes. Astrocytes execute homeostatic functions such as the regulation of the extracellular potassium ion concentration and the water balance[84]. Besides, they recycle neurotransmitters from synaptic clefts, but also release gliotransmitters themselves[85]. Furthermore, they take up nutrition from blood vessels, and can regulate vessel constriction and dilation[86]. Recent studies have shown that in particular the homeostasis of the water and ion balance at the capillary blood vessels is dysregulated after SAH[87,88]. Astrocytes normally contact the blood vessel by end-feet that get retracted after SAH, preventing them to execute their functions at the blood vessel[87]. This leads to disruption of the water homeostasis and this has also consequences for the glymphatic system[89]. This system filters the parenchyma of the brain to clear it from metabolic waste products[89]. If this system is impaired, toxic products will accumulate in the parenchyma of the brain[90]. The glymphatic system gets disrupted after SAH, contributing to post ictus brain damage[91]. Others have shown that the buffering of potassium ions is disrupted at the end-feet, causing reversed vasoconstriction of blood vessels[88,92]. These neurovascular changes occur at a delayed stage after SAH[93]. Impaired neurovascular coupling may lead to ischemia, and this impairment may, therefore, be important in the onset of DCI. Astrocytes also get immune-activated after SAH[6,94]. This response is also likely represented in a continuous spectrum of astrocyte-phenotypes. However, recent studies have proposed to name the neuroprotective state as “A2 astrocytes” and the neurotoxic state as “A1 astrocytes”, which are likely pro-inflammatory[95], in analogy to the outdated “M1-M2” microglia phenotypes. While A1 astrocytes are induced by C1q, TNF-α, and IL1β expressing microglia, neuroprotective A2 astrocytes are induced by TNF-α, IL-1β, and IL-6, and through downregulation of the P2Y receptor on astrocytes[95,96]. This suggests that the combination of cytokines depends on complement C1q to produce the neurotoxic astrocytes. Several markers have been identified for A1 astrocytes, one of which is the intracellular complement C3[95]. In **chapter 3**, we found an increase in C3 positive astrocytes in the mouse hippocampus after SAH. More importantly, the number of C3 positive astrocytes in the hippocampus correlated negatively with long-term memory for objects, in mice. This suggests that these astrocytes are harmful to the hippocampus, which can lead to memory impairments in mice after SAH. It would be interesting to further investigate the harmfulness of the A1-activated astrocytes to the hippocampus, and whether the A2 astrocyte can be beneficial.

Beneficial responses

Judging the growing body of studies investigating the glial response after SAH, including our own findings in **Chapter 1-3**, the glial response seems to be mainly detrimental in contrast to a few studies that report on the beneficial effect of a glial response in SAH[6]. One of the beneficial properties is the gain of stem cell properties of glia in response to an injury, which can facilitate brain repair[97,98]. It has been shown that astrocytes can adapt stem cell properties in several types of brain injury[98,99]. In **Chapter 4** we investigated changes in glial proliferation after SAH, which is an indication that astrocytes adopt stem cell properties. There are two neurogenic niches in the brain, the subventricular zone (SVZ), and the subgranular zone (SGZ) of the dentate gyrus of the hippocampus[97,100]. In mice, there is a constant renewal and addition of glutamatergic and GABAergic interneurons in the olfactory bulb and in the dentate gyrus of the hippocampus[100,101]. These zones harbor neurogenic astrocytes that proliferate, migrate, and differentiate into newborn neurons. In response to ischemic stroke, astrocytes in the striatum (near the subventricular zone) can regenerate and differentiate into neurons[102]. Furthermore, cells from the SVZ can migrate toward the site of injury[103]. We observed this might also be the case in SAH in **Chapter 4**. A third possible way for repair is the direct transdifferentiation from a glial cell to a neuron, without the need to proliferate[104].

The complement system is also involved in the maintenance of neurogenic astrocytes in the SVZ and dentate gyrus. Progenitor cells in the dentate gyrus express complement receptor 2 (CR2). Activation of CR2 inhibits neurogenesis in the dentate gyrus[105]. Neurogenic astrocytes in the SVZ have receptors for C3a and C5a[106]. Activation through C3aR signaling stimulates the neurogenic astrocytes to proliferate, migrate, and differentiate[106,107]. However, others have reported that C3aR antagonists promote neurogenesis[108]. Treatment to inhibit or stimulate properties of complement activation in neurogenic astrocytes needs to be carefully investigated. Likely, the dose of treatment affects these properties[106,108]. Interestingly, C5a has no effects on the proliferation of SVZ resident neurogenic astrocytes in adult mice[109]. Therefore, blocking C5 as a treatment against brain damage after SAH will likely not affect adult regenerative properties of the complement system of upstream C2/C3a signaling. In the acute phase after an SAH, the complement activation seems to be mainly detrimental. Blocking or suppressing the complement activation in the acute phase would therefore be advantageous.

In **chapter 4**, we did not see changes in the number of proliferative cells at

the SVZ of mice two weeks after SAH, which suggests that the effects on progenitor proliferation, if any, are not long-lasting. It is however possible that there were effects before our timepoint of investigation. However, we observed many $BrdU^+$ cells at damaged areas of the brain after SAH, that sometimes were also positive to premature neuronal marker doublecortin. This would suggest that there is an intrinsic repair mechanism. It would be interesting to study this further, to know the scale by which this happens, and whether this beneficial glial response can be stimulated as part of a therapy, while reducing the detrimental glial response.

Modeling SAH

We used mice to model SAH, and aimed to translate findings in these rodents to human SAH. Although the genes and cells in both organisms are highly similar, of course mice are hugely different from human beings[110]. This is also true for the glial response[111–113]. As we are interested in the process how glia respond to an SAH in patients, experiments on human brain tissue samples are very valuable. By understanding the glial response to SAH in both mice and humans, we can make a better translation from the mouse data to the actual patients. Although the glial response after SAH in rodents has been amply studied, the glial response in human brain tissue is still uncharted territory. This is largely due to the scarceness of post-mortem human SAH brain tissue. The human frontal cortex autopsy material used in **chapter 3**, was obtained from SAH patients who died 1-20 days after the initial hemorrhage. We only had access to frontal cortex of 11 patients, and we lacked autopsy material of SAH patients with known long-term cognitive impairment, and patients with good recovery. Our brain sample collection did not contain a sufficient number of patient material to make distinct groups (e.g. for age or sex). The Netherlands Brain Bank provided us with frontal cortex tissue of neurological controls. SAH brain material is normally not collected by the Netherlands Brain Bank and is not systematically present in brain tissue collections of neuropathology departments. Including SAH brain tissue in brain bank collections would be tremendously beneficial to study brain injury in patients who died in the first month after the ictus and in those with long-term survival (with or without cognitive impairments). Presence of such brain samples in brain bank collections would greatly improve our understanding of molecular and cellular consequences of an SAH in patients. Besides, human cell culture models could be used to study the consequences of an SAH. Induced pluripotent stem cells derived from human skin cells

can be cultured as cerebral mini-brains, so-called organoids[114]. These organoids consist of many brain cell types, including neurons, astrocytes, and microglia[115–117]. However, limitations are that they have no vasculature and are not confined in a skull. Nevertheless, it would be interesting to model SAH in cerebral organoids and to study how the organoids respond to a combination of exposure to blood, increased pressure, and ischemia. This would allow us to investigate glial response after SAH in human samples in a more standardized and controllable approach in comparison to autopsy tissue of SAH patients. Furthermore, as the cells are alive, it is possible to study neuronal and glial activity in these organoids, and a change in glial phenotype over time[117].

Finally, analyzing the glial response by non-invasive measurements in living human SAH survivors is possible through molecular imaging. Translocator protein (TSPO) is a protein in mitochondria that is upregulated in microglia and astrocytes when these cells are immune activated[118]. Using ligands of TSPO in positron emission tomography (PET) scanners, the glial response can be measured in living humans and rodents[119,120]. Interestingly, in rats, the intensity of TSPO positivity in living animals correlated with the severity of the SAH at 48 hours after induction of the SAH[120]. This is particularly of interest when studying the long-term glial response in human[119]. SAH patients with cognitive impairments could have repetitive TSPO PET scans over long periods of time, to study the correlation between cognitive status and the glial response. Furthermore, other functional molecular imaging techniques could be applied to measure physiological changes after brain injury. With a CO_2 challenge, the neurovascular coupling can be measured, and this may show impairments in neurovascular coupling in humans as has been seen in mice[92,121]. Moreover, functional MRI can be applied to detect brain activity differences after cognitive impairment[122]. Using a combination of these imaging techniques, the glial response can be correlated to functional changes in living human SAH survivors. Furthermore, these imaging techniques can be utilized in rodents, making these methods very valuable in translating the mouse data to the human situation[123]. However, there are also some limitations. There is currently a limited number of PET tracers to measure glial response[124]. Therefore, it is now impossible to characterize whether the glial activation is a pro-inflammatory or neuroprotective response. With functional MRI, measuring the blood oxygenation level-dependent (BOLD) signal may reflect astrocyte function and gliovascular coupling[125,126]. Moreover, with a maximum resolution of approximately 0.5mm^3 for MRI, it is impossible to

study (sub)cellular changes such as, for example, to study loss of synapses. To study the temporal cellular changes in combination with cognitive impairments, as well as studying novel therapeutic interventions, and known genetic modifications, we still need animal models.
There are several different animal models for SAH, as described in **Chapter 1, box 1**. The two most used models in recent years are the intracisternal blood injection model and the endovascular perforation model[127,128]. Both models are utilized in this thesis, and both models have their advantages and disadvantages. The advantage of the blood injection model is that the amount of blood in the subarachnoid space can be tightly controlled. Therefore, variation of the bleeding impact between mice is small, there is no risk of rebleeding, and the mortality is low. The endovascular perforation model is less controllable in the amount of blood in the subarachnoid space and has a chance of rebleeding. Outcome is therefore less homogeneous, with higher mortality, and animals with poor and good outcome. The endovascular perforation model, however, mimics human SAH more closely than the blood injection model. In the endovascular perforation model, the circle of Willis is perforated. This leads to tissue repair mechanisms close to the puncture, which may be of importance when modeling aneurysmal SAH. Although these models mimic human SAH, no animal model can fully mimic the complete pathophysiology of aneurysmal SAH. However, the endovascular perforation model is the closest to human SAH, and is indispensable for SAH research.

Therapeutic interventions.
Complement activation after brain injury induced by SAH seems to be mainly detrimental. Autologous inhibitory proteins of the complement pathway can restrict activation of the pathway, but application of these proteins is insufficient to stop a complement reaction after injury[29,30]. Several therapeutic compounds are utilized that reduce or block complement activation[129]. These treatments can act on initiation factors C1q/MBL, C3 convertase, and C5 convertase, but can also act as agonists of C3a/C5a receptors (Figure 1). C1-inhibitor is an endogenous complement inhibitor, and recombinant C1-inhibitor (C1-INH) can be beneficial in patients after stroke and in mice after experimental stroke[130,131]. Several other endogenous inhibitors are utilized to target the complement system and are tested in preclinical studies. One example is Crry-Ig, a C3b inhibitor[132]. Crry-Ig has been shown to have neuroprotective properties when administered after traumatic brain

injury (TBI)[133,134]. Furthermore, CR2-Crry has been tested to block the convertase of C3, and has been shown to have beneficial effects after TBI[135]. Hexapeptide-derived macrocycle AcF is a C5aR antagonist that was shown to be beneficial after intracranial hemorrhage, especially in synergy with a C3aR antagonist[76]. However, the role of the C3aR antagonist is controversial, as it also acts as an agonist[136]. Preventing the assembly of the Membrane Attack Complex, which makes pores into the membrane of cells and induces cell death, by C6 antisense, can also be beneficial after TBI[74]. These, and other interventions on complement activation in neurologic diseases have been described in a recent review[137].

Another way to suppress complement activation is by the use of antibodies. In **chapter 2**, we used an antibody as a treatment to block C5 fragmentation. This antibody is directed against murine C5 (BB5.1)[138]. The human analog of this antibody (Eculizumab) is used in the clinic for a variety of disorders such as generalized myasthenia gravis, atypical hemolytic uremic syndrome, and paroxysmal nocturnal hemoglobinuria[139–141]. It would be interesting to see whether it is also beneficial for the outcome after SAH. For this, a clinical trial (phase 2) has recently started. Several other antibodies have been used in experimental models, targeting C1q, mannose-binding protein-associated serine protease 2 (MASP-2), C3b, properdin, and other complement components[129]. Antibodies for treatment are distributed through blood circulation, and need to enter the brain by passage over the BBB. Therefore, only a limited amount of antibodies reaches the brain in normal circumstances. However, as both the hemorrhage and the secondary damage cause disrupted BBB, antibodies may still end up in high numbers in the brain. Many more therapeutics against complement activation are being tested, some of which are in clinical trials. Developments of these trials are nicely summarized in a recent review[142].

> Figure 1. Scheme of the complement system and examples of therapeutic interventions. The complement system consists of over 30 components that are activated after damage or an infection[29]. Therapeutic interventions can block or reduce complement activation ranging from targeting each step between the initiation and terminal components. C1-INH blocks the initiation of the classical and lectin pathways[130]. CR2-Crry targets the convertases of C3, while Crry-Ig blocks the alternative pathway C3b[132,135]. The human antibody Eculizumab and mouse antibody BB5.1 prevent the conversion of C5 into C5a and C5b[138,139]. The membrane attack complex assembly is blocked by C6 antisense treatment[74]. Furthermore, C5a receptors can be blocked by AcF to prevent the anaphylatoxin C5a from binding to its receptor C5aR1[76].

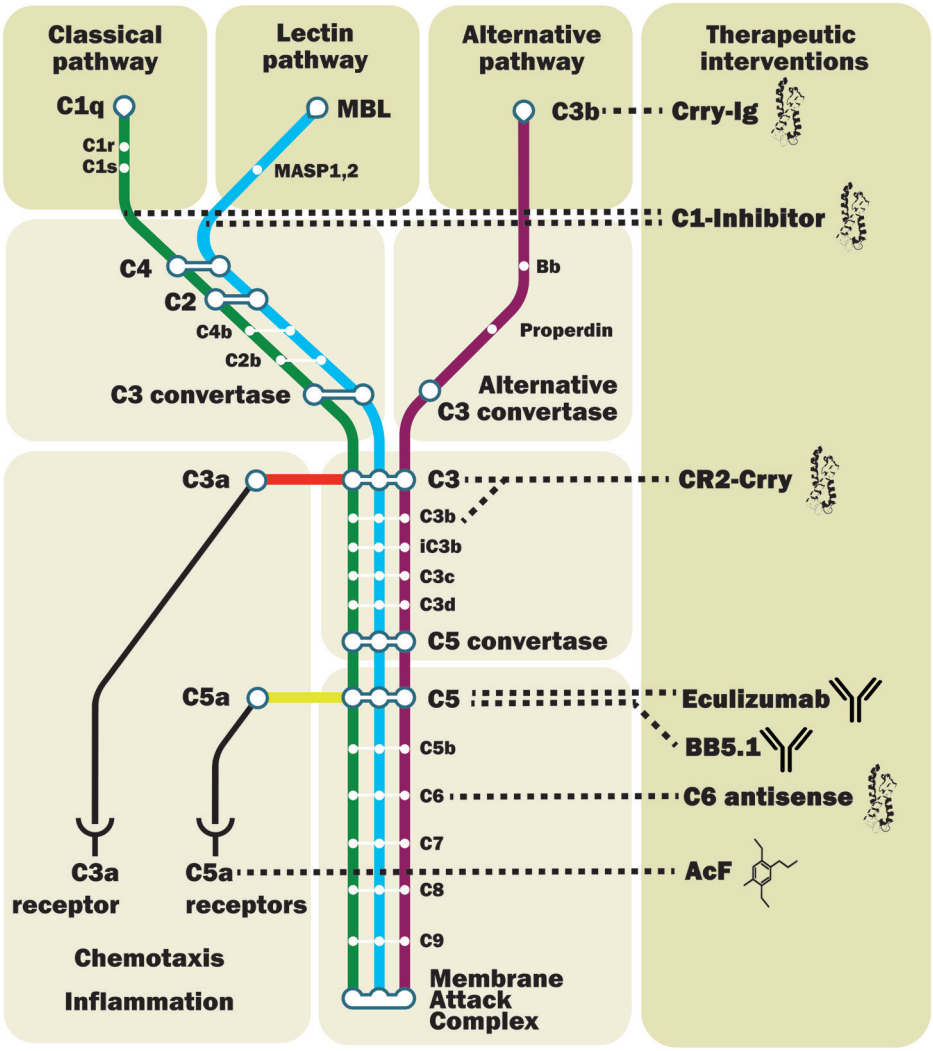

The complement system responds to brain injury and may cause additional damage. Therefore, treatment targeting the complement system may be beneficial. However, the complement system is also a defense mechanism against infections. Side effects of treatments targeting the complement system are an increased risk of bacterial and viral infections. Antibiotics should, therefore, be administered to minimize the chance of infection. Treatment against the complement system also acts against the homeostatic functions that the complement system has in the uninjured central nervous system.

These include the removal of weak synapses, and the potential involvement in neurogenic niches[47,52,83]. However, the impact of complement targeted treatment on these physiologic mechanisms, such as regulation of synapses, in adulthood is not known yet. Moreover, treatment against complement to reduce brain injury likely outweighs the potential suppression of these homeostatic functions.

The focus of this discussion and thesis has predominantly been on immune-related responses after SAH, like the complement system and glia response. Finding therapeutic targets against these responses may attenuate the poor outcomes seen after SAH. However, it should be noted that the poor outcome is multifactorial, meaning that there are more pathways or mechanisms involved in the damage after SAH. Although some of the clinical trials targeting these pathways did not have a satisfying outcome [143–145], they should not yet be discarded. Perhaps, as the poor outcome after SAH is multifactorial, the treatment should also be a combination of interventions.

Future directions

In this thesis, we gave insights into the functional consequences and clinical implications of the glial response after SAH. We studied the role of the complement system in the development of brain injury after SAH and found that complement C5 contributes to brain injury after SAH. Furthermore, we found that SAH mice had impaired memory, and that this impairment correlates to C3 expression in astrocytes in the CA1 region of the hippocampus. As the number of synapses did not seem to change, we do not know what exactly changed that caused the memory impairment. It could be that the neuronal conductance had changed, or that there was more neuronal cell death. Furthermore, we also do not know whether blocking the complement system would also reduce long term cognitive impairment. In this section, we will highlight some future experiments that should be conducted to get a better understanding of the functional implications of our findings.

The memory impairment in SAH mice is presumably due to impaired neuronal communication, as a result of complement and glia activation. As astrocytes retract their end-feet from blood vessels after SAH, we assume that the astrocytic processes on the synapses would also retract[87]. With these synapse enwrapping processes, they form the so-called tripartite synapse[146]. While the amount of neuronal synapses does not seem to change, it would be interesting to study the extent of the synaptic coverage of the astrocytic processes. The astrocytic compartment of the synapse, however, is very

small, below the diffraction limit of conventional light microscopy. To count tripartite synapses, we would, therefore, need super-resolution microscopy to visualize the astrocytic compartment[147]. One such super-resolution method is expansion microscopy, a method to physically enlarge the sample, instead of using a higher magnification by microscopy[148,149]. Expansion microscopy is a promising technique to use super-resolution microscopy analyzed by a normal confocal microscope. Expansion microscopy got many adaptations in recent years. Using conventional antibodies, it is now possible to expand various tissues from drosophila, zebrafish, mice, and even human paraffin tissue[149–152]. Furthermore, novel techniques allow for double expansion, enlarging the sample by roughly 20 times in all spatial dimensions[153]. Moreover, as samples get transparent, they are suitable for light-sheet microscopy, which recently led to the 3D reconstruction of all presynaptic sites in the drosophila brain in superb resolution[154]. With the right tools and antibodies, expansion microscopy can have great value to answer research questions that need super-resolution microscopy. In neuroscience, glial research lags behind on neuronal oriented science, due to technical restrictions. Unfortunately, this also seems to be the case in the expansion microscopy technique. While there are many protocols to visualize neuronal markers, protocols for astrocytic markers are not available. Instead, the GFAP-cre/ERT2 x Gt(ROSA)26Sor$^{tm14(CAG-TdTomato)}$ mouse line, which express the red fluorescent protein TD-tomato in GFAP^{+} cells after tamoxifen injection may be of value. In a preliminary study, we imaged pre- and post-expansion with the use of a normal confocal microscope (Figure 2A and 2B, respectively). Note that the scale bars in Figure 2A and 2B are both 10µm, but the astrocyte in Figure 2B is around 4x larger in all spatial dimensions than the astrocytes in Figure 2A. To investigate synapse numbers in the hippocampus, we imaged pre- (Bassoon) and post-synapse (Homer-1; Figure 2C) after expansion of the tissue with confocal microscopy. Note that the pre- and post-synapse are nicely aligned, but do not overlap. We intended to use this technique to investigate the number of tripartite synapses after SAH, but this still remains to be investigated.

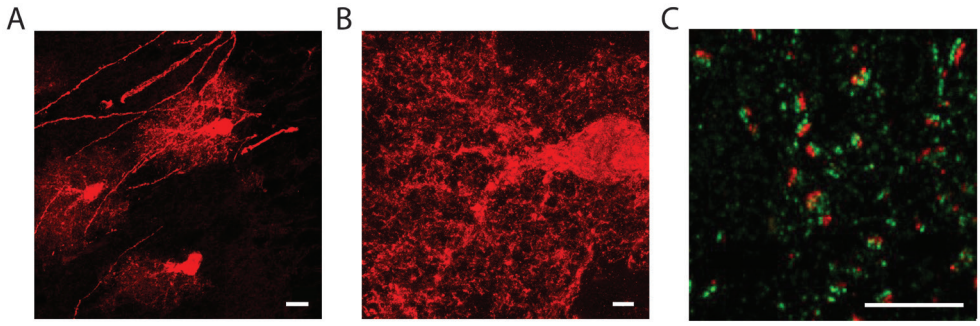

Figure 2. Expansion microscopy. A) Td-tomato positive astrocytes (and neuronal dendrites) of GFAP-cre/ERT2 x Gt(ROSA)26Sor$^{tm14(CAG-TdTomato)}$ mouse in the dentate gyrus, scale bar 10 µm, without expansion; and B) with expansion, scale bar also 10µm; C) Synapses in C57Bl/6J mouse cortex, green: Homer-1 (post-synaptic marker), red: Bassoon (presynaptic marker); scale bar 10µm. Use of GFAP-cre/ERT2 x Gt(ROSA)26Sor$^{tm14(CAG-TdTomato)}$ mouse line slices with the courtesy of Ketharini Senthilkumar, MSc. Figure 2B processed and imaged by Viktor al-Naqib, BSc.

The microglial response to SAH seems to be mainly detrimental. However, microglia can respond to damage by becoming neuroprotective. Thus far, little is known on how to stimulate the neuroprotective state of microglia, while suppressing the pro-inflammatory state. The neuroprotective state of activation is helpful for the repair after injury. It would be interesting to investigate whether we can stimulate or increase the presence of neuroprotective microglia, while repressing the pro-inflammatory ones. While many drugs can reduce the pro-inflammatory microglia response, there are currently few microglia-targeting drugs to drive their response to a neuroprotective state. However, several cytokines are known inducers of neuroprotective microglia, such as IL-4 and IL-10[155,156]. It would be interesting to study whether stimulating the receptors for IL-4/IL-10 in combination with pro-inflammatory suppressors can enhance recovery after SAH.
Lastly, it remains to be investigated whether the suppression of the complement pathway has long term advantages, in both mice and human. We have shown that suppression of complement C5 cleavage by antibody can reduce brain damage in mice 2 days after SAH. We have also shown that mice have memory impairment at 14 days after SAH. It would be interesting to know whether C5 also contributes to long term memory impairment after SAH,
and whether antibodies against C5 are a good treatment option against these impairments in mice. Similarly, clinical trials should be conducted to inves-

tigate whether these anti-C5 antibodies can reduce brain damage and poor functional outcome and cognitive impairment in SAH patients. To study the glial activation effects on cognition in patients, non-invasive imaging techniques like PET, with tracers against TSPO and synapses could be utilized, and measurements should then be correlated to cognitive impairment severity[157]. Unfortunately, there are no clinically available molecular imaging tracers to measure complement activation. We found that C5a measurements in plasma levels did not correlate to functional outcome, and therefore, it could not be used as a biomarker. Measuring the C5a levels in CSF may yield better results, but sampling CSF from patients is too invasive. Therefore, non-invasive ways to measure complement activation in the brain are not yet available. It would be of great value to invent such non-invasive measurement techniques for complement activation in the brain. It would greatly improve our knowledge about the role of complement activation in cognitive impairments in SAH patients. Preclinical use of the Single Photon Emission Computed Tomography (SPECT) imaging agent ^{99}mTc-rCR2 gives promising results to measure complement activation in mice, however, this compound has yet to be investigated in human[158]. For now, data from long-term follow-up studies of patients treated with complement suppressors will give valuable insights about whether these suppressors are also beneficial in reducing cognitive impairments.

These proposed further investigations are just the tip of the iceberg. Obviously, there are many more questions to be answered. However, we hope that many of these questions will soon be answered, and will, together with the results from this thesis, help find better treatment options for SAH patients.

Conclusion

Subarachnoid hemorrhage is a severe subtype of stroke that can cause profound injury to the brain. The immune response, activated by the complement system and through involvement of microglia and astrocytes, seems to worsen outcome after SAH. Blocking this immune response may outweigh the potential beneficial effects of the immune response, and therefore is an attractive approach in treating patients after SAH. We showed that in preclinical studies the complement and glial response are associated with damage and memory impairments. Targeting the complement response may thus be a promising novel therapeutic target to help to improve functional and cognitive outcome of SAH patients.

References

1. van Gijn, J., Kerr, R. S. & Rinkel, G. J. Subarachnoid haemorrhage. *The Lancet* **369**, 306–318 (2007).

2.Al-Khindi, T., Macdonald, R. L. & Schweizer, T. A. Cognitive and Functional Outcome After Aneurysmal Subarachnoid Hemorrhage. *Stroke* **41**, (2010).

3.Vergouwen, M. D., Jong-Tjien-Fa, A. V., Algra, A. & Rinkel, G. J. Time trends in causes of death after aneurysmal subarachnoid hemorrhage: A hospital-based study. *Neurology* **86**, 59–63 (2016).

4.Roos, Y. B. *et al.* Complications and outcome in patients with aneurysmal subarachnoid haemorrhage: a prospective hospital based cohort study in the Netherlands. *J. Neurol. Neurosurg. Psychiatry* **68**, 337–341 (2000).

5.Vergouwen, M. D. *et al.* Definition of delayed cerebral ischemia after aneurysmal subarachnoid hemorrhage as an outcome event in clinical trials and observational studies: proposal of a multidisciplinary research group. *Stroke* **41**, 2391–2395 (2010).

6.van Dijk, B. J., Vergouwen, M. D., Kelfkens, M. M., Rinkel, G. J. & Hol, E. M. Glial cell response after aneurysmal subarachnoid hemorrhage - Functional consequences and clinical implications. *Biochim.Biophys.Acta* **1862**, 492–505 (2016).

7.van Dijk, B. J. *et al.* Complement C5 Contributes to Brain Injury After Subarachnoid Hemorrhage. *Transl. Stroke Res.* (2019) doi:10.1007/s12975-019-00757-0.

8.Backes, D., Rinkel, G. J. E., Laban, K. G., Algra, A. & Vergouwen, M. D. I. Patient- and Aneurysm-Specific Risk Factors for Intracranial Aneurysm Growth: A Systematic Review and Meta-Analysis. *Stroke* **47**, 951–957 (2016).

9.Juvela, S., Hillbom, M., Numminen, H. & Koskinen, P. Cigarette smoking and alcohol consumption as risk factors for aneurysmal subarachnoid hemorrhage. *Stroke* **24**, 639–646 (1993).

10.Vlak, M. H., Algra, A., Brandenburg, R. & Rinkel, G. J. Prevalence of unruptured intracranial aneurysms, with emphasis on sex, age, comorbidity, country, and time period: a systematic review and meta-analysis. *Lancet Neurol.* **10**, 626–636 (2011).

11.Rinkel, G. J. E., Djibuti, M., Algra, A. & van Gijn, J. Prevalence and Risk of Rupture of Intracranial Aneurysms: A Systematic Review. *Stroke* **29**, 251–256 (1998).

12.Etminan, N. *et al.* Worldwide Incidence of Aneurysmal Subarachnoid Hemorrhage According to Region, Time Period, Blood Pressure, and Smoking Prevalence in the Population: A Systematic Review and Meta-analysis. *JAMA Neurol.* **76**, 588 (2019).

13.Lovelock, C. E., Rinkel, G. J. E. & Rothwell, P. M. Time trends in outcome of subarachnoid hemorrhage: Population-based study and systematic review. *Neurology* **74**, 1494–1501 (2010).

14.Zoerle, T. *et al.* Intracranial Pressure After Subarachnoid Hemorrhage*: *Crit. Care Med.* **43**, 168–176 (2015).

15.Trojanowski, T. How intracranial aneurysm rupture damages the brain. *Interv. Neuroradiol. J. Peritherapeutic Neuroradiol. Surg. Proced. Relat. Neurosci.* **14 Suppl 1**,

9–12 (2008).

16.Macdonald, R. L. Delayed neurological deterioration after subarachnoid haemorrhage. *Nat. Rev. Neurol.* **10**, 44–58 (2014).

17.Geraghty, J. R. & Testai, F. D. Delayed Cerebral Ischemia after Subarachnoid Hemorrhage: Beyond Vasospasm and Towards a Multifactorial Pathophysiology. *Curr. Atheroscler. Rep.* **19**, (2017).

18.Kozarcanin, H. *et al.* The lectin complement pathway serine proteases (MASPs) represent a possible crossroad between the coagulation and complement systems in thromboinflammation. *J. Thromb. Haemost.* **14**, 531–545 (2016).

19.Markiewski, M. M., Nilsson, B., Nilsson Ekdahl, K., Mollnes, T. E. & Lambris, J. D. Complement and coagulation: strangers or partners in crime? *Trends Immunol.* **28**, 184–192 (2007).

20.Ikeda, K. *et al.* C5a induces tissue factor activity on endothelial cells. *Thromb.Haemost.* **77**, 394–398 (1997).

21. Fortin, J. P., Bouthillier, J., St-Pierre, S. A. & Marceau, F. Contractile effect of anaphylatoxin C5a and of a mimetic peptide on the human umbilical artery: further evidence for leukocyte-dependent vasomotion. *J.Cardiovasc.Pharmacol.* **40**, 815–821 (2002).

22. Appelboom, G. *et al.* Role of the complement cascade in cerebral aneurysm formation, growth, and rupture. *Neuroimmunol. Neuroinflammation* **2**, 93 (2015).

23. Chaudhry, S. *et al.* Role of Damage Associated Molecular Pattern Molecules (DAMPs) in Aneurysmal Subarachnoid Hemorrhage (aSAH). *Int. J. Mol. Sci.* **19**, 2035 (2018).

24. Ricklin, D. & Lambris, J. D. Complement in Immune and Inflammatory Disorders: Pathophysiological Mechanisms. *J. Immunol.* **190**, 3831–3838 (2013).

25. Cai, J. Y., Sun, J. & Yu, Z. Q. Serum mannose-binding lectin levels after aneurysmal subarachnoid hemorrhage. *Acta NeurolScand* **134**, 360–367 (2016).

26. Llull, L. *et al.* Ficolin-1 Levels in Patients Developing Vasospasm and Cerebral Ischemia After Spontaneous Subarachnoid Hemorrhage. *Mol. Neurobiol.* **54**, 6572–6580 (2017).

27. Zanier, E. R. *et al.* Ficolin-3-mediated lectin complement pathway activation in patients with subarachnoid hemorrhage. *Neurology* **82**, 126–134 (2014).

28. Orsini, F. *et al.* Targeting Mannose-Binding Lectin Confers Long-Lasting Protection With a Surprisingly Wide Therapeutic Window in Cerebral Ischemia. *Circulation* **126**, 1484–1494 (2012).

29. Merle, N. S., Church, S. E., Fremeaux-Bacchi, V. & Roumenina, L. T. Complement System Part I â€“ Molecular Mechanisms of Activation and Regulation. *Front. Immunol.* **6**, (2015).

30. Merle, N. S., Noe, R., Halbwachs-Mecarelli, L., Fremeaux-Bacchi, V. & Roumenina, L. T. Complement System Part II: Role in Immunity. *Front. Immunol.* **6**, (2015).

31. Moraes, L. *et al.* Immune cells subpopulations in cerebrospinal fluid and peripheral blood of patients with Aneurysmal

Subarachnoid Hemorrhage. *SpringerPlus* **4**, (2015).

32. Atangana, E. *et al.* Intravascular Inflammation Triggers Intracerebral Activated Microglia and Contributes to Secondary Brain Injury After Experimental Subarachnoid Hemorrhage (eSAH). *Transl. Stroke Res.* **8**, 144–156 (2017).

33. Egashira, Y., Zhao, H., Hua, Y., Keep, R. F. & Xi, G. White Matter Injury After Subarachnoid Hemorrhage: Role of Blood–Brain Barrier Disruption and Matrix Metalloproteinase-9. *Stroke* **46**, 2909–2915 (2015).

34. Chou, S. H.-Y. *et al.* Elevated Peripheral Neutrophils and Matrix Metalloproteinase 9 as Biomarkers of Functional Outcome Following Subarachnoid Hemorrhage. *Transl. Stroke Res.* **2**, 600–607 (2011).

35. Xu, Z. *et al.* Resident Microglia Activate before Peripheral Monocyte Infiltration and p75NTR Blockade Reduces Microglial Activation and Early Brain Injury after Subarachnoid Hemorrhage. *ACS Chem. Neurosci.* (2018) doi:10.1021/acschemneuro.8b00298.

36. Lu, Y. *et al.* Peroxiredoxin 2 activates microglia by interacting with Toll-like receptor 4 after subarachnoid hemorrhage. *J. Neuroinflammation* **15**, 87 (2018).

37. Kawabori, M. & Yenari, M. A. The role of the microglia in acute CNS injury. *Metab. Brain Dis.* **30**, 381–392 (2015).

38. Xie, Y. *et al.* Human albumin attenuates excessive innate immunity via inhibition of microglial Mincle/Syk signaling in subarachnoid hemorrhage. *Brain. Behav. Immun.* **60**, 346–360 (2017).

39. Huang, X.-P. *et al.* Peli1 Contributions in Microglial Activation, Neuroinflammatory Responses and Neurological Deficits Following Experimental Subarachnoid Hemorrhage. *Front. Mol. Neurosci.* **10**, 398 (2017).

40. Xu, H. *et al.* Methylene blue attenuates neuroinflammation after subarachnoid hemorrhage in rats through the Akt/GSK-3beta/MEF2D signaling pathway. *Brain. Behav. Immun.* **65**, 125–139 (2017).

41. Zhang, X. *et al.* Astaxanthin mitigates subarachnoid hemorrhage injury primarily by increasing sirtuin 1 and inhibiting the Toll-like receptor 4 signaling pathway. *FASEB J. Off. Publ. Fed. Am. Soc. Exp. Biol.* **33**, 722–737 (2019).

42. Xie, Z. *et al.* Recombinant Netrin-1 binding UNC5B receptor attenuates neuroinflammation and brain injury via PPARgamma/NFkappaB signaling pathway after subarachnoid hemorrhage in rats. *Brain. Behav. Immun.* **69**, 190–202 (2018).

43. Zhao, Q. *et al.* Thioredoxin-interacting protein links endoplasmic reticulum stress to inflammatory brain injury and apoptosis after subarachnoid haemorrhage. *J. Neuroinflammation* **14**, 104 (2017).

44. You, W. *et al.* Inhibition of mammalian target of rapamycin attenuates early brain injury through modulating microglial polarization after experimental subarachnoid hemorrhage in rats. *J. Neurol. Sci.* **367**, 224–231 (2016).

45. Li, Z. & Han, X. Resveratrol alleviates early brain injury following subarachnoid hemorrhage: possible involvement of the AMPK/SIRT1/autophagy signaling pathway. *Biol. Chem.* **399**, 1339–1350 (2018).

46. Zhang, X.-S. *et al.* Resveratrol Attenuates Acute Inflammatory Injury in Experimental Subarachnoid Hemorrhage in Rats via Inhibition of TLR4 Pathway. *Int. J. Mol. Sci.* **17**, (2016).

47. Haruma, J. *et al.* Anti-high mobility group box-1 (HMGB1) antibody attenuates delayed cerebral vasospasm and brain injury after subarachnoid hemorrhage in rats. *Sci. Rep.* **6**, 37755 (2016).

48. Liu, F.-Y. *et al.* Fluoxetine attenuates neuroinflammation in early brain injury after subarachnoid hemorrhage: a possible role for the regulation of TLR4/MyD88/NF-kappaB signaling pathway. *J. Neuroinflammation* **15**, 347 (2018).

49. Zhang, T. *et al.* Apigenin protects blood-brain barrier and ameliorates early brain injury by inhibiting TLR4-mediated inflammatory pathway in subarachnoid hemorrhage rats. *Int. Immunopharmacol.* **28**, 79–87 (2015).

50. Tu, L. *et al.* Bexarotene attenuates early brain injury via inhibiting micoglia activation through PPARgamma after experimental subarachnoid hemorrhage. *Neurol. Res.* **40**, 702–708 (2018).

51. Chen, T. *et al.* PARP inhibition attenuates early brain injury through NF-kappaB/MMP-9 pathway in a rat model of subarachnoid hemorrhage. *Brain Res.* **1644**, 32–38 (2016).

52. Li, J. *et al.* Minocycline Protects Against NLRP3 Inflammasome-Induced Inflammation and P53-Associated Apoptosis in Early Brain Injury After Subarachnoid Hemorrhage. *Mol. Neurobiol.* **53**, 2668–2678 (2016).

53. Peng, Y. *et al.* Rolipram Attenuates Early Brain Injury Following Experimental Subarachnoid Hemorrhage in Rats: Possibly via Regulating the SIRT1/NF-kappaB Pathway. *Neurochem. Res.* **43**, 785–795 (2018).

54. Wei, S. *et al.* Erythropoietin ameliorates early brain injury after subarachnoid haemorrhage by modulating microglia polarization via the EPOR/JAK2-STAT3 pathway. *Exp. Cell Res.* **361**, 342–352 (2017).

55. Zhang, X. *et al.* Resveratrol Attenuates Early Brain Injury after Experimental Subarachnoid Hemorrhage via Inhibition of NLRP3 Inflammasome Activation. *Front. Neurosci.* **11**, 611 (2017).

56. LeBlanc, R. H. 3rd, Chen, R., Selim, M. H. & Hanafy, K. A. Heme oxygenase-1-mediated neuroprotection in subarachnoid hemorrhage via intracerebroventricular deferoxamine. *J. Neuroinflammation* **13**, 244 (2016).

57. Zhu, Q. *et al.* Aggf1 attenuates neuroinflammation and BBB disruption via PI3K/Akt/NF-kappaB pathway after subarachnoid hemorrhage in rats. *J. Neuroinflammation* **15**, 178 (2018).

58. Zhang, X.-S. *et al.* Sirtuin 1 activation protects against early brain injury after experimental subarachnoid hemorrhage in rats. *Cell Death Dis.* **7**, e2416 (2016).

59. Li, R. *et al.* TSG-6 attenuates inflammation-induced brain injury via modulation of microglial polarization in SAH rats through the SOCS3/STAT3 pathway. *J. Neuroinflammation* **15**, 231 (2018).

60. Turan, N. *et al.* Effect of Progesterone on Cerebral Vasospasm and Neurobehavior-

al Outcomes in a Rodent Model of Subarachnoid Hemorrhage. *World Neurosurg.* **110**, e150–e159 (2018).

61. Zhang, Z.-Y. *et al.* Enhanced Therapeutic Potential of Nano-Curcumin Against Subarachnoid Hemorrhage-Induced Blood-Brain Barrier Disruption Through Inhibition of Inflammatory Response and Oxidative Stress. *Mol. Neurobiol.* **54**, 1–14 (2017).

62. Cao, S. *et al.* Hydrogen sulfide attenuates brain edema in early brain injury after subarachnoid hemorrhage in rats: Possible involvement of MMP-9 induced blood-brain barrier disruption and AQP4 expression. *Neurosci. Lett.* **621**, 88–97 (2016).

63. Yuan, J. *et al.* Curcumin attenuates blood-brain barrier disruption after subarachnoid hemorrhage in mice. *J. Surg. Res.* **207**, 85–91 (2017).

64. Xu, J., Xu, Z. & Yan, A. Prostaglandin E2 EP4 Receptor Activation Attenuates Neuroinflammation and Early Brain Injury Induced by Subarachnoid Hemorrhage in Rats. *Neurochem. Res.* **42**, 1267–1278 (2017).

65. Peng, Y. *et al.* Neuroprotective Effects of Magnesium Lithospermate B against Subarachnoid Hemorrhage in Rats. *Am. J. Chin. Med.* **46**, 1225–1241 (2018).

66. Goksu, E. *et al.* Pentoxifylline Alleviates Early Brain Injury in a Rat Model of Subarachnoid Hemorrhage. *Acta Neurochir. (Wien)* **158**, 1721–1730 (2016).

67. Wu, Y. *et al.* An apoE-derived mimic peptide, COG1410, alleviates early brain injury via reducing apoptosis and neuroinflammation in a mouse model of subarachnoid hemorrhage. *Neurosci. Lett.* **627**, 92–99 (2016).

68. Veldeman, M. *et al.* Xenon Reduces Neuronal Hippocampal Damage and Alters the Pattern of Microglial Activation after Experimental Subarachnoid Hemorrhage: A Randomized Controlled Animal Trial. *Front. Neurol.* **8**, 511 (2017).

69. Fang, R., Zheng, X. & Zhang, M. Ethyl pyruvate alleviates early brain injury following subarachnoid hemorrhage in rats. *Acta Neurochir. (Wien)* **158**, 1069–1076 (2016).

70. Samanci, M. Y. *et al.* Neuroprotective Effects of Nasopharyngeal Perfluorochemical Cooling in a Rat Model of Subarachnoid Hemorrhage. *World Neurosurg.* **121**, e481–e492 (2019).

71. Zhang, X.-S. *et al.* Astaxanthin reduces matrix metalloproteinase-9 expression and activity in the brain after experimental subarachnoid hemorrhage in rats. *Brain Res.* **1624**, 113–124 (2015).

72. Li, J.-R. *et al.* Fluoxetine-enhanced autophagy ameliorates early brain injury via inhibition of NLRP3 inflammasome activation following subrachnoid hemorrhage in rats. *J. Neuroinflammation* **14**, 186 (2017).

73. Ransohoff, R. M. A polarizing question: do M1 and M2 microglia exist? *Nat. Neurosci.* **19**, 987 (2016).

74. Fluiter, K., Opperhuizen, A. L., Morgan, B. P., Baas, F. & Ramaglia, V. Inhibition of the Membrane Attack Complex of the Complement System Reduces Secondary Neuroaxonal Loss and Promotes Neurologic Recovery after Traumatic Brain Injury in Mice. *J. Immunol.* **192**, 2339–2348 (2014).

75. Brennan, F. H. *et al.* The Complement Receptor C5aR Controls Acute Inflammation and Astrogliosis following Spinal Cord Injury. *J.Neurosci.* **35**, 6517–6531 (2015).

76. Garrett, M. C. *et al.* Synergistic neuroprotective effects of C3a and C5a receptor blockade following intracerebral hemorrhage. *Brain Res.* **1298**, 171–177 (2009).

77. Stevens, B. *et al.* The Classical Complement Cascade Mediates CNS Synapse Elimination. *Cell* **131**, 1164–1178 (2007).

78. Iram, T. *et al.* Megf10 Is a Receptor for C1Q That Mediates Clearance of Apoptotic Cells by Astrocytes. *J. Neurosci.* **36**, 5185–5192 (2016).

79. Chung, W.-S. *et al.* Astrocytes mediate synapse elimination through MEGF10 and MERTK pathways. *Nature* **504**, 394 (2013).

80. Han, S. M. *et al.* Molecular Alterations in the Hippocampus after Experimental Subarachnoid Hemorrhage. *J. Cereb. Blood Flow Metab.* **34**, 108–117 (2014).

81. Chechik, G., Meilijson, I. & Ruppin, E. Neuronal Regulation: A Mechanism for Synaptic Pruning During Brain Maturation. *Neural Comput.* **11**, 2061–2080 (1999).

82. Schafer, D. P. *et al.* Microglia Sculpt Postnatal Neural Circuits in an Activity and Complement-Dependent Manner. *Neuron* **74**, 691–705 (2012).

83. Nguyen, P. T. *et al.* Microglial Remodeling of the Extracellular Matrix Promotes Synapse Plasticity. *Cell* **182**, 388-403.e15 (2020).

84. Min, R. & van der Knaap, M. S. Genetic defects disrupting glial ion and water homeostasis in the brain: Glial ion and water homeostasis in disease. *Brain Pathol.* **28**, 372–387 (2018).

85. Araque, A. *et al.* Gliotransmitters travel in time and space. *Neuron* **81**, 728–739 (2014).

86. Haydon, P. G. & Carmignoto, G. Astrocyte Control of Synaptic Transmission and Neurovascular Coupling. *Physiol. Rev.* **86**, 1009–1031 (2006).

87. Anzabi, M. *et al.* Hippocampal Atrophy Following Subarachnoid Hemorrhage Correlates with Disruption of Astrocyte Morphology and Capillary Coverage by AQP4. *Front. Cell. Neurosci.* **12**, 19 (2018).

88. Pappas, A. C., Koide, M. & Wellman, G. C. Astrocyte Ca2+ Signaling Drives Inversion of Neurovascular Coupling after Subarachnoid Hemorrhage. *J. Neurosci. Off. J. Soc. Neurosci.* **35**, 13375–13384 (2015).

89. Jessen, N. A., Munk, A. S. F., Lundgaard, I. & Nedergaard, M. The Glymphatic System: A Beginner's Guide. *Neurochem. Res.* **40**, 2583–2599 (2015).

90. Iliff, J. J. *et al.* Impairment of Glymphatic Pathway Function Promotes Tau Pathology after Traumatic Brain Injury. *J. Neurosci.* **34**, 16180–16193 (2014).

91. Gaberel, T. *et al.* Impaired Glymphatic Perfusion After Strokes Revealed by Contrast-Enhanced MRI: A New Target for Fibrinolysis? *Stroke* **45**, 3092–3096 (2014).

92. Koide, M. *et al.* Reduced Ca^{2+} Spark Activity after Subarachnoid Hemorrhage Disables BK Channel Control of Cerebral

Artery Tone. *J. Cereb. Blood Flow Metab.* **31**, 3–16 (2011).

93. Balbi, M., Koide, M., Schwarzmaier, S. M., Wellman, G. C. & Plesnila, N. Acute changes in neurovascular reactivity after subarachnoid hemorrhage *in vivo*. *J. Cereb. Blood Flow Metab.* **37**, 178–187 (2017).

94. Sofroniew, M. V. Multiple Roles for Astrocytes as Effectors of Cytokines and Inflammatory Mediators. *The Neuroscientist* **20**, 160–172 (2014).

95. Liddelow, S. A. *et al.* Neurotoxic reactive astrocytes are induced by activated microglia. *Nature* **541**, 481–487 (2017).

96. Shinozaki, Y. *et al.* Transformation of Astrocytes to a Neuroprotective Phenotype by Microglia via P2Y 1 Receptor Downregulation. *Cell Rep.* **19**, 1151–1164 (2017).

97. Magnusson, J. P. & Frisén, J. Stars from the darkest night: unlocking the neurogenic potential of astrocytes in different brain regions. *Development* **143**, 1075–1086 (2016).

98. Saha, B., Peron, S., Murray, K., Jaber, M. & Gaillard, A. Cortical lesion stimulates adult subventricular zone neural progenitor cell proliferation and migration to the site of injury. *Stem Cell Res.* **11**, 965–977 (2013).

99. Arvidsson, A., Collin, T., Kirik, D., Kokaia, Z. & Lindvall, O. Neuronal replacement from endogenous precursors in the adult brain after stroke. *Nat. Med.* **8**, 963 (2002).

100. Gonçalves, J. T., Schafer, S. T. & Gage, F. H. Adult Neurogenesis in the Hippocampus: From Stem Cells to Behavior. *Cell* **167**, 897–914 (2016).

101. Brill, M. S. *et al.* Adult generation of glutamatergic olfactory bulb interneurons. *Nat. Neurosci.* **12**, 1524–1533 (2009).

102. Magnusson, J. P. *et al.* A latent neurogenic program in astrocytes regulated by Notch signaling in the mouse. *Science* **346**, 237–241 (2014).

103. Yamashita, T. *et al.* Subventricular Zone-Derived Neuroblasts Migrate and Differentiate into Mature Neurons in the Post-Stroke Adult Striatum. *J. Neurosci.* **26**, 6627–6636 (2006).

104. Guo, Z. *et al.* In Vivo Direct Reprogramming of Reactive Glial Cells into Functional Neurons after Brain Injury and in an Alzheimer's Disease Model. *Cell Stem Cell* **14**, 188–202 (2014).

105. Moriyama, M. *et al.* Complement Receptor 2 Is Expressed in Neural Progenitor Cells and Regulates Adult Hippocampal Neurogenesis. *J. Neurosci.* **31**, 3981–3989 (2011).

106. Rahpeymai, Y. *et al.* Complement: a novel factor in basal and ischemia-induced neurogenesis. *EMBO J.* **25**, 1364–1374 (2006).

107. Shinjyo, N., Ståhlberg, A., Dragunow, M., Pekny, M. & Pekna, M. Complement-Derived Anaphylatoxin C3a Regulates In Vitro Differentiation and Migration of Neural Progenitor Cells: C3a Regulates Neural Progenitor Cell Fate and Migration. *STEM CELLS* **27**, 2824–2832 (2009).

108. Ducruet, A. F. *et al.* Complement inhibition promotes endogenous neurogenesis and sustained anti-inflammatory neuroprotection following reperfused stroke. *PloS*

One **7**, e38664 (2012).

109. Bogestål, Y. R. *et al.* Signaling through C5aR is not involved in basal neurogenesis. *J. Neurosci. Res.* **85**, 2892–2897 (2007).

110. Perlman, R. L. Mouse Models of Human Disease: An Evolutionary Perspective. *Evol. Med. Public Health* eow014 (2016) doi:10.1093/emph/eow014.

111. Gosselin, D. *et al.* An environment-dependent transcriptional network specifies human microglia identity. *Science* **356**, eaal3222 (2017).

112. Galatro, T. F. *et al.* Transcriptomic analysis of purified human cortical microglia reveals age-associated changes. *Nat. Neurosci.* **20**, 1162–1171 (2017).

113. Zhang, Y. *et al.* Purification and Characterization of Progenitor and Mature Human Astrocytes Reveals Transcriptional and Functional Differences with Mouse. *Neuron* **89**, 37–53 (2016).

114. Lancaster, M. A. & Knoblich, J. A. Generation of cerebral organoids from human pluripotent stem cells. *Nat. Protoc.* **9**, 2329–2340 (2014).

115. Bagley, J. A., Reumann, D., Bian, S., Lévi-Strauss, J. & Knoblich, J. A. Fused cerebral organoids model interactions between brain regions. *Nat. Methods* **14**, 743–751 (2017).

116. Sloan, S. A. *et al.* Human Astrocyte Maturation Captured in 3D Cerebral Cortical Spheroids Derived from Pluripotent Stem Cells. *Neuron* **95**, 779-790.e6 (2017).

117. Ormel, P. R. *et al.* Microglia innately develop within cerebral organoids. *Nat. Commun.* **9**, (2018).

118. Hamelin, L. *et al.* Early and protective microglial activation in Alzheimer's disease: a prospective study using ^{18}F-DPA-714 PET imaging. *Brain* **139**, 1252–1264 (2016).

119. Ramlackhansingh, A. F. *et al.* Inflammation after trauma: Microglial activation and traumatic brain injury. *Ann. Neurol.* **70**, 374–383 (2011).

120. Thomas, C. *et al.* Detection of Neuroinflammation in a Rat Model of Subarachnoid Hemorrhage Using [^{18}F]DPA-714 PET Imaging. *Mol. Imaging* **15**, 153601211663918 (2016).

121. Liu, P., De Vis, J. B. & Lu, H. Cerebrovascular reactivity (CVR) MRI with CO2 challenge: A technical review. *NeuroImage* (2018) doi:10.1016/j.neuroimage.2018.03.047.

122. Binnewijzend, M. A. A. *et al.* Resting-state fMRI changes in Alzheimer's disease and mild cognitive impairment. *Neurobiol. Aging* **33**, 2018–2028 (2012).

123. Dijkhuizen, R. M. & Nicolay, K. Magnetic Resonance Imaging in Experimental Models of Brain Disorders. *J. Cereb. Blood Flow Metab.* **23**, 1383–1402 (2003).

124. Janssen, B., Vugts, D., Windhorst, A. & Mach, R. PET Imaging of Microglial Activation—Beyond Targeting TSPO. *Molecules* **23**, 607 (2018).

125. Takata, N. *et al.* Optogenetic astrocyte activation evokes BOLD fMRI response with oxygen consumption without neuronal activity modulation. *Glia* **66**, 2013–2023

(2018).

126. Koide, M., Sukhotinsky, I., Ayata, C. & Wellman, G. C. Subarachnoid Hemorrhage, Spreading Depolarizations and Impaired Neurovascular Coupling. *Stroke Res. Treat.* **2013**, 1–10 (2013).

127. Peng, J. *et al.* Single clip: An improvement of the filament-perforation mouse subarachnoid haemorrhage model. *Brain Inj.* 1–11 (2018) doi:10.1080/02699052.2018.1531310.

128. Sabri, M., Ai, J., Lakovic, K. & Macdonald, R. L. Mechanisms of microthrombosis and microcirculatory constriction after experimental subarachnoid hemorrhage. *Acta NeurochirSuppl* **115**, 185–192 (2013).

129. Ricklin, D. & Lambris, J. D. Complement in immune and inflammatory disorders: therapeutic interventions. *J.Immunol.* **190**, 3839–3847 (2013).

130. De Simoni, M. G. *et al.* The Powerful Neuroprotective Action of C1-Inhibitor on Brain Ischemia-Reperfusion Injury Does Not Require C1q. *Am. J. Pathol.* **164**, 1857–1863 (2004).

131. De Simoni, M. G. *et al.* Neuroprotection by Complement (C1) Inhibitor in Mouse Transient Brain Ischemia. *J. Cereb. Blood Flow Metab.* **23**, 232–239 (2003).

132. Foley, S., Li, B., Dehoff, M., Molina, H. & Holers, V. M. Mouse Crry/p65 is a regulator of the alternative pathway of complement activation. *Eur. J. Immunol.* **23**, 1381–1384 (1993).

133. Leinhase, I. *et al.* Pharmacological complement inhibition at the C3 convertase level promotes neuronal survival, neuroprotective intracerebral gene expression, and neurological outcome after traumatic brain injury. *Exp. Neurol.* **199**, 454–464 (2006).

134. Rancan, M. *et al.* Central Nervous System–Targeted Complement Inhibition Mediates Neuroprotection after Closed Head Injury in Transgenic Mice. *J. Cereb. Blood Flow Metab.* **23**, 1070–1074 (2003).

135. Alawieh, A., Langley, E. F., Weber, S., Adkins, D. & Tomlinson, S. Identifying the Role of Complement in Triggering Neuroinflammation after Traumatic Brain Injury. *J. Neurosci.* **38**, 2519–2532 (2018).

136. Mathieu, M.-C. *et al.* The C3a receptor antagonist SB 290157 has agonist activity. *Immunol. Lett.* **100**, 139–145 (2005).

137. Brennan, F. H., Lee, J. D., Ruitenberg, M. J. & Woodruff, T. M. Therapeutic targeting of complement to modify disease course and improve outcomes in neurological conditions. *Semin. Immunol.* **28**, 292–308 (2016).

138. Frei, Y., Lambris, J. D. & Stockinger, B. Generation of a monoclonal antibody to mouse C5 application in an ELISA assay for detection of anti-CS antibodies. *Mol. Cell. Probes* **1**, 141–149 (1987).

139. Martí-Carvajal, A. J., Anand, V., Cardona, A. F. & Solà, I. Eculizumab for treating patients with paroxysmal nocturnal hemoglobinuria. *Cochrane Database Syst. Rev.* (2014) doi:10.1002/14651858.CD010340.pub2.

140. Dhillon, S. Eculizumab: A Review in Generalized Myasthenia Gravis. *Drugs* **78**, 367–376 (2018).

141. Wijnsma, K. L., Duineveld, C., Wetzels, J. F. M. & van de Kar, N. C. A. J. Eculizumab in atypical hemolytic uremic syndrome: strategies toward restrictive use. *Pediatr. Nephrol.* (2018) doi:10.1007/s00467-018-4091-3.

142. Ricklin, D., Mastellos, D. C., Reis, E. S. & Lambris, J. D. The renaissance of complement therapeutics. *Nat. Rev. Nephrol.* **14**, 26 (2017).

143. Dorhout Mees, S. *et al.* Calcium antagonists for aneurysmal subarachnoid haemorrhage. in *Cochrane Database of Systematic Reviews* (John Wiley & Sons, Ltd, 2007). doi:10.1002/14651858.CD000277.pub3.

144. Dorhout Mees, S., van den Bergh, W. M., Algra, A. & Rinkel, G. J. Antiplatelet therapy for aneurysmal subarachnoid haemorrhage. *Cochrane Database Syst. Rev.* (2007) doi:10.1002/14651858.CD006184.pub2.

145. Guo, J., Shi, Z., Yang, K., Tian, J. H. & Jiang, L. Endothelin receptor antagonists for subarachnoid hemorrhage. *Cochrane Database Syst. Rev.* (2012) doi:10.1002/14651858.CD008354.pub2.

146. Perea, G., Navarrete, M. & Araque, A. Tripartite synapses: astrocytes process and control synaptic information. *Trends Neurosci.* **32**, 421–431 (2009).

147. Panatier, A., Arizono, M. & Nagerl, U. V. Dissecting tripartite synapses with STED microscopy. *Philos. Trans. R. Soc. B Biol. Sci.* **369**, 20130597–20130597 (2014).

148. Asano, S. M. *et al.* Expansion Microscopy: Protocols for Imaging Proteins and RNA in Cells and Tissues. *Curr. Protoc. Cell Biol.* **80**, e56 (2018).

149. Chen, F., Tillberg, P. W. & Boyden, E. S. Expansion microscopy. *Science* **347**, 543–548 (2015).

150. Jiang, N. *et al.* Superresolution imaging of *Drosophila* tissues using expansion microscopy. *Mol. Biol. Cell* **29**, 1413–1421 (2018).

151. Freifeld, L. *et al.* Expansion microscopy of zebrafish for neuroscience and developmental biology studies. *Proc. Natl. Acad. Sci.* **114**, E10799–E10808 (2017).

152. Zhao, Y. *et al.* Nanoscale imaging of clinical specimens using pathology-optimized expansion microscopy. *Nat. Biotechnol.* **35**, 757–764 (2017).

153. Chang, J.-B. *et al.* Iterative expansion microscopy. *Nat. Methods* **14**, 593–599 (2017).

154. Gao, R. *et al.* Cortical column and whole-brain imaging with molecular contrast and nanoscale resolution. *Science* **363**, eaau8302 (2019).

155. Liu, X. *et al.* Interleukin-4 Is Essential for Microglia/Macrophage M2 Polarization and Long-Term Recovery After Cerebral Ischemia. *Stroke* **47**, 498–504 (2016).

156. Lively, S. & Schlichter, L. C. Microglia Responses to Pro-inflammatory Stimuli (LPS, IFNγ+TNFα) and Reprogramming by Resolving Cytokines (IL-4, IL-10). *Front. Cell. Neurosci.* **12**, 215 (2018).

157. Mercier, J., Provins, L. & Valade, A. Discovery and development of SV2A PET

tracers: Potential for imaging synaptic density and clinical applications. *Drug Discov. Today Technol.* **25**, 45–52 (2017).

158. Sharif-Paghaleh, E. *et al.* Non-Invasive whole-body detection of complement activation using radionuclide imaging in a mouse model of myocardial ischaemia-reperfusion injury. *Sci. Rep.* **7**, 16090 (2017).

Supplementary table 1. Intervention studies investigating microglia response after SAH

Drug/investigated compount	Species / strain	Model	Time after SAH	Pathways (if mentioned)	Other outcome	References
Human albumin	Sprague-Dawley rats	Endovascular perforation	1 and 7d	microglial Mincle/Syk signaling	Reduced M1 activation	38
Methylene blue	Sprague-Dawley rats	Endovascular perforation	3, 6, 12, 24, 48 and 72 h	Akt/GSK-3β/MEF2D signaling pathway	Attenuation of microglia activation, reduce EBI	40
Astaxanthin	Sprague-Dawley rats C57BL/6 mice TLR4 -/-	Prechiasmatic cistern blood injection	2, 6, 12, 24, 48 and 72 h	TLR4 pathway	Attenuation of microglia activation, reduce EBI	41
Netrin-1	Sprague-Dawley rats	Endovascular perforation	3, 6, 12, 24 and 72h	PPARγ/NFκB signaling pathway	Attenuation of microglia activation, reduce EBI	42
Thioredoxin-interacting protein	Sprague-Dawley rats	Endovascular perforation	12, 24, 48 and 72h	PERK and IRE1α pathway involved, activates Thioredoxin, that increases damage after SAH	Thioredoxin activated in astrocytes and microglia	43
Rapamycin	Sprague-Dawley rats	Prechiasmatic cistern blood injection	3, 24 and 72h	mTOR	Attenuation of microglia activation, reduce EBI	44
Resveratrol	Sprague-Dawley rats	Endovascular perforation	24 and 72h	MPK/SIRT1/autophagy signaling; TLR4 Pathway	Attenuation of microglia activation reduce EBI	45,46

Supplementary Table 1 continued.

Complement C5 antibody	BALB/c mice	Prechiasmatic cistern blood injection	48h	Complement pathway	Attenuation of microglia activation and cell death	7
High mobility group box-1 (HMGB1) antibody	Wistar rats	Cisterna magna blood injection	48h	TLR4 pathway	Antibody also reduces microglia activation	47
Fluoxetine	Sprague-Dawley rats	Endovascular perforation	24h	TLR4/MyD88/NF-κB signaling pathway	Attenuates of microglia activation reduce EBI	48,72
Apigenin	Sprague-Dawley rats	Endovascular perforation	24h	TLR4 pathway	Attenuation of microglia activation, reduce EBI	49
Bexarotene	C57BL/6J mice	Endovascular perforation	24h	PPARγ	Attenuation of microglia activation, reduce EBI	50
PARP inhibition	Sprague-Dawley rats	Endovascular perforation	24h	NF-κB/MMP-9 pathway	Attenuation of microglia activation, reduce EBI	51
Minocycline	Sprague-Dawley rats	Endovascular perforation	24h	NLRP3 Inflammasome-Induced Inflammation	Attenuation of microglia activation, reduce EBI	52
Rolipram	Sprague-Dawley rats	Endovascular perforation	24h	promotes the expression of SIRT1 while inhibited NF-κB activation	Attenuation of microglia activation, reduce EBI	53
Erythropoietin	C57BL/6J mice	Prechiasmatic cistern blood injection	24h	EPOR/JAK2-STAT3 pathway	Attenuation of microglia activation, reduce EBI	54

Supplementary Table 1 continued.

Resveratrol	Sprague-Dawley rats	Prechiasmatic cistern blood injection	24h	NLRP3 inflammasome activation inhibition	Attenuation of microglia activation, reduce EBI	55
Deferoxamine	Conditional HO-1 knockout C57BL/6 mice	Prechiasmatic cistern blood injection		microglial/macrophage HO-1 expression	Attenuation of microglia activation, reduce EBI	56
Aggf1	Sprague-Dawley rats	Endovascular perforation	3, 6, 12h; 1d, 3d, 7d, 14d, 21d	PI3K/Akt/ NF-kappaB pathway	Attenuation of microglia activation, reduce EBI better performance memory task	57
Sirtuin 1 activation	Sprague-Dawley rats	Prechiasmatic cistern blood injection	2, 6, 12, 24, 48 and 72 h	FoxOs, NF-κB and p53	SIRT1 expressed in microglia, not astrocytes	58
TSG6	Sprague–Dawley	Endovascular perforation	6, 12, 24, 48 and 72 h	SOCS3/STAT3 pathway	Reduced M1 activation	59
Progesterone	C57BL/6J mice	Prechiasmatic cistern blood injection	1, 6, 9 and 10d		Attenuation of microglia activation, reduce EBI and DCI, and more	60
Astaxanthin	Sprague-Dawley rats	Prechiasmatic cistern blood injection	24 and 72h		Attenuation of microglia activation, reduce EBI	71
Nano-Curcumin	Sprague-Dawley rats	Endovascular perforation	24 and 48h		Attenuation of microglia activation, reduce EBI	61
Hydrogen sulfide	Sprague-Dawley rats	Endovascular perforation	24h		Attenuation of microglia and astrocyte activation, reduce EBI and DCI	62

Supplementary Table 1 continued.

Curcumin	C57BL/6 J mice	Endovascular perforation	24h		Attenuation of microglia activation, reduce EBI	63
Prostaglandin	Sprague-Dawley rats	Endovascular perforation	24h		Attenuation of microglia activation, reduce EBI	64
Magnesium Lithospermate B	Sprague–Dawley	Endovascular perforation	24h	SIRT1/NF-κB pathway	Reduced microglia activity and apoptosis	65
Pentoxifylline	Wistar rats	Prechiasmatic cistern blood injection	24h		Attenuation of microglia activation, reduce EBI	66
ApoE-derived mimic peptide, COG1410	C57BL/6J mice	Endovascular perforation	24h		Attenuation of microglia activation, reduce EBI	67
Xenon	Sprague-Dawley rats	Endovascular perforation	24h		Attenuation of microglia activation, reduce EBI	68
Ethyl pyruvate	Sprague-Dawley rats	Endovascular perforation	24h		Attenuation of microglia activation, reduce EBI	69
NP-PFC-mediated hypothermia	Sprague-Dawley rats	Cisterna magna blood injection	3h		Attenuation of microglia activation, reduce EBI	70

EBI: Early Brain Injury; DCI: Delayed Cerebral Ischemia; M1: pro-inflammatory state of microglia activation.

ADDENDA

Het complementeren van een subarachnoïdale bloeding.

Voor alles wat we doen, gebruiken we onze hersenen. De hersenen zitten veilig afgesloten; een harde schedel zorgt voor bescherming van buitenaf. Ook in de schedel hebben de hersenen voldoende bescherming. Zo zitten er drie membranen rondom de hersenen. Eén daarvan heet het arachnoidea membraan, met daaronder de subarachnoïdale ruimte die gevuld is met cerebrospinale vloeistof, en er liggen enkele bloedvaten. De hersenen hebben ook nog bescherming tegen vreemde stoffen in de bloedcirculatie, door middel van de bloed-hersenbarrière. Dit alles zorgt ervoor dat ons brein beschemd en in relatieve rust kan blijven functioneren.
In en rond de hersenen gaat er ook nog wel eens wat mis. Aan de bloedvaten rondom de hersenen, in de subarachnoïdale ruimte, kunnen verwijdingen ontstaan, genaamd aneurysmata. Bij teveel druk vanuit de binnenkant kan een aneurysma knappen, waardoor bloed de subarachnoïdale ruimte in stroomt, en een aneurysmale subarachnoïdale bloeding (SAB) veroorzaakt. Vervolgens kunnen verschillende factoren leiden tot hersenletsel:

- Omdat de subarachnoïdale ruimte wordt beperkt door de schedel, stijgt de intracraniële druk. Deze kan zo hoog worden dat de bloedtoevoer naar de hersenen tijdelijk stopt, wat leidt tot ischemisch hersenletsel.
- Bloed in de subarachnoïdale ruimte wordt afgebroken, en er ontstaat een bloedsstolling. Veel van de afbraakproducten en stollingsfactoren zijn schadelijk voor de hersenen, wat meer hersenletsel kan veroorzaken.
- Bovendien wordt de bloed-hersenbarrière beschadigd, en biedt dat geen bescherming meer van tegen schadelijke stoffen in de bloedcirculatie. Deze stoffen kunnen nu de hersenen indringen en beschadigen.

Door alle schade is een SAB is een ernstige soort van beroerte met een hoog sterftecijfer. De mediane leeftijd waarop een aneurysmale SAB optreedt is 55 jaar. Vanwege deze jonge leeftijd en de slechte prognose is het verlies aan productieve levensjaren hoog. Eén derde van de patiënten sterft binnen 3 maanden na de bloeding en patiënten die de bloeding overleven hebben vaak langdurige functionele en cognitieve stoornissen.
De schade aan de hersenen veroorzaakt ook een immunologische reactie.

Dat heeft te maken met verschillende cellen in de hersenen en hun specifieke functies. Neuronen zorgen voor de signaaloverdracht. Daarnaast zijn er heel veel soorten gliacellen, die allemaal talloze functies hebben om de signaaloverdracht in goede banen te leiden. In dit proefschrift hebben we er maar een paar van benoemd, en hebben we ons voornamelijk gefocust op de astrocyten en de microglia. Onder normale omstandigheden zijn astrocyten onder andere betrokken bij de regulatie van energie, de signaaloverdracht tussen neuronen en het in stand houden van een goede ion- en waterhomeostase. Microglia zijn onder andere betrokken bij neurogenese en reguleren het aantal synapsen; de connecties tussen neuronen. Dit laatste doen ze door alle synapsen te scannen voor stofjes die behoren tot het complement systeem. Het complement systeem is onderdeel van een immunologisch proces. Echter, doordat de hersenen afgesloten zijn van de rest van het lichaam en normaal weinig in contact komen immunologische processen, voert het complement systeem in de gezonde hersenen andere functies uit. Als de synaps zich presenteert met onderdelen van het complement, wordt de synaps door de microglia verwijderd. Dit kan nuttig zijn, bijvoorbeeld voor het geval van het afleren van slechte gewoontes, of het vergeten van nutteloze herinneringen.

Het complement systeem is bij een subarachnoïdale bloeding sterk geactiveerd. Ook astrocyten en microglia veranderen van functie, ze reageren op de schade en de immuun- en complementactivatie in de subarachnoïdale ruimte en worden onderdeel van het immuunsysteem. Daarbij verliezen ze hun normale functies.

Het complement systeem is een immuun-cascade dat uit meer dan 30 eiwitten bestaat. De cascade kan worden geactiveerd via drie verschillende routes, die allemaal tot de productie van een belangrijk onderdeel leiden: complement C3 en C5, die beide gesplitst kunnen worden in weer kleinere eiwitten. Onder andere hierdoor worden immuuncellen, zoals astrocyten en microglia, geactiveerd.

Het proces van immuun-geactiveerde astrocyten en microglia heet ook wel gliose. Gliose kan mild zijn, door alleen cytokines uit te scheiden, maar het kan ook ernstig zijn, als gevolg van de vorming van een soort littekenweefsel rond beschadigde hersengebieden. Na een SAB proberen zowel het complement systeem als de gliose de schade aan de hersenen te beperken of te herstellen, maar het kan de hersenen ook verder beschadigen. Een voorbeeld

daarvan is dat een lage productie van cytokines een genezende uitwerking hebben op beschadigde neuronen, maar dat te veel cytokines giftig kunnen zijn voor het omliggende hersenweefsel. Bovendien worden de processen van de gezonde hersenen erg verstoord, doordat de astrocyten en microglia niet meer hun normale functies uitvoeren. Een aanhoudende gliose kan de schade van de SAB dus *complementeren*.

In dit proefschrift hebben we de gliose na een SAB onderzocht. In **hoofdstuk 1** van dit proefschrift hebben we een overzicht gemaakt van alle literatuur van vóór juli 2015 over gliose na SAB. Daarin geven we ook inzicht in de functionele gevolgen en klinische implicaties van de gliose. Een update daarvan wordt gegeven in de andere hoofdstukken en in de discussie.

In **hoofdstuk 2** hebben we de rol van het complementsysteem in de ontwikkeling van hersenletsel na de SAB bestudeerd. We vonden een toename van de aanwezigheid van complementcomponenten C1q en C3 in de hersenen van SAB-patiënten. Verder vonden we een verband tussen genetische polymorfismen in het gen van complement C5 en een slechte functionele uitkomst bij patiënten. Patiënten met dit risico-allel hadden lagere C5a-plasmaspiegels, hoewel de plasmaspiegels niet correleerden met een slecht functioneel resultaat. Daarbij vonden we ook dat de C5a-niveaus van complementcomponenten in cerebrospinale vloeistof 1 dag na SAB sterk waren verhoogd. Bij muizen zonder de C5a-receptor vonden we een verminderde microglia activatie en verminderde neurale celdood na een experimenteel geïnduceerde SAB. Bovendien waren de microglia activatie en neurale celdood ook verminderd bij wildtype muizen die injecties kregen met een antilichaam dat de splitsing van C5 in C5a en C5b voorkomt. Dit zou mogelijk een goede behandeling kunnen zijn tegen schade in de hersenen van SAB patiënten.

In **hoofdstuk 3** hebben we de gliosis in de frontale cortex van SAB-patiënten onderzocht. We vonden een toename van GFAP, een eiwit in astrocyten dat verhoogd is bij gliose, en zagen een toename van het aantal microglia, wat duidt op zowel geactiveerde astrocyten als microglia na een SAB bij mensen. Vervolgens hebben we ons gericht op de gliosis en cognitieve veranderingen in een muismodel voor SAB. We ontdekten dat muizen na een SAB geheu-

genstoornissen hebben. Bovendien was er een toename van complement C3 in de astrocyten van de hippocampus van muizen met een SAB, en dit correleerde met geheugenstoornissen. Dit suggereert dat complementactivatie in astrocyten bijdraagt aan cognitieve stoornissen na een SAB.

In **hoofdstuk 4** hebben we onderzocht of de gliose ook gunstig kan zijn, door regeneratieve eigenschappen te activeren om na een SAB het hersenweefsel te herstellen. We vonden echter geen verschil in de hoeveelheid proliferatieve neurogene astrocyten binnen de neurogene niche van de muizenhersenen, twee weken na SAB, maar zagen wel dat er mogelijk nieuwe neuronen groeide in hersengebieden met veel schade.

Subarachnoïdale bloedingen kunnen ernstige schade aan de hersenen veroorzaken. De immuunreactie, geactiveerd door het complementsysteem, microglia en astrocyten in de hersenen, lijkt de SAB voornamelijk te verslechteren. Het blokkeren van deze immuunreactie zou een goede uitwerking kunnen hebben op het herstel van patiënten met een SAB.

Complimenting Colleagues and Friends

Bart J. van Dijk[1].

1. UMC Utrecht Brain Center, Department of Translational Neurosciences, University Medical Center Utrecht, Utrecht University, Heidelberglaan 100, Utrecht, The Netherlands

Published with this thesis.

Abstract
A thesis without an acknowledgements section is not a finished thesis, in my opinion. It is also the only section most of you will read. If you did read more than just this, I appreciate it. For my acknowledgements, I would like to start with saying that being born in the Netherlands, with a prosperous economic situation, certainly helped in reaching my goals, and I am thankful of that. Many thanks to the countless number of teachers from elementary school to my last completed study who put in their effort to teach me something. But most importantly, I will have to thank you all. In this section I will elaborate my acknowledgements a bit. In case you are reading this and there is no mention of you and you expected otherwise, I am sorry for that, but thank you anyway.

Introduction
It is already more than 6 years ago when I got the following email from Niek Maas:

> *"Beste Bart,*
> *Ik heb via Jeroen de Vrij, post-doc binnen onze groep, vernomen dat er bij de groep van Prof. Elly Hol een AIO positie komt mbt tot het opzetten van een diermodel voor stroke.*
>
> *Omdat jij zowel animal tech bent en neuroscience hebt gestudeerd, moest ik aan jou denken. Ik heb Elly Hol in de cc van deze mail gevoegd zodat je gemakkelijk contact kan opnemen.*
>
> *Groet,*
>
> *Niek"*

This happened to be the initiation of my time in the group of Elly Hol, as after several talks to my supervisors I could start as a PhD student in her lab. Niek, thank you very much for initiating this. We know each other for a very long time now and I am glad we are still friends. I also would like to share my gratitude that you will be one of my paranymphs, and thereby will also end this adventure with me.

I probably could write several pages to why I would thank Elly Hol, but I'll keep it short. First of all you gave me the chance to continue my studies in the direction I really wanted, namely glia. Furthermore, you let me be me, and gave me the freedom to find out how to carry out the project. I liked to experiment with many different methods, of which most did not make it into this thesis, but I learned a lot from it. You invited me to join many outings and encouraged me to get out of my comfort zone and just invite myself. I enjoyed the networking and I have had quite some nice dinners and drinks. Even though you are quite a busy person, you always had time to talk about the project, about problems, about potential plans, or just about stuff. You try to involve people, and thereby making the lab and it's surrounding a very fun place to work. Elly, thank you very much for all the things you did to make my PhD to a success and the enjoying 5±1 years.

If I did not have Mervyn Vergouwen as one of my supervisors, this thesis would have been very different. Mervyn, you were always there, and your input and knowledge about the patient was of great value. You kept us organized. If the plans became too vague, you stepped in and got the plans back to the main aim; how it would benefit the SAH patient. You truly were a complementing factor to the supervision and the direction of this thesis. Thank you very much!

Gabriël Rinkel, thank you for the supervision. You helped us get forward. The monthly meetings were something to look forward to, and after each one of them, I exactly knew what I had to do for the months to come. I would also like to thank you for the way you correct written manuscripts. Your constructive criticism and the comments, with a nice dose of humour, made the texts a lot better.

The department of Translational Neuroscience was a nice place to work in. While different groups work there on different subjects, there always was unity. I think a lot of this can be attributed to Peter Burbach. Peter, thank you very much for the nice work environment you stimulated.

I would like to thank the defence committee, Prof dr. Rick Dijkhuizen, Prof. dr. Diederik van den Beek, Prof dr. Elga de Vries, Prof dr. Bart van der Zwan, Prof dr. Manon Benders and dr. Cora Nijboer for their time and effort and to make my defence possible.

I would also like to thank all my internship supervisors during my prior studies, as they paved the way towards my PhD. During my MLO, Nancy Schuurman, Jan van Amsterdam, Edwin Willems helped me in understanding that I should continue my studies. Internships with Huib Versnel and Tonny Mulder during my HLO introduced me to the fascinating world of Neurosciences, and got me into the Neurosciences master at the VU. I really enjoyed my time during the internship with Tom Würdinger and Tonny Lagerweij, where I learned a lot, and I am really thankful for the encouragement to look for an internship in Tokyo. I thank Prof. Shigeo Okabe for giving me the opportunity to do research in his lab at the University of Tokyo. Even though it was one of the toughest things I have done, my time in Tokyo was also one of the best.

Material and methods

Essential workers
My PhD mainly happened in the lab. As my project was a new project in an collaboration between Translational Neurosciences and the Neurology department, and as I did not have prior experience in the department, I had to rely on the knowledge of many people. These people are the essential workers in and around the lab.

One thing that saved a lot of time was all the administration and IT matters. Joke, Ria, Vicki, Sandra, Krista and Roger Koot, thank you for your help and all the reminders on the paperwork that were required to complete this PhD. I am also glad I did not have to vacuum the floor every week, wipe my desk or change the garbage bag daily. A big thank you to the cleaning facility with-

in our department. It saves a lot of time that we could now spend on our research.

One. Labs on the 5th floor

Within the HolLab, I was the only one to start out doing work with animals. Finding my way on the 5th floor through labs that were predominantly occupied by the Adan- and KasLab was not easy at first, but luckily they were all very helpful to assist me. Special thanks to Mieneke, for taking her time to correct all work-protocols. Thanks to Mark Broekhoven on suggestions on the surgery and thanks to the IVD, both Fred and Harry, who were very helpful in how to approach the severe disease model I would be using. The caretakers of the animals had great suggestions on how to minimize the discomfort in a practical way. Together with Marjolein Heil and Annemieke we were able to build a good intensive care unit. Thank you for your help. Jos, for keeping me company during the surgeries, and for building a higher surgery table, without that I would still have an aching back. Thanks to the good connections Prof. Jeroen Pasterkamp has in Amsterdam, a mouse breeder was hired that helped me a lot in managing the mice. Thank you Chris for always thinking of me when you had some left over C57bl/6Js, and for the fun we had organizing the Easter-lunch. At the start of the project, I was glad to get some feedback advice on the Subarachnoid Hemorrhage research from Rick Dijkhuizen. You helped in creating nice ideas for the project, and I am sad the plans to involve a MRI-scanner did not work out as planned. I guess my plans were only feasible if a PhD takes 16 years. One of the things that I did get to work was the behavioural tests. Thanks to Martien Kas, Kim van Elst and Remco Molenhuis for the guidance and providing the right protocols. Thanks to Jelle, Véronne and Jiska for keeping me company during the long behavioural sessions. It sometimes felt like I was the test subject in a social deprivation study, but seeing one of you during the weekends made me feel I was not.

Two. Labs on the 4th floor

Different from the 5th floor, where I had to claim a spot for the HolLab, some HolLab pioneers had already colonized the 4th floor on my arrival. Thanks to Manja, Miriam and Jacqueline, who already filled some fridges and freezers with the basic needs to do some experiments, and claimed enough work-

benches for all HolLab members to come. Luckily, the indigenous technicians were not hostile to these new inhabitants. On the contrary, they were most welcoming. Thanks to Henk Spierenburg for always knowing where to discard our chemical waste. This got a lot messier, stinkier and more difficult after you left. Leo, you were always helping out everyone, everywhere. You're truly a special person, I think people should make a movie about your work in the lab, it will be a blockbuster. During my pioneering time I was always looking for the best way to resolve my experiments into nice images. Thank you Youri for all the guidance in choosing the right microscopes and for teaching how to handle them. Thanks to Marina for the help in and around the histology lab. There, I had to embed some of the scarcely available human brain tissue from SAH patients into paraffin, that I had obtained from an obduction. Most of the tissue however, we got already embedded from Rinie Frijns, who had stored this most valuable collection for many years. Thank you for entrusting the collection for our research. Furthermore, thanks to the Netherlands Brain Bank for providing tissue from control patients.

Hong Kong
For my research I was in need of a good model. Luckily, the UMCU just established a new programme to collaborate with the Chinese University of Hong Kong at the start of my PhD. Thanks to Mervyn and Gabriel for establishing contact with Prof. George Wong, who happened to have ample experience with a model for Subarachnoid Hemorrhage in his group. I had the oppotunity to visit his lab. Many thanks to George Wong for the hospitality and giving me the chance to learn the technique, and thanks to Don and Vera for teaching me.

Staying focused
There are several ways to stay focused in the department of Translational Neuroscience. To stay focussed, you sometimes need to relax a bit. Since the view from most parts of the department is just another building, looking out the window is not part of relaxing. A well-deserved break is an option, and to also stay focussed, one would drink a coffee during their break. Coffee in the department could be obtained through the big black machine in the lunch room. It's disgusting, but it gets the job done. Thanks to the suppliers for sometimes refilling this machine on time. Luckily, there is a department

just next to Translational Neuroscience that has a small black machine, that produces significantly better coffee. Thanks to Nienke Derks for pointing this out to me. Then there is MiCafe, with their fancy barista coffee machine. This coffee is better, but is not cheap. Although I do not smoke, I really liked joining Nefeli, Emma and Renata's breaks outside, usually enjoying a good MiCafe coffee. Last, there was the special Jenifer Aniston coffee machine. Next to it, there was a comfortable sofa, and most importantly, there always were good people in that office to talk to. Thank you Marjolein for always taking time to have coffees with me. I did not have to say much and still you knew exactly what I wanted. And if Marjolein was not present, either Jelle, Oliver, Max, Jeroen or Katherine were always in for a chat, thanks.

Satiation and energy balance
Although I have often complained about the food quality, the restaurant de Brink did have food, which is nice. Broodjes Amsterdam were sold by MiCafe, a better alternative to the Brink. Even better, was broodje Ben, but came with a bit of a walk. The most amazing lunch one could get, was the Indian lunch from ~~New Delhivery~~ ~~Curier~~ Rice and Spice, made and delivered by Anuj and Divya. Thank you for the very delicious meals.

Results
As you would have noticed by now, this acknowledgement section is written in the layout of a publication, and it needs a result section. As the result of doing my PhD, I got to know the following people, who I worked with, or did some side activities. You made my PhD a lot more enjoyable.

Emma van Bodegraven is also one of the HolLab pioneers I talked about in the method section, but I wanted to elaborate a bit on why I would thank you Emma. Although our projects had little overlap, I always felt we were working in a great collaboration. We were the first to start as PhD students in the HolLab after it moved to Utrecht, so we had to set the mood. I think we managed by having a high ratio of fun/science. This demonstrates well in the Superawesomejournalclub we set up, together with Sharon and Rosalie. We never only did science, it always came with a good story, a snack, or several beers. In our view, a high science/fun ratio would be strange. I really liked our collaboration. Thank you for making me go to work with a smile.

Yujie, you are so funny. You never cease to surprise me. On top of that, your cooking skills are phenomenal, I think you won all the prices in the savoury category during each Easter-lunch. My okonomiyakies were no match. Thank you for teaching me Majong and inviting me for hot-pot. Delicious!

Sophietje, it would not surprise me to hear you wear a Superwoman suit beneath your cloths. Like Clark Kent, you act like a normal person, but you're not. The things you achieved during our time in Translational Neuroscience are out of this world. Doing night-shifts as a neurosurgeon, then coming back to the lab to pass your cells, and then ice-climb a mountain. Petje af. I enjoyed working with you, thank you for all the fun we had and thank you for your enthusiasm.

Marjolein, I already mentioned you above, thanking you for having coffee breaks with me. Moreover, I really liked our common interests, the running, the singing, the science. Thanks!

I was glad to have a desk in room STR4.129. They placed some amazing people in there. Like Emma Sudria Lopez, a girl from Catalonia, spontaneous, elated. Aai Emma, your presence enlightens. You decorated the office. Or Renata, from Terceira, with an incredibly warm personality. You made the office an inviting place to come to. I think more people thought so, as there weren't many days without guests. Andrea, you're the cherry on top. Thank you all for making the office awesome.

Nefeli, you're one of the kindest persons I know. I think in your first year you needed some more help, but only Keith dared to come close. Luckily the storm settled down, and you got better at managing your lab work. It was great to have you around and thank you for the borrels. Moreover, thank you for guiding me on how to finish a thesis. You helped a lot these last few months.

Ketharini, thank you for always being uplifting. I do not know how you do it, but you always seem so positive. I'll hop by at the Jeruzalemstraat soon to be happy.

Although it is not hard to combine science with creativity, my experiments did not fully satiate my urge to be creative. I feel this was also the case for Daniëlle van Rossum. Thank you Daniëlle, for sparking my creativity with all the side projects we had going on. Too bad we did not win the prize for Nature's Scientist at Work Photography contest. I think we should have won.

Amber, I like your genuine interest in others and your constructive feedback. For me personally, this meant that I could really clear my thoughts. Thank you for the talks in that bar in Düsseldorf, or just any talk in the hallway. I am glad you and Jessy are good at making movies. Jessy, I am glad you joined the HolLab. Your lively presence made it more enjoyable. Tamar, thank you for the nice time in Bertinoro and in the lab, and thank you for being such a good model for my photography. Jinte, I like that we level quite nicely. The ease to talk with you about things in and around science and other stuff was a nice way to get out for lunch. Let's go again soon. Sara Schaafsma, Saskia, Hans and Gijsje, Lianne, Christiaan and Marloes, Werner, thank you for the great time in the HolLab! And thank you Jeroen, Jacques, Frank, Anna, Özge, Janna, Mateja, Lieke, Marieke, Mark Verheijen, Vamshi, Valeria, Pavol, Anna, Eljo, Geoffrey, Erwin, Desiré, Asami, and others for the fun in the Translational Neuroscience department.

I would also like to thank all the people I really collaborated with in my scientific work. These include all the people that are co-authors on my other chapters, thank you. Most help I got are from my students. Marije, Zelonna and Viktor, you all did an amazing job for doing a ~6 month masters internship with me. Loads of work was performed that I did not have time for, resulting in nice data. Myrna, Jeanneke and Danny, your writing assignments helped me a lot. Daniëlle Vonk, thank you for helping out with the surgeries, it really made a difference in the amount of surgeries I could do in a day. Isadora, thank you for the imaging and tracing. Claudia, your tiramisu is amazing! Thank you for your help on the project. Thank you Inez for the help on the behavioural data and on the talks about SAH science, and Science in Transition. Vanessa, thank you for the help in setting up additional experiments. Many thanks to Roland for continuing the surgeries. Mark and Dick, thank you for the help in explaining the statistical difficulties I had with the genetic data analysis.

During my PhD I did several nice side activities. I was glad to be part of the Pizza-Journal club committee, to organize journal clubs for master students, while eating pizza. Thank you Geert for making this possible, and Roland, Véronne and Dick for helping setting it up. I also enjoyed the teaching part in the behaviour course of Roger Adan. Thank you Inge Wolterink for organizing this mouse behaviour practical with the Bachelor students. It was a very small part of my PhD, but definitely a fun one. Thanks to the borrel committee for occasionally organizing drinks.

I also did a lot of sports, and most sports come with competition. Suzanne, you always made a competition out of everything, and I am happy you did. The Singel loop, the MudRun, the triathlon, the Swimming through the Amsterdam Canals for ALS were all a whole lot of fun.
Climbing is not something to compete in, and rather encourage others to get better. Thank you Roland for introducing this amazing sport to me. Thank you Lill Eva, Onur, Paul, and Edu for encouraging me to climb a level higher. You can do it!

Paul, that was not the only mention of you. I saved you for last, at least for the result section. In research articles the last mentioned experiment is often the most conclusive for the story. Well, you are too. We have had an amazing time. When I first saw you I did not think we would go well together, but don't judge someone on his suit. I got to know you as a very interested and kind guy, who is also in for fun or a joke. Like Suzanne, you are also always making things into a competitions, and you want others to make the most out of things. In combination with your kindness brings a lot of aspiration, that helped me both professionally and personally. This usually shows in our regular climbing sessions, where you push me to do that run-jump-dyno. Or, it shows during a karaoke sessions, singing André Hazes' songs with full dedication. But also in the completion of this thesis, as you had a big hand in pushing me to finish it correctly. Thank you for being my paranymph, and thank you for the amazing time we had during our PhD, and hopefully will have somewhere between Utrecht and Voorburg in the future.

Discussion

It obviously does not need to be discussed that the friends and family from

outside your PhD should also be acknowledged. They are the people that shape you, and are the people you go to and discuss problems, spend time and have fun with.

I'd like to thank Niek and Bashel for the nice rijstwafelmeetings, we try to organize once a month since we could not be at Club Delicious anymore. Whether it was ordered from Ying Bin, Djakarta or Tai Soen, I think the quality of the food did not matter, the gathering mattered. I am sad Leo Eigeman could not see the completion of this thesis, but I would like to thank him for everything he did.

Martijn, we bumped into each other during our first year of the MLO, and I cannot remember a time since then that we lost track of each other's whereabouts. I am still glad you visited me in Tokyo, and I am sorry I cannot visit you more often in London. Thank you for being such a good friend. Mark, your hospitality is like no other. Even if I rang you out of your sleep, you would still just open the door at the FC Donderstraat. Thank you for the ease to have a good time. Together with Peter, we should soon go and see the Grand Mexican Warlock.

Merijn, thank you for being so warm-hearted. Even though we see each other only once every two years, whether it is in Tokyo, Pohang, Edinburg or Eelde, we just continue our previous conversation. I hope to visit you, Hearim and Matthijs in Hong Kong, or elsewehere, soon. Thank you for your support.

Berto, thank you for all the great talks we've had and the fun trips we have made. Furthermore, thank you for introducing Siem, Egbert, Amber, Marieke, Neline to make the 030 group. It is nice to be part of it. Thank you for all the escapes!

Egbert and Chris, thank you for the belaying!

Shashini, Tim, Linda, my (neuro)biological family, you guys are a fun bunch of people. Shashini, thank you for the nice Japanese/Korean dinners. Tim and

Linda, you two are suuperleuk! I really like our casual group of (ex)neuroscientists that go on adventures in London, hiking in Poland, or watch ~~Disney~~ movies on a couch.

Emma, Eelke en Sven, thank you for sharing a room with me in Amsterdam, it was a lot of fun. Truus, Bonnie and the rest, thank you for your support.

Vassillis, thank you for introducing me to the Camera Japan film festival. It is a nice way to feed my fascination for Japan. I hope we can go there together next time, or to the one in Barcelona.

Harukata Miki, first of all, thank you very much for the invitation to eat at Darjeeling in Nippori. It was life changing. Since then, we have been on multiple hiking trips and went to many restaurants in and around Tokyo. And, when I could not be in Japan, you sent treats from Japan in a box, or just have a chat online. Thank you for the friendship. Thanks to Hayashi-san, Higashi-san, Kashiwagi-san, Arnaud, Kevin, George, Billy, Xiaojing and Li for making Tokyo a lot more enjoyable.

To all my family, Schroten, Korenhof; Marry and Rob, van Dijk; Gerrie and Joke, van Baren/van Dijk, thank you for your interest in my study!

Marieke, Menno en Veerle, thank you for bringing more joy in life. Sanne, and Tjeerd, thank you for the nice family gatherings. Gerrit, Anneke, thank you for everything, you have always supported me during the studying and the non-studying, and I appreciate it very much.

Lisanne, thank you for making me go home with a smile too.

Curriculum Vitae

Bart van Dijk was born in Utrecht, the Netherlands, on 23 August 1985. After graduating from the MAVO at the Blaucapel College (currently called Gerrit Rietveld college) in 2003, he attended the MLO (Secondary Laboratory Education) in Utrecht, combined with two internships. He did one internship at the department of Virology at the faculty of Veterinary, University Utrecht, studying strains of the feline calicivirus. The other internship was done at the Dutch National Institute for Public Health and the Environment (RIVM), in the Toxicity department, studying the carcinogenicity of cigarettes. Thereafter, he attended the HLO (Higher Laboratory Education), leading to a Bachelor in Applied Science degree in 2010. During the HLO, he did another two internships, working at the otorhinolaryngology department of the UMCU studying the regenerative properties of hair cells in the vestibular system. The other internship was at the neuroanatomy department of the Vrije Universiteit in Amsterdam, studying neuronal activity in the medial prefrontal cortex of awake rats during attention. Thereafter he solo-travelled the world, visiting South-East Asia, Japan, Canada and the United States of America. He then started studying at the Vrije Universiteit in Amsterdam, enrolling in the research master programme Neurosciences. He did internships at the Cancer Center Amsterdam, VUMC, studying novel treatment options against paediatric glioblastoma and went on an internship abroad, at the Neurobiology department at the University of Tokyo, studying synaptogenesis in the presence of astrocytic exosomes. Thereafter, he started his PhD in the lab of Prof. dr. Elly Hol, co-supervized by Prof. dr. Gabriël Rinkel and dr. Mervyn Vergouwen, which resulted in this thesis. During this time he travelled to the lab of Prof. dr. George Wong, at the Chinese University of Hong Kong to learn the surgery operation for a subarachnoid haemorrhage mouse model. After his PhD he started a post-doc position at the lab of Prof. dr. Marjo van der Knaap, studying the disease mechanisms of the leukodystrophy Vanishing White Matter, for one year.

UMC Utrecht

Universiteit Utrecht

ISBN 978-94-93184-69-5